

# **Block Copolymer Micelles and Emulsions for Bactericidal Filter Paper**

by

**Renata Vyhnalkova**

A thesis submitted to McGill University in partial  
fulfillment of the requirements for the degree of

**Doctor of Philosophy**

Department of Chemistry  
McGill University  
Montreal, Quebec  
Canada

## Abstract

The main objective of the present thesis is to prepare bactericidal filter paper by employing hydrophobic biocides of very low water solubility. To achieve this goal, two different strategies were proposed. One involves the use of amphiphilic block copolymer micelles which serve as a carrier for loaded biocides, and are subsequently attached to the pulp fibres; the other utilizes biocide emulsions stabilized with polymeric materials. As a part of first strategy, the mechanisms of loading of biocide into and release from the block copolymer micelles of poly(styrene)-b-poly(acrylic acid) were elucidated. It was found that loading is a two step process; first, the micelle surface is saturated with biocide molecules. In the next step, the biocide penetrates as a front into the hydrophobic polystyrene core, while lowering the glass transition temperature of the polystyrene. The release of the biocide from the micelles was found to be a slower process than loading; the rate determining step of the release is the removal of the biocide molecules from the surface of the micelles, since the biocide molecules have to pass over an energy barrier to go into the aqueous solution. *E. coli* bacteria deactivation by biocide loaded micelles in solution was studied next. As a main conclusion, it was found that block copolymer micelles loaded with triclosan biocide are efficient in deactivating the bacteria in less than two minutes. Also, the mechanism of biocide uptake by the bacteria was elucidated, which involves transfer of biocide molecules during transient collisions between loaded micelles and bacteria. An antibacterial filter paper was prepared by modifying commercial filter papers or paper towels by changing the natural negative charge of the pulp fibres to positive by adsorption of cationic poly(acryl)amide, followed by attachment of negatively charged biocide loaded micelles to the pulp fibres. After passage through the modified filter paper, the bacteria were found to be no longer viable. Optimal parameters and conditions for bactericidal efficiency of the filter paper were determined. As a part of the second strategy, biocide emulsions stabilized by two different polymeric stabilizers were prepared, one of them being poly(ethylene imine), while the other consisted of micelles of poly(caprolactone)-b-poly(acrylic acid) block copolymer. These emulsions were tested for their efficiency in bacteria deactivation and both were found to be efficient. The deactivation mechanisms differ depending on the nature of the stabilizing agent. The key difference lies in the ionic charge of the stabilizing agents.

## Résumé

L'objectif principal de la présente thèse est de préparer un papier filtre bactéricide en employant des biocides hydrophobiques ayant une très faible solubilité dans l'eau. Pour atteindre ce but, deux différentes stratégies furent proposées. L'une implique l'utilisation de micelles de copolymère bloc amphiphiles qui servent au transport de biocides dopés, et sont subséquemment attachées aux fibres de pâte; l'autre utilise des émulsions biocides stabilisées avec des matériaux polymères. Comme partie de la première stratégie, les mécanismes de dopage du biocide ainsi que de la libération des micelles de copolymère bloc de poly(styrène)-b-poly(acide acrylique) furent élucidés. Il fut découvert que le dopage est un processus à deux étapes; premièrement, la surface de la micelle est saturée avec des molécules biocides. Dans l'étape qui suit, le biocide pénètre de front dans le cœur hydrophobique de polystyrène, diminuant la température de transition vitreuse du polystyrène. La libération du biocide des micelles fut déterminée comme étant un processus plus lent que celui du dopage; l'étape déterminante de la vitesse de libération est l'enlèvement des molécules biocides de la surface des micelles, étant donné que les molécules de biocide doivent passer au-dessus d'une barrière énergétique pour aller dans la solution aqueuse. La désactivation de bactéries *E. coli* par les micelles dopées de biocide en solution fut ensuite étudiée. Comme conclusion générale, il fut découvert que les micelles de copolymère bloc dopées avec le biocide triclosan sont efficaces pour désactiver les bactéries en moins de deux minutes. Aussi, le mécanisme de consommation du biocide par les bactéries fut élucidé, impliquant le transfert des molécules de biocide durant les collisions transitoires entre les micelles dopées et les bactéries. Un papier filtre antibactérien fut préparé en modifiant des papiers filtres commerciaux ou des papiers essuie-tout en changeant la charge négative naturelle des fibres de pâte pour une charge positive par adsorption de poly(acryl)amide cationique, suivi par l'attachement des micelles dopées de biocide chargées négativement aux fibres de pâte. Après leur passage à travers le papier filtre modifié, il fut déterminé que les bactéries n'étaient plus viables. Les paramètres et conditions optimales pour l'efficacité bactéricide du papier filtre furent déterminés. Comme partie de la deuxième stratégie, les émulsions biocides stabilisées par deux différents stabilisateurs polymériques furent préparées, un d'entre eux étant le poly(éthylèneimine), l'autre consistant en des micelles de copolymère bloc de poly(caprolactone)-b-poly(acide acrylique). Ces émulsions furent testées pour leur efficacité à la désactivation de bactéries et se sont avérées toutes deux efficaces. Les mécanismes de

désactivation différent dépendant de la nature de l'agent stabilisateur. La différence clé repose en la charge ionique des agents stabilisateurs.

## Foreword

In addition to a general introduction provided in Chapter 1, and a summary of the main conclusions given in Chapter 6, this dissertation includes four papers, each of which comprises one chapter. Slightly modified version of one paper was published in a scientific journal: three are to be submitted for publications:

Chapter 2: Journal of Physical Chemistry *B*, **2008**, 112, 8477.

Chapter 3: the manuscript is to be submitted to Journal of Applied Polymer Science

Chapter 4: the manuscript is to be submitted to Macromolecular Bioscience

Chapter 5: the manuscript is to be submitted to Journal of Colloids and Surfaces B, Biointerfaces

## Contribution of Authors

All the papers were co-authored by research directors Dr. Adi Eisenberg and Dr. Theo van de Ven. Ms. Gurpreet Manku helped with some bacteria experiments presented in Chapter 4. Ms. Gurpreet Manku was undergraduate student working under the direct supervision of the author. Other than the supervision, advice and direction of Dr. Adi Eisenberg and Dr. Theo van de Ven, and the aforementioned contribution to the Chapter 4, all the work presented in this dissertation was performed by the author.

## Acknowledgements

First and foremost, I would like to thank to my supervisors, Dr. Adi Eisenberg and Dr. Theo van de Ven for their guidance in my research over past 3.5 years, for their valuable advice, and for sharing their great knowledge and scientific enthusiasm with me. I also appreciate their patience and understanding, while I was trying to combine both, being a good student and a good mother. For this, and so much more, I want to thank you both, Dr. Eisenberg and Dr. van de Ven.

My heartfelt thanks especially go to my husband Zdeněk, who was always very understanding, helpful, encouraging, supportive, and optimistic during my studies. I am not sure, if I would be able to finish my degree without his endless support. His love, optimism, and care were a great motivation. I also want to thank to my parents Jitka and Vojtěch, my mother-in-law Vlasta, and my sisters, Andrea and Ivana. They have always been there for me, and I cannot thank them enough. Also I want to thank to my children Alex and Vanessa for their understanding that their mom had to travel sometimes and work long hours.

I also would like to thank to:

Alvaro Tejado, for his friendship and for his support, which kept me going. I want to thank him for all the help and all the laughter.

Annie Castonguay, for the translation of my abstract.

Dr. Tony Azzam and George Rizis, for their friendship, help, and advice, we always had a good time, and shared many scientific and life discussions. They were very helpful with TEM imaging and DLS.

Petr Fjurasek, for his friendship and his help with DSC.

Ms. Gurpreet Manku, for being such wonderful student to work with.

All members of Dr. Eisenberg's and Dr. van de Ven's groups, past and present: Leon, Jimmy, Jurek, Laura, Louis, Luca, Miro, Nur, Nura, Shawn, Zeinab, Zoreh. I have learned a lot from working with them. I also would like to thank them for all the help and all the laughter.

My friends Negin, Lojza, Gabriela, Jana, Robert, Monica, Dana, Ernest, Françoise; for all the unforgettable moments we shared. I am happy to be their friend.

All the members of Dr. Gray's group, especially to Tiffany and Teri.

Mrs. Jeannie Mui and Mrs. Line Mongeon, for their training and advice in electron microscopy.

Mrs. Colleen McNamie, who always "had ears for me" and was always very helpful.

Chantal Marotte, Sandra Aerssen, Fay Nurse, and other staff at the chemistry department. Their help is very much appreciated.

## Table of Contents

Abstract.....	ii
Résumé.....	iii
Foreword.....	v
Contribution of Authors.....	v
Acknowledgements.....	vi
Table of Contents.....	viii
List of Figures.....	xvii
List of Tables.....	xxii
List of Symbols.....	xxiv
<b>Chapter 1: Introduction.....</b>	<b>1</b>
<b>Introduction to the Thesis.....</b>	<b>1</b>
<b>1.1. Bactericidal Paper.....</b>	<b>3</b>
<i>1.1.1. Importance of Bactericidal Paper .....</i>	<i>4</i>
1.1.1.1. <u>Potential Uses</u> .....	5
1.1.1.2. <u>Related Commercial Products or Patented Ideas</u> .....	5
1.1.1.2.1. Bactericidal Paper Patents.....	5
1.1.1.2.2. Other Available Products.....	7
<i>1.1.2. Bactericidal Agents.....</i>	<i>7</i>
1.1.2.1. <u>TCMTB</u> .....	8
1.1.2.2. <u>Triclosan</u> .....	9
<i>1.1.3. Advantage of Bactericidal Paper.....</i>	<i>10</i>



<b>1.2. Polymers</b> .....	10
<i>1.2.1. Poly-meros (many parts)</i> .....	10
<i>1.2.2. Self Assembly of Block Copolymers in Solution</i> .....	14
1.2.2.1. <u>Self Assembly</u> .....	15
1.2.2.2. <u>Formation and Morphologies of Aggregates</u> .....	16
1.2.2.3. <u>Aggregation Numbers</u> .....	19
<i>1.2.3. Micelles</i> .....	20
1.2.3.1. <u>Micelles as Carriers in Drug Delivery</u> .....	21
1.2.3.2. <u>Micelle Loading</u> .....	23
1.2.3.2.1. Loading Capacity .....	24
1.2.3.2.1.1. <u>Compatibility between Solubilizate and the Core Forming Block</u> .....	24
1.2.3.2.1.2. <u>Partition Coefficient</u> .....	26
1.2.3.2.1.3. <u>Other Factors which Influence the Loading into Micelles</u> .....	27
1.2.3.2.2. Glass Transition Temperature .....	28
1.2.3.2.3. Mechanism of Loading – Case II Diffusion .....	29
1.2.3.3. <u>Release from Micelles</u> .....	31
<b>1.3. Emulsions</b> .....	34
<i>1.3.1. Stabilizers (Surfactants)</i> .....	36
<i>1.3.2. Block Copolymers as Stabilizers for Emulsions</i> .....	38
<i>1.3.3. Bactericidal Emulsions</i> .....	42
<b>1.4. Bacteria</b> .....	43
<i>1.4.1. The Bacteria Cell</i> .....	45
<i>1.4.2. The Cell Wall</i> .....	47
<i>1.4.3. Bacterial Reproduction</i> .....	48
<i>1.4.4. Pathogenic Bacteria</i> .....	49

<i>1.4.5. Mechanism of Bacteria Deactivation</i> .....	49
<b>1.5. Objectives of the Thesis</b> .....	51
<b>References</b> .....	53

<b>Chapter 2: Loading and Release Mechanisms of a Biocide in PS-b-PAA Block-copolymer Micelles</b> .....	62
<b>Abstract</b> .....	62
<b>2.1. Introduction</b> .....	63
<b>2.2. Experimental Section</b> .....	66
<i>2.2.1. Materials</i> .....	66
<i>2.2.2. Micelle Preparation</i> .....	67
<i>2.2.3. Characterization of the Micelles</i> .....	68
2.2.3.1. <u>Transmission Electron Microscopy</u> .....	68
2.2.3.2. <u>Dynamic Light Scattering</u> .....	69
<i>2.2.4. Micelle Loading</i> .....	69
2.2.4.1. <u>UV-vis Spectroscopy</u> .....	69
<i>2.2.5. Kinetics of Micelle Loading</i> .....	70
<i>2.2.6. Kinetics of Release of Biocide from Micelles</i> .....	70
<i>2.2.7. <math>T_g</math> of PS/Biocide Mixtures</i> .....	71
<i>2.2.8. Partition Coefficients</i> .....	71
<b>2.3. Results and discussion</b> .....	72
<i>2.3.1. Size of the Micelles and their Core and Corona</i> .....	72
<i>2.3.2. TCMTB Saturation Concentration</i> .....	73
<i>2.3.3. Maximum Adsorption Capacity of Biocide on the Surface of the Micelle Core</i> .....	73
<i>2.3.4. Kinetics of Micelle Loading</i> .....	74

2.3.4.1. <u>Depletion of Biocide Molecules from Solution</u> .....	74
2.3.4.2. <u>Initial Loading Kinetics</u> .....	76
2.3.4.3. <u>Biocide Transfer from Biocide Film to Micelles</u> .....	77
2.3.4.4. <u>T<sub>g</sub> for the Mixtures of Polystyrene and TCMTB Biocide</u> .....	80
2.3.4.5. <u>Non-Fickian Diffusion - Penetrating Front</u> .....	82
2.3.4.6. <u>Maximum Loading</u> .....	83
2.3.4.7. <u>Partition Coefficient of Biocide/Polymer and Biocide/Ethylbenzene</u> .....	85
2.3.5. <i>Kinetics of Biocide Release from Micelles</i> .....	86
2.3.6. <i>Mechanisms of Biocide Loading and Release</i> .....	88
2.3.6.1. <u>Mechanism of Biocide Transfer from Biocide Film to Micelles</u> .....	88
2.3.6.2. <u>Mechanism of Biocide Incorporation into the Micelles</u> .....	89
2.3.6.3. <u>Mechanism of Biocide Release from the Micelles</u> .....	90
<b>2.4. Conclusions</b> .....	91
<b>2.5. Reference List</b> .....	92
<b>Bridging Section between Chapters 2 and 3</b> .....	95
<b>Chapter 3: Bactericidal Block Copolymer Micelles</b> .....	97
<b>Abstract</b> .....	97
<b>3.1. Introduction</b> .....	97
<b>3.2. Experimental Section</b> .....	100
3.2.1. <i>Materials</i> .....	100
3.2.2. <i>Experimental Techniques and Procedures</i> .....	102
<b>3.3. Results and discussion</b> .....	103
3.3.1. <i>Size and Structure of the Micelles</i> .....	103

3.3.2. <i>Deactivation of Bacteria by TCMTB</i> .....	104
3.3.2.1. <u>Saturation Concentration of TCMTB in Water</u> .....	104
3.3.2.2. <u>Effect of Micelle Loading</u> .....	104
3.3.2.3. <u>Bacteria Exposure to Biocide Loaded Micelles/Re-growth in the Presence of Micelles</u>	105
3.3.2.4. <i>Cationic Poly(acrylamide)</i> .....	109
3.3.2.5. <u>Deactivation of E. coli by TCMTB loaded PS<sub>297</sub>-b-PVP<sub>30</sub> Micelles</u> .....	112
3.3.2.6. <u>Bacteriostatic and Bactericidal Properties of TCMTB Loaded Micelles</u> .....	113
3.3.3. <i>Deactivation of Bacteria by Triclosan (TCN)</i> .....	115
3.3.3.1. <u>Saturation Concentration of Triclosan</u> .....	116
3.3.3.2. <u>Bacteria Killing Time</u> .....	117
3.3.4. <i>Deposition of Micelles on E. coli Bacteria</i> .....	120
3.3.4.1. <u>Effect of Time of Fixation</u> .....	120
3.3.4.2. <u>Dead vs. Live Bacteria</u> .....	122
3.3.4.3. <u>Number of Micelles per Monolayer on Bacteria</u> .....	122
3.3.4.4. <u>Drying Effect</u> .....	124
3.3.5. <i>Proposed Mechanism of Bacteria Deactivation</i> .....	125
3.3.5.1. <u>Amount of Biocide in Bacteria</u> .....	125
3.3.5.2. <u>Mechanism of Biocide Transfer to Bacteria</u> .....	127
<b>3.4. Conclusions</b> .....	129
<b>3.5. Reference List</b> .....	131
<b>Bridging Section between Chapters 3 and 4</b> .....	133
<b>Chapter 4: Bactericidal Filter Paper</b> .....	134
<b>Abstract</b> .....	134

<b>4.1. Introduction</b>	134
<b>4.2. Experimental Section</b>	139
4.2.1. <i>Materials</i>	139
4.2.2. <i>Experimental Techniques</i>	142
4.2.3. <i>Micelle Preparation</i>	142
4.2.4. <i>Characterization of the Micelles</i>	142
4.2.5. <i>Micelle Loading</i>	143
4.2.6. <i>Preparation of the Bactericidal Filter Paper</i>	143
4.2.7. <i>Test for Antibacterial Paper Efficiency</i>	145
<b>4.3. Results and Discussion</b>	146
4.3.1. <i>Efficiency of Antibacterial Filter Paper</i>	146
4.3.2. <i>Effect of Pore Size of Filter Paper on Antibacterial Efficiency</i>	149
4.3.2.1. <u>Whatman Filter Papers</u>	149
4.3.2.2. <u>Commercial Paper Towel</u>	152
4.3.3. <i>Optimization of Bactericidal Efficiency of Filter Paper</i>	154
4.3.4. <i>Re-usability of Antibacterial Filter Paper</i>	157
4.3.5. <i>Bacteria Deactivation with the Paper Left in the Bacteria Suspension</i>	159
<b>4.4. Conclusions</b>	160
<b>4.5. Reference List</b>	163
<b>Bridging Section between Chapters 4 and 5</b>	164
<b>Chapter 5: Bactericidal Filter Paper</b>	165
<b>Abstract</b>	165
<b>5.1. Introduction</b>	166

<b>5.2. Experimental Section</b>	171
5.2.1. <i>Materials</i>	171
5.2.2. <i>Experimental Techniques</i>	173
5.2.3. <i>Micelle Preparation</i>	173
5.2.4. <i>Characterization of the Micelles</i>	174
5.2.5. <i>Emulsion Preparation</i>	174
5.2.6. <i>Bacteria Deactivation Using Emulsion</i>	175
5.2.7. <i>Kinetics of Emulsion Dissolution</i>	176
<b>5.3. Results and Discussion</b>	176
5.3.1. <i>Emulsions Properties</i>	176
5.3.1.1. <u>Stability of TCMTB Emulsions</u>	176
5.3.1.2. <u>Emulsions Stabilized by PEI</u>	177
5.3.1.3. <u>Emulsions Stabilized by PCL-b-PAA Micelles</u>	178
5.3.2. <i>Bacteria Deactivation by Emulsions</i>	180
5.3.2.1. <u>Bacteria Deactivation by PEI/TCMTB Emulsions</u>	181
5.3.2.2. <u>Bacteria Deactivation by PCL-b-PAA/TCMTB Emulsions</u>	184
5.3.2.3. <u>Comparison of PEI and PCL-b-PAA/TCMTB Emulsions in Bacteria Deactivation</u>	186
5.3.3. <i>Mechanisms of Bacteria Deactivation</i>	187
5.3.3.1. <u>Kinetics of Emulsion Dissolution</u>	187
5.3.3.1.1. PEI/TCMTB Emulsion	187
5.3.3.1.2. PCL-b-PAA/TCMTB Emulsion	189
5.3.3.1.3. <u>Comparison of Kinetic Results for PEI and PCL-b-PAA/TCMTB Emulsions</u>	191
5.3.3.2. <u>Deactivation Mechanisms</u>	192

5.3.3.2.1. Mechanism of Bacteria Deactivation by PEI/TCMTB Emulsions .....	192
5.3.3.2.2. Mechanism of Bacteria Deactivation by PCL-b-PAA/TCMTB Emulsions .....	194
5.3.3.2.3. Comparison of Mechanisms of Bacteria Deactivation by PEI/TCMTB and PCL-b-PAA /TCMTB emulsions .....	196
5.3.3.3. <u>Properties of Emulsion Droplets after Deactivation</u> .....	198
5.3.3.3.1. Residual Shells of PEI after Bacteria Deactivation .....	200
5.3.3.3.2. Residual Shells of PCL-b-PAA after Bacteria Deactivation .....	201
<b>5.4. Conclusions</b> .....	202
<b>5.5. Reference List</b> .....	205
 <b>Chapter 6: Conclusions, Contributions to Original Knowledge and Suggestions for Future Work</b> .....	207
<b>6.1. Conclusions and Contributions to Original Knowledge</b> .....	207
6.1.1. <i>Loading and Release Mechanisms of a Biocide in PS-b-PAA Block-copolymer Micelles</i>	208
6.1.2. <i>Bactericidal Block-copolymer Micelles</i> .....	210
6.1.3. <i>Bactericidal Filter Paper</i> .....	212
6.1.4. <i>Effect of Stabilizers on the Deactivation Efficiency of Bactericidal Emulsions</i> .....	215
<b>6.2. Suggestions for Future Work</b> .....	217
6.2.1. <i>Loading and Release Mechanisms of a Biocide in PS-b-PAA Block-copolymer Micelles</i>	18
6.2.2. <i>Bactericidal Block-copolymer Micelles</i> .....	218

<i>6.2.3. Bactericidal Filter Paper .....</i>	<i>219</i>
<i>6.2.4. Effect of Stabilizers on the Deactivation Efficiency of Bactericidal Emulsions .....</i>	<i>221</i>
<b>Appendix to Chapter 1 .....</b>	<b>223</b>
<b>Appendix to Chapter 3 .....</b>	<b>230</b>
<b>Appendix to Chapter 4 .....</b>	<b>240</b>
<b>Appendix to Chapter 5 .....</b>	<b>246</b>



## List of Figures

<b>Figure 1.1:</b> Schematic representation of types of copolymers: A – Statistical, B – Alternating, C – Graft, D – Block, E – Diblock .....	12
<b>Figure 1.2:</b> Schematic representation of crew-cut (A) and star like (B) block copolymer micelles .....	14
<b>Figure 1.3:</b> Schematic representation and TEM images of: A) spherical micelles, B) rod like micelles, C) vesicles, D) large compound micelles .....	17
<b>Figure 1.4:</b> Schematic representation of loaded micelles (from reference 53) .....	22
<b>Figure 1.5:</b> Schematic representation of A) bacterial inner structure, B) the cell wall of gram negative (LHS) and gram-positive (RHS) bacteria (image taken from reference 135) .....	45
<b>Figure 2.1:</b> Structure and properties of polymer and biocide used .....	67
<b>Figure 2.2:</b> TEM image of PS <sub>197</sub> -b-PAA <sub>47</sub> micelles with schematic representation of micellar structure .....	68
<b>Figure 2.3:</b> Kinetics of micelle loading (% intake of biocide vs time). Initially the uptake is linear with a loading rate constant $k = 2.0 \times 10^{-5}$ kg/s. The solid curve is a single exponential fit with a characteristic time of 18 min. Triangles are result of a separate experiment.....	76
<b>Figure 2.4:</b> Schematic representation of experimental setup for maximum biocide uptake by micelles ~ 35 wt % - Biocide molecules diffuse through the dialysis bag into the micelle solution and adsorb onto the micelles.....	80

**Figure 2.5:** Glass transition temperature  $T_g$  for the mixtures of Polystyrene and TCMTB biocide. The line is given by the equation shown in the inset, with  $T_{g1} = 373$  K and  $T_{g2} = 200$  K, respectively.....81

**Figure 2.6:** The L.H.S. of eq. 9, plotted vs.  $t - t_r$ . The slope equals  $v/R$ ,  $v$  being the velocity of the penetrating front. The inset shows the schematics of a penetrating front .....83

**Figure 2.7:** TEM images and loading efficiency of PS<sub>197</sub>-b-PAA<sub>47</sub> micelles, with micelle diameters measured by TEM and DLS .....84

**Figure 2.8:** Kinetics of biocide release from micelles (% of release vs time). The curves are given by Equation 10. The fitting parameter,  $\tau_{\text{release}}$ , for the two curves measured up to 30 hours, are 286 min (diamonds) and 278 min (squares) .....87

**Figure 2.9:** Schematic representation of TCMTB biocide uptake by PS<sub>197</sub>-b-PAA<sub>47</sub> micelles. A) Early stage uptake: Biocide molecules transfer from the film to the micelle during transient collisions, until a monolayer of biocide on the micelle surface is formed. B) Later stage uptake: Internalization of the biocide molecules into the micelles by case II diffusion (moving front) with the empty surface spots being replenished by biocide transfer from the film .....89

**Figure 2.10:** Schematic representation of biocide release. A) Early stage release from the micelles – Molecules are released from the surface of the PS core with a constant rate, determined by the energy barrier of escape; B) Later stage release - Biocide is not released from the micelles in the later stage because of increase in  $T_g$  during release .....90

**Figure 3.1:** Deactivation of *E. coli* by exposing bacteria for 2 hours to 30 wt % TCMTB loaded micelles of PS<sub>197</sub>-b-PAA<sub>47</sub>, followed by exchange of half amount of micelles for growth medium and subsequent 3 hours growth. For comparison the bacteria growth was also tested in water and in the presence of empty (non-loaded) micelles. Full circles: control bacteria sample in water, empty circles: bacteria in the presence of empty micelles, full triangles: bacteria in the presence of loaded micelles .....106

**Figure 3.2:** SEM images of *E. coli*: A) control sample, B and C) in the presence of non-loaded micelles of PS<sub>197</sub>-b-PAA<sub>47</sub>, D – F) in the presence of 30% TCMTB loaded micelles .....108

**Figure 3.3:** TEM images of microtomed cross sections of *E. coli* bacteria: A) control sample; B, C) in the presence of 30% TCMTB loaded micelles.....109

**Figure 3.4:** Effect of cationic poly(acrylamide) on *E. coli* bacteria deactivation and comparison with effect of non-loaded and TCMTB loaded PS<sub>197</sub>-b-PAA<sub>47</sub> micelles. Schematic representation of effect of c-PAM on bacteria: *E. coli* in the presence of A) empty micelles and c-PAM; B) empty micelles; C) c-PAM. *E. coli* flocculates in the presence of loaded micelles and c-PAM 111

**Figure 3.5:** Deactivation of *E. coli* bacteria by empty and TCMTB biocide loaded PS<sub>297</sub>-b-PVP<sub>30</sub> micelles .....113

**Figure 3.6:** Deactivation or killing of *E. coli* by TCMTB loaded micelles of PS<sub>197</sub>-b-PAA<sub>47</sub>. *E. coli* exposed for various times (0 to 90 min) in the presence of 30 wt % TCMTB loaded micelles of PS<sub>197</sub>-b-PAA<sub>47</sub>, followed by exchange of micelles for growth medium and subsequent 22 hour growth .....114

**Figure 3.7:** Killing time of *E. coli* by TCMTB loaded micelles of PS<sub>197</sub>-b-PAA<sub>47</sub> as a function of exposure times of bacteria to loaded micelles prior to re-growth .....115

**Figure 3.8:** Deactivation of *E. coli* by exposure of the bacteria to a saturated solution of TCN for 2 hours followed by incubation of the bacteria for various time periods .....117

**Figure 3.9:** Killing time of *E. coli* by TCN loaded micelles of PS<sub>275</sub>-b-PAA<sub>47</sub> as a function of exposure time to loaded micelles prior to bacteria re-growth .....119

**Figure 3.10:** SEM images of *E. coli* bacteria killed by micelles of PS<sub>275</sub>-b-PAA<sub>47</sub> loaded with TCN (images A and B); image C is bacteria in absence of TCN loaded micelles (control sample). (The image scale for image C is the same as in case of image B) .....119

**Figure 3.11:** SEM images for various fixation times of *E. coli* deactivation by TCMTB loaded PS<sub>197</sub>-b-PAA<sub>47</sub> micelles with glutaraldehyde: A, B) immediate fixation; C, D) fixation after two weeks .....121

**Figure 3.12:** SEM images of *E. coli*: Number of micelles per monolayer on bacteria .....123

**Figure 3.13:**SEM image of *E coli* in the presence of TCMTB loaded PS<sub>197</sub>-b-PAA<sub>47</sub> micelles125

**Figure 3.14:** Schematic representation of mechanism of bacteria deactivation .....128

**Figure 4.1:** Schematic representation of antibacterial filter paper. (Not to scale) .....138

**Figure 4.2:** Efficiency of the variously treated antibacterial filter paper on *E. coli* (ATCC11229 strain) solution passed through a grade 3 Whatman filter paper with a pore size of 6 µm. The experimental conditions were the following: concentration of both c-PAM and triclosan loaded micelles was 1 mg/g of paper each; the volume of 100 mL of bacteria solution of absorbance of 0.1, filtering time was between 30 to 60 minutes, depending on the treatment of the filter paper .....148

**Figure 4.3.** Efficiency of the variously treated filter papers on solution of *E. coli* (ATCC11229 strain) passing through Whatman filter papers of 90 mm diameter of various pore sizes. Symbols: square - grade 3 (pores size 6 µm), triangle –grade 2 (pore size 8 µm), circle – grade 1 (pore size 11 µm). The experimental conditions were the following: weight ratios of c-PAM and triclosan loaded micelles were 1 mg/g of paper each, the volume was 100 mL of bacteria solution of absorbance of 0.1, and the filtering time was between 30 to 60 minutes, depending on the treatment of the filter paper .....150

**Figure 4.4:** Efficiency of the modified paper towel on *E. coli* ATCC11229 strain. The experimental conditions were the following: weight ratios of c-PAM and triclosan loaded micelles was 1 mg/g of paper each, the volume was 100 mL of bacteria solution of absorbance of 0.1, and the filtering time was slower than one minute .....153

**Figure 5.1:** TEM (A, B) and SEM (C - E) images of 50/50 ratios of PEI/TCMTB emulsion ...178

<b>Figure 5.2:</b> TEM (A,B) and SEM (C) images of 50/50 ratios of PCL- <i>b</i> -PAA/TCMTB emulsion .....	180
<b>Figure 5.3:</b> Bacteria deactivation by PEI/TCMTB emulsions .....	183
<b>Figure 5.4:</b> Effect of supernatant of PEI/TCMTB emulsions on bacteria deactivation (control experiment). (SN) - emulsion supernatant, (EM) – emulsion .....	184
<b>Figure 5.5:</b> Bacteria deactivation by PCL- <i>b</i> -PAA /TCMTB emulsions .....	185
<b>Figure 5.6:</b> Kinetics of PEI/TCMTB emulsion dissolution for 66/33 and 50/50 % ratios of PEI and TCMTB in emulsion .....	186
<b>Figure 5.7:</b> Kinetics of PCL- <i>b</i> -PAA/TCMTB emulsion dissolution for 66/33 and 50/50 % ratios of PCL- <i>b</i> -PAA and TCMTB in emulsion .....	190
<b>Figure 5.8:</b> SEM images (A-D) of <i>E. coli</i> bacteria deactivated by PEI/TCMTB emulsion (0.136 g/L of PEI and TCMTB), (E, F) – <i>E. coli</i> control .....	194
<b>Figure 5.9:</b> SEM images of bacteria deactivated by PCL- <i>b</i> -PAA/TCMTB .....	195
<b>Figure 5.10:</b> Schematic representation of mechanisms of bacteria deactivation by PEI/TCMTB (A1 and A2) and PCL- <i>b</i> -PAA /TCMTB (B) emulsions .....	197
<b>Figure 5.11:</b> TEM (A – C) and SEM (D – F) images of PEI/TCMTB shells remaining after emulsion dissolution for 50/50 % ratios of PEI and TCMTB after 1400 minutes of dialysis (at the end of the kinetics of emulsion dissolution experiment) .....	200
<b>Figure 5.12:</b> TEM (A, B) and SEM (C – E) images of PCL- <i>b</i> -PAA /TCMTB shells remaining after emulsion dissolution for 50/50 % ratios of PCL- <i>b</i> -PAA and TCMTB after 1400 minutes of dialysis (at the end of the kinetics of emulsion dissolution experiment) .....	202

## List of Tables

<b>Table 1.1:</b> Structure and properties of TCMTB and Triclosan biocides .....	9
--	---

<b>Table 2.1:</b> Biocide concentrations in the ethylbenzene phase and the water phase as determined experimentally, and the resulting partition coefficients .....	85
---	----

<b>Table 3.1:</b> Structure and properties of the polymers .....	101
--	-----

<b>Table 3.2:</b> Structure and properties of the biocides .....	102
--	-----

<b>Table 3.3:</b> Amount of TCMTB biocide in bacteria. Bacteria <i>E. coli</i> were starved in the presence of TCMTB loaded for various times (5 to 195 min). The solution was centrifuged and the concentration of TCMTB in the supernatant was compared to the TCMTB concentration in the original samples .....	126
--	-----

<b>Table 4.1:</b> Structure and properties of polystyrene- <i>block</i> -poly(acrylic acid) polymer and of cationic polyacrylamide .....	140
--	-----

<b>Table 4.2:</b> Structure and properties of triclosan biocide .....	141
---	-----

<b>Table 4.3:</b> The antibacterial efficiency of the filter paper as influenced by changes in various parameters: weight ratio of biocide loaded micelles deposited onto the filter paper, weight ratio of c-PAM deposited onto the filter paper, concentration of bacteria solution passed through the filter paper and volume of bacteria solution passed through the filter paper. Boxes highlighted in grey refer to conditions inefficient in bacteria deactivation since the value of relative absorbance is higher than 1.03 .....	156
--	-----

<b>Table 5.1:</b> Structure and properties of thiocyanomethylthiobenzothiazole biocide. <sup>16,17</sup> .....	171
--	-----

**Table 5.2:** Structure and properties (molecular weight and polydispersity indices) of stabilizing agents of polyethyleneimine and poly(caprolactone)<sub>33</sub>-*b*-poly(acrylic)<sub>33</sub> acid polymer .....173

## List of Symbols

A	maximum uptake of biocide per unit volume
$a_1$	radius of bacterium
$a_2$	radius of micelle
ATRP	atom transfer radical polymerization
B	concentration of the biocide in the micelle
$B_0$	initial biocide concentration (at the start of release)
$B_f$	final biocide concentration (at the end of release)
C	total concentration
cmc	critical micelle concentration
c-PAM	cationic poly(acryl amid)
cwc	critical water concentration
$c_{EB}, c_{water}$	concentration of biocide in ethylbenzene or in water
$\delta$	solubility parameter
DHT	dihydrotestosterone
DLS	dynamic light scattering
Dox	doxorubicin
DSC	differential scanning calorimetry
EB	ethylbenzene
<i>E. coli</i>	<i>Escherichia coli</i> bacteria
FDA	Food and Drug Administration
HPLC	High Performance Liquid Chromatography
ICP	Inductively Coupled Plasma
k	Boltzman constant = $1.38 \times 10^{-23} \text{ m}^2 \text{ kg s}^{-2} \text{ K}^{-1}$



$K_{\text{EB/water}}$	ethylbenzene-water partition coefficient
$\chi$	Flory-Huggins interaction parameter
L.H.S.	left hand side
$\text{LD}_{50}$	lethal dose to kill half the members of a tested population
milli-Q water	water that has been purified and deionized to a high degree
$M_n$	number average molar mass
$\eta$	viscosity of water ( $10^{-3}$ Pas)
$n_2$	number of micelles per unit volume
$N_{\text{agg}}$	aggregation number
O/W	oil in water
O/W/O	oil in water in oil
PAA	poly(acrylic acid)
PCL	poly(caprolactone)
PCL-b-PAA	poly(caprolactone)- <i>block</i> -poly(acrylic acid) block copolymer
PEO	poly(ethylene oxide)
PEI	poly(ethylene imine)
PLA	poly(ethylene oxide)-poly(lactide)
PMMA	poly(methyl methacrylate)
PPO	poly(propylene oxide)
PS	polystyrene
PS-b-PAA	poly(styrene)- <i>block</i> -poly(acrylic acid) block copolymer
PS-b-P4VP	poly(styrene)- <i>block</i> -poly(vinyl pyridine)
Py	pyrene
$r$	location of the moving front at time $t$
ROP	ring opening polymerization

SEM	scanning electron microscopy
SOC	N-Succinyl-N'-octyl chitosan
t	time
T	absolute temperature (K)
T <sub>g</sub>	glass transition temperature (°C)
T <sub>m</sub>	melting temperature(point) (°C)
τ <sub>release</sub>	average residence time (related to biocide release)
<i>t</i> BA	<i>tert</i> -butyl acrylate
TCMTB	thiocyanomethylbenzothiazole biocide
TCN	triclosan biocide
TEM	transmission electron microscopy
THF	tetrahydrofuran
v	velocity (m/s)
V <sub>s</sub>	molecular volume of solubilizate
W/O	water in oil
W/O/W	water in oil in water
W <sub>x</sub>	weight fraction of material x

*To my husband Zdeněk  
and to my children Alex and Vanessa  
with all my love*

# Chapter 1: Introduction

---

## **Introduction to the Thesis:**

Polymeric materials have become ubiquitous in everyday life. They are encountered in a wide spectrum of applications, ranging on one hand from plastics and paints all the way to biomedical applications. One example of such an application involves nano-sized drug delivery systems, in which nano- or micro- spheres or even block copolymer micelles are used as carriers for hydrophobic materials of biomedical interest.

The present thesis deals with a practical application of polymers in an area which is relatively unexplored, i.e. their application as carriers for hydrophobic bactericidal materials. This project study is part of a collaborative research project within a network on bioactive paper (Sentinel), which has as its objective to capture, detect and deactivate pathogens, using paper as a substrate. Part of the strategy is to incorporate biocides into paper to deactivate bacteria. Our methods are based on loading a hydrophobic antibacterial agent into amphiphilic block copolymer micelles. Another way involves emulsions of biocides, stabilized by polymeric materials, to increase the overall biocide concentration in the solution. The work, therefore, focuses on a wide range of topics. On one hand it impinges on block copolymer self assembly, preparation of the polymeric nanostructures or polymer protected emulsions, loading into and release of biocide from

micelles, partitioning of the biocide between water and the hydrophobic core material, the glass transition temperature of the loaded carrier and attachment of loaded micelles onto the pulp fibers. On the other hand it deals with bacteria deactivation using biocide loaded block copolymer micelles or emulsions stabilized by polymeric material, evaluation of the bactericidal efficiency of the treated paper when used as a filter, and a number of related topics. Because of the wide range of topics, the subjects discussed in the introduction are, necessarily, also very broad.

The introduction will be presented in four major parts. First part will deal with bactericidal paper and currently available hydrophobic bactericidal agents, and other topics related to bactericidal materials. The next subject, treated in greater depth, describes block copolymers and their self assembly to yield micellar aggregates. The third topic will focus on emulsions and their stabilization using polymeric materials. The fourth and final topic will describe the bacteria and methods of bacteria deactivation.

This thesis consists of six main Chapters. Chapter 1 is divided into four sections, with a view to providing introductory information relevant to the work presented in this thesis, such as bactericidal paper, polymers, emulsions and bacteria.

Chapter 2 mainly focuses on description of mechanisms of loading of the biocide into PS-b-PAA block copolymer micelles and its release from the micelles.

Chapter 3 is devoted to the behavior of bactericidal block-copolymer micelles in solution and the efficiency of bacteria deactivation.

Chapter 4 deals with preparation, efficiency and optimization of the parameters in bactericidal paper.

Effects of stabilizers on the deactivation efficiency of bactericidal emulsions are discussed in Chapter 5.

The final conclusions, contributions to the original knowledge and suggestions for future work are presented in Chapter 6.

### **1.1. Bactericidal Paper**

The main aim of the present study was to prepare antibacterial paper. Since some of the bactericidal materials, usually the most potent ones, are hydrophobic, and since their saturated solutions are in water not concentrated enough to kill bacteria, there was a need of finding a strategy to increase the concentration of such materials in an aqueous environment. It is well known that block copolymer micelles and dispersions or emulsions stabilized by block copolymers are widely used in many applications, for example in drug delivery.<sup>1-6</sup> In the work described in this thesis, block copolymer micelles and homopolymers were employed as carriers for hydrophobic antibacterial materials to increase locally the total concentration of these materials in aqueous solutions while maintaining efficient material transfer to the bacteria and thus assuring their bactericidal effectiveness. The block copolymer micelles in such application do not serve only as a carrier for the bactericidal hydrophobic materials, but are also effective as a reservoir to be used when needed. Based on a survey of the literature, it appears that the use of block copolymer micelles or homopolymer stabilized emulsions is innovative in this context, since it has never been used in the preparation of antibacterial paper.

Bactericidal paper has many potential applications, for example as an antibacterial filter paper, in food packaging or to obtain water free of bacteria in remote areas. The use of paper as an antibacterial system has many advantages. Among others, paper is a biodegradable material of

low cost. In addition, block copolymer micelles or emulsions stabilized by block copolymers or by homopolymers serve as a carrier and storage medium for the hydrophobic biocides of low water solubility and toxicity and, therefore, their total concentration in solution is highly increased. If the block copolymer micelles are attached to the pulp fibers, no micelles are found in the solution after filtration, which is now free of viable bacteria. An additional advantage of such a system, aside of killing of the bacteria, is the trapping of bigger nonbacterial particulates on the filter paper. Also, the expected long shelf life and ease of transport of such filter paper to remote areas is advantageous.

#### *1.1.1. Importance of Bactericidal Paper*

Public health implications make the killing of bacteria in water a very important topic. It becomes especially relevant in third world countries, where a lack of safe drinking water is common. Even in developed countries, such as Canada, drinking water might not be easily accessible, for example while camping in remote areas. In the case of a major catastrophe, for example a flood, the quality of the drinking water can be compromised even in metropolitan areas.

To prepare bactericidal filter paper for water purification, the strategy involves the use of hydrophobic biocides, which have very low water solubility. They are incorporated into the hydrophobic cores of amphiphilic block copolymer micelles or are used as emulsions stabilized by block copolymer micelles or by homopolymers. These micelles or emulsions can be attached to the filter paper; bacteria from the solution are killed by the biocide released while the water with bacteria is passing through the filter paper. Due to extremely low solubility of the antibacterial agent in water, the water containing the killed bacteria remains safe to drink.

#### 1.1.1.1. Potential Uses

A potential application of such antibacterial filter paper would be in small scale disposable filters for drinking water in remote areas, with additional benefits of filtration such as removal of small particulates. Another potential application could involve filters for sludges in the pulp and paper industry. Many other applications can be anticipated in situations where bacteria free water is important. An antibacterial paper can be used in other potential applications, for example in food wrapping.

#### 1.1.1.2. Related Commercial Products or Patented Ideas

Products which produce potable water free of bacteria have already been developed, and are employed in commercially available systems such as antimicrobial paper,<sup>6-11</sup> drinking straws,<sup>12-14</sup> or disinfecting pills.<sup>15</sup> These systems will be discussed in next sections.

##### 1.1.1.2.1. Bactericidal Paper Patents

An antimicrobial paper made from silver ion-containing polyacrylic fibers and polyester fibers was studied by Akihiro *et al.*<sup>7</sup> for its antimicrobial properties and its bactericidal activity. This paper exhibited a broad and high antibacterial activity against 13 bacteria. In the presence of sodium chloride or peptone, the bactericidal activity was almost nullified at 1.5% or 0.05%, respectively. Hydroxyl radicals and C-centered radicals were identified on the basis of the electron spin resonance spectra, and the bactericidal activity was inhibited by radical scavengers such as superoxide dismutase or potassium iodide. In addition, even when the antibacterial paper was removed from the cell suspension, the bactericidal effect was still maintained. The produced radical was proved to be a bactericidal chemical species, and moreover, the living radical to which the OH group was converted within the bacterial cells was found to be the bactericidal



factor. It was suggested that bacterial cells pull the silver ions out from the paper. The antibacterial paper was found to have a high antimicrobial activity due to the effectiveness of the OH group and the bacteria cells absorbing the silver ions and also due to the oxidizing properties of silver.<sup>7</sup>

Sacura et al.<sup>8</sup> prepared an enzyme containing filter paper which kills airborne bacteria caught on the its surface. The use of such paper results in protection against secondary contamination from bacteria in air filtration systems; dust tends to accumulate at one third depth of the paper thickness along the air flow direction. In the absence of protective measures, bacteria caught with the dust multiply on the surface portion of the filter papers and go through the filter.<sup>8</sup>

An antimicrobial paper was prepared by Intilli;<sup>9</sup> in his application, an antimicrobial additive is incorporated into the binding agent of a heavy-duty, kraft-type paper of substantial density, air impermeability, and improved printability. The antimicrobial additive migrates from within the binding agent onto the paper fibres and inhibits the growth of microorganisms.<sup>9</sup>

An antibiotic paper was patented previously.<sup>10</sup> The author claims that cellulose fibres possess strong antibiotic properties (including antiviral properties) when they have a uniform content of a small amount of a 2-(C<sub>8</sub> -C<sub>18</sub> substantially straight chain alkyl) *pseudourea*. The fibres remain antimicrobial when, in addition, they contain a normal water-soluble thermosetting wet strength resin in the thermoset state.<sup>10</sup>

An antibacterial filter paper based on Ag containing glass fibres of a size smaller than 1  $\mu\text{m}$  diameter was previously described in a Japanese patent.<sup>11</sup> Another patent<sup>12</sup> dealing with anti-microbial filters includes a silicone-based filter membrane. This anti-microbial filter device filters out microorganisms in a fluidic system.<sup>12</sup>

To our knowledge, a bactericidal paper based on block copolymer micelles as carriers containing hydrophobic biocides or based on biocide emulsions coated with block copolymer micelles or homopolymer has not been described yet and is not available commercially. Thus, the filter paper systems described in this thesis appear to be novel.

#### 1.1.1.2.2. Other Available Products

LifeStraw is one example of straws used to drink water directly from a water source.<sup>13</sup> This straw-like device is manufactured by the Vestergaard Frandsen Group in Denmark and is based on a combination of mesh filters, iodine-impregnated beads and active carbon to remove particulate matter and bacteria. Another example of a drinking straw is Survival Straw,<sup>14</sup> produced by Alloy Safe – USA, which is based on alloy media. Yet another example of a drinking straw is Pioneer,<sup>15</sup> manufactured by Pristine - Canada, which does not remove pathogens of a size smaller than 3  $\mu\text{m}$ .

Disinfecting pills represent another method of bacteria deactivation in water. Commercially available disinfecting pills are manufactured by Camping Survival<sup>16</sup> and usually contain chlorine, chlorine dioxide, iodine or colloidal silver.

However, clearly, none of these commercially available products have the simplicity of passing the water through antibacterial filter paper to achieve potability, while simultaneously removing particulates.

#### *1.1.2. Bacterial Agents*

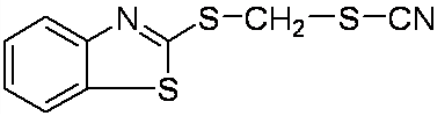
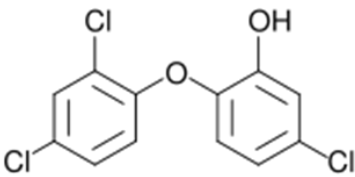
Many desirable biocides are hydrophobic in nature. Since the solubility of these antibacterial materials in water is too low to be efficient in killing the bacteria, delivering such biocides to bacteria in a dry or aqueous environment is difficult. Thus, it would be advantageous to find

methods of delivering biocides to bacteria while keeping the concentration in water very low, and yet to have a highly efficient concentration of the biocide in a reservoir in water. Within this range of parameters or prospective applications, micellar delivery systems or biocide emulsions stabilized by block copolymers or homopolymers are ideal, because they allow us to use a very poorly soluble biocide, which, therefore, does not contaminate the aqueous solution, while the total concentration of biocide in the solution is high, since it is stored in micelles or emulsions.

From among the many available biocides, such are chlorine, chlorine dioxide, amines, copper salts, organo-sulphur compounds, quaternary ammonium salts, and chlorinated phenolics,<sup>22</sup> two examples of hydrophobic antibacterial materials were chosen to be explored in the present study; i.e. thiocyanomethylbenzothiazole (TCMTB), which is already used in the pulp and paper industry, and triclosan, a very potent antibacterial material used in many industries. Detailed information about these two biocides is given in the next two sections.

#### 1.1.2.1. TCMTB

TCMTB is a hydrophobic bactericidal material of low water solubility (12.7 mg/L), of low toxicity and of low melting point (34 °C). Its structure and properties are given in Table 1.1, and, in more detail, in Chapters 2, 3 and 5. It is commercially used in many industries such as paper, wood, leather, agricultural and marine as an antibacterial and antifungal material. TCMTB is an organo-sulphur compound. Such compounds act as biocides by inhibiting bacteria growth.<sup>22</sup> The energy is transferred in bacterial cells when iron reacts from  $\text{Fe}^{3+}$  to  $\text{Fe}^{2+}$ . Organo-sulphur compounds remove the  $\text{Fe}^{3+}$  by complexation as an iron salt. The transfer of energy through the bacteria is then stopped and immediate cell death follows.

<b>Molecular structure</b>		
<b>Biocide</b>	<b>Thiocyanomethylthiobenzothiazole (TCMTB)</b>	<b>Triclosan (TCN)</b>
<b>M<sub>w</sub> (g/mol)</b>	238	289
<b>Water solubility (mg/L)</b>	12.7	11.0
<b>Melting point (°C)</b>	34	55 - 57
<b>Oral LD<sub>50</sub> (g/kg)</b>	0.75 (on rats) <sup>21</sup>	5 (on rats) <sup>19</sup>

**Table 1.1:** Structure and properties of TCMTB and Triclosan biocides.

#### 1.1.2.2. Triclosan

Triclosan, is a potent wide spectrum antibacterial and antifungal agent commercially used in soaps, deodorants, toothpastes, shaving creams, mouth washes, cleaning supplies etc. Triclosan is a chlorinated aromatic compound which has functional groups representative of both esters and phenols. Phenols often show anti-bacterial properties. The mechanism of action of triclosan on the *E. coli* bacteria is known to be the blocking of lipid synthesis in the bacteria.<sup>18</sup> The chlorinated phenolics first adsorb to the cell wall of the microorganisms by interaction involving hydrogen bonds. After adsorption to the cell wall, they diffuse into the cell where they go into suspension and precipitate proteins. Due to this mechanism the growth of the microorganisms is inhibited.<sup>22</sup> The molecular structure, together with other properties of triclosan, including water solubility and oral LD<sub>50</sub>, are given in Table 1.1 and discussed in more detail in Chapters 3 and 4.

It is noteworthy that, in spite of its potency, the oral LD<sub>50</sub> value for triclosan on rats is 5 g/kg of animal,<sup>19</sup> higher than that for NaCl (3 g/kg).<sup>20</sup>

### 1.1.3. Advantages of Bactericidal Paper

As briefly highlighted above, bactericidal paper has many advantages. Among others, is the low cost of the paper as a substrate as well as its biodegradability. In addition, the advantage of “packing” the bactericidal agent in a micelle and emulsion is that it combines the low toxicity of a saturated aqueous solution with the high storage capacity of an organic medium. In the absence of such a water compatible hydrophobic storage system, the use of the hydrophobic biocides in an aqueous environment would not be feasible. It should be recalled that, because of the low solubility, the toxicity of saturated aqueous solutions of the biocides used here is very low, and no health hazard to humans is involved. If, in case of antibacterial filter paper, the biocide loaded micelles are attached to the pulp fibers, no block copolymer micelles should be contained in the solution after filtration independent of whether the deactivated bacteria have been filtered out or not. Also, an additional advantage of such a filter paper that it traps the bigger particulates, such as sand or particles of a few mm, on the filter paper, while the killing of the bacteria. Still another advantage of the use of micelles contained in antibacterial paper lies in its expected long shelf life. Finally, the ease of transport of such filter paper to remote areas should be mentioned.

## 1.2. Polymers

### 1.2.1. Poly-Meros (Many-Parts)

The term *Makromolecül* was first introduced by Staudinger in 1924 to describe high molecular weight molecules - *polymers*. Today, eighty six years later, everybody is familiar with these

“substances that are all pervasive in our everyday lives, that indeed we would have difficulty in avoiding that may be handled, used, ignored, commented on, and normally taken for granted. Some of these substances are new and are recent products resulting from the ingenuity of the chemists, some are naturally occurring and have been used by man for several thousand years, some form parts of our bodies.”<sup>23</sup>

A *polymer* is defined as a naturally occurring or synthetic large molecule (*macromolecule*), constructed from many (poly = many) relatively simple repeating units, smaller building blocks called *monomers* (meros = parts) before polymerization, that become covalently bonded. Natural polymers include proteins, starch, DNA and others, while polystyrene, poly (acrylic acid), and polycaprolactone are examples of synthetic polymers.

When a macromolecule is built only from one type of monomer, the product is called a *homopolymer*, normally referred to simply as a polymer. If the chains are composed of two or more types of monomer units, the material is known as *copolymer*.<sup>23</sup>

Depending on the arrangement of the monomers in the chain, copolymers prepared from bifunctional monomers can be subdivided further into four main categories: a *statistical copolymer* (distribution of the two monomers in the chain is statistical), an *alternating copolymer* (units are alternating), a *graft copolymers* (blocks of one monomer type are grafted on to a backbone of the other as branches), and *block copolymer* (composed of a substantial sequence of each repeat unit). A *diblock copolymer* is a type of block copolymer composed of two sequences of different repeat units. Figure 1.1. shows a schematic representation of these four types of copolymers, including a diblock copolymer.

*Copolymer block length* is the term which describes the *length* of each block, i. e. the number of repeat units of each species in the diblock. For example PS<sub>197</sub>-b-PAA<sub>47</sub> contains 197 styrene units and 47 units of acrylic acid.

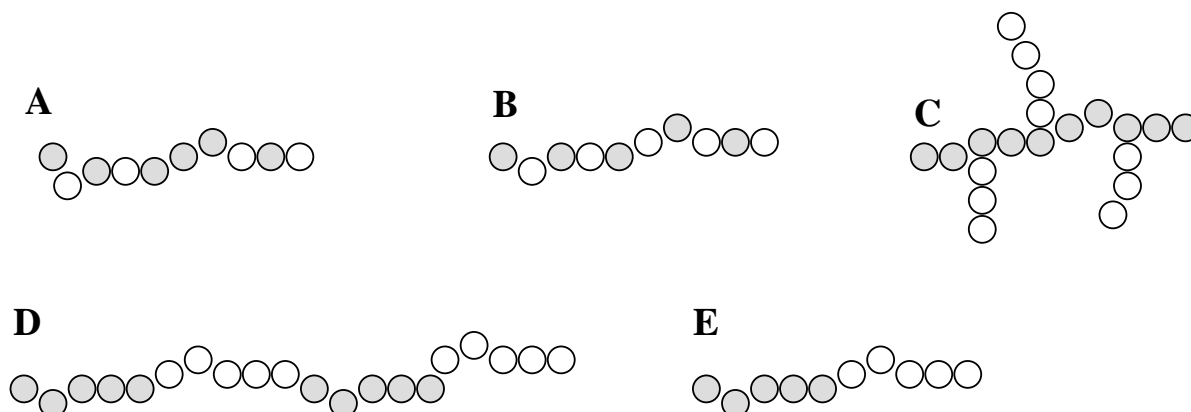


**Figure 1.1:** Schematic representation of types of copolymers: A – Statistical, B – Alternating, C – Graft, D – Block, E - Diblock

The process through which small molecules are covalently bonded to form large macromolecules is called *polymerization*.<sup>24</sup> Two types of polymerization are distinguished, based on differences in the mechanisms of the process: *condensation* and *addition*.

Condensation, also known as *step-growth* polymerization, is the process of forming polymers through a series of chemically identical steps (one step at the time), high molecular weight materials result in large yield from a large number of steps. Step-growth polymerization can be schematically represented by one of the individual reaction steps  $\sim A + B \sim \rightarrow \sim ab \sim$ . A covalent bond is formed between two functional groups, A and B, of two different monomers in each step. Dimers grow into trimers, tetramers etc. as the reaction progresses. The growth of the chain continues until the supply of monomer is exhausted.<sup>23-26</sup>

Addition, a second type of polymerization, also called *chain-growth* polymerization, occurs by introducing an active growth center into a monomer, followed by the addition of monomers to that center by a chain type kinetic mechanism. The active center is ultimately killed off by a termination step. The average *degree of polymerization*, (usually equal to the number of monomers that react as a result of a single initiation step) that characterizes the system, depends on the frequency of addition steps relative to the termination steps. Thus high molecular weight polymers are achieved almost immediately.<sup>23</sup> Chain-growth polymerization requires three distinct kinetic steps in the chain growth mechanism: (1) *Initiation*, the reaction, where an active center  $I^*$  is formed by the decomposition of an initiator molecule  $I$ :  $I \rightarrow I^*$ . (2) *Propagation*, the reaction whereby the initiator fragment reacts with a monomer  $M$  to begin the conversion to polymer; the active center is retained in the adduct. Monomers continue to add in some way until molecules with degree of polymerization  $n$  are formed:  $I^* + M \rightarrow IM^* \rightarrow IMM^* \rightarrow \rightarrow \rightarrow \rightarrow IM_n^*$ . (3) *Termination*, the reaction generally involving two polymers containing active centers, whereby the growth centers are deactivated, resulting in dead polymer:  $M_n^* + M_m^* \rightarrow M_{n+m}$  dead polymer.<sup>(25)</sup>

Chain-growth polymerization can be further classified according to the nature of the growth-propagating center as a *free radical polymerization* or *ionic (cationic or anionic) polymerization*. Free radical polymerization is a process whereby the propagating center possesses one unpaired electron. The process in which the positively or negatively charged group is present at the end of the propagating chain, is referred to as ionic polymerization.<sup>24</sup> *Atom transfer radical polymerization* (ATRP), is one type of free radical polymerization in which the active center has a very long life time. It should be noted that the ATRP method was used to synthesize the amphiphilic block copolymer of PS<sub>197</sub>-b-PAA<sub>47</sub> (Chapters 2 – 4).<sup>27</sup> Amphiphilic block copolymer



of poly(caprolactone)<sub>33</sub>-*b*-poly(acrylic)<sub>33</sub> acid (PCL-*b*-PAA) was prepared by ring opening polymerization (ROP is a form of addition polymerization) of  $\epsilon$ -caprolactone ( $\epsilon$ -CL), followed by ATRP of *tert*-butyl acrylate (*t*BA) (Chapter 5).<sup>28</sup>

### 1.2.2. Self Assembly of Block Copolymers in Solution

*Amphiphilic* is a term commonly used to describe molecules that possess both hydrophilic (water compatible) and hydrophobic (water incompatible) moieties.<sup>30</sup> Amphiphilic block copolymers are macromolecules consisting of covalently bonded blocks or segments of opposite water-compatibility. The amphiphilic nature of these copolymers containing incompatible parts gives rise to their unique properties in selective solvents, at surfaces and in the bulk, due to microphase separated morphologies. Their characteristic self-organization in the presence of selective media (solvent or surface) often results in the formation of aggregates such as *micelles*, and other colloidal size structures.<sup>30</sup> Block copolymer micelles consist of a compact core of the insoluble chains, surrounded by a corona composed of the soluble chains. Based on the relative length of each block, two types of micelles can be distinguished: *crew-cut* and *star like*. Crew-

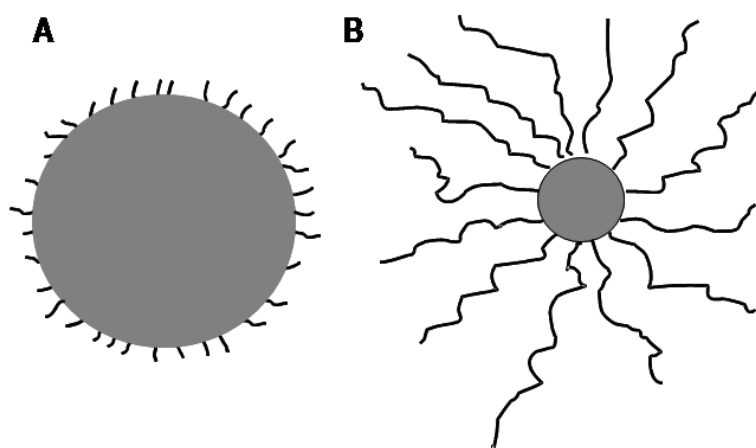


**Figure 1.2:** Schematic representation of crew-cut (A) and star like (B) block copolymer micelles.

cut micelles have large cores and short coronal “hair”, and are formed from block copolymer consisting of relatively longer insoluble block than the soluble one. Star like micelles, on the other hand, contain longer soluble corona-forming block, thus, the coronal “hair” is long. Figure 1.2 shows a schematic representation of crew-cut (A) and star like (B) block copolymer micelles.

#### 1.2.2.1. Self Assembly

The *self assembly* (formation) of block copolymer micelles requires the presence of two opposite forces: an *attractive force* between the core-forming chains, which brings about their aggregation, and a *repulsive force* between corona chains, which prevents the continual growth of the micelles into one macroscopic phase. In aqueous media, the aggregation arises mainly from the “hydrophobic effect” and its driving force is entropic in nature. The hydrophobic effect is described by the increase in entropy that accompanies the destruction of the well-structured water molecules organized around the hydrophobic chain, as this chain is removed from the aqueous solution, into the micelle core.<sup>31,32</sup> In selective organic solvents, however, the formation of block copolymer micelles is exothermic and driven mainly by enthalpy.<sup>32</sup> As to the repulsive force, it arises among the hydrophilic chains due to electrostatic interactions, in the case of ionic block copolymers, or because of steric repulsive forces (either entropic or due to preference for hydration, rather than association), in the case of non-ionic blocks.<sup>31</sup>

Crew-cut micelles normally cannot be prepared by direct dissolution of the block copolymer in a solvent selective for the long block. Instead, the diblock copolymers are first dissolved in a solvent good for both blocks, and then a precipitant for the solvophobic (usually long) block is added, resulting in the aggregation of these long blocks. The underlying principle of self-assembly is that two fundamentally different sub-units of the amphiphile (hydrophobic and

hydrophilic blocks) are driven to phase separate like oil and water, with the limiting condition that they are covalently attached to each other. Macromolecules are therefore thermodynamically driven to self-assemble in order to minimize the contact between immiscible components (the solvent and the insoluble block).<sup>34</sup>

An important parameter in characterizing the process of micellization is the *critical micelle concentration, cmc*. The cmc is defined as the threshold polymer concentration for micellization. At concentrations lower than the cmc, the copolymer exists in solution as free chains. Above the cmc, micelles are present, and for monodisperse systems<sup>29</sup>, the concentration of free chains remains constant upon further increase in the copolymer concentrations. The cmc for a given copolymer depends on solution properties such as temperature and solvent nature. However, in a given solvent and at a constant temperature, the cmc is a function of copolymer properties such as relative block length, total molecular weight and architecture.<sup>31</sup>

At equilibrium, the micelles exchange chains with one another (via the free chains), but this exchange in block copolymer systems is generally slow, due to a number of factors, including the high molecular weight, the low cmc and the possible entanglement and low mobility of the chains in the core.<sup>31</sup> Depending on system details, e.g. the glass transition temperature of the core, the aggregate may even be dynamically frozen.

#### 1.2.2.2. Formation and Morphologies of Aggregates

The existence of multiple morphologies in selective solvents is one of the interesting phenomena seen in the aggregate systems made from amphiphilic block copolymers. The first report on the formation of various morphologies in solutions of amphiphilic block copolymers appeared in 1995.<sup>27</sup> Since then, many studies dealt with the polymorphism of block copolymers

in solution, using various copolymers, in different solvents and under various solution conditions.<sup>27,34,37-49</sup> In addition to well known spherical micelles, other morphologies have also been observed, including, for example, rod like micelles, vesicles, large compound micelles (Figure 1.3) etc.

There are two main methods to prepare block copolymer micelles, the *direct dissolution* method and the *solvent modification* method. The choice of method depends on the solubility of the block copolymer in water. The direct dissolution method can be employed if the copolymer is marginally soluble in water, otherwise, the solvent modification method is used in case of limited solubility of hydrophobic segment of the copolymer in water.<sup>50</sup>

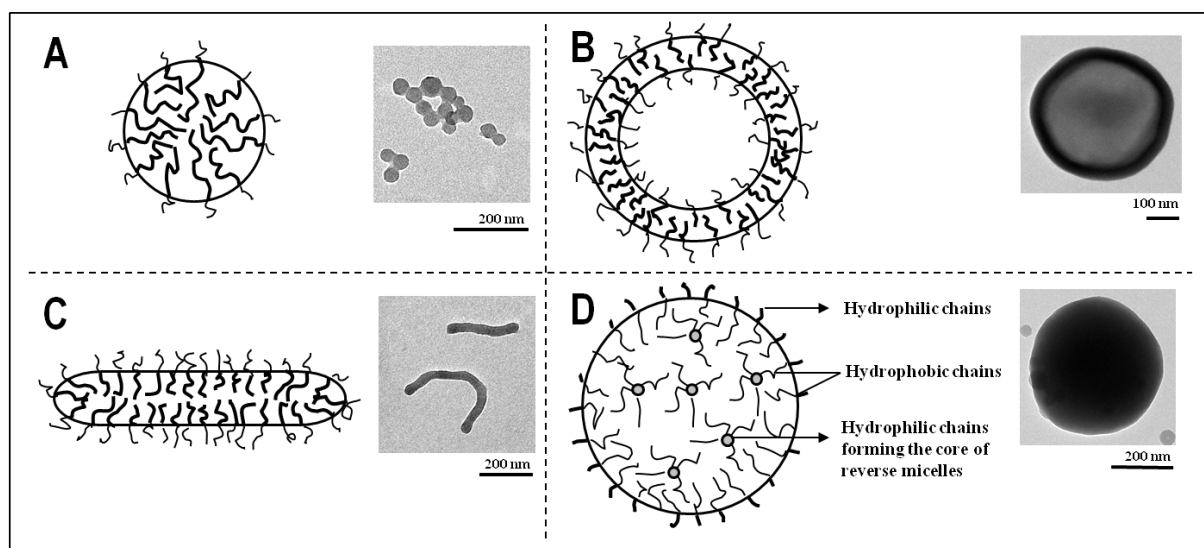


**Figure 1.3:** Schematic representation and TEM images of: A) spherical micelles, B) vesicles, C) rod like micelles, D) large compound micelles.

In the case of the solvent modification method, the copolymers (initial copolymer concentration is about 1 wt %) are first dissolved in an organic solvent, which is good for both segments and which is miscible with water, i.e. dioxane or tetrahydrofuran (THF). To induce

aggregation of the hydrophobic blocks, mili-Q water, the precipitant, is added slowly to the solution.

Self-assembly of the block copolymers begins when the water concentration reaches the *critical water concentration*, *cwc*, which can be defined as the water content at which phase separation of the polymer solution starts. Phase separation in the copolymer solution results in the formation of micelles consisting of a hydrophobic block (for example polystyrene), with core surrounded by and a corona shell of the hydrophilic block.<sup>49</sup>

As the water concentration increases above the *cwc*, the kinetics of chain exchange becomes slow and it is possible to trap the morphologies present at a high enough precipitant content. When the water content reaches the desired concentration, the sample is quenched and dialyzed against mili-Q water to remove the organic solvent.<sup>49</sup> The solvent modification method was employed for the present study to prepare the aggregates from the block copolymers. Detailed procedures for micelle preparation are described (for block copolymers used here) in Chapters 2 – 5. A brief description of the background of the formation of multiple morphologies is given in the Appendix at the end of the thesis.

In the study of self-assembly and polymorphism of block copolymer aggregates, the determination of the shape, size, and aggregation number of the structure is very important. Techniques such as transmission electron microscopy (TEM), scanning electron microscopy (SEM) and dynamic light scattering (DLS) are commonly used in such determinations. All three of these techniques were used extensively in the work presented in this thesis and will be discussed in more detail in Chapters 2 to 5.

### 1.2.2.3. Aggregation Numbers

Important parameters relevant to aggregate formation are the *aggregation numbers*,  $N_{agg}$ , and the dimensions of the core and interface at equilibrium. The aggregation number is defined as the number of block copolymer molecules in the micelle. Some characteristics of the aggregate structures, such as the degree of stretching of the core-forming blocks and the density of corona chains at the core-solvent interface, can be calculated based on this parameter.<sup>48</sup>  $N_{agg}$ , at equilibrium, is a function of copolymer composition and molecular weight, the quality of the solvent, etc.; for example, the poorer the solvent quality, the larger the  $N_{agg}$ .

Experimentally, most of the methods used to obtain  $N_{agg}$ , such as light scattering, involve changing the polymer concentration. These methods are very useful for systems in which the aggregates are frozen and  $N_{agg}$  does not change.

The  $N_{agg}$  can be also estimated using transmission electron microscopy, where the size of the micelles can be determined from the micrographs and the  $N_{agg}$  can be subsequently calculated from the volume of the single chain in the micelle. This technique of  $N_{agg}$  estimation was used in Chapter 2 for PS<sub>197</sub>-b-PAA<sub>47</sub> block copolymer.

The core dimensions can be directly determined by the aggregation number of the micelle and the solvent content in the core, assuming a sharp interface between the core and the corona of a micelle. The core dimension should change in the course of the water addition, since  $N_{agg}$  and solvent content are a function of the water content.  $N_{agg}$  for the micelles at equilibrium can also be estimated from its relationship to the cmc from the theory for small molecule surfactants micelles,<sup>52</sup> as shown in the following equation:

$$N_{agg} = 2(C / cmc)^{1/2} \quad (1-1)$$

where  $C$  is the total copolymer concentration. The cmc is a function of the water content, and  $N_{\text{agg}}$  as a function of the water content can be calculated. The core dimensions increase as the water content increases, owing to the increase in the aggregation number; simultaneously, solvent is extracted from the core, but the effect of this process on core size is minor.<sup>48</sup>

### 1.2.3. Micelles

The self assembly of amphiphilic block copolymers into aggregates of different morphologies, including spherical micelles, was discussed in the previous sections. The present section focuses exclusively on spherical block copolymer micelles, since they were used in the work of this thesis described in Chapters 2 to 5.

As highlighted above, amphiphilic block copolymers with large solubility differences between the hydrophilic and hydrophobic segments, self assemble in an aqueous environment into polymeric micelles of the size of tens of nanometers (10 – 50 nm).<sup>53-60</sup> These micelles have a fairly narrow size distribution, and are characterized by their unique core-shell architecture, where hydrophobic segments are segregated from the aqueous exterior to form an inner core surrounded by the corona composed of hydrophilic block copolymer segments. Solvent selectivity and, hence, copolymer self-assembly, have been observed for a variety of block copolymers in aqueous systems as well as in polar and nonpolar organic solvents. Because of the great variability in block copolymer size, architecture and composition, amphiphilic block copolymer micelles can be used in a wide range of applications, including solubilization of drugs or pollutants, as nanoreactors, in controlled drug delivery,<sup>53-60</sup> in toxic waste removal<sup>61, 62</sup> and as carriers for hydrophobic materials or DNA, among others.

#### 1.2.3.1. Micelles as Carriers in Drug Delivery

Polymeric micelles have a range of properties which makes them attractive as drug carriers, such as high stability and good biocompatibility for some copolymer systems.<sup>53-60</sup> In addition, they have been shown to be able to incorporate poorly soluble pharmaceuticals and to deliver them efficiently to pathological areas.

Pharmaceutical drug carriers are expected to be biodegradable, have small particle size, possess high loading capacity, demonstrate prolonged blood circulation (where applicable), and, ideally, accumulate in required pathological sites in the body.<sup>63</sup> The development of drug carriers meeting all these requirements for poorly soluble pharmaceuticals represents a challenging problem. Therapeutic application of hydrophobic, poorly water-soluble agents is known to be associated with some serious problems; the low water-solubility frequently results in poor absorption and bioavailability, as well as drug aggregation-related complications.<sup>64,65</sup> Low solubility in water is characteristic of many drugs, including anticancer agents.<sup>66</sup> The hydrophobicity helps a drug molecule to penetrate a cell membrane in cases where the molecular target for the drug is located intracellularly.<sup>67</sup> In addition, it has also been observed that a drug, or more generally, a biologically active molecule, may need a hydrophobic group to have a sufficient affinity toward the appropriate target receptor.<sup>68</sup> By some estimates, almost a half of the potentially valuable drug candidates identified by high throughput screening technologies demonstrate poor solubility in water and are, for this reason, rejected.<sup>69</sup>

To overcome the poor solubility of some drugs, certain excipients are used in formulations, such as clinically acceptable organic solvents.<sup>8</sup> Still, organic solvents might result in a frequent non-specific toxicity. Another option is to use certain micelle-forming surfactants in formulations of insoluble drugs.<sup>70</sup> Here also the hydrophobic fragments of the amphiphilic



molecules form the core of the micelle, which can solubilize poorly soluble pharmaceuticals (Figure 1.4).<sup>71</sup> The hydrophilic parts of the amphiphilic molecules form the micelle corona. Micellar encapsulation increases the solubility and bioavailability of poorly soluble drugs, increases their stability in biological surroundings, improves their pharmacokinetics and biodistribution, and decreases the toxicity of the drug.<sup>72-74</sup>

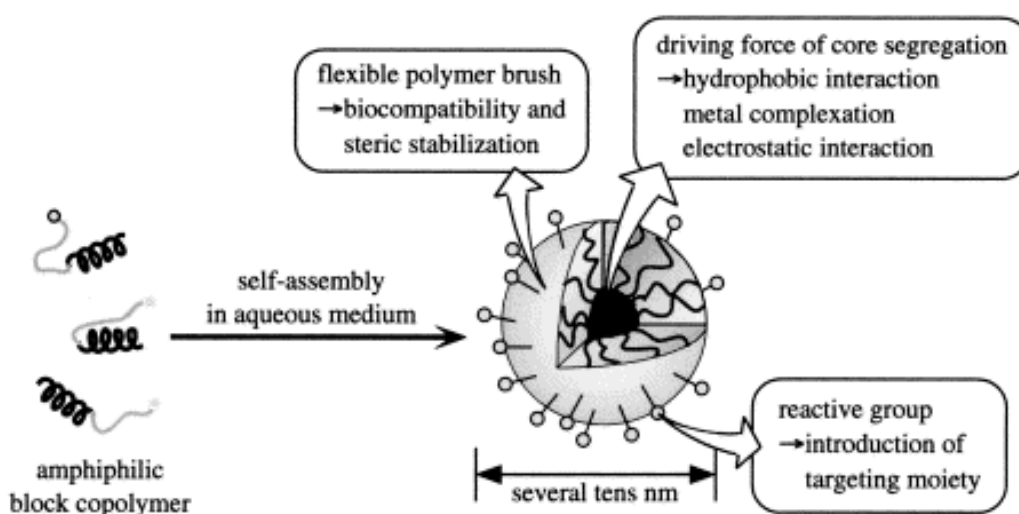


**Figure 1.4:** Schematic representation of loaded micelles prepared (from reference 53).

Most of the drug is incorporated inside the micelles and is, thus, rendered non toxic. In addition, because of their small size, micelles demonstrate spontaneous accumulation in pathological areas with leaky vasculature and impaired lymphatic drainage, such as tumors and infarcts, via the mechanism of the enhanced permeability and retention effect.<sup>75-78</sup>

In the work of this thesis, in parallel to the use of block copolymers in drug delivery systems, as published previously by many groups, block copolymer micelles were used as a carriers and

storage sites for hydrophobic biocides of low water solubility and toxicity to increase their total concentration in solution. These systems are discussed in detail in Chapters 2 to 4.

#### 1.2.3.2. Micelle Loading

The method used to incorporate the solubilize (loaded material) into the micelles depends mostly on the micelle preparation method involved for the particular block copolymer. In general, there are three main ways to load the solubilize. If the micelles are formed by direct dissolution in water, then an aliquot of copolymer water stock solution is often added to a vial, which contains the solubilize to be incorporated. For example, a solubilize stock solution in acetone is made and then an aliquot is added to an empty vial, the acetone is allowed to evaporate, and then the copolymer/water mixture is added.<sup>56</sup>

In the case of the solvent modification method, the copolymers are first dissolved in an organic solvent, which is good for both segments and which is miscible with water, i.e. dioxane or tetrahydrofuran (THF). To induce aggregation of the hydrophobic blocks, milli-Q water is added slowly to the system which leads to the formation of micelles consisting of a core formed from the hydrophobic blocks with core surrounded by a corona shell of the hydrophilic blocks. In the next step, the solubilize stock solution in acetone is prepared and then an aliquot is added to an empty vial, the acetone is allowed to evaporate, and then the micelles/water mixture is added,<sup>56</sup> followed by the vigorous stirring to allow the micelles to be loaded with hydrophobic solubilize. This technique was chosen to load the hydrophobic material into micelles as described in Chapters 2, 3, 4.

Finally, if the micelles are prepared by the solvent modification method alone, the solubilize is added with the copolymer to the common organic solvent and then water is added drop-wise,

as the core is formed, the hydrophobic solubilize partitions into the core, which leads to the formation of the solubilize loaded micelles.<sup>56</sup>

#### 1.2.3.2.1. Loading Capacity

The micelle core serves as the cargo space for various hydrophobic materials, as discussed above. However, this cargo space is limited. In order to exploit maximally the minimal loading space available, many factors which control the loading capacity and loading efficiency have to be manipulated. The major factors which influence both the loading capacity and loading efficiency of block copolymer micelles are nature of the solute, nature of the core-forming block, core block length, total copolymer molecular weight, solute concentration, and to a lesser extent, the nature and block length of the corona. Many studies have indicated that the overriding factor is the compatibility between the solubilize and the core-forming block.<sup>56</sup>

##### 1.2.3.2.1.1. Compatibility between the Solubilize and the Core Forming Block

Extensive studies have been performed to explore the influence of the properties of the solubilizes on their extent of incorporation into block copolymer micelles. Several of the important properties of the solubilize that have been identified are molecular volume, polarity, hydrophobicity, charge, degree of ionization, and interfacial tension against water, if it forms a separate phase.<sup>79</sup>

As was mentioned above, the nature of the core forming polymer, i.e. the solute, including its polarity, hydrophobicity, charge and degree of ionization, has been found to influence greatly the degree of incorporation. Controlling the compatibility between the solute and the core-forming block can be used to enhance incorporation of the solubilize most effectively. One way of

expressing the compatibility is in terms of the Flory-Huggins interaction parameter,  $\chi_{s-p}$ , which is defined by the following equation:<sup>79,80</sup>

$$\chi_{s-p} = (\delta_s - \delta_p)^2 V_s / kT \quad (1-2)$$

where  $\delta_s$  and  $\delta_p$  are the Scatchard-Hildebrand solubility parameters of the solubilize and the core forming polymer, respectively.,  $V_s$  is the molecular volume of the solubilize,  $k$  is the Boltzmann constant, and  $T$  is the absolute temperature. Nagarajan *et al.*<sup>79</sup> and Gadelle *et al.*<sup>80</sup> used  $\chi$  as a correlation parameter to predict the extent of solubilization of aromatic and aliphatic hydrocarbons in block copolymer micelles. These studies, which considered solubilization to occur in the micelle core only, showed that molecules which are more compatible with the core-forming block (i.e. with smaller  $\chi$  parameter) are solubilized to a higher extent. However, these studies pointed out that using  $\chi$  alone to predict the extent of solubilization is insufficient in cases when solubilization occurs at the micelle interface.

Giacomelli *et al.*<sup>85</sup> points out the importance of developing systems in which the active molecule “matches” the micellar core in terms of compatibility (Flory-Huggins interaction parameter  $\chi \approx 0$ ). The specific interactions between hydrophobic guest molecules and core-forming block were studied, and it was suggested that probe/micelle systems exhibiting the ability to form  $R_1\text{-COOH/NH}_2$  acid-base pairs within the micellar core, display high loading capacities (> 100%), which decrease considerably, for example, after esterification of carboxylic acid moieties.<sup>85</sup> A remarkable example of optimal drug delivery system, for which loadings as high as 190 % were observed, is the 17  $\beta$ -estradiol/PEO-b-PCL.<sup>86</sup>

Due to the fact that each solubilize is unique, it seems reasonable that no single core-forming block will allow maximum loading levels to be achieved for all solubilizes. Thus, it is unlikely that any one micelle system will serve as an efficient storage medium for all solubilizes.

### 1.2.3.2.1.2. Partition Coefficient

Besides the  $\chi$  parameter, another way to define the stability of the material loaded into micelle – micelle complex against dilution is the partition coefficient. Partition coefficient can be also used to determine the amount of material solubilized by the micelles; to ascertain whether the solubilize loading is governed by thermodynamics, the micelle-water partition coefficient can be used. The partition coefficient is a thermodynamic parameter that represents the affinity of a given solubilize for the micellar phase, relative to that for the aqueous phase.<sup>99,100</sup>

As described in Chapter 2 in detail, the partition coefficient of biocide between ethylbenzene (EB), a low molecular weight analog of PS, and water was measured in order to determine the relative affinity of the biocide for the polystyrene micelle core versus that of the aqueous solution.<sup>99,100</sup> The ethylbenzene-water partition coefficient,  $K_{EB/water}$ , can be calculated using the following equation:

$$K_{EB / water} = \frac{c_{EB}}{c_{water}} \quad (1 - 3)$$

where  $c_{EB}$  is the concentration of biocide in the EB phase and  $c_{water}$  is concentration of biocide in the water phase. Ethylbenzene was chosen, as described in Chapter 2 of this thesis, as a model solvent due to its structural similarity to the styrene repeat unit; therefore, the solubility of TCMTB biocide in ethylbenzene can be considered as an approximation for the solubility for the biocide in the polystyrene micelle core. If the partition coefficients of the biocide between the polystyrene core of the micelles and water are in a good agreement with those of the biocide between ethylbenzene and water, one can conclude that the solubilize loading is governed by thermodynamics.

*1.2.3.2.1.3. Other Factors which Influence the Loading into Micelles*

Aside from polymer–solubilizate compatibility and interactions, there are other factors which influence the extent of incorporation of a solubilizate into block copolymer micelles. For a given solubilizate, the extent of incorporation is a function of factors that affect the micelle size or aggregation number. These factors include the ratio of the hydrophilic to hydrophobic block lengths,<sup>80-83</sup> as well as the copolymer molecular weight<sup>80,82</sup> and the copolymer and solute concentrations.<sup>84</sup>

For example, the solubilisation capacity of poly(ethylene oxide)-b-poly(propylene oxide)-b-poly(ethylene oxide) triblock copolymer micelles (PEO-b-PPO-b-PEO) increases with the hydrophobic PPO block length.<sup>80-83</sup> This effect is attributed to the decrease in the cmc, and also increase in the aggregation number and, therefore, in the micelles size, that accompany an increase in the hydrophobic block length.<sup>80-83</sup>

The hydrophilic block length also affects the extent of the solubilisation; increasing the PEO percentage in the PEO-b-PPO-b-PEO triblock copolymers increases the cmc and decreases the aggregation number; therefore, with the formation of smaller micelles, the solubilisation capacity decreases.<sup>80,81,83</sup>

Incorporation into micelles is also influenced by the copolymer molecular weight; higher molecular weight polymers form larger micelles and, therefore, show a higher loading capacity.<sup>80,82</sup> Increasing the solute concentration has also been found to increase the aggregation number of the copolymer under dynamic equilibrium conditions, which causes formation of larger micelles and to increase the solubilisation capacity per micelle.<sup>84</sup>

## 1.2.3.2.2. Glass Transition Temperature

It is well known that small molecules, when loaded into the micelle core, can act as plasticizers and, therefore, lower the glass transition temperature ( $T_g$ ) of the core forming polymer; the decrease in  $T_g$  would speed up the diffusion of the small molecules through the hydrophobic region.<sup>87</sup> The glass transition temperature is the temperature range in which the transition in the amorphous regions occurs between the glassy and rubbery state. Substantially, above  $T_g$ , an amorphous polymer is in its rubbery state and therefore soft and flexible. Small molecules, for example biocides, can act as plasticizers for the poly(styrene) (PS) and, therefore, decrease its  $T_g$  and thus speed up the diffusion of the small molecules into the hydrophobic micelles core.

Singh *et al.*<sup>87</sup> reported for PS films ( $M_w = 212$  kDa) of thickness of 20 – 30 nm a thickness related drop in  $T_g$  of less than 10°C. To explore the  $T_g$  depression of PS by small molecules, such as those of the biocide, the differential scanning calorimetry (DSC) technique can be employed for mixtures of various compositions. DSC was used in this work to study the  $T_g$  of the mixture of PS and TCMTB biocide, as shown in detail in Chapter 2. The Fox equation<sup>88</sup> is, by far, the simplest which describes the  $T_g$  behavior of plasticized systems. The equation is:

$$\frac{1}{T_g} = \frac{W_1}{T_{g1}} + \frac{W_2}{T_{g2}} \quad (1 - 4)$$

where  $T_g$  is the glass transition temperature of the plasticized system (K),  $W_1$  and  $W_2$  are the weight fractions of pure material 1 and material 2 (the polymer and the biocide), respectively, and  $T_{g1}$  and  $T_{g2}$  are the glass transition temperatures of pure material 1 and material 2, respectively.

## 1.2.3.2.3. Mechanism of Loading - Case II Diffusion

The term “case II diffusion” was first applied by Alfrey *et al.*<sup>89</sup> to penetration of low molecular weight materials into a glassy polymer substrate characterized by zero-order kinetics and a sharp penetrant advancing front. This phenomenon appeared to constitute a limiting form of the deviation from normal Fickian penetration kinetics (correspondingly termed “case I diffusion”) commonly exhibited by glassy polymer-micromolecular penetrant systems. In the absence of externally applied stresses, the diluents penetrate into the glassy polymer in the form of moving fronts at constant velocity under constant conditions of the given levels of external activity of the diluent and the prevailing temperature.<sup>90</sup> Case II behavior is characterized by the existence of (1) a sharp solvent front in the polymer advancing at a constant velocity, (2) a negligible solvent concentration gradient behind the sharp solvent front, and (3) an induction time leading to the onset of front movement.

Such non-Fickian diffusion processes have been investigated extensively over the past four decades. For example, Thomas and Windle<sup>91-93</sup> studied the characteristic features of Case II diffusion during methanol sorption in glassy poly(methyl methacrylate) (PMMA) and modeled this Case II diffusion process in terms of the viscous response of polymer glass to the osmotic swelling pressure generated by the penetrating solvent. Hui *et al.*<sup>94-96</sup> refined Thomas and Windle’s mechanistic model and employed Rutherford backscattering spectrometry for the determination of penetrant concentration profiles in the polystyrene/iodohexane system. Their results clearly demonstrate that the initiation of Case II front movement can only take place after the volume fraction of penetrant has reached a critical value at the surface of the glassy polymer, after which the polymer viscosity would be lowered sufficiently and the diffusion coefficient of the penetrant increased to the level necessary to establish the Case II front.<sup>96</sup> Rossi *et al.*<sup>97</sup>



proposed a description of Case II diffusion which is based on the concept of plasticization at a sufficiently high solvent concentration where the slow plasticization kinetics sets an upper limit for the solvent flux into the glassy region. More recently, Lee et al.<sup>98</sup> report on a sample size-dependent induction time and front penetration rate during Case II diffusion of methanol in spherical glassy PMMA beads. With increasing sample diameter, the observed induction time generally increases, while the front penetration rate exhibits a weak decreasing trend.<sup>98</sup>

Because the small molecules act as plasticizers for the core forming block, the penetration in the core occurs, to the greatest extent, when the  $T_g$  is lowered sufficiently by the small molecules. The velocity of the moving front can be calculated assuming that the small molecules form a penetrating front moving at constant velocity,  $v$ , towards the interior of a micelle (i.e. by case II diffusion).<sup>91-97</sup> If the small molecule concentration at one side of the front is at saturation and zero at the other side, the increase in concentration of the small molecules in the micelle,  $B$ , with time is:

$$B = A \frac{4\pi}{3} (R^3 - r^3) \quad (1 - 5)$$

where  $A$  is the maximum uptake per unit volume and  $r$  the location of the front at time  $t$ , given by  $r = R - vt$ , valid for  $0 \leq \tau \leq 1$  with  $\tau = vt / R$ . Hence

$$B = \frac{4\pi}{3} A [R^3 - (R - vt)^3] = B_\infty [1 - (1 - \tau)^3] \quad (1 - 6)$$

where  $B_\infty = 4/3 \pi R^3 A$ , the maximum micelle loading. eq. (1 - 6) can be re-written as

$$1 - \left( \frac{B_\infty - B}{B_\infty} \right)^{1/3} = \tau \quad (1 - 7)$$

If the plot of the left hand side of equation 1 - 7 vs. time shows a straight line, it can be concluded that penetration follows case II diffusion. The velocity of the penetrating front can be

calculated using equation 1 – 6. The speed of the penetrating front was calculated using the above equations for the constant velocity of the biocide moving on a front inside the PS core of the micelles, as described in detail in Chapter 2.

### 1.2.3.3. Release from Micelles

The release of material from block copolymer micelles depends upon several factors such as the rate of diffusion of the incorporated material through the micelle, micelle stability and the rate of biodegradation of the copolymer.<sup>56</sup> If the micelle is stable and the rate of biodegradation of the copolymer is slow, the release rate will be mostly influenced by several of the following factors: the strength of the interactions between the incorporated material and the core-forming block,<sup>102</sup> the physical state of the micelle core,<sup>101</sup> the amount of loaded material into micelles,<sup>103</sup> the molecular volume of the incorporated material, the length of the core-forming block<sup>103</sup> and the localization of the loaded material within the micelle.

The stronger the interaction between the incorporated material and the core-forming block, the slower the release of the loaded material from the micelle. For example, studies by La *et al.*<sup>102</sup> found that the in vitro release rate of indomethacin from PBLA-*b*-PEO micelles increased with increasing pH of the external medium. As the pH of the medium is increased, more of the carboxylic acid groups become ionized, weakening the hydrophobic–hydrophobic interaction which holds the drug within the micelle core.<sup>102</sup> Thus, strong polymer–solubilize interactions will enhance loading and decrease the release rate of the loaded material from the micelles.

The incorporated material may lie within the micelle core, at the interface between the micelle core and the corona or even within the corona itself. The localization of the solubilize will largely depend upon its physical properties and the interaction parameters between the

solubilizate and the micelle core and corona – forming blocks.<sup>99,100</sup> It has been found that the more soluble compounds are localized in the inner corona or the core–corona interface while the more hydrophobic compounds are situated mostly in the micelle core.<sup>99</sup> The release rate of the drug will largely be a function of its localization within the micelle. The outer corona region of the micelle is quite mobile; as a result, release from this area will be rapid. The release of drug localized in the corona or at the interface is said to account for ‘burst release’ from the micelle.<sup>99</sup> The localization of the biocide within the micelle is discussed in detail in Chapter 2.

Another factor influencing the rate of the solubilizate release from the micelle is the state of the micelle core, i.e. whether it is liquid-like or solid-like, which determines the diffusion coefficient of the small molecules. The physical state of the core under normal physiological conditions (37°C) will depend largely upon the glass transition temperature of the core-forming block and the degree of crystallinity, if any. Far below the glass transition temperature the polymer is in a solid-like state, while far above it the polymer is in a liquid-like state; the changes in properties such as viscosity through the region are gradual.<sup>104</sup> Micelles containing polystyrene cores are glassy at room temperature since the glass transition temperature of polystyrene is ca. 100°C; however, if a solvent can diffuse into the core, plasticization can lower the  $T_g$  appreciably, as discussed above. Many of the biocompatible polymers have glass transition temperatures which are well below that of polystyrene. For example, the glass transition temperatures for several of the biocompatible polymers are 35°C for poly(glycolic acid) (mol. wt. 50 000), 54°C for poly(L-lactic acid) (mol. wt. 50 000), - 62°C for polycaprolactone (mol. wt. 44 000) and -75°C for poly(propylene oxide).<sup>105</sup> The movement of the incorporated material from a glassy core will be slower in comparison to the movement of materials out of cores which are more mobile. This effect was seen, for example, in studies by

Teng et al.<sup>106</sup> who found that the diffusion constant for pyrene in poly(styrene) is lower than it is in poly(tert-butyl acrylate). This result was expected since the  $T_g$  of polystyrene is 100°C while that of poly(tert-butyl acrylate) is 42°C.<sup>106</sup> Micelle cores formed from the more hydrophilic polymers may contain appreciable amounts of water. The release of loaded material from cores of this nature has been found to proceed rapidly.<sup>106</sup>

The properties of the micelle core, including core radius, influence the release rate if the loaded material is primarily situated in the micelle core. The longer the core-forming block, the larger the core, and the slower the release of the incorporated material from the micelle. However, the release kinetics of loaded material which reside at the core–corona interface or in the outer shell are rapid because the molecules do not have to diffuse through the core, and are thus not influenced by the core radius, and thus length of the core-forming block.

The size or molecular volume of the incorporated material will also affect its rate of diffusion from the micelle.<sup>105</sup> Materials with larger molecular volumes will have a smaller diffusion constant resulting in a decreased release rate. Once again, the burst release or release of materials localized at the micelle surface should be independent of the molecular volume.

The physical state of the drug within the delivery vehicle can have a significant effect on the release kinetics. If the loaded material is dissolved molecularly, it may act as a plasticizer and lower the glass transition temperature of the core-forming block; this, in turn, may accelerate the release.

### 1.3. Emulsions

Another way of increasing the concentration of the hydrophobic materials of low water solubility in aqueous solutions, aside of loading the hydrophobic materials into micelles, is the incorporation of such materials into emulsion droplets.

An *emulsion* is a mixture of two or more immiscible liquids, usually water and oil. In an emulsion, one liquid (the dispersed phase) is dispersed in the other (the continuous phase), in which it is essentially insoluble; the boundary between these phases is called the interface.<sup>107,108</sup> Emulsions tend to have a cloudy appearance, because the many phase interfaces scatter light that passes through the emulsion. Emulsions are unstable and thus do not form spontaneously. Emulsions are usually produced by dispersion, because dispersion is much easier for a fluid than for a solid. The formation of a large interfacial area between two phases normally requires the expenditure of a significant amount of energy (vigorous shaking or stirring), but this can be dramatically reduced in the presence of a surfactant, which may act as a dispersing or stabilizing agent, which prevents the emulsion from coalescing.<sup>107,108</sup> The surfactant molecules adsorb at the interface between the oil and water, and by their adsorption, they lower the interfacial tension and increase the interfacial viscosity. Emulsifying agents may also be ionic compounds, in which case they impart a charge to the surface, which, in turn, establishes an ion atmosphere of counter-ions in the adjacent aqueous phase. The electrical charge produces a repulsive force between approaching droplets, and this prevents them from making close contact during a collision and coalescing.<sup>107,108</sup>

Energy input through shaking, stirring or homogenizing processes is needed to initially form an emulsion. Over time, and especially in the absence of stabilizers, emulsions tend to revert to

the stable state of the phases comprising the emulsion; an example of this is seen in the separation of the oil and vinegar components of Vinaigrette, an unstable emulsion that will quickly separate unless shaken. Whether an emulsion is stable as a water-in-oil emulsion or an oil-in-water emulsion depends on the volume fraction of the two phases and on the type of emulsifier. Generally, emulsifiers and emulsifying particles tend to promote dispersion of the phase in which they do not dissolve very well; for example, proteins dissolve better in water than in oil and so tend to form oil-in-water emulsions (that is they promote the dispersion of oil droplets throughout a continuous phase of water).

Typically, emulsions by themselves are not thermodynamically stable.<sup>112</sup> “Emulsion stability refers to the ability of an emulsion to resist change in its properties over time.”<sup>109</sup> There are three types of emulsion instability: flocculation, creaming, and coalescence. Flocculation describes the process by which the dispersed phase comes out of suspension in flakes. Coalescence is another form of instability, which is observed when small droplets combine to form progressively larger ones. Emulsions can also undergo creaming, the migration of one of the substances to the top (or the bottom, depending on the relative densities of the two phases) of the emulsion under the influence of buoyancy or centripetal force when a centrifuge is used.

An *emulsifier* is a substance which stabilizes an emulsion by increasing its kinetic stability. One important class of emulsifiers is known as *surfactants* (discussed in the next section).

Emulsions are widely used in many industries, such as the food industry, coatings industries, in pharmaceuticals, hairstyling, personal hygiene and cosmetics. Microemulsions are, for example, used to deliver vaccines and kill microbes.<sup>110</sup> Typically, the emulsions used in these techniques are nanoemulsions of soybean oil, with particles that are 400-600 nm in diameter.<sup>111</sup> The

emulsification process is not chemical, as with other types of antimicrobial treatments, but mechanical. The smaller the droplet, the greater energy, and thus, the greater the driving force to merge with other lipids. The oil is emulsified using a high shear mixer with detergents added to stabilize the emulsion, so when the droplets encounter the lipids in the membrane or envelope of bacteria or viruses, they force the lipids to merge with themselves.<sup>111</sup> On a mass scale, this effectively disintegrates the core membrane and kills the pathogen. This soybean oil emulsion does not harm normal human cells nor the cells of most other higher organisms.<sup>111</sup> The most effective application of this type of nanoemulsion is for the disinfection of surfaces. Some types of nanoemulsions have been shown to effectively destroy HIV-1 and various tuberculosis pathogens, for example, on non-porous surfaces.<sup>111</sup>

### 1.3.1. Stabilizers (Surfactants)

To stabilize the oil emulsion in water, an emulsifying compound is used; this is a chemical that stabilizes the emulsion, and is often a surfactant-type molecule.<sup>112</sup> A shortened form of "SURFace-ACTive AgeNT", a *surfactant* is a chemical that stabilizes mixtures of two immiscible liquids (oil and water) by reducing the surface tension at the interface between the oil and water molecules. Because water and oil do not dissolve in each other, a surfactant has to be added to the mixture to keep it from separating into layers. Surfactants can increase the kinetic stability of emulsions greatly so that, once formed, and stored in an appropriate environment the emulsion does not change significantly over years of storage.

Surfactants are usually organic compounds that are amphiphilic, meaning they contain both hydrophobic groups (their *tails*) and hydrophilic groups (their *heads*). Therefore, they are soluble in both organic solvents and water. The term surfactant was coined by Antara products in 1950.

Surfactants reduce the surface tension of water at the liquid-liquid interface. Many surfactants can also assemble in solution into aggregates. Examples of such aggregates are micelles and vesicles. The concentration at which surfactants begin to form micelles is known as the critical micelle concentration (cmc). When micelles form in water, their tails form a core that can encapsulate hydrophobic material, and their (ionic/polar) heads form an outer shell that maintains favourable contact with water. Surfactants are also often classified into four primary groups; anionic, cationic, non-ionic, and zwitterionic (dual charge).

Thermodynamics of surfactant systems are of great importance, theoretically and practically.<sup>113</sup> The importance is due to the fact that surfactant systems represent systems between ordered and disordered states of matter. Surfactant solutions may contain ordered phases and disordered phases.

Examples of food emulsifiers are egg yolk (where the main emulsifying agent is lecithin); mayonnaise and Hollandaise sauce are oil-in-water emulsions that are stabilized with egg yolk lecithin. Detergents are another class of surfactant, and will physically interact with both oil and water, thus stabilizing the interface between oil or water droplets in suspension. This principle is exploited in soap to remove grease in the process of cleaning. Emulsions are also frequently used in pharmaceuticals, hairstyling, personal hygiene and cosmetics. These are usually oil and water emulsions, but which of these is dispersed and which is continuous depends on the specific formulation. These emulsions may be called creams, ointments, liniments (balms), pastes, films or liquids, depending mostly on their oil and water proportions and their route of administration.<sup>114,115</sup>



### 1.3.2. Block Copolymers as Stabilizers for Emulsions

The use of block copolymers as emulsion stabilizers is very extensive and only a few representative examples can be given in this thesis.

Polymeric surfactants, mainly block copolymers, but also functionalized oligomers and polysoaps, have been the subject of increasing interest over the last decades in a variety of applications as emulsifiers, dispersion stabilizers, wetting agents, and others.<sup>116</sup> The interest in these polymeric amphiphiles, and especially in block copolymers with well-defined structure, molecular weight, and composition, arises mainly from their unique solution and associative properties. Block copolymers, consisting in the simplest case of hydrophilic and hydrophobic blocks, behave similarly to low-molecular-weight surfactants; however, polymeric surfactants have, in general, much lower diffusion coefficients and critical micelle concentrations than “classic” surfactants.<sup>116</sup>

Despite certain limitations, block copolymers may, under some conditions, have advantages over conventional low-molecular-weight surfactants. In fact, block copolymers with very low cmc and low diffusion coefficients, may become strongly attached to the colloidal particles and thus provide excellent steric or electrosteric stabilization against flocculation and coalescence.<sup>116</sup> Their stabilization efficiency is related to parameters like surface or interfacial tension or cmc, and results from an extensive interaction between the block copolymer sequences and the immiscible phases. Moreover, block copolymers present a wider range of possibilities than the classical low-molecular-weight surfactants as they are suitable for the preparation of a “polymeric water-in-water” emulsions.<sup>116</sup> Compared with conventional surfactants, block copolymers in latex technology may serve not only as a stabilizer in the polymerization process, but also as an active component in the finished product formulation, for example, as plasticizers, compatibilizers, antistatic agents and oil and/or water repellents.

The major application possibilities of block copolymer-stabilized dispersions, in both aqueous and nonaqueous systems, are, therefore, in the fields of coatings, inks, toners, adhesives, and functional packing materials for chromatography. One minor limitation of block copolymers, and of polymeric surfactants in general, in their use as stabilizers is that, with increasing molecular weight, their diffusion coefficient, and hence their efficiency as stabilizers, decreases by surfactant entrapment in the latex particles. For industrial applications, a suitable compromise is a molecular weight range of about 1 000 to 20 000.<sup>116</sup>

In addition to these more conventional applications, nanostructured colloidal particles have a potential use in advanced technologies such as information storage, controlled drug delivery and photonic devices, which might be accessible with ABC triblock copolymers and stimuli responsive latexes, as was recently demonstrated by Armes.<sup>124</sup>

The research on block copolymers as polymeric surfactants and their colloidal behaviour was developed from the pioneering work of Molau<sup>117</sup> in the mid 1960s. These colloidal aspects of block copolymers in solution have been surveyed from experimental and theoretical points of view by Price,<sup>118</sup> Piirma,<sup>119</sup> Tuzar and Kratochvil,<sup>120</sup> Riess,<sup>121</sup> Alexandridis and Hatton,<sup>122</sup> and quite recently by Alexandridis and Lindman.<sup>123</sup>

Classic oil and water emulsions can be classified as O/W (oil in-water) or W/O (water-in-oil) depending on the nature of the continuous and dispersed phase. More complex multiple emulsions are also possible, i.e. either W/O/W (water-in-oil-in water) or O/W/O emulsions.

Hydrophilic–hydrophobic block copolymers, such as poly(ethylene oxide)-poly(propylene oxide)-poly(ethylene oxide) triblocks (PEO–PPO–PEO), poly(styrene)-b-poly(ethylene oxide) diblocks (PS–PEO), and poly(methyl methacrylate)-poly(ethylene oxide) diblocks (PMMA–PEO) are typical examples of systems used as polymeric surfactants. For styrene–water

emulsions, stabilized with PS-PEO or PEO-PS-PEO di- and triblock copolymers, it was shown that stable O/W emulsions of small droplet size are preferably prepared with PS-PEO and PEO-PS-PEO with a PEO content of 60–80 wt.-% and a molecular weight in the range of 1 000 to 20 000. In contrast, stable W/O emulsions are obtained with PS-PEO and PS-PEO-PS copolymers having a 60–80 wt. % PS content.<sup>116</sup>

Some properties of block copolymers such as surface activity, emulsifying properties, and applications as stabilizers of colloidal systems, such as polymeric dispersions, would need further investigation as these topics have only been examined to a small extent up till now. Gilbert *et al.*<sup>125</sup> reported that an electrosteric stabilizer (poly(styrene)-*b*-poly(acrylic acid) PS-*b*-PAA) has the effect of a major reduction in the rate coefficients for both entry and exit in an emulsion polymerization, compared to what is seen in the same latex with an ionic stabilizer. This reduction varies significantly with changes in both pH and ionic strength and therefore clearly has its origin in the polyacrylate moieties in the interfacial region, where radicals diffuse through the hairy layer, due to substantial change in the viscosity in the interfacial region.<sup>125</sup>

Block copolymers of PS-*b*-PAA of various molar masses, topologies and compositions were studied by Burguiere *et al.*<sup>126</sup> as emulsion stabilizers. The diblock copolymers with 10 styrene units and a maximum of 50 acrylic acid units were found to be most efficient stabilizers; an increase in the size of the hydrophilic segment did not lead to any improvement in efficiency. The triblock or starblock copolymers did not behave differently from the diblocks. In contrast, it was found that the efficiency of triblocks with an internal hydrophilic segment strongly depends on the respective length of both blocks.<sup>126</sup>

Antoinetti *et al.*<sup>127</sup> investigated the application of block copolymers with one charged block as emulsion stabilizers. It was found that the stabilizing properties of these polyelectrolyte block

copolymers strongly depend on the ionic strength and the architecture of the charged block. The lower the ionic strength the better is the ability of the block copolymer to stabilize latex particles.<sup>127</sup>

Prestidge *et al.*<sup>128</sup> studied PEO-PPO-PEO block copolymers at the emulsion droplet-water interface. The adsorbed layer thickness was shown to depend on the copolymer structure, the surface chemistry of the absorbent, and the level of cross-linking within the droplets.<sup>128</sup>

Lips *et al.*<sup>129</sup> studied curvature effects and phase inversion on the thermodynamics of particle-stabilized emulsions. The authors found that if the particles are not densely packed, the interfacial bending moment and the spontaneous curvature (due to the particles) are equal to zero; if the particles are closely packed, then the particle adsorption monolayer possesses a significant bending moment, and the interfacial energies of bending and dilatation become comparable. In this case, the bending energy can either stabilize or destabilize the emulsion, depending on whether the particle contact angle is smaller or greater than 90°. <sup>129</sup>

Recently, Deming *et al.*<sup>112</sup> (Nature 2008) prepared double emulsions composed of water-in-oil-in-water. These complex emulsions allow both water-soluble and oil-soluble compounds to be delivered in the same droplet; the oil-coated water droplets were on the order of 100 nm in diameter. The authors have shown that these emulsions can be prepared in a simple process and stabilized over many months (more than nine) using single-component, synthetic amphiphilic diblock copolypeptide surfactants (poly(L-lysine HBr)<sub>x</sub>-b-poly(racemic-leucine)<sub>y</sub>). These surfactants even stabilize droplets subjected to extreme flow, leading to the direct production of robust double nanoemulsions that are amenable to nanostructured encapsulation applications in foods, cosmetics and drug delivery.<sup>112</sup>

### 1.3.3. Bacterial Emulsions

The literature dealing with bactericidal emulsions is very limited. Only one publication (a patent) which deals with this topic was found. Lipecki *et al.*<sup>130</sup> presented an invention which relates to a process for preparing stable emulsions of biologically active compounds that are water insoluble or have low water solubility directly before introducing them to an environment of use. More particularly, the invention is directed to a process for preparing emulsions of biocides and biocidal formulations directly using a micro-mixing device wherein the resulting emulsions are free of additives including surfactants, co-surfactants, emulsifiers, stabilizers, polymers, copolymers and solvents. Emulsions of water insoluble biocides including reduced amounts of organic solvents are also prepared directly before use. These emulsions are stable toward the phase separation for periods measured in years. Active ingredients are compounds and polymers selected from biocides and are provided as neat liquids, concentrates and dispersions.<sup>130</sup>

The authors<sup>130</sup> claim that the invention provides several advantages. Water insoluble active ingredients are difficult to emulsify using conventional mixing technology and require significant quantities of added surfactants and solvents. In some instances, certain solvents are utilized to render the active ingredient soluble and have adverse environmental impacts associated with such solvents. The micro-mixers emulsify the water insoluble active ingredients of the invention using solvents that have little to no adverse environmental impact. Micro-mixers can be used to prepare emulsions of water insoluble biocides including isothiazolones, but do not require significant quantities of added surfactants and solvents to form stable micro-emulsions.<sup>130</sup>

Although it is used industrially, no literature was found related to the use of thiocyanomethylbenzothiazole (TCMTB) biocide in emulsions. In the present study, emulsions of biocide were prepared in order to increase local concentration of the hydrophobic biocide in water, and are along with the preparation techniques discussed in Chapter 4.

#### 1.4. Bacteria

Since the present thesis deals primarily with self assembled block copolymer micelles in bacterial deactivation, it seems appropriate to include a very brief section on bacteria for the convenience of the reader.

*Bacteria* are a large group of unicellular, prokaryote, microorganisms. Typically a few micrometres in length, bacteria have a wide range of shapes, ranging from spheres to rods and spirals. Bacteria are ubiquitous in every habitat on earth, growing, for example, in soil, as well as in organic matter and in the live bodies of plants, animals and humans. There are, typically, 40 million bacterial cells in a gram of soil and a million bacterial cells in a milliliter of fresh water; in all, there are approximately five nonillion ( $5 \times 10^{30}$ ) bacteria on earth,<sup>131</sup> forming much of the world's biomass.<sup>131</sup>

There are approximately ten times as many bacterial cells in the human flora of bacteria as there are human cells in the body, with large numbers of bacteria on the skin and as gut flora.<sup>132</sup> The vast majority of the bacteria in the body are rendered harmless by the protective effects of the immune system, and a few are beneficial. However, a few species of bacteria are pathogenic and cause infectious diseases, including cholera, syphilis, anthrax, leprosy and tuberculosis. In

developed countries, antibiotics are used to treat bacterial infections in humans and animals; repeated exposure has the unintentional consequence that antibiotic resistance is becoming common. In industry, bacteria are important in sewage treatment, in the production of cheese and yoghurt through fermentation, as well as in biotechnology and the manufacture of antibiotics and other chemicals.<sup>133</sup>

Bacteria are classified as prokaryotes. Unlike cells of animals and other eukaryotes, bacterial cells do not contain a nucleus and rarely harbour membrane-bound organelles. Prokaryotes consist of two very different groups of organisms: Bacteria and Archaea.<sup>134</sup> Most bacteria cells are either rod-shaped, called bacilli (e.g. *Escherichia coli*) or spherical, called cocci (e.g. *Micrococcus Luteus*).

*Escherichia coli* (*E. coli*) is a Gram negative (defined on page 46) rod-shaped bacterium of about 2  $\mu\text{m}$  long and 0.5  $\mu\text{m}$  in diameter, with a cell volume of 0.6 - 0.7  $\mu\text{m}^3$ .<sup>153</sup> *E. coli* bacteria are commonly found in the lower intestine of humans. Most *E. coli* strains are harmless, but some, such as serotype O157:H7, can cause serious food poisoning in humans.<sup>154</sup> The harmless strains are part of the normal flora of the gut, and can benefit their hosts by producing vitamin K<sub>2</sub>,<sup>155</sup> and by preventing the establishment of pathogenic bacteria within the intestine.<sup>156,157</sup> *E. coli* bacteria can be grown easily (optimal growth of *E. coli* occurs at 37°C), and its genetics are simple and easily-manipulated or duplicated, making it one of the best-studied prokaryotic model organisms, and an important species in biotechnology and microbiology. In the present thesis, harmless *E. coli* bacteria of strain ATCC11229 were used as a model pathogen to study bacteria deactivation by biocide loaded micelles, as described in Chapters 3 and 4 and by biocide emulsions described in Chapter 5.

*1.4.1. The Bacteria Cell*

The bacterial cell is surrounded by a lipid membrane, or cell membrane, which encloses the contents of the cell and acts as a barrier to hold nutrients, proteins and other essential components of the cytoplasm within the cell. A schematic representation of the bacterial structure is shown in Figure 1.5.<sup>135</sup> As they are prokaryotes, bacteria do not tend to have membrane-bound organelles in their cytoplasm and thus contain few large intracellular structures. Many important biochemical reactions, such as energy generation, occur by concentration gradients across membranes. The general lack of internal membranes in bacteria means reactions such as electron transport occur across the cell membrane between the cytoplasm and the periplasmic space.<sup>136</sup> Other proteins serve to import nutrients across the cell membrane, or expel undesired molecules from the cytoplasm. Bacteria do not have a membrane-bound nucleus, and their genetic material is typically a single circular chromosome located in the cytoplasm in an irregularly shaped body called the nucleoid.<sup>137</sup> The nucleoid contains the chromosome with associated proteins and RNA. Like all living organisms, bacteria contain ribosomes for the production of proteins.<sup>138</sup>

Flagella are rigid protein structures, about 20 nanometres in diameter and up to 20 micrometres in length that are used for mobility. Flagella are driven by the energy released by the transfer of ions down an electrochemical gradient across the cell membrane.<sup>142</sup> Fimbriae are fine filaments of protein, just 2–10 nm in diameter and up to several micrometers in length. They are distributed over the surface of the cell, and resemble fine hairs when seen under the electron microscope. Pili are cellular appendages that can transfer genetic material between bacterial cells.<sup>143</sup> Capsules are produced by many bacteria to surround their cells, and vary in structural



complexity, ranging from a disorganised slime layer of extra-cellular polymer, to a highly structured capsule. These structures can protect cells from engulfment by eukaryotic cells.<sup>144</sup> They can also act as antigens and be involved in cell recognition, as well as aiding attachment to surfaces and the formation of biofilms.<sup>144</sup>

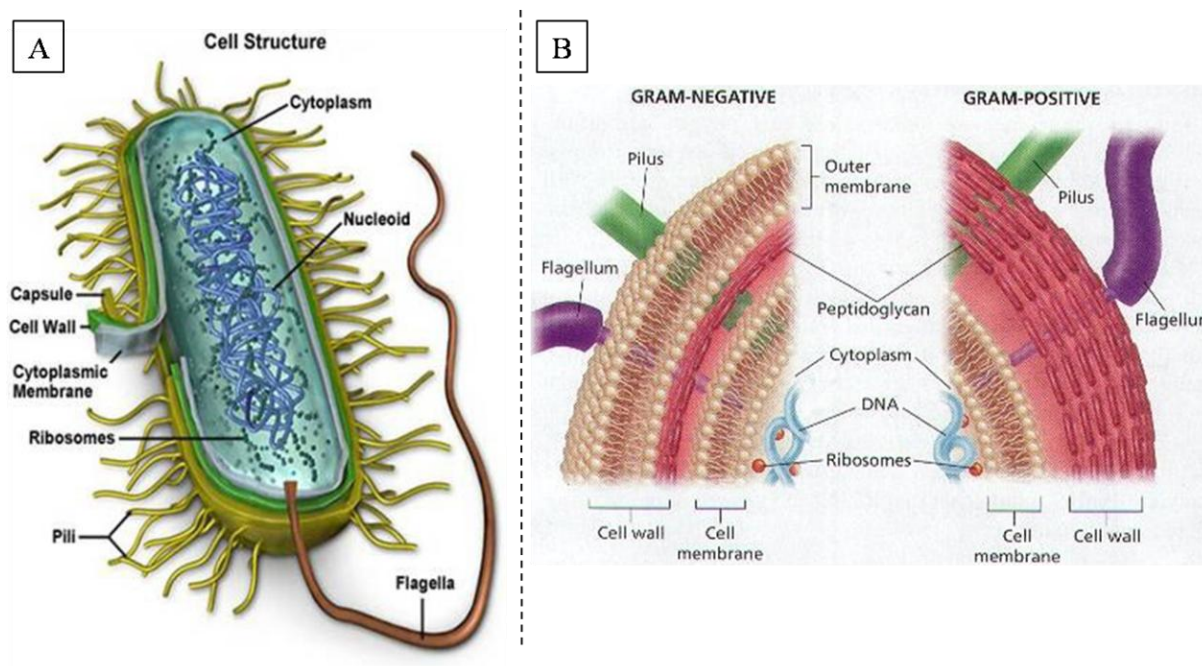


**Figure 1.5:** Schematic representation of A) bacterial inner structure, B) the cell wall of gram-negative (LHS) and gram-positive (RHS) bacteria (image taken from reference 135).

A bacterium very often moves using a flagella. Many bacteria (such as *E. coli*) have two distinct modes of movement: forward swimming movement and tumbling. Swimming bacteria frequently move near 10 body lengths per second. This makes them at least as fast as fish, on a relative scale.<sup>148</sup> The tumbling allows them to reorient and makes their movement a three-dimensional random walk.<sup>149</sup>

#### 1.4.2. The Cell Wall

The bacterial cell wall is located around the outside of the cell membrane. (Figure 1.5 A and B) Bacterial cell walls are made of peptidoglycan, which is made from polysaccharide chains cross-linked by unusual peptides containing D-amino acids.<sup>139</sup> The cell wall is essential to the survival of many bacteria, and the antibiotic penicillin is able to kill bacteria by inhibiting a step in the synthesis of peptidoglycan.<sup>140</sup>

There are two different types of cell wall in bacteria, called *Gram-negative* (e.g. *E. coli* bacteria) and *Gram-positive* (e.g. *Micrococcus Luteus* bacteria) (Figure 1.5. B). Gram positive and gram negative refers to how a bacteria reacts to a gram stain. Gram stain test, a counterstain (commonly safranin) is added after the crystal violet, coloring all Gram-negative bacteria with a red or pink color. On the other hand, Gram-positive bacteria will retain the crystal violet dye when washed in a decolorizing solution. The test itself is useful in classifying two distinct types of bacteria based on the structural differences of their cell walls. Gram-negative bacteria have a relatively thin cell wall consisting of a few layers of peptidoglycan surrounded by a second lipid membrane containing lipopolysaccharides and lipoproteins. The outer membrane prevents the initial stain from penetrating. In contrast, Gram-positive bacteria possess a thick cell wall containing many layers of peptidoglycan (a sugar-protein shell) that the stain can penetrate, and teichoic acids. Most bacteria have a Gram-negative cell wall.<sup>141</sup> Gram negative bacteria have overall negative charge.

### 1.4.3. Bacterial Reproduction

The increases in the size of bacteria (cell growth) and their reproduction by cell division are tightly linked in unicellular organisms. Bacteria grow to a fixed size and then reproduce through binary fission (a form of asexual reproduction).<sup>145</sup> Under optimal conditions (at 37°C and good access of oxygen), bacteria can grow and divide extremely rapidly, and bacterial populations can double every 9.8 min.<sup>146</sup> In cell division, two identical clone daughter cells are produced. In the laboratory, bacteria are usually grown using solid or liquid media. Solid growth media such as agar plates are used to isolate pure cultures of a bacterial strain. However, liquid growth media are used when measurement of growth or large volumes of cells are required.

Bacterial growth follows three phases. When a population of bacteria first enter a high-nutrient environment that allows growth, the cells need to adapt to their new environment; the first phase of growth is the *lag phase*, a period of slow growth when the cells are adapting to the high-nutrient environment and preparing for fast growth. The second phase of growth is the logarithmic phase - *log phase* (exponential phase). The log phase is marked by rapid exponential growth. During log phase, nutrients are metabolised at maximum speed until one of the nutrients is depleted and starts limiting growth. The final phase of growth is the *stationary phase* and is caused by depleted nutrients. The cells reduce their metabolic activity and consume non-essential cellular proteins.<sup>147</sup>

#### 1.4.4. Pathogenic Bacteria

If bacteria form a parasitic association with other organisms, they are classed as *pathogens*. Pathogenic bacteria are a major cause of human death and disease and cause infections such as tetanus, diphtheria, syphilis, cholera, food-borne illnesses, pneumonia, tuberculosis and others. Each species of pathogen has a characteristic spectrum of interactions with its human hosts. While some bacteria are part of the normal human flora, some, such as *Staphylococcus* or *Streptococcus*, can cause skin infections, pneumonia, meningitis and even overwhelming sepsis, a systemic inflammatory response producing shock, massive vasodilation and death.<sup>150</sup>

Bacterial infections may be treated with antibiotics, which are classified as *bactericidal* if they kill bacteria, or *bacteriostatic* if they just prevent bacterial growth. There are many types of antibiotics and each class inhibits a process that is different in the pathogen from that found in the host. An example of how antibiotics produce selective toxicity are chloramphenicol and puromycin, which inhibit the bacterial ribosome, but not the structurally different eukaryotic ribosome.<sup>151</sup> While antibiotics are used in treating disease, they may be contributing simultaneously to the development of antibiotic resistance in bacterial populations.<sup>152</sup> Infections can be prevented by antiseptic measures such as, for example, sterilizing the skin prior to piercing it with the needle of a syringe. Disinfectants such as bleach are used to kill bacteria or other pathogens on surfaces to prevent contamination and further reduce the risk of infection.

#### 1.4.5. Mechanisms of Bacteria Deactivation

Biocides are used to reduce populations of bacteria, a situation from which the microorganisms cannot easily recover. There are many different biocides, some of which have a wide range of

effects on different bacteria. They can be divided up into oxidising agents and non-oxidising agents. The main biocides used the present thesis are TCMTB, Triclosan, and poly(ethylene imine). All these above mentioned biocides are non-oxydising, and are described in more detail in sections 1.1.2.1. and 1.1.2.2.

TCMTB is an organo-sulphur compound. Such compounds act as biocides by inhibiting bacteria growth.<sup>22</sup> The energy is transferred in bacterial cells when iron reacts from  $\text{Fe}^{3+}$  to  $\text{Fe}^{2+}$ . Organo-sulphur compounds remove the  $\text{Fe}^{3+}$  by complexion as an iron salt. The transfer of energy is then stopped and immediate cell death follows.<sup>22</sup>

The mechanism of growth inhibition of *E. coli* bacteria by triclosan is known to be blocking of lipid synthesis in the bacteria.<sup>18</sup> The chlorinated phenolics first adsorb to the cell wall of the microorganisms by interaction involving hydrogen bonds. After adsorption to the cell wall, they diffuse into the cell where they go into suspension and precipitate proteins.<sup>22</sup>

Polyethylene imine contains secondary amines. These compounds are, generally, most effective against bacteria in alkaline pH ranges. They are positively charged and will thus bond to the negatively charged sites on the bacterial cell wall.<sup>22</sup> These electrostatic bonds will cause the bacteria to die of stresses in the cell wall. They also cause the normal flow of life-sustaining compounds through the cell wall to stop, by reducing its permeability.<sup>22</sup>

The topics such as bactericidal paper, bacteria deactivation, bactericidal agents, and the types of bactericidal agents used in the present study, as well as current commercial methods used for bacterial deactivation, are relevant to the present section. But since these topics have already been discussed in sections 1.1.1 and 1.1.2., they are omitted from the present section.

## **1.5. Objectives of the Thesis**

As mentioned in Introduction to the Thesis, the present study deals with a practical application of polymers in an area which is relatively unexplored, i.e. their application as carriers for hydrophobic bactericidal materials. The main objective of this dissertation was to find a strategy to prepare an antibacterial filter paper which would contain biocides of a hydrophobic nature and, therefore, of low water solubility. Since the saturation concentrations of these biocides in water are too low to kill the bacteria, the biocides had to be concentrated locally in the solution and a mechanism needs to exist to transfer them to the bacteria. Two approaches of preparation of bactericidal filter paper were explored in this work, such as using encapsulation of the biocide into amphiphilic block copolymer micelles, followed by attachment of the biocide loaded micelles to the pulp fibers of the filter paper (described in Chapters 2 to 4), and preparation of biocide emulsions stabilized by polymer or block copolymer micelles (described in Chapter 5).

Following the introduction in Chapter 1, Chapter 2 focuses on loading and release mechanism of a biocide in polystyrene<sub>197</sub>-block-poly (acrylic acid)<sub>47</sub> (PS<sub>197</sub>-b-PAA<sub>47</sub>) block copolymer micelles. The kinetics of loading of PS-b-PAA micelles, suspended in water, with thiocyanomethylthiobenzothiazole (TCMTB) biocide, and its subsequent release, was investigated. In addition, the glass transition temperature of polystyrene mixtures with TCMTB was determined, along with the partition coefficients of TCMTB in polystyrene and ethylbenzene in water. The detailed mechanisms of loading and release of TCMTB into and from the block copolymer micelles were elucidated and are described.

Chapter 3 deals with bactericidal block copolymer micelles in solution. The deactivation efficiencies of PS-b-PAA and polystyrene-block-poly(vinyl pyridine) (PS-b-P4VP) block

copolymer micelles, loaded with TCMTB and triclosan (TCN) biocides on *E. coli* bacteria were studied. Also, the mechanism of biocide transfer from micelles to the bacteria was investigated in aqueous solutions.

In Chapter 4 the preparation of the bactericidal filter paper is described. The efficiency of the filter paper containing PS-*b*-PAA block copolymer micelles loaded with triclosan was tested on *E. coli* bacteria. In addition, the parameters of the bactericidal filter paper affecting the efficiency of the bacteria deactivation were optimized and are discussed in Chapter 4. Finally, the mechanism of the biocide transfer from the loaded micelles on the filter paper to the bacteria was elucidated.

In Chapter 5 a description of the effects of two different stabilizers on the deactivation efficiency of bactericidal emulsions is given. This Chapter focuses specifically on finding stabilizing agents to prepare stable emulsions. The efficiencies in bacteria deactivation of those stable emulsions were studied as well. In addition, the kinetics of emulsion dissolution and mechanisms of bacteria deactivation using biocide emulsions were elucidated and are discussed in Chapter 5.

Finally, Chapter 6 summarizes the main conclusions drawn from this work, discusses contributions to the original knowledge, and outlines some suggestions for future studies.

It should be noted that the main techniques used in this dissertation were dynamic light scattering, scanning and transmission electron microscopy and UV-vis spectroscopy. These techniques are described in Appendices at the end of the thesis.

**References:**

- (1) Kabanov, A.V, Bartakova, E.V., Melik-Nubarov, N.S., Fedoseev, N.A., Dorodnich, T.Y., Alakhov, V.Y., Chekhonin, V.P., Nazarova, I.R., Kabanov, V.A., *J. Controlled Release*, **1992**, 22, 141.
- (2) Kwon. G., Naito, M., Yokoyama, M., Okano, T., Sakurai, Y., Kataoka, K.J., *J. Controlled Release*, **1997**, 48, 195.
- (3) Jones, M., Leroux, J., *Eur. J. Pharm., Biopharm.*, **1999**, 48, 101.
- (4) Allen, C., Han, J., Yu, Y., Maysinger, D., Eisenberg, A., *J. Controlled Release*, **2000**, 63, 275.
- (5) Savich, R., Luo, L., Eisenberg, A., Maysinger, D., *Science*, **2003**, 300, 615.
- (6) Gaucher, G., Dufresne, M.H., Sant, V.P., Kang, N., Maysinger, D., Leroux, J. Ch., *J. Controlled Release*, **2005**, 109, 165.
- (7) Akihiro, S., Takako, S., Miho, A., Hirokazu, M., Takuya, M., Hiroki, K., *J. of Antibacterial and Antifungal Agents*, **2003**, 31, 4, 173.
- (8) Sakura, O., Shoj, Y., Mikiko, G., Takashi, A., Kazuro, I., *Kuki Seijo to Kontamineshyon Kontororu Kenkyu Taikai Yokoshu*, **1999**, 17, 108.
- (9) Intilli, H.S., U.S. patent 4533435, 1985
- (10) United States Patent 3728213
- (11) U.S. patent 7201846, 2007
- (12) Japanese Patent JP06285314
- (13) <http://www.vestergaard-frandsen.com/lifestraw.htm>
- (14) <http://www.alloysafe.com/search.php?search=survival straw>
- (15) <http://www.airport.ca/news/Water-Purifier-for-Your-Travels-PRISTINE-Pioneer-mergency-Water-Filter-System-022497.php>
- (16) <http://www.campingsurvival.com/watpur.html>
- (17) [http://www.pesticideinfo.org/Detail\\_Chemical.jsp?Rec\\_Id=PC34528](http://www.pesticideinfo.org/Detail_Chemical.jsp?Rec_Id=PC34528)
- (18) [www.mindfully.org/Pesticide/Triclosan-Lipid-Synthesis](http://www.mindfully.org/Pesticide/Triclosan-Lipid-Synthesis)
- (19) Barbolt, T.A., *Surg Infect (Larchmt)*, **2002**, (3), Suppl 1:S45-53.
- (20) [www.sciencelab.com/xMSDS-Sodium\\_chloride-9927593](http://www.sciencelab.com/xMSDS-Sodium_chloride-9927593)



- (21) Manninen, A., Auriola, S., Vartiainen, M., Liesivuori, J., Turunen, T., Pasanen, M., *Arch Toxicology*, **1996**, 70, 579.
- (22) <http://www.lenntech.com/biocides.htm>
- (23) Cowie, J. M.G.: *Polymers: Chemistry and Physics of Modern Materials*; 2<sup>nd</sup> ed.; Chapman and Hall; New York, **1991**.
- (24) Szwarc, M.; *Carbanions, Living Polymers and Electron Transfer Process*; John Wiley and Sons Inc., **1968**.
- (25) Hiemenz, P.C.; *Polymer Chemistry The Basic Concepts*; Marcel Dekker; New York, **1984**
- (26) Elias, H.G., *An Introduction to Polymer Science*, 1<sup>st</sup>ed.; VCH Publishers, Inc., New York, **1997**
- (27) Zhang, L., Eisenberg, A.; *Science*, **1995**, 268, 1728.
- (28) Edward, Q.Z., Remsen, E., Wooley, K.L., *J. Am. Chem. Soc.* **2000**, 122, 3641.
- (29) Gao, Z; Eisenberg, A.; *Macromolecules*, **1993**, 26, 7353.
- (30) Velichkova, R. S., Christova, D. C., *Prog. Polym. Sci.*, **1995**, 20, 819.
- (31) Price, C., *Developments in Block Copolymers*, Goodman, I., Ed., Applied Science Publisher, New York, **1982**, 1, 39.
- (32) Liu, T., Liu, L.Z., Chu, B., *Amphiphilic Block Copolymers : Self Assembly and Applications*, Lindman, B., Ed., Elsevier, Amsterdam, **2000**, 115.
- (33) Yu, Y., Zhang, L., Eisenberg, A., *Langmuir*, **1997**, 13, 2578.
- (34) Zhang, L., Eisenberg, A.; *J.Am. Chem. Soc.*, **1996**, 118, 3168..
- (35) Hamley, I., *The Physics of Block Copolymers*; Oxford Science Publication: New York, **1998**.
- (36) Zhang, L., Eisenberg, A.; *Science*, **1995**, 268, 1728 –1731.
- (37) Cameron, N. S., Corbierre, M. K., Eisenberg, A.; *Can. J. Chem.*, **1999**, 77, 1311.
- (38) Shen, H.; Zhang, L.; Eisenberg, A; *J.Am. Chem. Soc.*, **1999**, 121, 2728.
- (39) Lim Soo, P., Eisenberg, A.; *J. Polym. Sci. Part B: Polym. Phys.*, **2004**, 42, 923.
- (40) Choucair, A., Eisenberg, A., *European Physical J. E*, **2003**, 10, 37.

- (41) Burge, S. E., Eisenber, A., *Langmuir*, **2001**, 17, 8341.
- (42) Zhang, L., Eisenberg, A.; *Macromolecules*, **1999**, 32, 2239.
- (43) Shen, H.; Zhang, L.; Eisenberg, A; *J. Phys. Chem. B*, **1997**, 101, 4697.
- (44) Shen, H.; Zhang, L.; Eisenberg, A; *J. Phys. Chem. B*, **1999**, 103, 9473.
- (45) Shen, H.; Zhang, L.; Eisenberg, A; *Macromolecules*, **2000**, 33, 2561.
- (46) Luo, L.; Eisenberg, A.; *J. Am. Chem. Soc.*, **2001**, 123, 5, 1012.
- (47) Luo, L.; Eisenberg, A.; *Angew. Chem. Int. Ed.*, **2002**, 41, 6, 1001.
- (48) Zhang, L., Eisenberg, A.; *Polym. Adv. Technol.*, **1998**, 9, 677.
- (49) Zhang, L., Eisenberg, A.; *J. Polym. Sci. Part B: Polym. Phys.*, **1999**, 37, 1469.
- (50) Allen, Ch., Maysinger, D., Eisenberg, A., *Coll. and Surf. B: Biointerfaces*, **1999**, 16, 3.
- (51) Nagarajan,R., Ganesh, K., *J. Chem. Phys.*, **1989**, 90, 5843.
- (52) Israelachvili, J. N., *Intermolecular and Surface Forces*, 2<sup>nd</sup> ed., Academic Press, London, **1992**.
- (53) Torchilin, V., *Drug Delivery Technology*, **2004**, 4, 2.
- (54) Kataoka, K., Nishiyama, N., *Pharmacology and Therapeutics*, **2006**, 112, 630.
- (55) Kataoka, K., Harada, A., Nagasaki, Y., *Advanced Drug Delivery Reviews*, **2001**, 47, 113.
- (56) Allen, Ch., Maysinger, D., Eisenberg, A., *Colloids and Surfaces B: Biointerfaces*, **1999**, 16, 3.
- (57) Gaucher, G., Dufresne, M.H., Sant, V.P., Kang, N., Mayisinger, D., Leourx, J.Ch., *J. Controlled Release*, **2005**, 109, 169.
- (58) Kataoka, K., Nishiyama, N., *Polymer Drugs in the Clinical Stage*, Ed. Madea, Kluwer Academic/Plenum Publishers, New York, **2003**.
- (59) Huh, K.M., Min, H.S, Lee, S.Ch., Lee, H.J., Kim, S., Park, K., *J. Controlled Release*, **2008**, 126, 122.
- (60) Miller, A.C., Bershteyn, A., Tan, W., Hammond, P.T., Cohen, R.E., Irvine, D.J., *Biomacromolecules*, **2009**, 10, 732.
- (61) Nagarajan, R., *Curr. Opin. Colloid Interface Sci.*, **1996**, 1, 391.

- (62) Haulbrook, W.R., Freerer, J.L., Hatton, T.A., Tester, J.W., *Environ. Sci. Technol.*, **1993**, 27., 2783.
- (63) Gref R, Minamitake Y, Peracchia MT, Trubetskoy V, Torchilin VP, Langer R. *Science*, **1994**; 263:1600-1603.
- (64) Lipinski CA, Lombardo F, Dominy BW, Feeney PJ., *Adv Drug Deliv Rev.*, **2001**;46:3-26.
- (65) Fernandez AM, Van Derpoorten K, Dasnois L, Lebtahi K, Dubois V, Lobl TJ, Gangwar S, Oliyai C, Lewis ER, Shochat D, Trouet A. *J Med Chem*, **2001**;44:3750-3753.
- (66) Shabner BA, Collings JM, eds. *Cancer Chemotherapy: Principles & Practice*, J.B. Lippincott Co: Philadelphia, PA; **1990**.
- (67) Hageluken A, Grunbaum L, Nurnberg B, Harhammer R, Schunack W, Seifert R., *Biochem Pharmacol*, **1994**;47:1789-1795.
- (68) Lipinski CA., *J Pharmacol Toxicol Met*, **2000**; 44:235-249.
- (69) Thompson D, Chaubal MV, *Drug Deliv Technol*, **2000**; 2:34-38.
- (70) Yalkowsky SH, ed. *Techniques of Solubilization of Drugs*. Marcel Dekker, Inc: New York and Basel; **1981**.
- (71) Lasic DD, Mixed micelles in drug delivery, *Nature*, **1992**;355:279-280.
- (72) Hammad MA, Muller BW, *Eur J Pharm Sci.*, **1998**;7:49-55.
- (73) Jones M, Leroux J, *Eur J Pharm Biopharm*, **1999**;48:101-111.
- (74) Torchilin VP., *J Contr Release*, **2001**;73:137-172.
- (75) Gabizon AA., *Adv Drug Deliv Rev*, **1995**;16:285-294.
- (76) Lukyanov AN, Hartner WC, Torchilin VP., *J Contr Release*, **2004**;94:187-193.
- (77) Maeda H, Wu J, Sawa T, Matsumura Y, Hori KJ., *J Contr Release*, **2000**;65:271-284.
- (78) Maeda H, Sawa T, Konno TJ., *J Contr Release*, **2001**;74:47-61.
- (79) Nagarajan, R., Barry, M., Ruckenstein, E., *Langmuir*, **1986**, 2, 210.
- (80) Gadelle, F., Koros, W.J., Schechter, R.S., *Macromolecules*, **1995**, 28, 4883.

- (81) Nagarajan, R., Ganesh, K., *Macromolecules*, **1989**, 22, 4312.
- (82) Hunter, P.N., Hatton, T.A., *Langmuir*, **1992**, 8, 1291.
- (83) Kozlov, M.Y., Melik-Nubarov, N.S., Bartakova, E.V., Kabanov, A.V., *Macromolecules* **2000**, 33, 3305.
- (84) Xing, L., Mattice, W.L., *Macromolecules*, **1997**, 30, 1711.
- (85) Giacomelli, C., Schmidt, V., Borsali, R., *Langmuir*, **2007**, 23, 6947.
- (86) Lim-Soo, P., Luo, L., Davidson, P., Maysinger, D., Eisenberg, A., *Mol. Pharm.*, **2005**, 2, 519
- (87) Singh, L.; Ludovice, P. J.; Henderson, C.; *Thin Solid Films*, **2004**, 449, 231.
- (88) Fox, T. G.; *Bul. Am. Phys. Soc.*, **1956**, 1, 123.
- (89) Alfrey, T., Gurnee, E.F., Lloyd, W.G., *J. Polymer Sci.*, **1966**, 12, 249.
- (90) Zhou, Q.Y., Argon, A.S., Cohen, R.E., *Polymer*, **2001**, 42, 613.
- (91) Thomas NL, Windle AH., *Polymer*, **1978**,19,255.
- (92) Thomas NL, Windle AH., *Polymer*, **1981**,22,627.
- (93) Thomas NL, Windle AH., *Polymer*, **1982**,23,529
- (94) Hui CY, Wu KC, Lasky RC, Kramer EJ., *J Appl Phys*, **1987**,61,5129.
- (95) Hui CY, Wu KC, Lasky RC, Kramer EJ., *J Appl Phys*, **1987**,61,5137.
- (96) Lasky RC, Kramer EJ., *Polymer*, **1988**,29,637.
- (97) Rossi G, Pincus PA, De Gennes PG., *Europhys Lett*, **1995**,32,391.

- (98).Li, J.-X., Lee, P.I., *Polymer*, **2006**, 47, 7726.
- (99) Choucair, A.; Eisenberg, A.; *JACS*, **2003**, 125, 39, 11993.
- (100) Choucair, A.; Lim Soo, P.; Eisenberg, A.; *Langmuir*, **2005**, 21, 9308.
- (101) Kwon, G., Naito, M., Yokoyama, M., Okano, T., Sakurai, O., Kataoka, K., *J. Controlled Release* **48**, **1997**, 195.
- (102) La, S.B., Okano, T., Kataoka, K., *J. Pharm. Sci.*, **1996**, 85, 85.
- (103) Kim, S.Y., Shin, G.I., Lee, Y.M., Cho, C.S, Sung, Y.K., *J. Controlled Release*, **1998**, 51, 13.
- (104) J.M.G. Cowie, *Polymers: Chemistry and Physics of Modern Materials*, 2nd Edition, Blackie Academic and Professional, New York, **1994**.
- (105) Teng, Y., Morrison, M.E., Munk, P., Webber, S.E., *Macromolecules*, **1998**, 31, 3578.
- (106) B.D. Ratner, A.S. Hoffman, F.J. Schoen, J.E. Lemons, *Biomaterials Science: An Introduction to Materials in Medicine*, Academic Press, New York, **1996**.
- (107) Hunter, R.J., *Introduction to Modern Colloid Science*, Oxford University Press, **1993**.
- (108) Hiemenz, P.C., *Principles of Colloid and Surface Chemistry*, 2<sup>nd</sup> edition, Marcel Dekker, Inc., New York and Basel, **1986**.
- (109) McClements, *Food Hydrocolloids*, **1999**, 13, 419.
- (110) [www.nano.med.umich.edu/Platforms/Adjuvant-Vaccine-Developement.html](http://www.nano.med.umich.edu/Platforms/Adjuvant-Vaccine-Developement.html).
- (111) [www.eurekalert.org/pub\\_releases/2008-02/uomh-nvs022608.php](http://www.eurekalert.org/pub_releases/2008-02/uomh-nvs022608.php).
- (112) Hanson, J.A., Chang, C.B., Graves, S.M., Li, Z., Mason, T.G., Deming, T.J., *Nature*, **2008**, 455, 85.
- (113) Baeurle, S.A., Kroener J., *J. Math. Chem.*, **2004**, 36, 409.
- (114) Aulton, M. E., *Aulton's Pharmaceutics: The Design and Manufacture of Medicines* (3rd ed.). Churchill Livingstone, **2007**.
- (115) Troy, D. A., Remington, J. P., Beringer, P., *Remington: The Science and Practice of Pharmacy* (21st ed.). Philadelphia, Pennsylvania, USA: Lippincott Williams & Wilkins, **2006**.
- (116) Riess, G., Labbe, C., *Macromol. Rapid Commun.*, **2004**, 25, 401.

- (117) Molau, G. E., *Colloidal and Morphological Behavior of Block and Graft Copolymers*, in: *Block Copolymers*, S.L. Aggarwal, Ed., Plenum Press, New York, **1970**, 79.
- (118) Price, C., *Colloidal Properties of Block Copolymers*, in: *Developments in Block Copolymers 1*, S. L. Aggarwal, Ed., Applied Science, London, **1982**, 39.
- (119) Piirma, I., *Polymeric Surfactants*, in: *Surfactant Science Series 42*, Marcel Dekker, New York, **1992**, 1.
- (120) Tuzar, Z., Kratochvil, P., *Micelles of Block and Graft Copolymers in Solution*, in: *Surface and Colloid Science*, E. Matijevic, Ed., Plenum Press, New York, **1993**, Vol. 15, 1, 1.
- (121) Riess, G., Dumas, P., Hurtrez, G., *Block Copolymer Micelles and Assemblies*, in: *MML Series 5*, Citus Books, London, **2002**, 69.
- (122) Alexandridis, P., Hatton, T.A., *Block Copolymers*, in: *Polymer Materials Encyclopedia 1*, CRC Press, Boca Raton, **1996**, 743.
- (123) Alexandridis, P., Lindman, B., *Amphiphilic Block Copolymers: Self Assembly and Applications*, Elsevier, Amsterdam, **2000**, 1.
- (124) Amalvy, J.I., Armes, S.P., Brinks, B.P., Rodrigues, J. A., G. F. Unali, G. F., *Chem. Commun.*, **2003**, 15, 1826.
- (125) Coen, E.M., Lyons, R.A., Gilbert, R.G., *Macromolecules*, **1996**, 29, 5128.
- (126) Burguiere, C., Pascual, S., Bui, Ch., Vairon, J.-P., Charleux, B., Davis, K.A., Matyjaszewski, K., Betremieux, I., *Macromolecules*, **2001**, 34, 4439.
- (127) Muller, H., Leube, W., Tauer, K., Forster, S., Antoinety, M., *Macromolecules*, **1997**, 30, 2288.
- (128) Barnes, T.J., Prestidge, C.A., *Langmuir*, **2000**, 16, 4116.
- (129) Kralchevsky, P.A., Ivanov, I.B., Ananthapadmanabhan, K.P., Lips, A., *Langmuir*, **2005**, 21, 50.
- (130) European Patent 1508276, Lipiecki, F.J., Maroldo, S.G., Pendell, B.J., Simon, E.S., Rohm and Hass, **2005**.
- (131) Whitman, W.B., Coleman, D.C., Wiebe, W.J, *Proceedings of the National Academy of Sciences of the United States of America*, **1998**, 95, 12, 6578.
- (132) Sears, C.L., *Anaerobe*, **2005**, 11, 5, 247.
- (133) Ishige, T., Honda, K., Shimizu, S., *Current Opinion in Chemical Biology*, **2005**, 9, 2, 174.

- (134) Woese ,C.R., Kandler, O., Wheelis, M.L *Proceedings of the National Academy of Sciences of the United States of America* , **1990**, 87, 12, 4576.
- (135) [http://silverfalls.k12.or.us/staff/read\\_shari/mysite/chapter\\_24\\_AB.htm](http://silverfalls.k12.or.us/staff/read_shari/mysite/chapter_24_AB.htm)
- (136) Harold, F.M., *Bacteriological Reviews*, **1972**, 36, 2, 172.
- (137) Thanbichler, M., Wang, S., Shapiro, L., *J. Cell. Biochem.*, **2005**, 96, 3, 506.
- (138) Poehlsgaard, J., Douthwaite, S., *Nat Rev Microbiol*, **2005**, 3, 11, 870.
- (139) van Heijenoort, J., *Glycobiology*, **2001**, 11, 3, 25R.
- (140) Koch, A., *Clin Microbiol Rev.*, **2003**, 16, 4, 673.
- (141) Walsh, F., Amyes, S., *Curr Opin Microbiol*, **2004**, 7, 5, 439.
- (142) Kojima, S., Blair, D., *Int Rev Cytol.*, **2004**, 233, 93.
- (143) Silverman, P., *Mol Microbiol.*, **1997**, 23, 3, 423.
- (144) Stokes, R., Norris-Jones, R., Brooks, D., Beveridge, T., Doxsee, D., Thorson, L.,. *Infect Immun*, **2004**, 72, 10, 5676.
- (145) Koch, A., *Crit Rev Microbiol* , **2002**, 28, 1, 61.
- (146) Eagon, R.G., *Journal of Bacteriology*, **1962**, 83, 4, 736.
- (147) Hecker, M., Völker, U., *Adv Microb Physiol*, **2001**, 44, 35.
- (148) Dusenbery, D. B., *Living at Micro Scale*, p. 136. Harvard University Press, Cambridge, Mass., **2009**.
- (149) Wu, M., Roberts, J., Kim, S., Koch, D., DeLisa, M., *Appl Environ Microbiol*, **2006**, 72, 7, 4987.
- (150) Fish, D., *Am J Health Syst Pharm.*, **2002**, 59, 1., S 13.
- (151) Yonath, A., Bashan, A., *Annu Rev Microbiol*, **2004**, 58, 233.
- (152) Khachatourians, G.G., *CMAJ*, **1998**, 159, 9, 1129.
- (153) Kubitschek, H.E., *J. Bacteriol.*, **1990**, 172, 1, 94–101.
- (154) Vogt, R.L., Dippold, L. *Public Health Rep.*, **2005**, 120, 2, 174.

- (155) Bentley, R., Meganathan, R., *Microbiol. Rev.*, **1982**, 46, 3, 241.
- (156) Hudault, S., Guignot, J., Servin, A.L., *Gut*, **2001**, 49,1,47.
- (157) Reid, G., Howard, J., Gan, B.S., *Trends Microbiol.*, **2001**, 9, 424.



## **Chapter 2:**

# **Loading and Release Mechanisms of a Biocide in PS-*b*-PAA Block Copolymer Micelles**

---

### **Abstract**

The kinetics of loading of polystyrene<sub>197</sub>-block-poly (acrylic acid)<sub>47</sub> (PS<sub>197</sub>-*b*-PAA<sub>47</sub>) micelles, suspended in water, with thiocyanomethylthiobenzothiazole (TCMTB) biocide, and its subsequent release was investigated. Loading of the micelles was found to be a two step process. First, the surface of the PS core of the micelles is saturated with biocide, with a rate determined by the transfer of solid biocide to micelles during transient micelle – biocide contacts. Next, the biocide penetrates as a front into the micelles, lowering the  $T_g$  in the process (Non-Fickian case II diffusion). The slow rate of release is governed by the height of the energy barrier which a biocide molecule must overcome to pass from the PS into the water, resulting in a uniform biocide concentration within the micelle, until the  $T_g$  is increased to the point that diffusion inside the micelles becomes very slow. Maximum loading of biocide into micelles is around 30 % (w/w) and is achieved in one hour. From partition experiments it can be concluded that the biocide has a similar preference for polystyrene as for ethylbenzene over water, implying that the maximum loading is governed by thermodynamics.

*\* Reproduced in part with permission from Journal of Physical Chemistry B, 2008, 112, 8477.  
Copyright 2008 American Chemical Society.*

## 2.1. Introduction

Self-assembling colloidal aggregates have been receiving much attention as a potential carriers for biologically active ingredients, specifically drugs.<sup>1-8</sup> It is well known that amphiphilic block copolymers have the ability to self-assemble into ordered structures, such spherical micelles, when dissolved in selective solvents (i.e., solvents thermodynamically poor for one block and good for the other).<sup>9-13</sup> In polar solvents the hydrophilic blocks of the polymer form the corona of the micelle, while the core consists of the hydrophobic blocks.

Many studies revealed that the core structure and composition enables the micelles to take up poorly water soluble materials; thus, they can be used as nanocontainers for hydrophobic materials in aqueous media, while the outer shell serves as a stabilizing interface between the hydrophobic core and the external medium.<sup>14-24</sup> By the use of micelles the solubility of hydrophobic materials in aqueous medium is greatly increased. For example, Wilhelm *et al.*<sup>14</sup> investigated partitioning of hydrophobic pyrene (Py) between the aqueous medium and polystyrene-block-poly(ethylene oxide) block copolymer micelles. Zhao *et al.*<sup>15</sup> discuss the partitioning of Py between PS<sub>500</sub>-*b*-PAA<sub>60</sub> crew-cut micelles and water/DMF solvent mixtures. Xing *et al.*<sup>16</sup> studied ABA type triblock micelle – solvent partition coefficient of small solubilize molecules in the solvents which selectively solvate the middle block of triblock copolymer.

More recently, Cho *et al.*<sup>17</sup> reported on the preparation of self-assembled nanoporous multilayered films of polystyrene-block-poly(4 vinyl pyridine) (PS-*b*-P4VP) and PS-*b*-PAA with tunable optical properties, where a water-insoluble photochromic dye was incorporated into the hydrophobic PS core. Giacomelli *et al.*<sup>18</sup> reported on improvement of the loading capacity of block copolymer micelles by specific interactions between hydrophobic guest molecules and

core-forming segments. In case of probes containing weak carboxylic acid groups the achieved loading capacities were high (> 100% weight/weight of polymer).<sup>18</sup> The hydrodynamic size of micelles increased by a factor of two due to high micelle loadings and, in some cases, the morphology even changed from micelles to cylinders.<sup>18</sup> Lee *et al.*<sup>19</sup> studied loading and release of a hydrophobic drug in poly(ethylene oxide)-poly(lactide) (PLA) block copolymers containing a small quantities of carboxylic acid in the hydrophilic PLA block. It was found that the loading efficiency increased with increasing carboxylic acid content in the block copolymer while the release of the drug was slower from micelles containing higher amounts of carboxylic acid in the copolymer.<sup>19</sup> Such results are attributed to the interactions between the carboxylic group of copolymers and the drug.<sup>19</sup>

When trying to load micelles as quickly as possible under industrial conditions, the kinetics and mechanism of loading becomes important;<sup>20</sup> on the other hand the kinetics and mechanism of release is important in assessing potential applications. Several studies have recently dealt with kinetics of loading and release of hydrophobic material into and from block copolymer micelles.<sup>18,20-24</sup> Xiangiang *et al.*<sup>21</sup> studied loading and release of hydrophobic anticancer drug doxorubicin (Dox) into polymeric micelles of N-Succinyl-N'-octyl chitosan (SOC). It was found<sup>21</sup> that the loading content of Dox increased with increasing drug-to-carrier ratio. Stevenson –Abouelnasr *et al.*<sup>22</sup> reported on the kinetics of the release of Dox from Pluronic P105 micelles during ultrasonication. The mechanism causing the release into solution was proved to be the destruction of the micelles during sonication.<sup>22</sup> Allen *et al.*<sup>23</sup> investigated the loading and release kinetics of dihydrotestosterone (DHT) into block copolymer micelles of poly(caprolactone)-b-poly(ethylene oxide). A high loading capacity for DHT in micelles was found<sup>23</sup> and the release profile of the drug from the micelle solution involved a slow steady release which continued over

a period of one month. The release kinetics of hydrophobic probes of pyrene and phenanthrene from block copolymer micelles of polystyrene-*b*-poly(methacrylic acid) and poly(2-vinylpyridine-*b*-poly(ethylene oxide) was studied by Teng *et al.*<sup>24</sup> The release was analyzed by a model of diffusion out of a sphere; diffusion constants were found to depend on both the core and the probe and were very small.<sup>24</sup> The mechanism of probe release from the block copolymer micelles reported by Giacomelli *et al.*<sup>18</sup> is governed by diffusion within the micelle. Thus, while there are a number of studies of kinetics of loading and release, to our knowledge, no publications deal with the detailed mechanisms of loading of hydrophobic material into block copolymer micelles.

In this paper we discuss the preparation of biocide loaded block copolymer micelles and the kinetics and mechanisms of the uptake and release of a particular biocide. The present study is part of a collaborative research project within a network on bioactive paper, which has as its objective to capture, detect and deactivate pathogens, using paper as a substrate. Part of the strategy is to incorporate biocides into paper to deactivate bacteria. Our approach is based on loading a hydrophobic antibacterial agent, thiocyanomethylthiobenzothiazole (TCMTB), into amphiphilic block copolymer micelles to increase the biocide concentration locally. TCMTB was chosen for this project because it is already used in pulp and paper applications and is FDA approved. Micelles selected for this project are prepared from PS<sub>197</sub>-*b*-PAA<sub>47</sub> amphiphilic block copolymer and consist of a hydrophobic polystyrene core and a hydrophilic poly(acrylic acid) (PAA) corona. The hydrophobic biocide preferentially partitions into the hydrophobic micelle core. It should be noted that TCMTB and PS<sub>197</sub>-*b*-PAA<sub>47</sub> are used as model materials to understand the mechanisms of loading and release of a hydrophobic probe into block copolymer micelles. The PS-*b*-PAA micelle system is very well explored from the point of view of

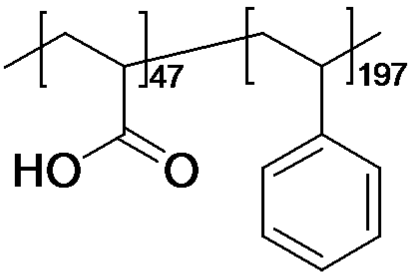
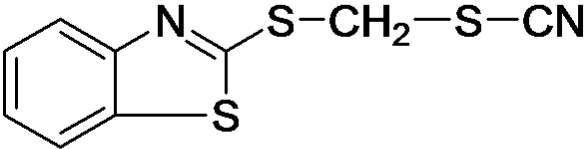
preparation of micelles and their characteristics, and studies have been performed on uptake of hydrophobic materials, their release and their localization within the micelle.<sup>14, 25</sup>

In the present paper we report specifically on the characterization of the micelles with and without biocide, on the kinetics of filling micelles with biocide and the release of the biocide from the micelles in an aqueous environment. Also, we discuss the localization of the biocide within the micelles; finally a mechanism of loading and release of biocide into and out of the micelles is proposed.

## **2.2. Experimental Section**

### *2.2.1. Materials*

The amphiphilic block copolymer of PS<sub>197</sub>-*b*-PAA<sub>47</sub> (Figure 1) was synthesized using atom transfer radical polymerization.<sup>26-29</sup> The number average molar mass ( $M_n$ ) of the polymer is 28900 and its polydispersity index is 1.10. TCMTB, the antibactericidal material (biocide), was provided by Buckman laboratories. The structure and properties of this slightly water-soluble material are also shown in Figure 2.1. The size of biocide grains was measured by confocal microscopy using the Sigma Scan image analysis. The average diameter was found  $1.7 \pm 0.3 \mu\text{m}$ . Dioxane was purchased from Sigma-Aldrich (HPLC grade) and used as received. The pH of the deionized water used in all experiments was approximately 6.

	
Polymer	Antibacterial material (biocide)
PS <sub>197</sub> - <i>b</i> -PAA <sub>47</sub> Poly(styrene) <sub>197</sub> - <i>b</i> - Poly(acrylic acid) <sub>47</sub>	TCMTB (Thiocyanomethylthiobenzothiazole)
$M_w$ =28 900 g/mol	$M_w$ =238 g/mol
Amphiphilic block copolymer	Water solubility = 12.7 mg /L

**Figure 2.1.** Structure and properties of polymer and biocide used

### 2.2.2. Micelle Preparation

PS<sub>197</sub>-*b*-PAA<sub>47</sub> block copolymer was dissolved in dioxane, a good solvent for both blocks. The initial block copolymer concentration was 1% (w/w). The sample was then stirred over night to ensure complete dissolution of the polymer. To induce self-assembly into micelles, milli-Q water was added drop-wise at a rate of 0.2 % (w/w)/min. Water addition was continued until a final water concentration of 50 % (w/w) was reached. The water concentration determines the resulting morphology.<sup>30</sup> Under these conditions only micelles are formed, no other morphology is observed. The solution was quenched into a large excess of water in order to freeze the aggregate morphology, and dialyzed for a period of three days to remove the organic solvent (dioxane).

### 2.2.3. Characterization of the Micelles

Transmission electron microscopy (TEM) and dynamic light scattering (DLS) were employed to characterize the micelles. The micelles are composed of a hydrophobic polystyrene core and a hydrophilic poly(acrylic acid) corona. A schematic drawing of the micelle composition is shown in Figure 2.2.

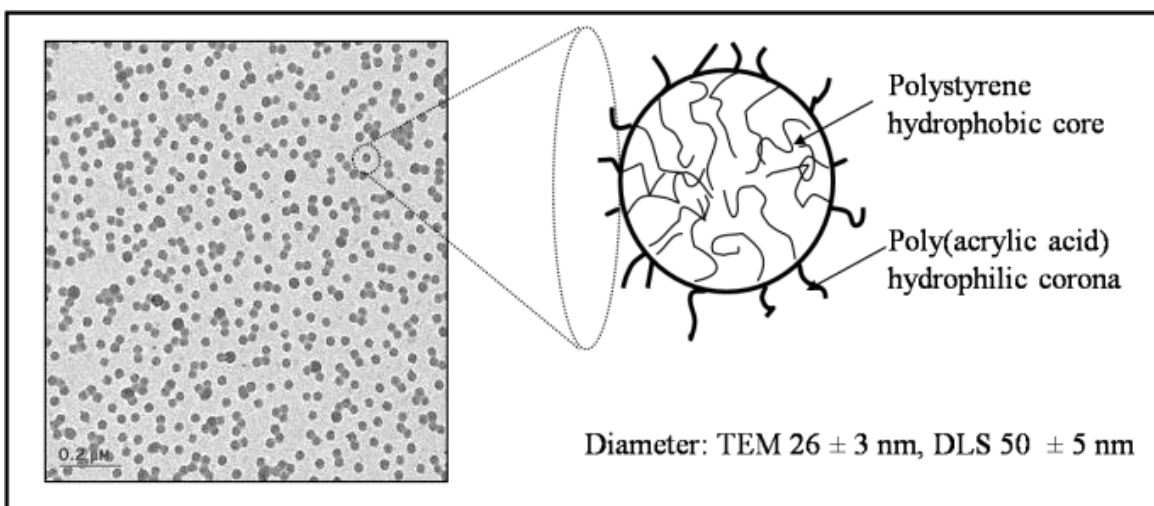


**Figure 2.2.** TEM image of PS<sub>197</sub>-*b*-PAA<sub>47</sub> micelles with schematic representation of micellar structure.

#### 2.2.3.1. Transmission Electron Microscopy

TEM was one of the techniques used to characterize the micelles. Samples for the TEM studies were prepared from the micellar solutions by applying one drop of the solution to a copper grid, which had been pre-coated with 0.5 % formvar solution and a layer of carbon. The drop was allowed to evaporate over night. TEM (without using any staining) was performed on a JEOL microscope model JEM 2000FX.<sup>31-32</sup> The average size of the micelles was evaluated from TEM images using the Sigma Scan image analysis.

#### 2.2.3.2. Dynamic Light Scattering

In addition to electron microscopy dynamic light scattering was used to determine the diameter of the micelles. The light scattering experiments were performed on a Brookhaven light scattering instrument with a BI9000 AT digital correlator. The data were collected by monitoring the scattered light intensity at a 90° scattering angle at 25 °C. The micelle solutions were prepared as described above in section 2.2.2.

#### 2.2.4. *Micelle Loading*

Upon completion of the dialysis of the micelle solution, the micelles were loaded with the TCMTB biocide. Prior to loading the biocide was dissolved in 2 mL acetone to a concentration of 5 mg/mL and placed in a vial. Acetone was allowed to evaporate over night from the vial, leaving a thin film of the biocide inside. The micelle solutions (10 mg of polymer in 10 mL) were afterwards transferred to the vials containing the biocide film and vigorously stirred for a period of 1 hour to achieve maximum loading. The excess of biocide was removed by a 0.45 µm filter. The kinetics of loading and release will be discussed in sections 2.3.4. and 2.3.5. It should be noted that it is a common practice to load micelles from a film<sup>25</sup> rather than loading from grains (granules), which is not as efficient. To our knowledge no explanation of the reason why loading from a film is so successful, has been given in the literature.

##### 2.2.4.1. UV-vis Spectroscopy

The concentration of the biocide in the loaded micelles was evaluated using UV-vis spectroscopy. All UV measurements were performed on a Varian UV-vis spectrophotometer (model Cary 300 Bio). First, a calibration curve of the absorbance vs. concentration for various



known biocide concentrations in dioxane/water 95/5 % (w/w) was constructed at three various wavelengths which show peaks in the spectrum at 300.2, 290.0 and 280.4 nm; absorbance increases linearly with the concentration. Samples of unknown biocide concentrations were also dissolved in dioxane/water ratio at 95/5 % (w/w), (in such mixture the micelles are completely dissolved) and then compared to the calibration curves.

It should be noted that UV-vis spectra of PS<sub>197</sub>-*b*-PAA<sub>47</sub> micelles without biocide show a low PS peak at wavelengths lower than those used for the preparation of the calibration curves; this peak does not interfere with the biocide spectra.

#### *2.2.5. Kinetics of Micelle Loading*

The unloaded micelles were added to a vial with biocide film and stirred. 250  $\mu$ L aliquots of the samples were taken from the bottom of the vial at given times for a period of 3 hours, and then were filtered (using a 0.45  $\mu$ m filter and a disposable syringe) into separate, clean vials. From each filtered sample, a 125  $\mu$ L aliquot was taken and added to dioxane to prepare 95/5 % (w/w) dioxane/sample solution; the absorbance of each sample was then measured at 300.2, 290.0 and 280.4 nm. The biocide content in the micelles was evaluated using the calibration curves (as described in section 2.2.4.1.).

#### *2.2.6. Kinetics of Release of Biocide from Micelles*

A sample of the loaded micelles was inserted into a dialysis bag and then placed into a container with 15 L of milli-Q water. 250  $\mu$ L aliquots of the sample were taken at given times for a period of 30 hours. The sample aliquots were afterwards added to dioxane to prepare a 95/5 % (w/w) dioxane/sample solution and then tested using UV-vis for their absorbance at 300.2, 290.0

and 280.4 nm. The results were then compared with calibration curves and the biocide content in the micelles was calculated.

#### *2.2.7. $T_g$ of PS/Biocide Mixtures*

Polystyrene and biocide were co-dissolved in dioxane in various styrene/biocide ratios (100, 95, 90, 85, 80, 70 and 60 % (w/w) of styrene in the mixture). The samples were freeze-dried to obtain solid mixtures. Glass transition temperatures of the samples were measured using differential scanning calorimeter model Q1000 from TA Instruments. The vapor pressure of the biocide is much smaller than that of dioxane ( $8.6 \times 10^{-7}$  vs. 37 Torr at 25 °C). Therefore no biocide loss is expected during freeze drying.

#### *2.2.8. Partition Coefficients*

The partition coefficient of biocide between ethylbenzene (EB), a low molecular weight analog of PS, and water was measured in order to determine the relative affinity of the antibacterial material for the polystyrene micelle core versus the aqueous solution.<sup>25,33</sup> A set of various known concentrations of biocide were dissolved in 5 mL of ethylbenzene, mixed with 5 mL of water and stirred. Each mixture, which consists of two immiscible phases, was stirred for a few minutes. The ethylbenzene phase was then allowed to separate over night from the aqueous phase and the concentration of biocide was evaluated in each phase of each sample using UV-vis spectroscopy. The ethylbenzene-water partition coefficient for each sample,  $K_{EB/water}$ , was then calculated using the following equation:

$$K_{EB / water} = \frac{C_{EB}}{C_{water}} \quad (1)$$

where  $c_{EB}$  is the concentration of biocide in the EB phase and  $c_{water}$  is concentration of biocide in the water phase. Ethylbenzene was chosen as a model solvent due to its structural similarity to the styrene repeat unit. It should be noted that polystyrene, of which the micelle core is composed, most likely has different solubility properties than those of ethylbenzene. Therefore, the solubility of TCMTB biocide in ethylbenzene should be considered as only an approximation for the solubility for the antibacterial material in the polystyrene micelle core.

## **2.3. Results and discussion**

### *2.3.1. Size of the Micelles and their Core and Corona*

The average diameter of the micelles is  $26 \pm 3.0$  nm (based on 2048 counts), evaluated from TEM micrographs using Sigma Scan image analysis. This average diameter includes both the PS core and the surrounding PAA corona in a collapsed state. The estimated diameter of the micelle core is 24.6 nm, since the calculated thickness of the collapsed corona is about 0.7 nm. The thickness of the collapsed corona is calculated from the volume of 250 PAA chains surrounding the core. A representative TEM picture of unloaded PS<sub>197</sub>-*b*-PAA<sub>47</sub> micelles is shown in Figure 2.2.

DLS revealed that the average effective diameter of the micelles before loading is  $50 \pm 5$  nm. The micelle diameter measured by DLS is about twice as large as that measured from TEM. The difference in micelle size measured by DLS and TEM can be explained by the fact that the corona is collapsed in TEM while in DLS the corona is expanded. Furthermore, TEM represents a number average diameter while DLS represents a z-average. At pH 6 PAA is highly expanded (as “brushes”); the planar zig-zag length of PAA<sub>47</sub> is estimated to be about 12 nm, accounting for most of the difference between TEM and DLS.

### 2.3.2. TCMTB Saturation Concentration

TCMTB biocide is a hydrophobic, very slightly water soluble white crystalline material. To determine the saturation concentration of the biocide in water, 0.025 % (w/w) of biocide was placed in milli-Q water. In order to dissolve the biocide, the solution was heated while stirring and then cooled. The undissolved excess of biocide in the samples was removed by two different methods. In the first sample, the excess was removed by filtering using 0.45  $\mu\text{m}$  filters, while in the second, it was centrifuged out. The saturation concentration of the biocide in the samples was examined independently using the 50/50 % (w/w) dioxane/water calibration curve. Biocide saturation concentrations found in the two sets of samples were similar, 14.0 mg/L and 11.4 mg/L, respectively. For subsequent calculations, the average of 12.7 mg/L was used.

### 2.3.3. Maximum Adsorption Capacity of Biocide on the Surface of the Micelle Core

The number of biocide molecules needed to cover totally the micellar surface area is estimated from

$$N_b A_b = 4\pi R_n^2 \quad (2)$$

where  $N_b$  is the number of biocide molecules on the external surface of a micelle core at saturation,  $A_b$  is the area of an adsorbed biocide molecule and  $R_n$  is the radius of the micelle core. Any adsorption in excess of this value must involve biocide located inside the PS core. For this calculation, the area of one biocide molecule was estimated (using a molecular model), the number of biocide molecules accommodated on one micelle was calculated, and finally, the maximum percentage of biocide adsorbed on the surface relative to the total amount taken up was estimated. The micelles have an average diameter of ca. 26 nm, as determined by TEM. This average diameter includes both the PS core and the surrounding PAA corona in a collapsed state.

Since the biocide would be adsorbed on the core of the micelle, for further calculations the radius of the micelle core, which was estimated as 12.3 nm, was used because the thickness of the collapsed corona is about 0.7 nm (see section 2.3.1.). The micellar interfacial area, calculated on the basis of the radius of the PS core, is  $1.93 \times 10^3 \text{ nm}^2/\text{micelle}$ . The average aggregation number, estimated from the volume of PS per micelle, is about 250 chains/micelle, and thus the weight of one micelle is  $1.2 \times 10^{-20} \text{ kg}$ . Assuming a 1.5 Å bond length between the atoms in TCMTB and similar distance of closest approach between them,  $A_b \approx 10 \times 4 \times 2.25 \approx 90 \text{ Å}^2$  and thus the number of biocide molecules on the surface of micelles at saturation is  $2.1 \times 10^3$  biocide molecules. Because the molar mass is 238, the maximum adsorption of biocide on the external micelle core surface at saturation is approximately 8 % (w/w). This estimate is for close-packed molecules. Random packing will lower this estimate by about half.

#### 2.3.4. Kinetics of Micelle Loading

##### 2.3.4.1. Depletion of Biocide Molecules from Solution

The time required for all biocide molecules in the water (12.7 mg/L – saturation value) to be taken up by the micelles was estimated as follows: The number of biocide molecules colliding with a single micelle per second is estimated from the Smoluchowski equation:<sup>34</sup>

$$J = \frac{2kT}{3\eta} \frac{(a_1 + a_2)^2}{a_1 a_2} n \cong \frac{2kTn}{3\eta} \frac{a_1}{a_2} \approx 33 \frac{kT}{\eta} n \quad (3)$$

where  $a_1$  is the radius of the micelle (25 nm by DLS),  $a_2$  is the radius of biocide ( $\sim 0.5 \text{ nm}$ ),  $k$  is the Boltzmann constant ( $1.38 \times 10^{-23} \text{ J/K}$ ),  $T$  is the temperature (K),  $\eta$  is the viscosity of water ( $\text{Ns/m}^2$ ) and  $n$  is number of biocide molecules per unit volume, which, at saturation, is  $3.2 \times 10^{22} \text{ biocide molecules/m}^3$ . The number of biocide molecules colliding with one micelle is thus  $4.3 \times 10^6 \text{ s}^{-1}$ . The number of biocide molecules per micelle is about 320, since the number of micelles

per unit volume is  $10^{20}$  micelles/ $\text{m}^3$  (calculated from 0.1 % (w/w) micelle solution). Hence it takes  $t = 320/4.3 \times 10^6 = 74 \text{ } \mu\text{s}$  for these biocide molecules to disappear from the solution by adsorption on the micelle surface assuming that all collisions are sticky. Since about  $3 \times 10^3$  biocide molecules are taken up per micelle at surface saturation, these 320 molecules, which are taken up in  $74 \text{ } \mu\text{s}$ , contribute a relatively small amount to the total biocide uptake (i.e. about 10 % of the external layer, or less than 3 % of the total uptake). To confirm that this estimate is realistic, we can also compare the average distance a biocide molecule travels in  $74 \text{ } \mu\text{s}$  with the average distance between micelles. The average distance traveled by a biocide molecule is given by the Einstein-Smoluchowski equation:<sup>35</sup>

$$\langle x^2 \rangle = 2Dt = \frac{2kT}{4\pi\eta a_2} t \quad (4)$$

where  $D$  is the diffusion coefficient and  $t$  ( $\sim 74 \text{ } \mu\text{s}$ ) is the time needed for a biocide molecule to travel from the solution to the micelle surface. Thus, the mean square displacement  $\langle x^2 \rangle = 630 \times 10^{-16} \text{ m}^2$ . Hence, the average distance traveled in  $74 \text{ } \mu\text{s}$  is about 250 nm, which seems reasonable since this is comparable to the average distance between micelles.

We can conclude from these estimates that all biocide molecules in the saturated water phase are captured in a very short time (less than 0.1 ms) by the micelles, and that the number of absorbed biocide molecules at this point is far less than that at maximum uptake. Thus, the biocide is quickly depleted from the solution and must be replaced by dissolution of the solid biocide. This suggests that, initially, the rate-determining step of micelle loading is the dissolution of biocide from the solid.

#### 2.3.4.2. Initial Loading Kinetics

The kinetics of micelle loading are presented in Figure 2.3, where the biocide content in the micelles (% (w/w)) is plotted vs. the loading time (min). It can be seen from the graph that, initially, the biocide content increases linearly with time up to about 10 min, which corresponds to about 10 % (w/w) and thus most likely reflects saturation of the micelles surface. The second part of the curve, the region from 10 min to about 60 min, corresponds to the penetration of the

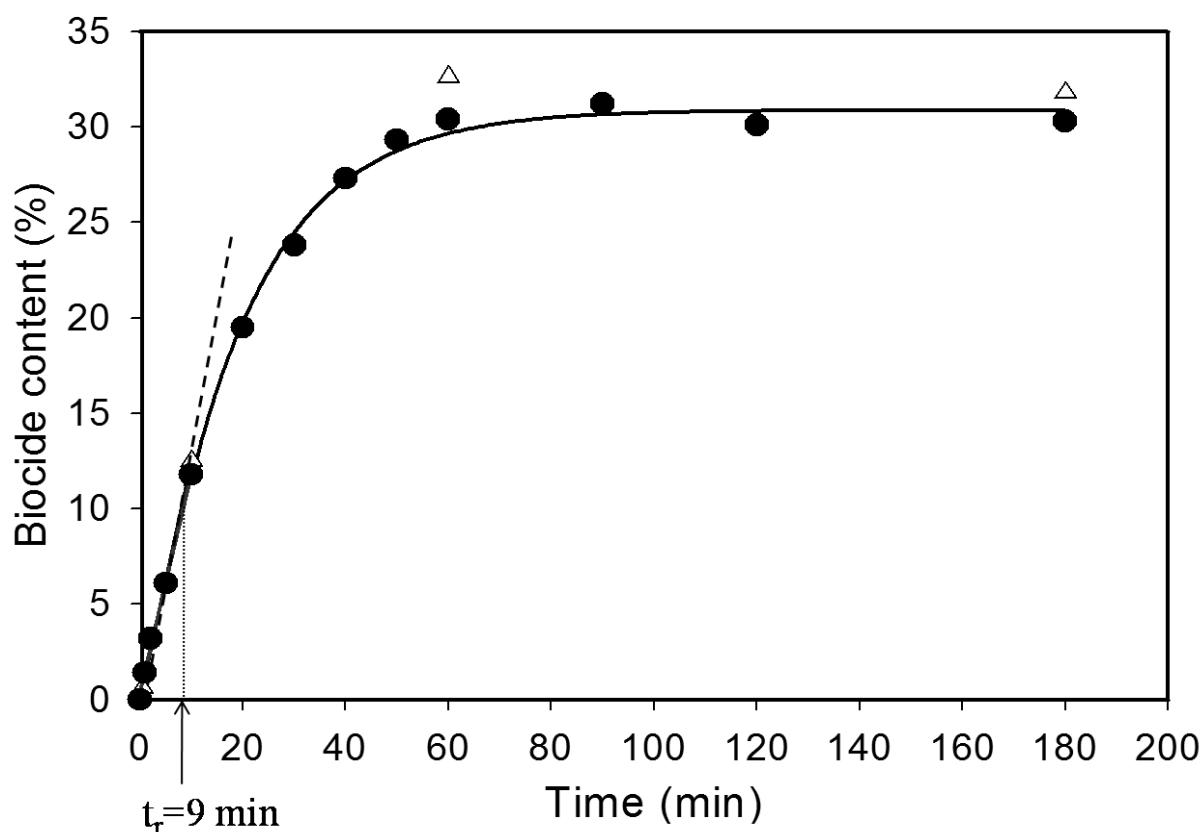


**Figure 2.3.** Kinetics of micelle loading (% intake of biocide vs time). Initially the uptake is linear with a loading rate constant  $k = 2.0 \times 10^{-5}$  kg/s. The solid curve is a single exponential fit with a characteristic time of 18 min. Triangles are result of a separate experiment.

biocide from the micelle surface into the PS core. The maximum loading of the micelles is about 32 % (w/w), which is achieved in about 60 minutes. The loading of the micelles does not increase further with time.

To establish if the initial loading rate is determined by dissolution of solid biocide from the solid film, we have to make an estimation of the desorption rate constant,  $k_{des}$ . This can be found from the dissolution of biocide emulsion droplets. A detailed description will be given in an upcoming publication. The desorption constant is estimated from the initial slope of the size of biocide emulsion droplets with time, with the result  $k_{des} = 2.5 \times 10^{-8} \text{ kg/m}^2\text{s}$ . The area of biocide film is estimated to  $7.25 \times 10^{-4} \text{ m}^2$ . Assuming that the initial rate is determined by biocide dissolution from the solid film, with an estimated area of  $7.2 \text{ cm}^2$ , the expected uptake is  $2.5 \times 10^{-8} \times 7.2 \times 10^{-4} = 1.8 \times 10^{-11} \text{ kg/s}$ .

The first part of the loading curve (Figure 2.3) (up to about 10 min) corresponds to the saturation of the micelle surfaces and can be described by:

$$B = kt, \text{ for } t < t_{tr} \quad (5)$$

where  $k$  is the adsorption rate constant and  $t_{tr}$  the transition time, at which the uptake becomes non-linear. From the initial linear increase of loading with time, a biocide uptake rate of  $2.0 \times 10^{-5} \text{ kg/s}$  is found. This is six orders of magnitude larger than the above estimate, implying that biocide transfer from solid biocide to the micelles does not proceed by dissolution, except perhaps if the film is not smooth, but consist of a large number of very small particles.

#### 2.3.4.3. Biocide Transfer from Biocide Film to Micelles

Before adopting the micelle loading procedure involving the biocide film deposited inside the glass vial, described in section 2.2.4., another technique was explored. It is based on the addition



of solid TCMTB biocide directly to the micelle solution and allowing loading to proceed for various periods of time, i.e. 3, 6 and 9 days. The remaining solid biocide is then removed using a 0.45  $\mu\text{m}$  filter. It was found that this technique is not efficient; the loading achieved is below 2.5 % (w/w). By contrast, when the micelles are loaded from the biocide film (section 2.2.4.), a maximum loading of  $\sim 32$  % (w/w) is achieved in 1 hour. A likely explanation for the apparently low loading levels using the direct loading technique is that the micelles stick to the biocide grains, and are thus filtered off along with the excess of biocide, since the size of the biocide grains is  $1.7 \pm 0.3$   $\mu\text{m}$ , while the filter pores are 0.45  $\mu\text{m}$ . A significant percentage of the loaded micelles is thus lost, and the calculation of the apparent loading level is based on the initial number of micelles. It is conceivable that the individual micelles may actually be fully saturated. However, the experimental error due to loss of micelles, coupled with the spectroscopic method of determining of the total uptake in the micelles remaining in solution, makes precise calculation of biocide uptake impractical.

A discussion of the loading mechanism involves both transfer from the biocide film or grain to the micelle surface and subsequent internalization. Two experiments were performed to explore the details of biocide transfer to the micelle, specifically whether the biocide loading can occur from solution by diffusion or whether contact between the biocide and the micelle is necessary. In order to explore the possibility of contactless loading, the micelles were placed in a dialysis bag (12 – 14 kDa cut off), while the biocide film was, in the first experiment, placed outside the dialysis bag. At the beginning of the experiment, milli-Q water was added into the vial, and the contents of the dialysis bag were stirred for 0.5, 1 and 48 hours. 250  $\mu\text{l}$  of the sample was tested using UV-vis for its absorbance as described in section 2.2.4.1. It was found that in 0.5 hour the loading level was 1.4 % (w/w), in 1 hour it was 2.5 % (w/w) and in 48 hours it reached 20.0 %

(w/w). Because the micelles do not come into the contact with biocide film, due to their placement in the dialysis bag, the loading rate is lower (compared to loading without the dialysis bag, see Figure 2.3). The micelles are loaded with biocide by diffusion through the solvent and dialysis bag. The possibility that some small nano-size pieces of the film are broken off, thus accelerating the transfer cannot be excluded.

In the second experiment (see experimental setup in Figure 2.4), the unloaded micelles were also placed into the dialysis bag. The dialysis bag was then put into the vial containing solid biocide granules. At the beginning of the experiment, milli-Q water was added into the vial and both the vial and the dialysis bag were stirred for 48 hours. 250  $\mu$ l of the sample was taken in 0.5, 1 and 48 hours and tested using UV-vis for its absorbance as described in section 2.2.4.1. It was found that the loading level in 0.5 hour was 1.7 % (w/w), in 1 hour it was 2.5 % (w/w) and in 48 hours it reached 34.7 % (w/w). The initial 0.5 and 1 hour loading levels are similar to those in which the loading occurred from the film. However, the loading level in 48 hours is 75 % larger since the surface area of the biocide grains is bigger than that of the biocide film and, therefore, more of biocide molecules will diffuse through the dialysis membrane to adsorb on the micelles. The difference in loading between micelles in a dialysis bag and those in direct contact with biocide grains proves that, indeed, the micelles adsorb on the biocide grains.

In general, the loading without contact between micelles and biocide film or grains takes longer than loading from the biocide film when contact can take place. Loading using the dialysis bag technique with biocide grains outside the dialysis bag (see Figure 4) is more efficient but slower than loading from the film, because there is no loss of adsorbed micelles on the broken biocide film pieces. These experiments show that the fast loading observed in Figure 3 must be due to transfer during transient micelle-biocide film contacts. These experimental

observations also explain the common use of films for loading as reflected in the literature,<sup>25</sup> instead of grains.

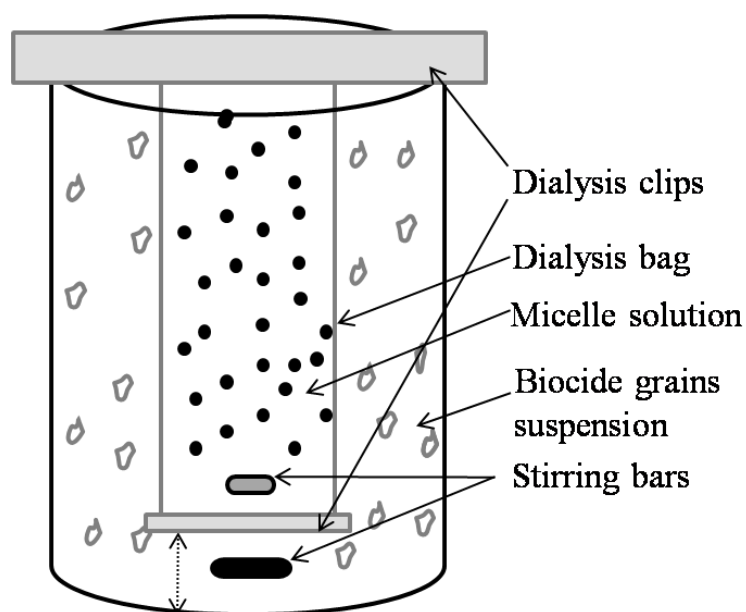


**Figure 2.4.** Schematic representation of experimental setup for maximum biocide uptake by micelles ~ 35 wt % - Biocide molecules diffuse through the dialysis bag into the micelle solution and adsorb onto the micelles.

#### 2.3.4.4. $T_g$ for the Mixtures of Polystyrene and TCMTB Biocide

Although the glass transition temperature ( $T_g$ ) of the PS micelle core might be different from that of bulk PS, the difference is likely to be small, similar to the  $T_g$  difference between bulk PS and that of thin PS films. Singh *et. al*<sup>36</sup> reported for PS films ( $M_w = 212$  kDa) of thickness of 20 – 30 nm a drop in  $T_g$  of less than 10°C. The glass transition temperature of PS is about 100 °C, which raises the question of how fast biocide molecules can diffuse through the PS core at room temperature? Also the possibility exists that biocide molecules act as plasticizers, lowering the  $T_g$  and speeding up diffusion. To explore this aspect, the  $T_g$  of mixtures of PS and biocide was measured over a range of compositions. The results are shown in Figure 2.5, where the  $T_g$  for the

mixtures of PS and biocide measured by differential scanning calorimetry (DSC) is plotted vs. biocide content for mixtures of various compositions. While there are many equations describing the  $T_g$  of plasticized systems, the Fox equation<sup>37</sup> is by far the simplest:

$$\frac{1}{T_g} = \frac{W_1}{T_{g1}} + \frac{W_2}{T_{g2}} \quad (6)$$

Here  $T_g$  is the glass transition temperature of the plasticized system (K),  $W_1$  and  $W_2$  are the weight fractions of pure polystyrene and biocide, respectively, and  $T_{g1}$  and  $T_{g2}$  are the glass transition temperatures of pure polystyrene and biocide, respectively. The dashed line was

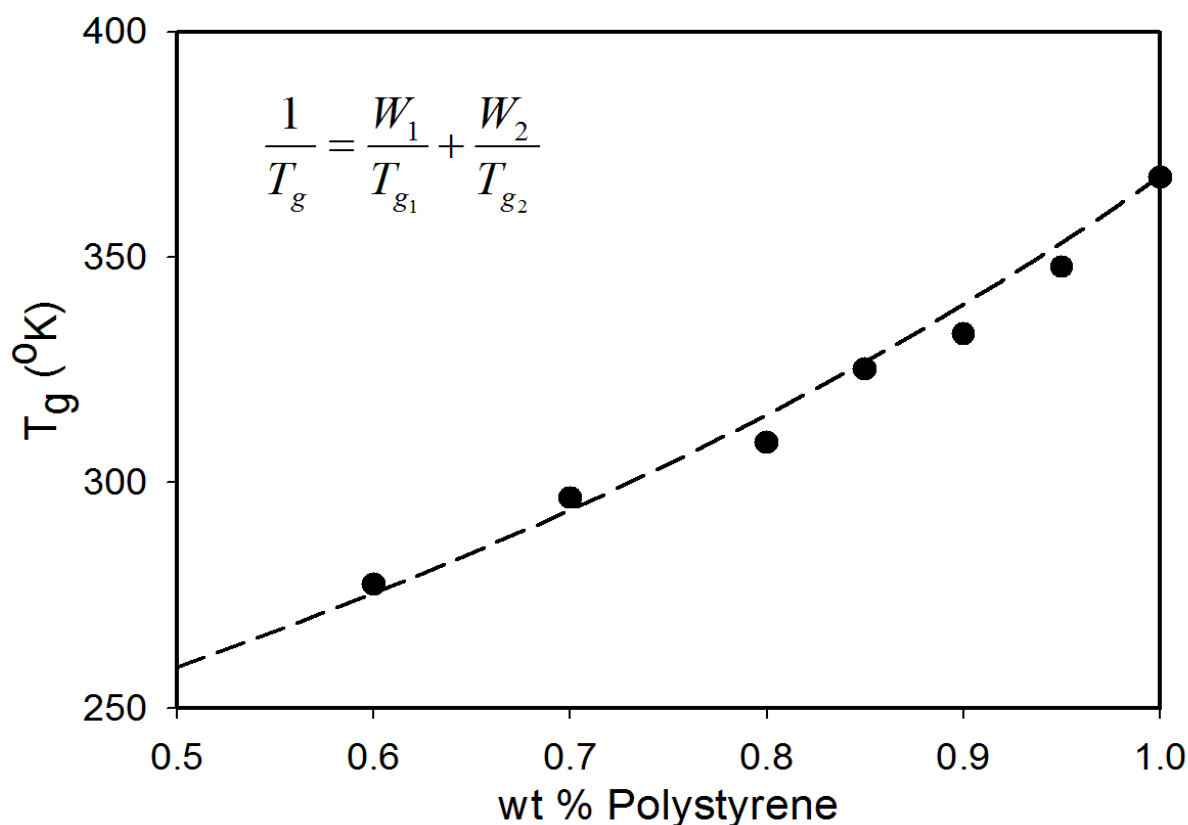


**Figure 2.5.** Glass transition temperature  $T_g$  for the mixtures of Polystyrene and TCMTB biocide. The line is given by the equation shown in the inset, with  $T_{g1} = 373$  K and  $T_{g2} = 200$  K, respectively.

calculated using equation 6 with the values of  $T_{g1} = 373$  K and  $T_{g2}$  (for the plasticizer) = 200 K. The melting point of the biocide is 307 K (34 °C), which gives a value of  $T_g/T_m$  for the biocide of 0.65, typical of a wide range of materials.<sup>38-40</sup>

#### 2.3.4.5. Non-Fickian Diffusion - Penetrating Front

Because the biocide molecules act as plasticizers for PS, it is likely that penetration in the core occurs to the greatest extent when the  $T_g$  is lowered sufficiently by the biocide. Thus, one expects that the biocide forms a penetrating front moving at constant velocity,  $v$ , towards the interior of a micelle (i.e. by case II diffusion<sup>41,42</sup>). Assuming further that the biocide concentration at one side of the front is at saturation and at the other side zero, then the increase in biocide concentration in the micelle,  $B$ , with time is:

$$B = A \frac{4\pi}{3} (R^3 - r^3) \quad (7)$$

$A$  being the maximum uptake per unit volume and  $r$  being the location of the front at time  $t$ , given by  $r = R - vt$ , valid for  $0 \leq \tau \leq 1$  with  $\tau = vt/R$ . Hence

$$B = \frac{4\pi}{3} A [R^3 - (R - vt)^3] = B_\infty [1 - (1 - \tau)^3] \quad (8)$$

where  $B_\infty = 4/3 \pi R^3 A$ , the maximum micelle loading. Eq. 8 can be written

$$1 - \left( \frac{B_\infty - B}{B_\infty} \right)^{1/3} = \tau \quad (9)$$

The loading data in Figure 3 were fitted by eq. 9, starting at  $t = t_r = 9$  min. The plot of biocide concentration in the micelles vs. time is shown in Figure 6. From the slope of the straight line it can be concluded that penetration follows case II diffusion with the penetrating front moving with a constant velocity of 0.2 nm/min.

It should be noted that no changes in morphology were observed as a result of biocide penetration the micelle core.

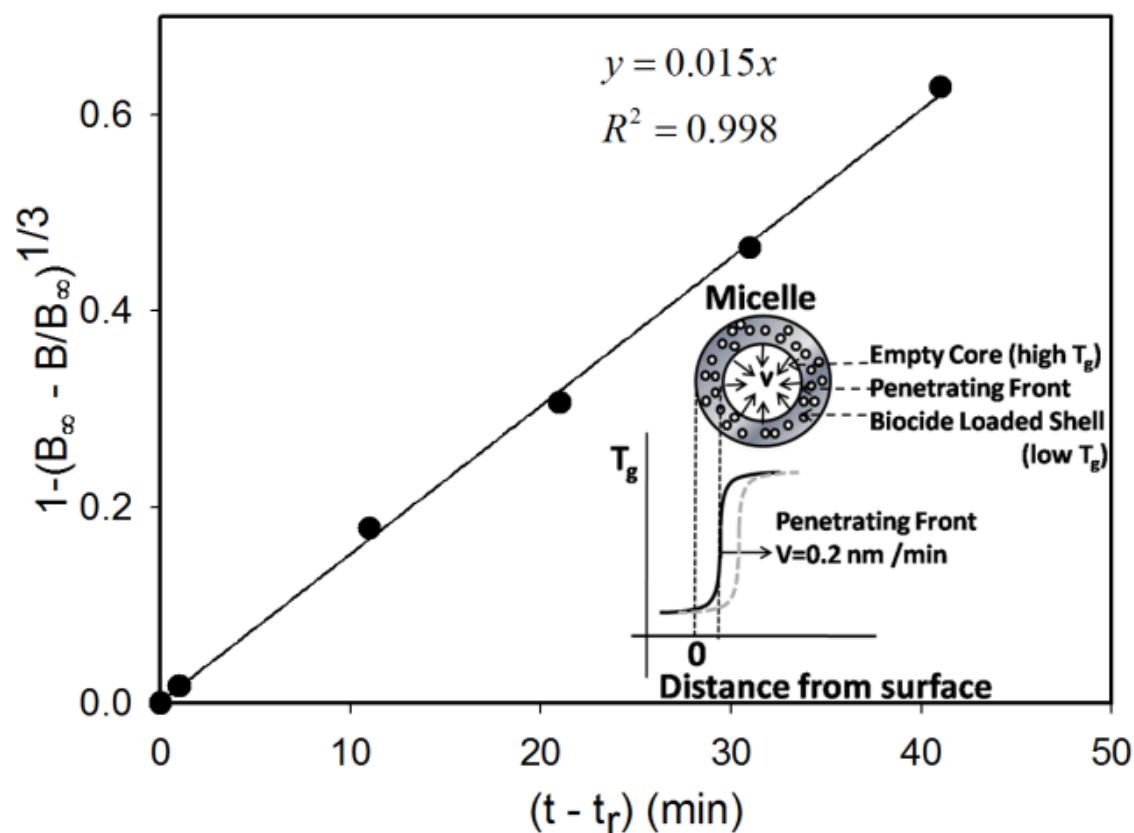


**Figure 2.6.** The L.H.S. of eq. 9, plotted vs.  $t - t_r$ . The slope equals  $v/R$ ,  $v$  being the velocity of the penetrating front. The inset shows the schematics of a penetrating front.

#### 2.3.4.6. Maximum Loading

As shown in Figures 2.3 and 2.7, the maximum micelle loading achieved experimentally is about 32% (w/w). Thus, since the maximum biocide adsorption on the micelle surface is estimated to be 8 % (w/w) at maximum monolayer surface coverage (see section 2.3.3.), the interior of the micelle core must contain at least 24 % (w/w) of biocide.

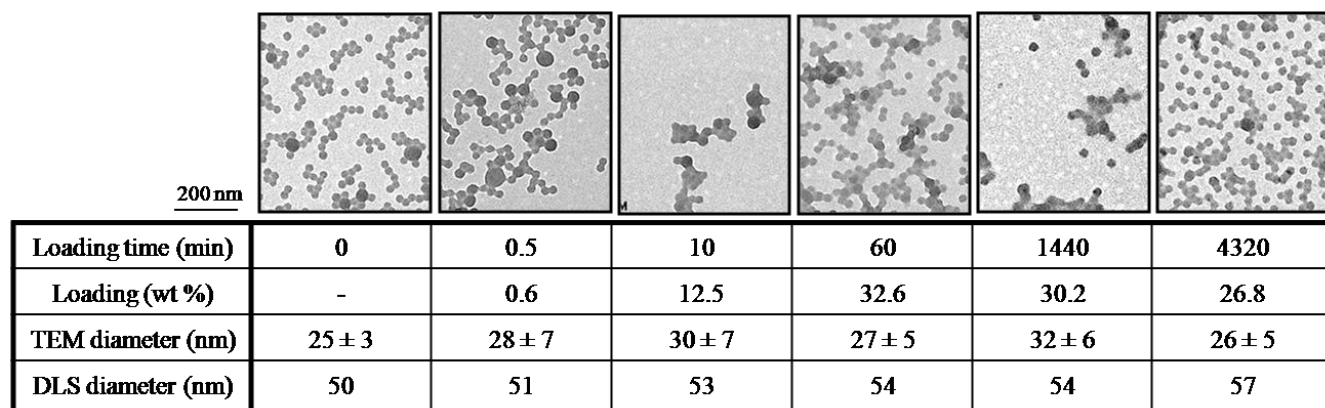


**Figure 2.7.** TEM images and loading efficiency of PS<sub>197</sub>-*b*-PAA<sub>47</sub> micelles, with micelle diameters measured by TEM and DLS.

TEM micrographs of the loaded micelles for various loading times and biocide uptakes are shown in Figure 2.7. As the loading of the micelles increases with time, the size of the micelles does not change significantly. The average size of the micelles as measured by TEM is about 28 nm with a standard deviation of  $\pm 5.5$  nm. The micelle diameter, measured by DLS, increases with loading time and total uptake by 5 nm after 60 minutes. The differences in diameters between TEM and DLS were already discussed in section 2.3.1. The expected increase of the core for 30 % (w/w) loading is 10 % (w/w) or 2.5 nm. Both TEM and DLS data are consistent with this increase within experimental error.

It should also be noted that the loading level decreased for loading times much longer than 90 minutes (72 hours) in case of loading from a biocide film as shown on Figure 2.7. The decrease in loading is most likely caused by the fact that the film starts to break into small pieces (visual observation) which afterwards float in the vial. Breaking of the biocide film is probably due to a weakening of the film in contact with the liquid induced by the stirring of the solution. Also, in

this case, the micelles stick to pieces of biocide film, and are filtered off along with the excess of biocide. This explains the apparent decrease in loading levels at long times.

#### 2.3.4.7. Partition Coefficient of Biocide/Polymer and Biocide/Ethylbenzene

To determine whether the final loading is governed by thermodynamics, partition experiment with ethylbenzene was performed. Ethylbenzene was chosen because it is a low molecular mass analog of PS. A set of five samples of various known biocide concentrations was prepared. The biocide concentrations were evaluated using UV-vis both in the ethylbenzene phase and the water phase. The partition coefficients for all the samples were then calculated using eq. 1, as discussed in section 2.2.8. The biocide concentration values and the resulting partition coefficients for each of the samples are given in Table 2.1.

Sample number	Biocide concentration (g/L)		Partition Coefficient
	Ethylbenzene phase	Water phase	
1	11.43	0.00053	21 600
2	15.83	0.00069	22 900
3	22.68	0.00093	24 400
4	35.81	0.00142	25 200
5	50.31	0.00214	23 500
Average	-	-	23 500 ± 14 00

**Table 2.1.** Biocide concentrations in the ethylbenzene phase and the water phase as determined experimentally, and the resulting partition coefficients.



The average value of the partition as determined by this experimental procedure is  $23500 \pm 1400$ . This value can be compared with that for the partition coefficient between the polystyrene core of the micelles and water, calculated as follows: The total weight concentration of the micelles in solution is 10 g/L. Since the polystyrene constitutes 86 % of the polymer mass, the mass of biocide in the core at 30 % uptake is  $0.36 \times 10^3$  g/L. At saturation, the concentration of the biocide in water is  $12.7 \times 10^{-3}$  g/L. Thus, the partition coefficient of biocide between micelles polystyrene core and water is 29,000. The average experimental values of the partition coefficients for biocide in ethylbenzene and in the PS core of the micelles are in a very good agreement. One can conclude that the biocide prefers the PS micelle core over water by a factor of 29,000, similar to the preference of the biocide for ethylbenzene over water. Thus, the maximum loading capacity of micelles by biocide is consistent with the biocide partition data in ethylbenzene and suggests that the maximum loading is dictated by thermodynamics

#### *2.3.5. Kinetics of Biocide Release from Micelles*

The kinetics of biocide release from the block copolymer micelles was studied on three samples of loaded micelles. The experiment is explained in section 2.2.6. The data for the kinetics of release are shown in Figure 2.8, where the micelle biocide content (% (w/w)) is plotted vs. the release time (min). It can be concluded from the graph that release from the micelles is a slower process than loading (characteristic time  $\tau$  for loading is 18 min – Figure 2.3 vs. ca. 280 min for release – Figure 2.8). Also, as shown in the graph, not all biocide molecules can be released from the micelles; the biocide concentration after 30 hours is still  $\sim 5$  % (w/w), which is caused by the increase of  $T_g$  of the micelle

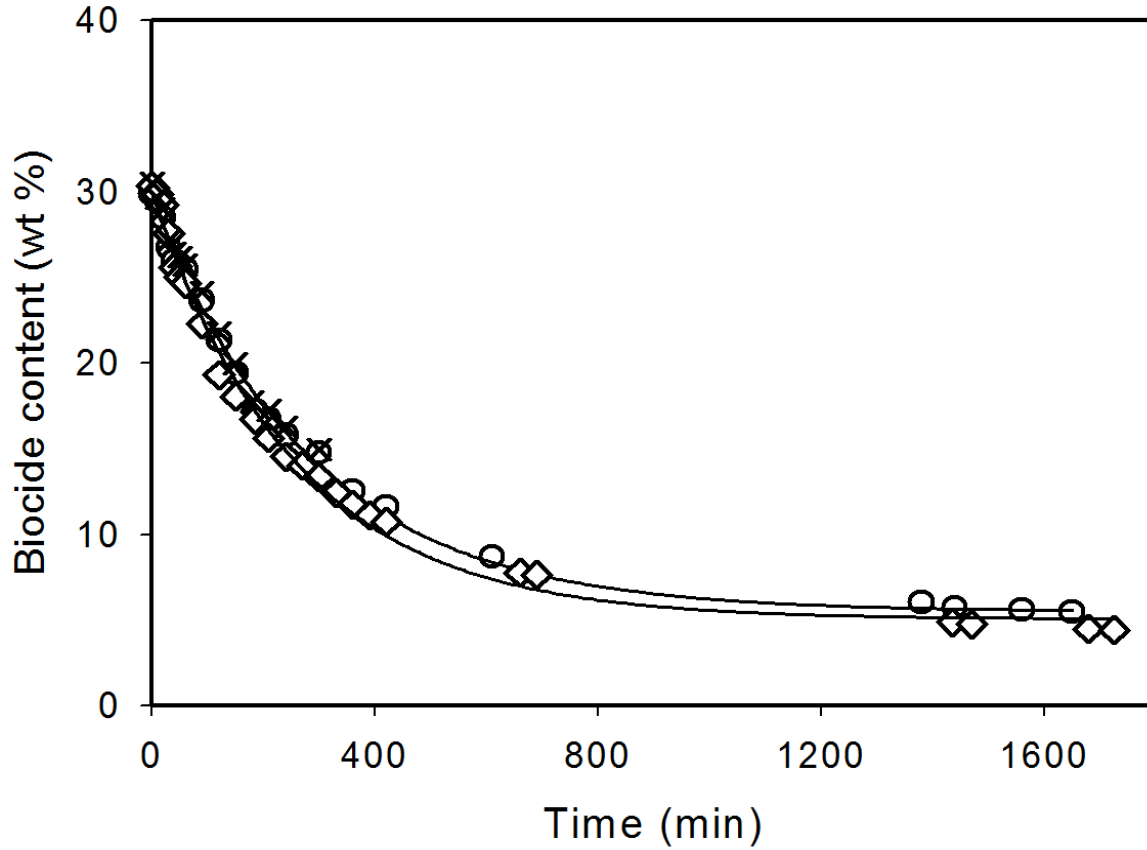


**Figure 2.8.** Kinetics of biocide release from micelles (% of release vs time). The curves are given by Equation 10. The fitting parameter,  $\tau_{\text{release}}$ , for the two curves measured up to 30 hours, are 286 min (diamonds) and 278 min (squares).

core upon biocide release. Both release data (measured for 30 hours) in Figure 2.8 were fitted to the single exponential:

$$B = (B_o - B_f) e^{-t/\tau_{\text{release}}} + B_f \quad (10)$$

where  $B$  is the biocide concentration,  $B_o$  the initial biocide concentration (at the start of release) and  $B_f$  the final biocide concentration. The release times,  $\tau_{\text{release}}$ , for the two curves measured up to 30 hours are 286 and 278 minutes, respectively. The release data do not fit a diffusion model in which the release should vary with the square root of the time but instead follows first order

release kinetics. This implies that the distribution of biocide within the core remains uniform and that the rate determining step of the release process is the release of biocide molecules from the surface of the core. Hence for most of the release process, the average residence time ( $\tau_{\text{release}}$ ) of a biocide molecule on the micelle surface is constant. Agreement with eq. 10 shows that the release rate is constant, till diffusion becomes too slow to transport biocide molecules from the interior to the surface of the PS core.

### *2.3.6. Mechanisms of Biocide Loading and Release*

#### 2.3.6.1. Mechanism of Biocide Transfer from Biocide Film to Micelles

The proposed mechanism of the transfer of biocide molecules from the biocide film to the micelle surfaces is summarized schematically in Figure 2.9A, which represents early stage uptake, i.e. the adsorption of biocide molecules onto the polymer micelle surface. As the polymer micelles come into contact with the biocide film, biocide molecules are adsorbed onto the surface of the micelles. Due to the stirring of the solution, the micelles with adsorbed biocide molecules are continuously in and out of contact with the biocide film, and during each contact additional biocide molecules are transferred from the film to the micelles. The adsorption of the biocide on the micelle surface takes place until saturation (monolayer) of the micelle surface is reached, which occurs, according to the kinetics of micelle loading (see linear part of the curve in Figure 2.3), in about 10 minutes. Maximum adsorption of biocide on the external surface of the micelles at saturation is approximately 8% (w/w) according to the calculations described in section 2.3.3.

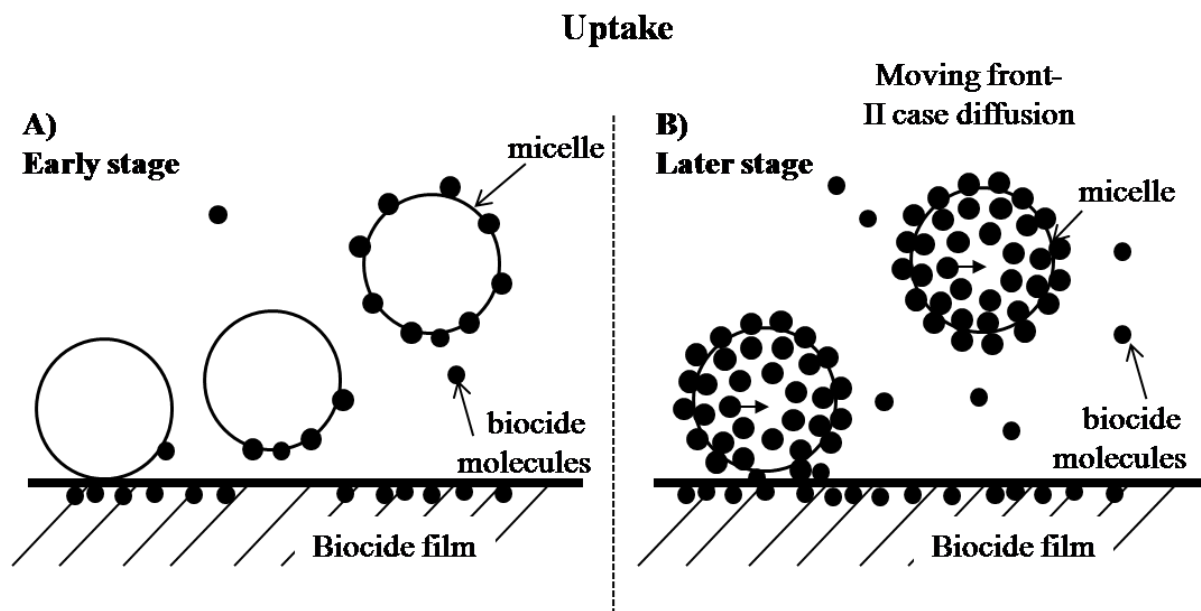


**Figure 2.9.** Schematic representation of TCMTB biocide uptake by PS<sub>197</sub>-*b*-PAA<sub>47</sub> micelles. A) Early stage uptake: Biocide molecules transfer from the film to the micelle during transient collisions, until a monolayer of biocide on the micelle surface is formed. B) Later stage uptake: Internalization of the biocide molecules into the micelles by case II diffusion (moving front) with the empty surface spots being replenished by biocide transfer from the film.

#### 2.3.6.2. Mechanism of Biocide Incorporation into the Micelles

The proposed mechanism of biocide molecules incorporation into the micelles is schematically shown in Figure 2.9 B. Figure 2.9 B deals with the later stage of the biocide uptake by the micelles, specifically the internalization of the biocide molecules from the micelle surface into the PS core of the micelles. This process is much slower than the adsorption of the biocide molecules on the micelle surface and thus it is the rate-determining step of the biocide loading. The molecules of the biocide are transferred from the surface inside the PS core by case II diffusion, (as shown in Figure 2.6) with a penetrating front moving at constant velocity of 0.2 nm/min towards the interior of a micelle. This velocity depends on how fast the biocide molecules plasticize the PS core. This process continues until the micelles are loaded with

biocide molecules to the thermodynamic limit. The empty biocide sites on the micelle surface are replenished from the biocide film by the mechanism discussed in section 2.3.6.1.

### 2.3.6.3. Mechanism of Biocide Release from the Micelles

The mechanism of biocide release is shown schematically in Figure 2.10. In general, the biocide release from the micelles takes longer than the loading, which is completed in 1 hour. The rate determining step of biocide release from the micelles is the release of biocide molecules from the surface of the micelles; biocide molecules have to pass over the energy barrier to go into aqueous solution. The surface of the micelles is afterwards replenished by diffusion of biocide molecules from the micelle interior in early stage release, (see Figure 2.10 A) resulting in a uniform biocide concentration within the micelle, until the  $T_g$  is increased to the extent that diffusion inside the micelles becomes very slow. Not all the biocide can be released from micelle

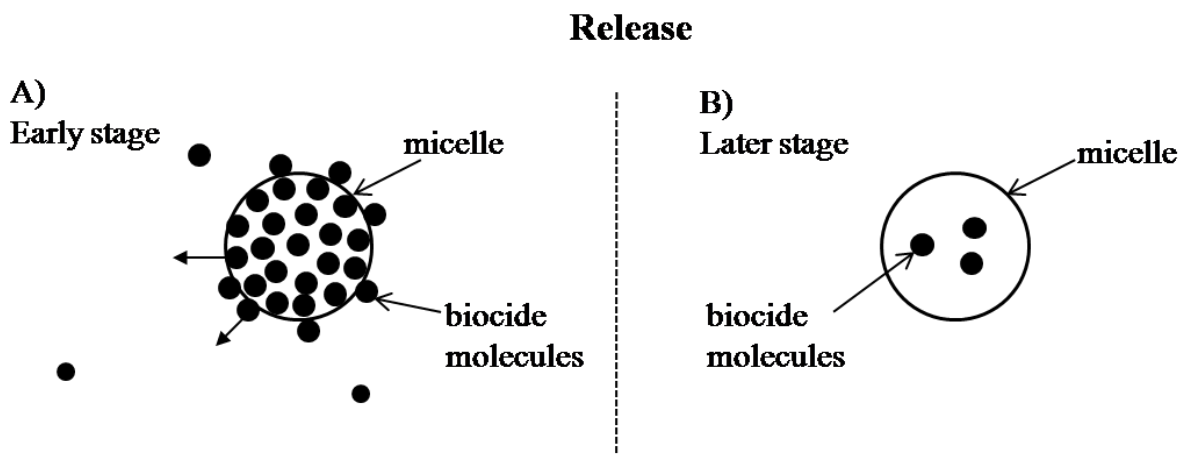


**Figure 2.10.** Schematic representation of biocide release. A) Early stage release from the micelles – Molecules are released from the surface of the PS core with a constant rate, determined by the energy barrier of escape; B) Later stage release -Biocide is not released from the micelles in the later stage because of increase in  $T_g$  during release.

interior within a reasonable time (see Figure 2.10 B) due to increase in glass transition temperature with decreasing biocide content, which slows down the release process.

## **2.4. Conclusions**

Crew-cut micelles of PS<sub>197</sub>-b-PAA<sub>47</sub> block copolymer were self assembled in dioxane by slow addition of water. The micelles size was found to be 26 nm by TEM and 50 nm by DLS. The micelles were loaded with the hydrophobic antibacterial agent, TCMTB, and the loading was measured by UV-vis. Maximum loading of biocide into micelles is around 32 % (w/w) and is achieved in one hour. Loading of TCMTB biocide into the PS-b-PAA micelles was found to be a two step process. First, the micelle surface is saturated with biocide molecules (monolayer of about 10 % (w/w) of biocide molecules) in about 10 minutes of loading by transient contacts between micelles and the biocide film. Next, the biocide penetrates as a front into the PS core with a speed of 0.2 nm/min, lowering the  $T_g$  in the process (Non-Fickian case II diffusion). From partition coefficient experiments it can be concluded that the biocide has a similar preference for polystyrene as for ethylbenzene over water, indicating that maximum loading is governed by thermodynamics. Loading from the biocide film is more effective than loading from biocide grains; the micelles adsorb onto the biocide grains and are filtered off together with the excess of biocide.

The release of biocide from the micelles is a slower process than loading. The rate of release is governed by the height of the energy barrier which a biocide molecule must overcome to pass into the aqueous phase, resulting in a uniform biocide concentration within the micelle, until the  $T_g$  is decreased to the extent that diffusion inside the micelles becomes very slow.

It should be noted that the loading kinetics described in this paper is expected to be quite general, while the release kinetics is an extreme case, in which the release is governed by the

height of an energy barrier. Another extreme case of release kinetics is reported by Giacomelli *et al.*,<sup>18</sup> in which the rate determining step of the release is governed by diffusion within the micelle.

## 2.5. Reference List

- (1) Yokoyama, M.; *Crit. Rev. Ther. Drug Carrier Syst.*, **1992**, 9.
- (2) Kwon, A. V.; Kataoka, K.; *Adv. Drug Delivery Rev.*, **1995**, 16, 295.
- (3) Kabanov, A.V.; Alakhov, V. Y.; Alexandris, P.; Lindman, B.; *Amphiphilic Block Copolymers: Self Assembly and Applications*, Eds.: Elsevier: Amsterdam, **1997**.
- (4) Allen, C., Maysinger, D., Eisenberg, A., *Colloids Surf., B*, **1999**, 16, 3.
- (5) Nakanishi, T., Fukushima, S., Okamoto, K., Suzuki, M., Matsumura, Y., Yokoyama, M., Okano, T., Sakurai, Y., Kataoka, K., *Journal of controlled Release*, **2001**, 74 (1-3), 295.
- (6) Kabanov, A.V., Bartakova, E.V., *Current Pharmaceutical Design*, **2004**, 10 (12), 1355.
- (7) Torchilin, V.P., *Pharmaceutical Research*, **2007**, 24 (1), 1.
- (8) Gindy, M.E., Panagiotopoulos, A.Z., Prud'homme, R.K., *Langmuir*, **2008**, 24, 83.
- (9) Nagarajan, R., Barry, M., Ruckenstein, E., *Langmuir*, **1986**, 2, 210.
- (10) Zhang, L.F., Eisenberg, A., *Science*, **1995**, 268, 1728.
- (11) Tao, J., Stewart, S., Liu, G.J., *Macromolecules*, **1997**, 30, 2738.
- (12) Discher, B.M., Won, Y.-Y., Ege, D. S., Lee, J. C.-M., Bates, F. S., Discher D. E., Hammer, D. A., *Science*, **1999**, 284, 1143.
- (13) Lodge, T.P., Pudil, B., Hanley, K.J., *Macromolecules*, **2002**, 35, 4707.

- (14) Wilhelm, M., Zhao, Ch.-L., Wang, Y., Xu, R., Winnik, M. A., Mura, J.-L., Riess, G., Croucher, M.D., *Macromolecules*, **1991**, 24, 1033.
- (15) Zhao, J.; Allen, Ch.; Eisenberg, A.; *Macromolecules*, **1997**, 30, 7143.
- (16) Xing, L., Mattice, W. L., *Macromolecules*, **1997**, 30, 1711.
- (17) Cho, J.; Hong, J.; Char, K.; Caruso, F.; *JACS*, **2006**, 128, 9935.
- (18) Giacomelli, C., Schmidt, V., Borsali, R., *Langmuir*, **2007**, 23, 6947.
- (19) Lee, J., Cho, E. Ch., Cho. K., *Journal of Controlled Release*, **2004**, 94, 323.
- (20) Zhu, Z., Anacker, J.L., Shengxiang, J., Hoyer, T.R., Macosko, Ch.W., Prud'homme, R.K., *Langmuir*, **2007**, 23, 10499.
- (21) Xiangyang, X., Ling, L., Jianping, Z., Shiyue, L., Jie, Y., Xiaojin, Y., Jinsheng, R., *Colloids and Surfaces B: Biointerfaces*, **2007**, 55, 222.
- (22) Stevenson-Abouelnasr, D., Ghaleb, A. H., Pitt, W. G., *Colloids and Surfaces B: Biointerfaces*, **2007**, 55, 59.
- (23) Allen, Ch., Han, J., Yu, Y., Maysinger, D., Eisenberg, A., *Journal of Controlled Release*, **2000**, 63, 275.
- (24) Teng, Y., Morrison, M. E., Munk, P., Webber, S. E., Prochazka, K., *Macromolecules*, **1998**, 31, 3578.
- (25) Choucair, A.; Eisenberg, A.; *JACS*, **2003**, 125, 39, 11993.
- (26) Luo, L.; Eisenberg, A.; *Langmuir*, **2001**, 17, 6804.
- (27) Azzam, T.; Eisenberg, A.; *Angew. Chem. Int. Ed.*, **2006**, 45, 7443.
- (28) Zhong, X. F.; Varshney, S. K.; Eisenberg, A.; *Macromolecules*, **1992**, 25, 7160.
- (29) Yu, K.; Eisenberg, A.; *Macromolecules*, **1998**, 31, 3509.
- (30) Shen, H.; Eisenberg, A.; *J. Phys. Chem. B*, **1999**, 103, 9473.



- (31) Evans, R. J.; *Encyclopedia of Physical Science and Technology*, 1<sup>st</sup> ed., Meyers, R.A., Ed.; Academic Press Inc., **1987**, vol. 8.
- (32) Reimer, L., *Transmission Electron Microscopy: Physics of Image Formation and Microanalysis*, 4<sup>th</sup> ed., Springer – Verlag, Berlin, **1997**.
- (33) Choucair, A.; Lim Soo, P.; Eisenberg, A.; *Langmuir*, **2005**, 21, 9308.
- (34) Smoluchowski, M. Z.; *Phys. Chem.*, **1917**, 92, 129.
- (35) van de Ven, T.G.M.; *Colloidal Hydrodynamics*, Academic Press, London, **1989**.
- (36) Singh, L.; Ludovice, P. J.; Henderson, C.; *Thin Solid Films*, **2004**, 449, 231.
- (37) Fox, T. G.; *Bul. Am. Phys. Soc.*, **1956**, 1, 123.
- (38) Krijgsman, J.; Feijen, J.; Gaymans, R. J.; *Polymer*, **2004**, 25, 8523.
- (39) Sakthivel, P.; Kannan, P. J.; *Polymer Sci. A.*, **2004**, 42, 20, 5215.
- (40) Kannan, P.; Senthil, S.; Vijayakumar, R.; Marimuthu, R.; *J. App. Polymer Sci.*, **2002**, 86, 14, 3494.
- (41) Ensore, D. J.; Hopfenberg, H. B.; Stannet, V. T.; *Polymer*, **1977**, 18, 793.
- (42) Ritgert, F.; Peppas, N. A.; *Fuel*, **1987**, 66, 815.

## **Bridging Section between Chapters 2 and 3**

---

The main aim of Chapter 2 was to develop techniques for the incorporation of a biocide into block copolymer micelles. PS-*b*-PAA block copolymer micelles were chosen as a model for the incorporation of the biocide, thiocyanomethylthiobenzothiazol, (TCMTB). The filled micelles, which are expected to be bactericidal, might have a wide range of applications, including possibly in a bactericidal paper. As a first step, it was of interest to see whether such micelles do, indeed, have bactericidal properties and in what environments they can be utilized. For this reason a study of the bactericidal properties of such micelles was performed in an aqueous environment.

Chapter 3 describes this study. Since TCMTB proved to be a relatively weak bactericidal agent, a parallel study of the bactericidal effectiveness of a more potent agent was also performed, and is also described in Chapter 3. This second bactericidal agent is triclosan (TCN). The uptake and release properties of this agent were also investigated briefly, a detailed study was not considered necessary, since the preliminary results, which paralleled those of TCMTB, were sufficient for the preparation of the loaded micelles. Because the PAA, like the bacterial surface, is negatively charged, it was considered important to investigate the intermediary action of a cationic polymer, such as a cationic polyacrylamide (c-PAM) in promoting the interactions

between micelles and bacteria. It was also considered important to elucidate the mechanism of biocide transfer from the micelles to the bacteria.

Another aspect of the study reported in Chapter 3 is the introduction of a different micelle former, i.e. PS-*b*-P4VP, which can have a positively charged corona under a wide range of conditions. This polymer was chosen because vinyl pyridine by itself has some bactericidal properties, which made it likely that the effectiveness of the PS-*b*-P4VP block copolymer micelles would be higher than those of PS-*b*-PAA.

## Chapter 3:

# Bactericidal Block-copolymer Micelles

---

### Abstract

Block-copolymer micelles with bactericidal properties were designed to deactivate pathogens such as *E. coli* bacteria. The micelles of polystyrene-block-poly(acrylic acid) (PS-b-PAA) and polystyrene-block-poly(vinyl pyridine) (PS-b-P4VP) block-copolymers were loaded with biocides of thiocyanomethylthiobenzothiazole (TCMTB) or triclosan (TCN), and the mechanism of biocide transfer to bacteria was investigated. Depending on the type of antibacterial agent, micelles with a diameter of 50 nm (in swollen state) were loaded with the hydrophobic biocide up to 20 to 30 % (w/w) of the unloaded micelles. Bacteria were exposed to loaded micelles and bacterial deactivation was evaluated. It was found that block-copolymer micelles loaded with TCMTB are bacteriostatic for short exposure times and only become bactericidal when exposed to the bacteria for long period of time (10 hours). The micelles loaded with TCN are bactericidal (bacteria are killed in less than two minutes). It was also shown that the biocide is, most likely, transferred to the bacteria by repeated micelle-bacteria contacts, and not *via* the solution.

### 3.1. Introduction

Colloidal particles, especially association-colloids such as self-assembled micelles, have been receiving much attention as potential carriers for biologically active ingredients, specifically hydrophobic drugs.<sup>1-8</sup> It is well known that amphiphilic block copolymers have the ability to self-assemble into ordered structures, such a spherical or rod-like micelles, when dissolved in selective solvents (i.e., solvents thermodynamically poor for one block and good for the other).<sup>9-</sup>

\* The manuscript is to be submitted to *Journal of Polymer Applied Science*

<sup>16</sup> In polar solvents the hydrophilic blocks of the polymer form the corona of the micelle, while the core consists of the hydrophobic blocks.

The advantages of using micellar delivery systems are many-fold. For example, the amount of hydrophobic toxic material that can be stored in micelles intended for animal or human use is far higher than the lethal dose ( $LD_{50}$ ) of the free material that the body can tolerate, primarily because most of the hydrophobic toxic material is incorporated in the micelle; the freely dissolved material is considerably below the toxic limit. In addition, the release rate can be controlled, among others, by the glass transition temperature of the core material, as well as the interaction parameter between the polymer and the toxic compound. Additional advantages of using micellar delivery systems are, for example, long circulation times in the body when using a poly(ethylene) oxide (PEO) corona, high loading levels, which can be orders of magnitude higher than the solubility limit of the compound, slow and sometimes controlled release, as well as possible localization on the surface of micelles<sup>17</sup>; in addition one can also control the charge of the corona (poly(acrylic acid) (PAA) negative, poly(vinyl pyridine) (P4VP) positive and PEO uncharged) which might be useful for specific applications. In addition, loaded micelles are generally very stable, and thus possess extended shelf life, which is also very advantageous.<sup>18</sup>

Many desirable biocides are hydrophobic in nature. Delivering such biocides to bacteria in a dry or aqueous environment is non-trivial because, frequently, the solubility of the antibacterial agent in water is too low to be effective in bacterial deactivation. Therefore, it would be very desirable to find methods of delivering biocides to bacteria while keeping the concentration in water very low, and yet to be able to have a high effective concentration of the biocide in a reservoir in water. Within this range of parameters or prospective applications, a micellar delivery system is ideal, in that it allows us to use a very poorly soluble biocide, so it does not

contaminate the aqueous solution, while the total concentration of biocide in the solution is high. Superficially, the above characteristics might appear antithetical to bacterial deactivation in view of the low concentration of free biocide in water and the need for effective deactivation. Therefore, it is necessary to find a micellar system in which the biocide can be transferred to bacteria without involving transport through the solution.

The present study is part of a collaborative research project within a network on bioactive paper, which has as its objective to capture, detect and deactivate pathogens, using paper as a substrate. Part of the strategy is to incorporate hydrophobic biocides into paper to prepare bioactive paper to deactivate bacteria. Our approach is based on loading a hydrophobic antibacterial agent into amphiphilic block copolymer micelles to increase the biocide concentration locally. In an earlier paper<sup>19</sup> the mechanisms of the uptake and release of thiocyanomethylthiobenzothiazole (TCMTB) biocide into and from polystyrene<sub>197</sub>-block-poly(acrylic acid)<sub>47</sub> (PS<sub>197</sub>-b-PAA<sub>47</sub>) micelles were reported. Loading of the micelles was found to be a two-step process. First, the surface of the PS core of the micelles is saturated with biocide, at a rate determined by the transfer of solid biocide to micelles during transient micelle-biocide contacts. Next, the biocide penetrates as a front into the micelles, lowering the glass transition temperature in the process (non-Fickian case II diffusion). The slow rate of release is governed by the height of the energy barrier that a biocide molecule must overcome to pass from polystyrene (PS) into water, resulting in a uniform biocide concentration within the micelle; the release continues until the glass transition temperature is increased to the point that diffusion inside the micelles becomes very slow. Maximum loading of biocide into micelles is ~30 % (w/w) and is achieved within 1 h. From partition experiments, it was concluded that the biocide

has a similar preference for polystyrene over water as for ethylbenzene over water, implying that the maximum loading is governed by thermodynamics.

In the present paper we describe a micellar delivery system for hydrophobic antibacterial agents that can be used in aqueous environments. Kinetics of bacteria deactivation, including the mechanism of biocide uptake by the bacteria were also studied. The deactivation of *E. coli* (gram negative) bacteria using polystyrene-block-poly (acrylic acid) diblocks (specifically PS<sub>197</sub>-b-PAA<sub>47</sub> and PS<sub>456</sub>-b-PAA<sub>103</sub>) and polystyrene<sub>297</sub>-block-poly (vinyl pyridine)<sub>30</sub> PS<sub>297</sub>-b-P4VP<sub>30</sub> block-copolymer micelles, loaded with TCMTB or triclosan (TCN) biocides was studied, and the mechanism of transfer of biocide to bacteria was elucidated. The micelles, of ca 50 nm diameter, are loaded with the hydrophobic antibacterial material from a biocide film, reaching maximum loading (20 – 30 % (w/w)) depending on the type of antibacterial agent. Bacterial deactivation was evaluated by UV-vis spectroscopy in terms of optical density (absorbance) at a wavelength of 600 nm. The absorbance of bacteria deactivated by biocide loaded micelles was compared to the absorbance of bacteria in water and to that of bacteria exposed to solutions containing empty micelles. In addition, the effect of cationic poly(acryl)amide (c-PAM) alone on bacteria deactivation was tested. Finally, the transfer of antibacterial agents from the core of the micelles to the bacteria during transient collisions was studied.

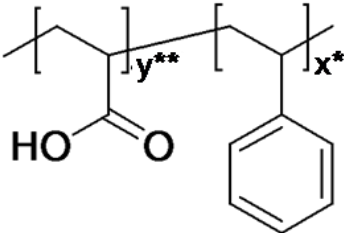
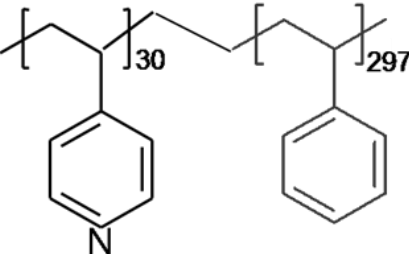
## 3.2. Experimental Section

### 3.2.1. Materials

The amphiphilic block copolymers of PS<sub>197</sub>-b-PAA<sub>47</sub> and PS<sub>456</sub>-b-PAA<sub>103</sub> (structures and properties are shown in Table 3.1.) were synthesized using atom transfer radical polymerization.<sup>20-23</sup> Block copolymer of PS<sub>297</sub>-b-P4VP<sub>30</sub> were synthesized by sequential anionic

polymerization of styrene followed by 4-vinylpyridine.<sup>24</sup> The number average molecular weight ( $M_w$ ) and polydispersity indices of the polymers used at this study are shown in Table 3.1. Cationic polyacryl amide (c-PAM) of 20 % of degree of substitution – PERCOL 292 was purchased from Allied Colloids (Canada) Inc (now BASF).

Thiocyanomethylthiobenzothiazole (TCMTB), the hydrophobic bactericidal material (biocide), was provided by Buckman laboratories. The second hydrophobic antibacterial material, Triclosan (TCN) (Irgasan), used in this study, was purchased from Fluka BioChemika (HPLC grade). The structure and properties of both very slightly water-soluble materials, TCMTB and TCN, are shown in Table 3.2. 1-4-Dioxane was purchased from Sigma-Aldrich (HPLC grade) and used as received. The pH of the milli-Q water used in all experiments was approximately 6.

<b>Molecular structure</b>			
<b>Polymer</b>	<b>PS<sub>197</sub>-b-PAA<sub>47</sub></b>	<b>PS<sub>456</sub>-b-PAA<sub>103</sub></b>	<b>PS<sub>297</sub>-b-P4VP<sub>30</sub></b>
<b><math>M_w</math> (g/mol)</b>	<b>23 900</b>	<b>50 900</b>	<b>34 100</b>
<b>PDI</b>	<b>1.10</b>	<b>1.04</b>	<b>1.10</b>

**\*x = number of styrene units, \*\*y = number of acrylic acid units**

**Table 3.1.** Structure and properties of the polymers



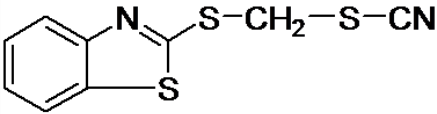
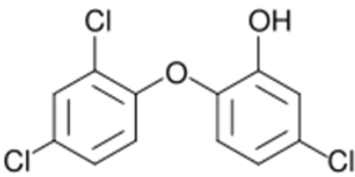
<b>Molecular structure</b>		
<b>Biocide</b>	<b>Thiocyanomethylthiobenzothiazole (TCMTB)</b>	<b>Triclosan (TCN)</b>
<b>M<sub>w</sub> (g/mol)</b>	238	289
<b>Water solubility (mg/L)</b>	12.7	11.0
<b>Melting point (°C)</b>	34	55 - 57
<b>Oral LD<sub>50</sub> (g/kg)</b>	0.75 (on rats) <sup>25</sup>	5 (on rats) <sup>26</sup>

Table 3.2. Structure and properties of the biocides

The bacteria used in this work consisted of gram negative *E. coli* bacteria of ATCC11229 strain. The bacteria were donated by Prof. Mansel Griffiths from Canadian Research Institute for Food Safety, University of Guelph, Canada. The medium used in this work was Miller-Hinton broth purchased from Fluka (microbiology grade); bacteria were grown in this broth at 37 °C while shaking. The bacteria fixative, glutaraldehyde, was donated by Dr. Hojatollah Vali, Facility for Electron Microscopy Research, McGill University.

### 3.2.2. Experimental Techniques and Procedures

The description of micelle preparation, characterization and of the loading procedure is given in detail in the Appendix to Chapter 3. Techniques to evaluate bacteria deactivation, such as transmission and scanning electron microscopy, UV-vis spectroscopy, electrophoretic mobility

measurements and hemacytometer bacteria counting, are also described in the Appendix to Chapter 3.

### **3.3. Results and discussion**

#### *3.3.1. Size and Structure of the Micelles*

The average diameter of PS<sub>197</sub>-b-PAA<sub>47</sub> micelles (unloaded) is  $26 \pm 3$  nm (based on 2048 counts), evaluated from TEM micrographs using Sigma Scan image analysis. This average diameter includes both the PS core and the surrounding PAA corona in a collapsed state. From stoichiometry, the calculated diameter of the micelle core is 24.6 nm, while the thickness of the collapsed corona is about 0.7 nm. The thickness of the collapsed corona is calculated from the volume of 250 PAA chains of 47 units each surrounding the core. A representative TEM picture of unloaded PS<sub>197</sub>-b-PAA<sub>47</sub> micelles was shown in Figure 3.2 of the previous publication<sup>19</sup> and can be also found in Figure 3.1 in the Appendix to Chapter 3 along with the schematic representation of the micelles.

DLS revealed that the average effective diameter of the micelles before loading is  $50 \pm 5$  nm. The micelle diameter measured by DLS is about twice as large as that measured from TEM images. The difference in micelle size measured by DLS and TEM can be explained by the fact that the corona is collapsed in TEM while in DLS the corona is expanded. Furthermore, TEM represents a number average diameter while DLS represents a z-average.

### 3.3.2. Deactivation of Bacteria by TCMTB

#### 3.3.2.1. Saturation Concentration of TCMTB in Water

TCMTB biocide is a hydrophobic, very slightly water soluble white crystalline material. The TCMTB saturation concentration was determined to be 12.7 mg/L.<sup>19</sup> A saturated aqueous solution of TCMTB was tested on *E. coli* bacteria for its deactivation effect. The bacteria samples of various concentrations (as measured by absorbance from 1.0 to 0.05) were exposed for 2 hours to the saturated solution; the bacteria solutions with the TCMTB were then centrifuged, the supernatant was exchanged for the growth medium, and the bacteria were then incubated at 37 °C while shaking for 2 hours. From the absorbance values it was found that the bacteria were growing after an exposure of 2 hours to the same extent as the control sample; the concentration of TCMTB in the saturated aqueous solution was therefore too low to be bactericidal for *E. coli*.

#### 3.3.2.2. Effect of Micelle Loading

The bacteria were then exposed to various concentrations of micelles loaded with TCMTB to find the concentration of TCMTB needed to deactivate the *E. coli* at a concentration giving an absorbance of 0.1 at the wavelength of 600 nm. For this purpose, the TCMTB loaded PS<sub>197</sub>-b-PAA<sub>47</sub> micelles (polymer concentration of 1 g/L equivalent to 10<sup>17</sup> micelles/L) containing TCMTB in the micelle core at a concentration of 30 % (w/w) – 0.3 g/L were used. Since the solubility of TCMTB in water is 12.7 mg/L (Table 3.2), the concentration of TCMTB in solution by loading the biocide into the micelles is increased by approximately 25 times at the given polymer concentration (1 g/L) and 30 (w/w) % loading (0.3 g of TCMTB/L). The growth medium was then added to the micelle solution at a volume ratio of 50/50. The micelle solution

was diluted then to the final TCMTB concentrations of 37.5 mg/L, 75 mg/L, 112.5 mg/L and 150 mg/L; also a sample without TCMTB was tested (the control sample); the total volume of each sample was 20 mL. The bacteria concentration was kept constant in each sample (0.1 absorbance). The samples were then incubated at 37 °C, while shaking, and the absorbance at 600 nm was monitored for 1.5 hours. It was found that the control sample (in the absence of loaded micelles) grows within 1.5 hour to an absorbance of 1.01, and that the bacteria growth slows down as the concentration of biocide increases. One can see that the bacteria become completely deactivated, at the micelle concentration corresponding to the TCMTB concentrations of 112.5 and 150 mg/L, because bacteria growth is inhibited and the absorbance does not change with time. The concentrations correspond to a loading of 11.2 and 15.0 % of 1 g/L micelle solution. For this reason we selected a micelle concentration of 1 g/L to be used in this study.

### 3.3.2.3. Bacteria Exposure to Biocide Loaded Micelles – Re-growth in the Presence of Micelles

SEM and TEM were used to visualize the effect of biocide loaded micelles of PS<sub>197</sub>-b-PAA<sub>47</sub> on *E. coli*, and to compare them with the controls, which consisted of bacteria in the presence of empty micelles and in the complete absence of micelles. Three samples were prepared: 1) no micelles; 2) empty micelles; 3) micelles loaded with 30 % (w/w) TCMTB (0.3 g of TCMTB/L). The total volume of each sample was 10 mL and the bacteria concentration was adjusted to reach an absorbance of 0.1. (Prior to that, the bacteria were grown over night to an absorbance of 1, diluted next day to an absorbance of 0.1 and re-grown again to yield a fresh sample). The samples were left for 2 hours in the incubator at 37 °C while shaking. In the next step, half the amount of each sample was taken for further analysis (SEM, TEM) while 5 mL of growth

medium was added to the other half. The samples were then incubated at 37 °C for 2 hours while shaking and monitoring the absorbance. The results of bacteria re-growth in absence of micelles, in the presence of empty micelles and of TCMTB loaded micelles are plotted in Figure 1 as relative absorbance vs. time. The concentration of block copolymer micelles was 0.5 g/L (equal to  $5 \times 10^{17}$  micelles/L) and the concentration of TCMTB in loaded micelles was 0.15 g/L.

Figure 3.1 shows that empty micelles affect the growth of bacteria slightly. The relative absorbances of the two samples are comparable; the bacteria growth is  $\sim 10\%$  slower in case of bacteria in the presence of non-loaded micelles than that of the control in water. Figure 3.1 also shows that the TCMTB loaded micelles deactivate bacteria, since the absorbance did not change within 3 hours.

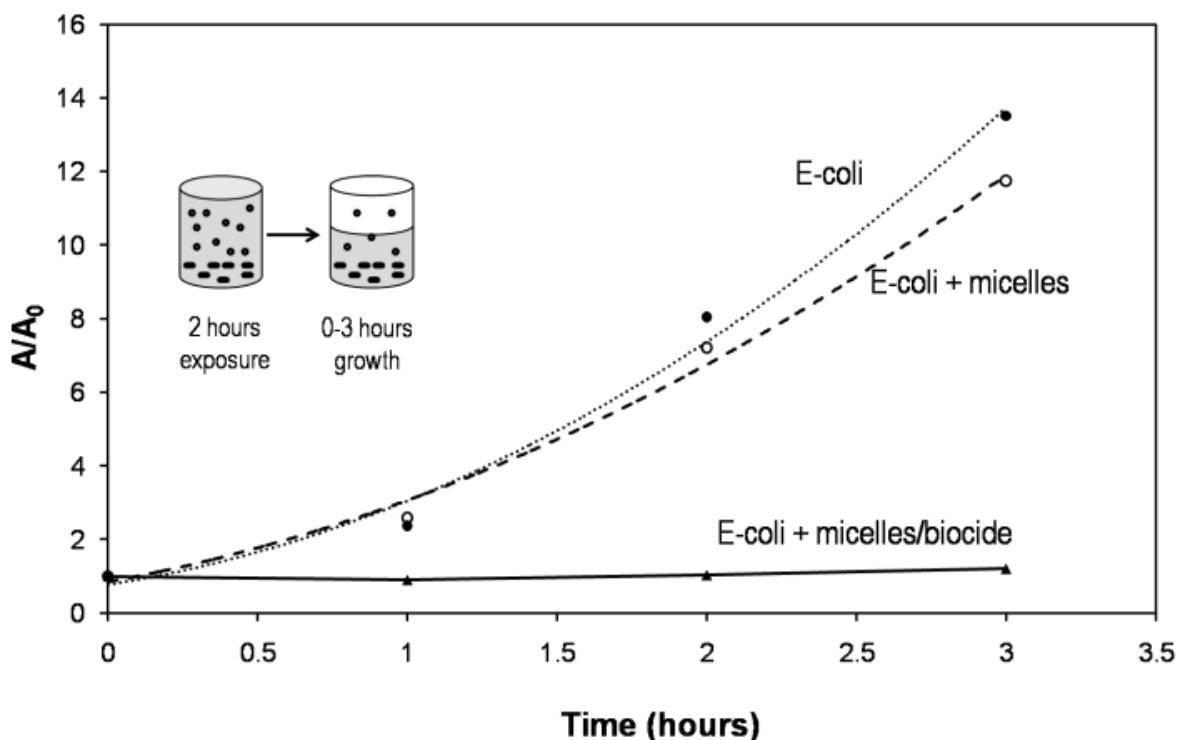


**Figure 3.1.** Deactivation of *E. coli* by exposing bacteria for 2 hours to 30 wt % TCMTB loaded micelles of PS<sub>197</sub>-b-PAA<sub>47</sub>, followed by exchange of half amount of micelles for growth medium and subsequent 3 hours growth. For comparison the bacteria growth was also tested in water and in the presence of empty (non-loaded) micelles. Full circles: control bacteria sample in water,

empty circles: bacteria in the presence of empty micelles, full triangles: bacteria in the presence of loaded micelles.

To explore the effect of absolute block length of the copolymer on bactericidal action the behavior of TCMTB loaded PS<sub>456</sub>-b-PAA<sub>103</sub> micelles on *E. coli* bacteria was studied. The total length of this polymer is higher by a factor of approximately two relative to the previously used polymer, but the ratio of PS to PAA is nearly identical, i.e. 4.19 for PS<sub>197</sub>-b-PAA<sub>47</sub> and 4.43 for PS<sub>456</sub>-b-PAA<sub>103</sub>. PS<sub>456</sub>-b-PAA<sub>103</sub> block copolymer micelles were loaded with TCMTB; in a manner similar to that of PS<sub>197</sub>-b-PAA<sub>47</sub> micelles; approximately 30 % (w/w) of loading was achieved in one hour by loading from biocide film. The same experimental approach as described in previous experiment was applied to test the efficiency of TCMTB loaded PS<sub>456</sub>-b-PAA<sub>103</sub> micelles on the bacteria. The results showed that the TCMTB loaded micelles of PS<sub>456</sub>-b-PAA<sub>103</sub> deactivate bacteria, similar to loaded PS<sub>197</sub>-b-PAA<sub>47</sub> micelles, since the relative absorbance did not increase with time, it even decreased slightly within 3 hours of incubation. The decrease in absorbance with time is, most likely, caused by the lysing some bacteria; the relative absorbance in 3 hours of bacteria incubation is almost identical for both polymers (PS<sub>197</sub>-b-PAA<sub>47</sub> and PS<sub>456</sub>-b-PAA<sub>103</sub>).

Before re-growth of *E. coli* bacteria, 5 mL of sample was taken for SEM imaging. SEM images of bacteria are shown in Figure 3.2; image A corresponds to the control sample (bacteria in absence of micelles), images B and C shows bacteria in the presence of non-loaded micelles of PS<sub>197</sub>-b-PAA<sub>47</sub>, and images D – F illustrate bacteria in the presence of TCMTB loaded micelles. Figure 3.2 shows that the surface of the bacterium, which is on the verge of division (Figure B), is fully covered by non-loaded micelles, as opposed to image A of non-treated bacteria. In image B, micelles are also clearly visible in the background of the bacteria, similar to image C, where the bacteria surface is almost devoid of micelle coverage. In general, about 30 % of the bacteria

exposed to non-loaded micelles are fully covered by micelles based on visual estimates from SEM images; the rest of the bacteria show little or no deposition. Moreover, about 30 % of the bacteria, upon exposure to TCMTB, excrete extra-cellular polysaccharides, as shown in images D – F. About 30 % of the bacteria in the presence of loaded micelles also show a high deposition of micelles on their surface (images E and F). However, about 70 % of the bacteria, in the presence of loaded micelles, do not exhibit any micelle deposition; two examples of uncovered bacteria are in images D and E. The bacteria exposed to the loaded micelles excrete much more extra cellular polysaccharides, on which micelles also deposit, than bacteria exposed to non-loaded micelles. Figure 3.2 also shows that if no micelles adsorb on the bacteria, no extra-cellular polysaccharides are excreted. The phenomenon of micelle deposition on bacteria surfaces vs. absence of micelle deposition will be discussed in section 3.3.4.

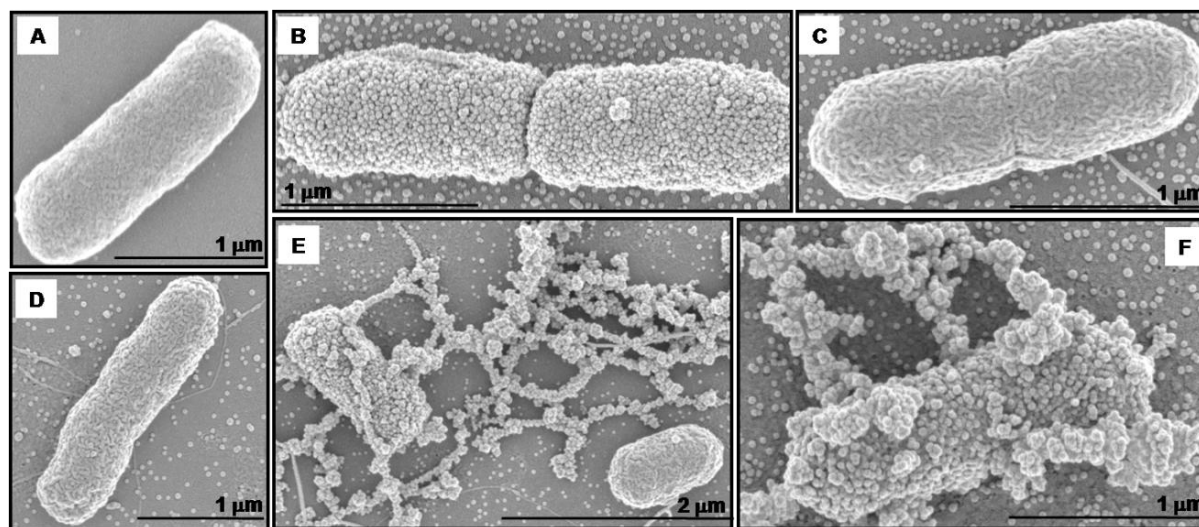


**Figure 3.2.** SEM images of *E. coli*: A) control sample, B and C) in the presence of non-loaded micelles of PS<sub>197</sub>-b-PAA<sub>47</sub>, D – F) in the presence of 30% TCMTB loaded micelles.

Figure 3.3 shows TEM microtomy images of *E. coli* cross sections: image A illustrates a control sample, images B and C show the bacteria in the presence of loaded micelles. Images B

and C demonstrate that some of the bacteria exposed to the loaded micelles are depleted in the middle (the intensity of light inside the bacteria is similar to that outside), what is seen in contrast to in control sample (A). The difference in appearance is caused by the presence of the TCMTB. For bacteria in the presence of loaded micelles, micelle deposition was expected on the outer surface of the bacteria, which is not observed (images B and C). Possibly, the deposition of micelles on *E. coli* as seen by SEM is an artifact for sample preparation.

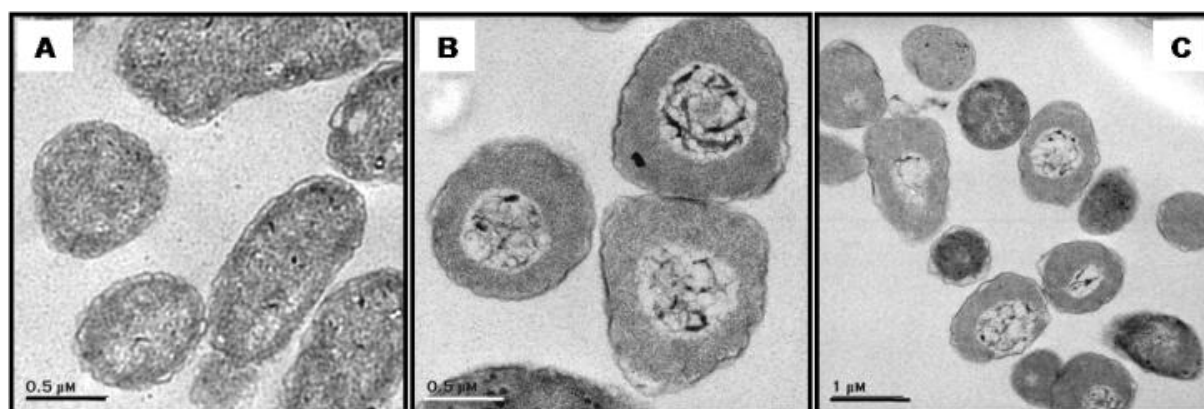


**Figure 3.3.** TEM images of microtomed cross sections of *E. coli* bacteria: A) control sample; B, C) in the presence of 30% TCMTB loaded micelles.

One of the advantages of the micellar systems is its stability.<sup>18</sup> Over a two years period, it was shown that as long as the loaded micelles are stored in a biocide saturated solution, the morphology, size and the concentration of the biocide in the micelles does not change with time.

#### 3.3.2.4. Cationic Poly(acrylamide)

To prepare bioactive paper which deactivates bacteria, one approach is to use c-PAM to attach negatively charged biocide loaded micelles onto negative pulp fibers. Therefore, we need to understand the effect of cationic poly(acrylamide) (c-PAM), the bridging material, on *E. coli* bacteria deactivation. The c-PAM, at a concentration of 0.2 g/L, was used in one series of



experiments along with empty and 30 % (w/w) (0.3 g of biocide/L) TCMTB loaded micelles of the PS<sub>197</sub>-b-PAA<sub>47</sub> block copolymer. The samples tested were in the following three ways: bacteria in the presence of c-PAM only, of empty micelles and c-PAM, and of TCMTB loaded micelles and c-PAM. The experimental procedures and conditions (exposure time, volume of the samples, temperature etc.) and concentrations of the empty and loaded micelles were kept the same as those described in section 3.3.2.3. The relative absorbance values for samples containing c-PAM were compared with those for the samples containing the same polymer micelles of PS<sub>197</sub>-b-PAA<sub>47</sub> block copolymer (non-loaded and TCMTB loaded) (Figure 3.4). In addition the schematic representations of the effect of c-PAM on bacteria in the presence of A: empty micelles and c-PAM; B: empty micelles; C: c-PAM is shown in Figure 3.4.

Figure 3.4 insert C shows that bacteria do not grow in the presence of c-PAM; therefore, it must be acting as a biocide on the bacteria, i.e. the c-PAM molecules adsorb on the surface of the bacteria, thus deactivating them. Since the bacteria surface has a net negative charge,<sup>27</sup> it seems reasonable to suggest that c-PAM, which is cationic, would adsorb on bacteria surface. Thus, it is not surprising that the effect of c-PAM itself on the bacteria is similar to that of TCMTB loaded micelles on the bacteria; the bacteria do not grow with time, i.e. they are deactivated, and since the relative absorbance decreases, they might be also lysed. By contrast, the effect of c-PAM on bacteria in the presence of empty micelles is very different. The relative absorbance of bacteria in the presence of c-PAM and empty micelles is, after 5 hours of bacterial incubation, similar to that of the control sample, which means that c-PAM, along with empty micelles, does not deactivate bacteria. The reason for such behavior is the following: The c-PAM is positively charged. Both, the micelles and the bacteria are negatively charged. In the absence of micelles, c-PAM adsorbs on the bacterial surface and deactivates the bacteria. However, in the presence of

micelles, since the surface area of the micelles is 100 times larger than that of the bacteria, the c-PAM adsorbs mainly on the micelles (schematic representation in Insert A in Figure 3.4). The relative absorbance of bacteria in the presence of empty micelles is  $\sim 20\%$  lower than that of bacteria in the presence of empty micelles and c-PAM; the empty micelles by themselves affect the growth of the bacteria only slightly and the bacteria are unaffected (schematic representation in Inset B in Figure 3.4). It was also found that combining TCMTB loaded micelles and c-PAM causes flocculation of *E. coli* likely caused by c-PAM/biocide interactions. The mechanism of this bacteria flocculation is unknown.

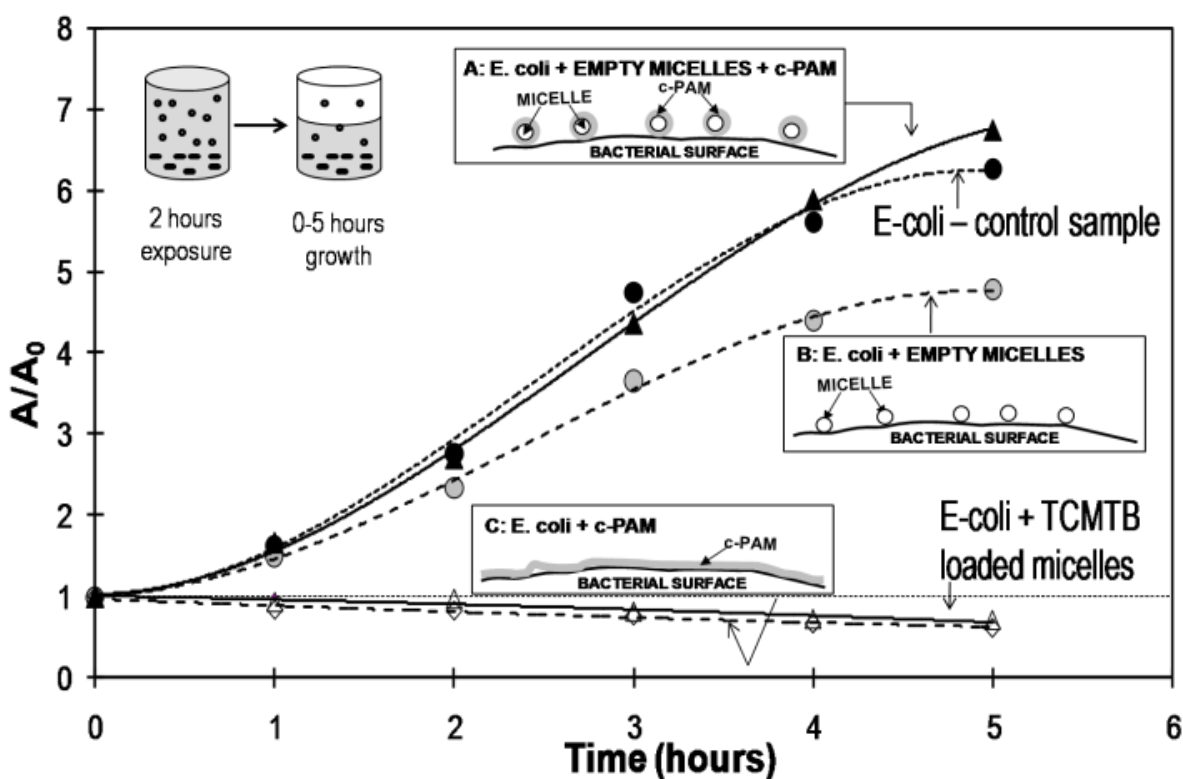


**Figure 3.4.** Effect of cationic poly(acrylamide) on *E. coli* bacteria deactivation and comparison with effect of non-loaded and TCMTB loaded PS<sub>197</sub>-b-PAA<sub>47</sub> micelles. Schematic representation of effect of c-PAM on bacteria: *E. coli* in the presence of A) empty micelles and c-PAM; B) empty micelles; C) c-PAM. *E. coli* flocculates in the presence of loaded micelles and c-PAM.

### 3.3.2.5. Deactivation of *E. coli* by TCMTB loaded PS<sub>297</sub>-b-PVP<sub>30</sub> Micelles

To explore the effect of a variation in corona composition, micelles containing hydrophilic negatively charged PAA polymer chains were replaced by those containing hydrophilic positively charged P4VP chains, and the deactivation of *E. coli* bacteria by TCMTB loaded PS<sub>297</sub>-b-PVP<sub>30</sub> micelles was studied. The bacteria samples were exposed to the loaded micelles for 2 hours. The experiment was performed in the same manner as that described in section 3.3.2.3.; i.e. separate runs for the bacteria samples in the presence of 30 % (w/w) of TCMTB loaded micelles (0.3 g of TCMTB/L), empty micelles and in absence of micelles (control sample). The only difference was that the bacteria were incubated in the growth medium for 18.5 hours at 37°C, and the absorbance was monitored with time. Figure 3.5 shows an increase in absorbance for control sample (bacteria in water, black symbols) to a value of 5. For the PS<sub>297</sub>-b-PVP<sub>30</sub> micelles, the experiment with empty micelles (without TCMTB loading) yields very different results than of those obtained for PS-b-PAA micelles. Only very limited bacteria growth is observed over the 18.5 hour incubation period for the P4VP corona system. By contrast, for the PS-b-PAA micelles (Figure 3.1), the rate of bacterial growth was nearly similar to that in nutrient medium alone. The difference lies in the bactericidal nature of the P4VP itself. Also, because P4VP is positively charged, since micelles deposit on the bacteria. TCMTB loaded PS<sub>297</sub>-b-PVP<sub>30</sub> micelles are efficient in deactivating bacteria as can be seen from the fact that the relative absorbance not only does not exhibit any increase, but actually decreases to 0.9, which means that the bacteria are lysed. Bacteria were incubated for 18.5 hours instead of 5 hours to see if the bacteria growth will become constant after 5 hours of incubation or will continue to

increase. No significant difference was observed in the relative absorbances for any of the samples at 5 hours and at 18.5 hours.

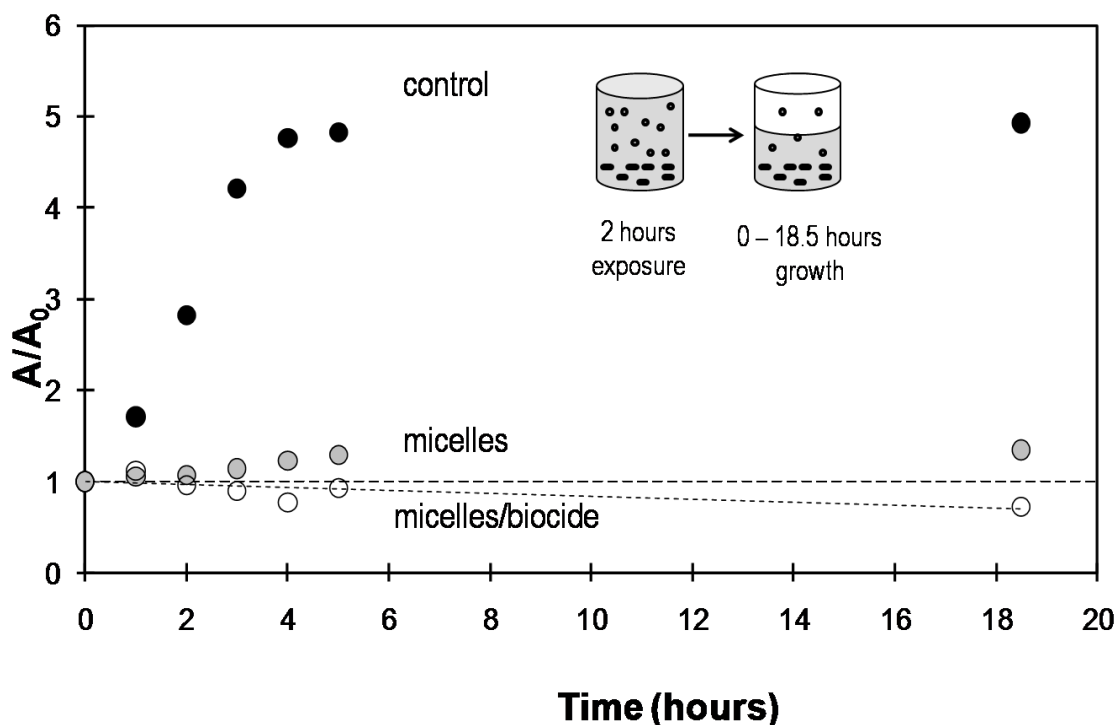


**Figure 3.5.** Deactivation of *E. coli* bacteria by empty and TCMTB biocide loaded PS<sub>297</sub>-b-PVP<sub>30</sub> micelles.

### 3.3.2.6. Bacteriostatic and Bactericidal Properties of TCMTB Loaded Micelles

To evaluate whether the micelles loaded with TCMTB are bacteriostatic or bactericidal, it was necessary to test bacteria re-growth in the absence of loaded micelles. To clarify this aspect, *E. coli* were exposed to 30 % (w/w) (0.3 g of biocide/L) TCMTB loaded PS<sub>197</sub>-b-PAA<sub>47</sub> micelles in an incubator at 37 °C while shaking for various periods of time (between 0 to 90 minutes) at the same micelle concentrations as previously described in section 3.3.2.3 (1 g/L). The samples taken after various exposure times were then centrifuged at 3000 RPM for 10 minutes and the entire supernatant containing the TCMTB loaded micelles was exchanged for growth medium,

keeping the volume the same as it was before centrifugation (10 mL). The samples were then incubated for up to 22 hours while monitoring the absorbance of individual samples (Figure 3.6). Bacteria continue to grow at a rate comparable to that of the control sample (black circles in Figure 3.6). It was found that the 90 minutes exposure time of bacteria to the TCMTB loaded PS<sub>197</sub>-b-PAA<sub>47</sub> micelles is not long enough to kill them.

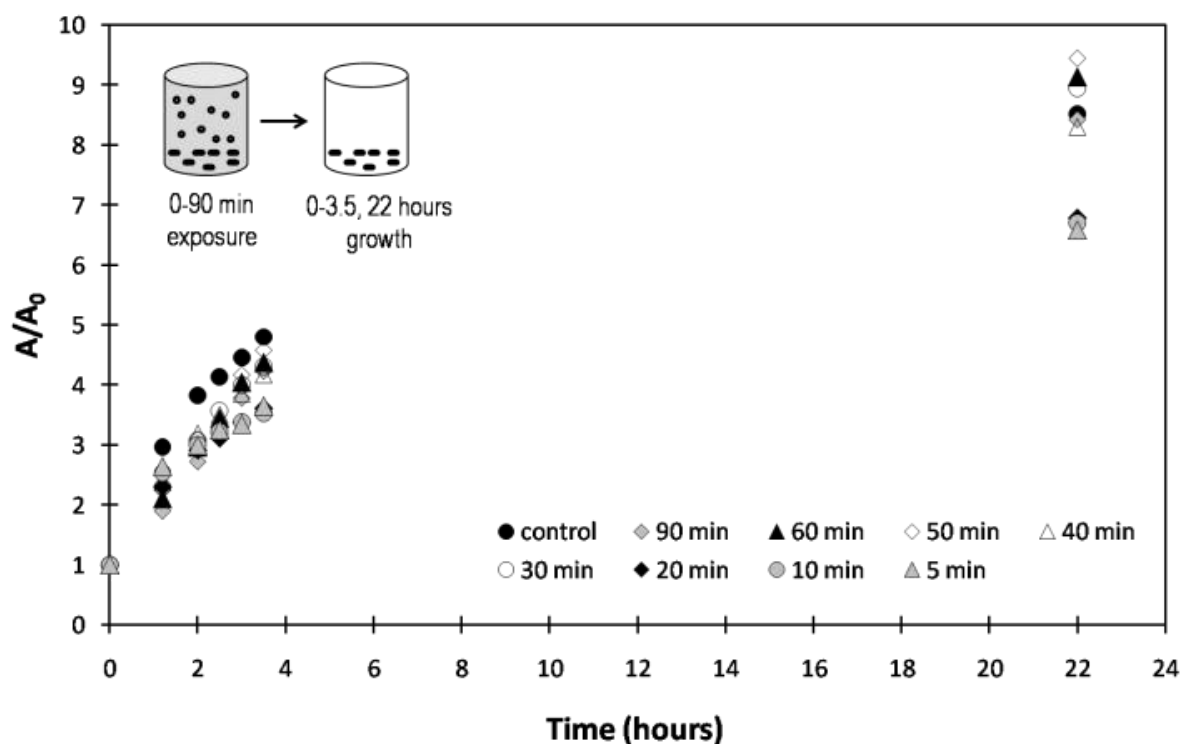


**Figure 3.6.** Deactivation or killing of *E. coli* by TCMTB loaded micelles of PS<sub>197</sub>-b-PAA<sub>47</sub>. *E. coli* exposed for various times (0 to 90 min) in the presence of 30 wt % TCMTB loaded micelles of PS<sub>197</sub>-b-PAA<sub>47</sub>, followed by exchange of micelles for growth medium and subsequent 22 hour growth.

To find the time needed to kill the *E. coli*, the experiment described above was repeated but with longer exposure times, i.e. 3 to 16 hours and the bacteria incubation time was also extended to 5 hours (Figure 3.7).

Bacteria grow at progressively slower rates, compared to the control sample (black circles), i.e. for samples which have been exposed to the TCMTB loaded micelles for 3, 6 and 8 hours. But those exposed for 12 and 16 hours do not grow at all. The bacteria killing time is thus approximately 10 hours. Hence, for the conditions shown in Figure 3.6 (short exposure time of 0 to 90 min), the TCMTB loaded micelles indicate bacteriostatic properties. In case of a much longer exposure time of the bacteria to the TCMTB loaded micelles (approximately 10 hours), the TCMTB loaded micelles show bactericidal properties (Figure 3.7).

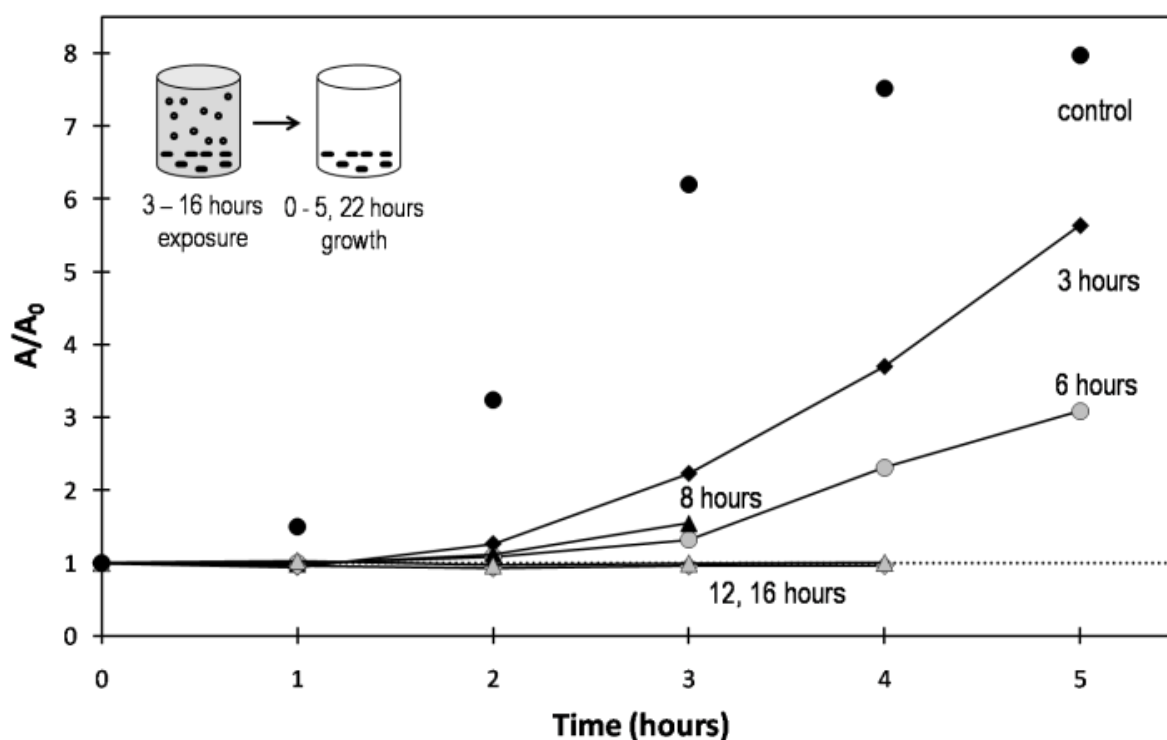


**Figure 3.7.** Killing time of *E. coli* by TCMTB loaded micelles of PS<sub>197</sub>-b-PAA<sub>47</sub> as a function of exposure times of bacteria to loaded micelles prior to re-growth.

### 3.3.3. Deactivation of Bacteria by Triclosan (TCN)

TCMTB is killing the *E. coli* in approximately 10 hours, which is a very long time for applications, such as, for example, in bactericidal filter paper. In that application, where the bacteria solution is passed through the filter paper containing micelles loaded with biocide, the killing time of bacteria should be short (on the order of minutes) for the paper to be efficient. For that reason, another hydrophobic biocide was evaluated. Triclosan, a potent wide spectrum antibacterial and antifungal agent commercially used in soaps, deodorants, toothpastes, shaving creams, mouth washes, cleaning supplies etc. was selected. The mechanism of action of triclosan on the *E. coli* bacteria is known to be blocking of lipid synthesis in the bacteria.<sup>28</sup> In contrast, the deactivation mechanism for TCMTB is unknown, and hence the deactivation mechanism is not necessarily the same. The molecular structure, together with other properties of triclosan, including water solubility and oral LD<sub>50</sub>, are given in Table 2. It is noteworthy that, in spite of its potency, the oral LD<sub>50</sub> value for triclosan on rats is 5 g/kg of animal,<sup>26</sup> higher than that for NaCl (3 g/kg).<sup>29</sup>

#### 3.3.3.1. Saturation Concentration of Triclosan

Even though the solubility of TCN in water is low (11.0 mg/L according to the literature<sup>30</sup>) it seems advisable to test the efficiency of TCN on *E. coli* deactivation. In order to find the TCN efficiency on *E. coli* bacteria, the TCN was dissolved in water, and the excess of the undissolved material was removed using a 0.45  $\mu$ m filter. The concentration of the TCN was tested by UV-vis and found to be 11.4 mg/L at pH of  $\sim$  5.4 using a wavelength of 281.4 nm in dioxane/water at 95/5% (w/w).<sup>19</sup> The *E. coli* were then exposed for 2 hours to saturated aqueous TCN solution in the incubator at 37 °C while shaking (the absorbance of the bacteria – TCN saturated solution was adjusted to 0.1, which corresponds to  $25 \times 10^6$  bacteria/mL); the control sample of bacteria

in only water was also exposed for 2 hours. Samples were then centrifuged for 10 min at 3000 RPM, the supernatant was replaced by growth medium and the samples were incubated for 3.5 hours while monitoring their absorbance.

The relative absorbance of *E. coli* bacteria exposed to the TCN saturated solution continues to increase with time even though the rate is much lower than that of the control sample (Figure 3.8). This means that the saturated TCN solution is not concentrated enough to kill the bacteria. Therefore, the TCN has to be loaded into micelles to be effective in killing the bacteria. A mechanism exists to transfer the TCN to the bacteria, and such a mechanism will be described in section 3.3.5.

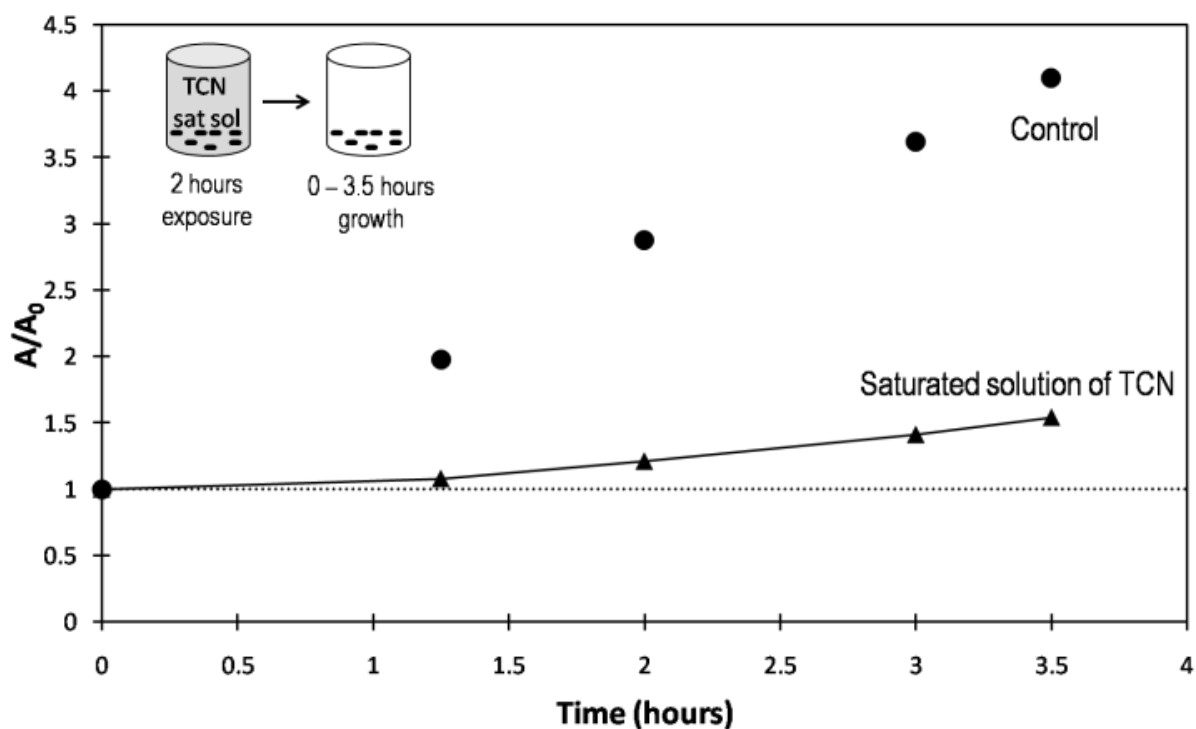


**Figure 3.8.** Deactivation of *E. coli* by exposure of the bacteria to a saturated solution of TCN for 2 hours followed by incubation of the bacteria for various time periods.

### 3.3.3.2. Bacteria Killing Time



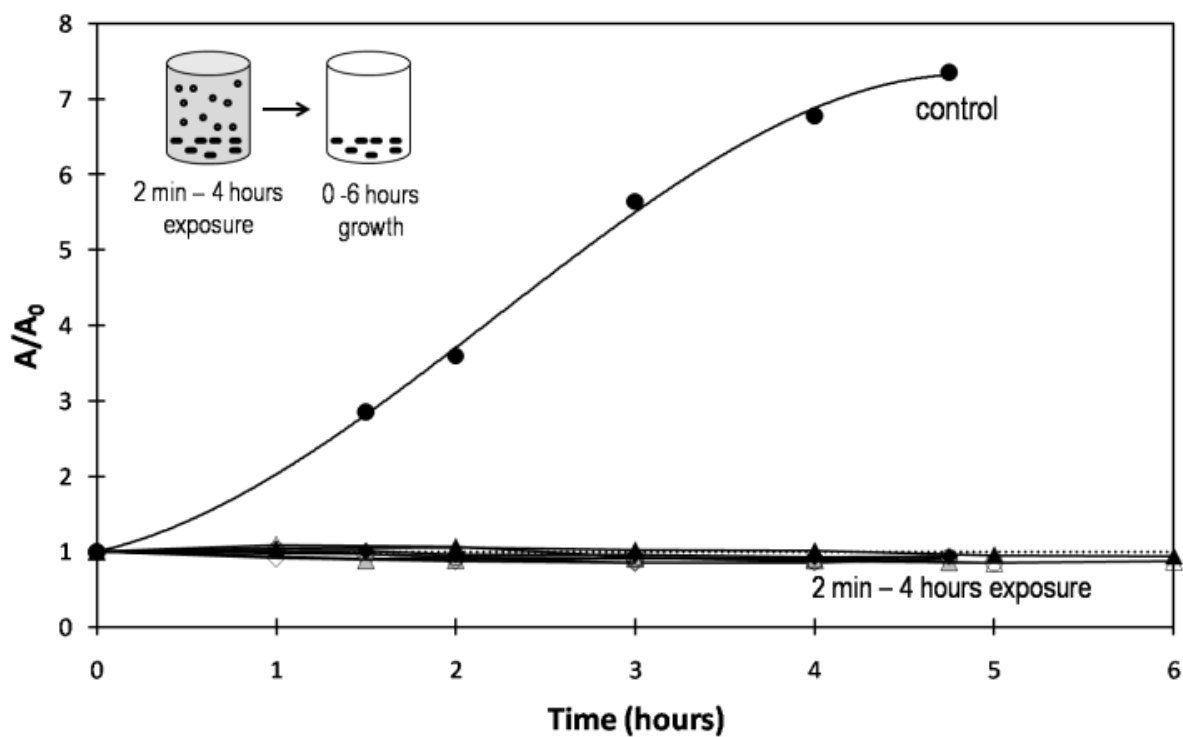
The loading of TCN into PS<sub>197</sub>-b-PAA<sub>47</sub> micelles was performed by following the same protocol as in case of TCMTB biocide loading into micelles, as described previously.<sup>19</sup> The loading efficiency was evaluated using UV-vis spectroscopy, at a wavelength of 281.4 nm in dioxane/water at 95/5% (w/w) (details are given in the previous publication<sup>19</sup> in section 3.2.4.). The maximum loading of approximately 20 % (w/w) of TCN into PS<sub>197</sub>-b-PAA<sub>47</sub> micelles is achieved by loading from the biocide film in 1 hour. Since the concentration of loaded TCN in the micelles was 200 mg/L while and its solubility in water is 11.4 mg/L, the total concentration of TCN is increased approximately 20 times at the given polymer concentration (1 g/L) and at a loading of 20 (w/w) %.

The TCN loaded PS<sub>197</sub>-b-PAA<sub>47</sub> micelles were also evaluated for their antibacterial activity. The micelles in a solution of concentration of 1 g/L, were loaded with TCN at a concentration of ~ 20 % (w/w) in 10 mL batches. The initial absorbance of the bacteria samples in solutions with TCN loaded micelles was set to be 0.1. Samples of loaded micelles were exposed to the *E. coli* for various times (2, 5, 10, 20, 30 min and 1, 2, 4 hours) along with the control sample (bacteria in water for 4 hours) in the incubator at 37 °C, while shaking. 1 mL of the sample was then taken for SEM imaging and treated as described in the Appendix to Chapter 3. The remainder of the samples was centrifuged for 10 min at 3000 RPM, the supernatant was replaced by growth medium and the samples were incubated for 6 hours while monitoring the absorbance.

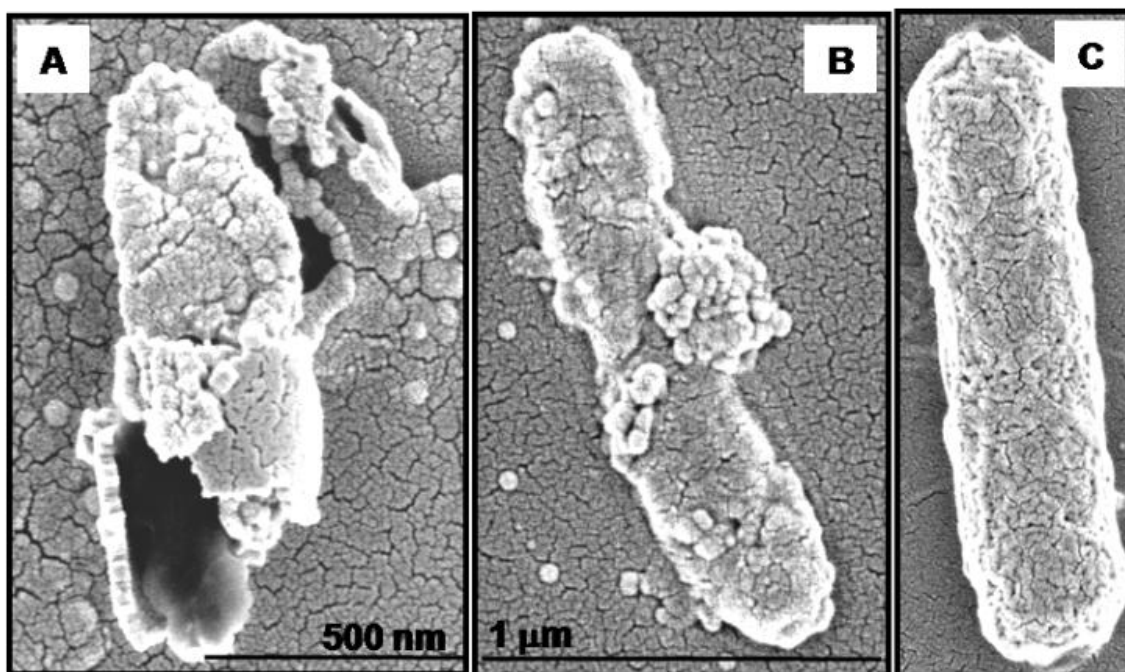
Figure 3.9 shows that the TCN loaded micelles are efficient in killing bacteria in two minutes or less. Shorter exposure times could not be explored due to sample manipulation time restrictions.

Figure 3.10 shows the SEM images of *E. coli* bacteria treated PS<sub>275</sub>-b-PAA<sub>47</sub> micelles loaded with TCN (images A and B). Interestingly, most of the bacteria observed in SEM images were

lysed similar to those in picture A, which is additional proof that the bacteria were killed by the TCN loaded micelles. Image C shows the control sample of *E. coli* in the absence of TCN loaded micelles.



**Figure 3.9.** Killing time of *E. coli* by TCN loaded micelles of PS<sub>275</sub>-b-PAA<sub>47</sub> as a function of exposure time to loaded micelles prior to bacteria re-growth.



**Figure 3.10.** SEM images of *E. coli* bacteria killed by micelles of PS<sub>275</sub>-b-PAA<sub>47</sub> loaded with TCN (images A and B); image C is bacteria in absence of TCN loaded micelles (control sample). (The image scale for image C is the same as in case of image B).

#### 3.3.4. Deposition of Micelles on *E. coli* Bacteria

As already mentioned in section 3.3.2.3. (Figure 3.2.) approximately 30 % of the bacteria exposed to the empty (2B) and loaded (2E, 2F) micelles are fully covered by deposited micelles. This was determined visually from SEM images. The rest of the bacteria (~ 70 %) exhibit little or no deposition, as illustrated in images 2C for empty micelles and 3D for loaded micelles. Bacteria which excrete extra-cellular polysaccharides and are covered by deposited micelles also exhibit micelle deposition on the extracellular polysaccharide fibers as shown on images 2E and 2F. In the following sections we will further discuss the above phenomena. In particular, we investigated whether or not micelle deposition depends on fixation time, or whether or not the bacteria are alive or dead, or if deposition is a drying effect.

##### 3.3.4.1. Effect of Time of Fixation

It was speculated that the micelle deposition on some bacteria could be attributed to the differences in the time of fixation of bacteria samples by glutaraldehyde. The following experiment was performed to explore this hypothesis: Two samples of *E. coli* bacteria of an absorbance of 0.1 at 600 nm were exposed to TCMTB loaded micelles of PS<sub>197</sub>-b-PAA<sub>47</sub> block copolymer of polymer concentration of 1 g/L for 2 hours. One of the two samples was then centrifuged and the supernatant was exchanged for the fixative (glutaraldehyde) right after 2 hours exposure time. SEM images of *E. coli* bacteria after immediate fixation are shown on Figure 3.11 A and B. The second of the two bacterial samples was also centrifuged right after the 2 hours exposure to the TCMTB loaded micelles and the supernatant was exchanged for water. However, in this case, the sample was kept in a refrigerator for two weeks. After two weeks of refrigeration, the supernatant was exchanged for the fixative (glutaraldehyde), and the sample taken for SEM imaging. SEM images of *E. coli* bacteria fixed after two weeks storage are shown on Figure 3.11 C and D.

Figure 3.11 shows that there is no appreciable difference between the images obtained by the immediate fixation (images A and B) vs. fixation after two weeks (images C and D). In both cases the bacteria are partially covered by micelles. Also, in both cases the bacteria release extracellular polysaccharides, which are covered by deposited micelles. According to these results, the deposition of the micelles on the bacteria does not correlate with fixation times.

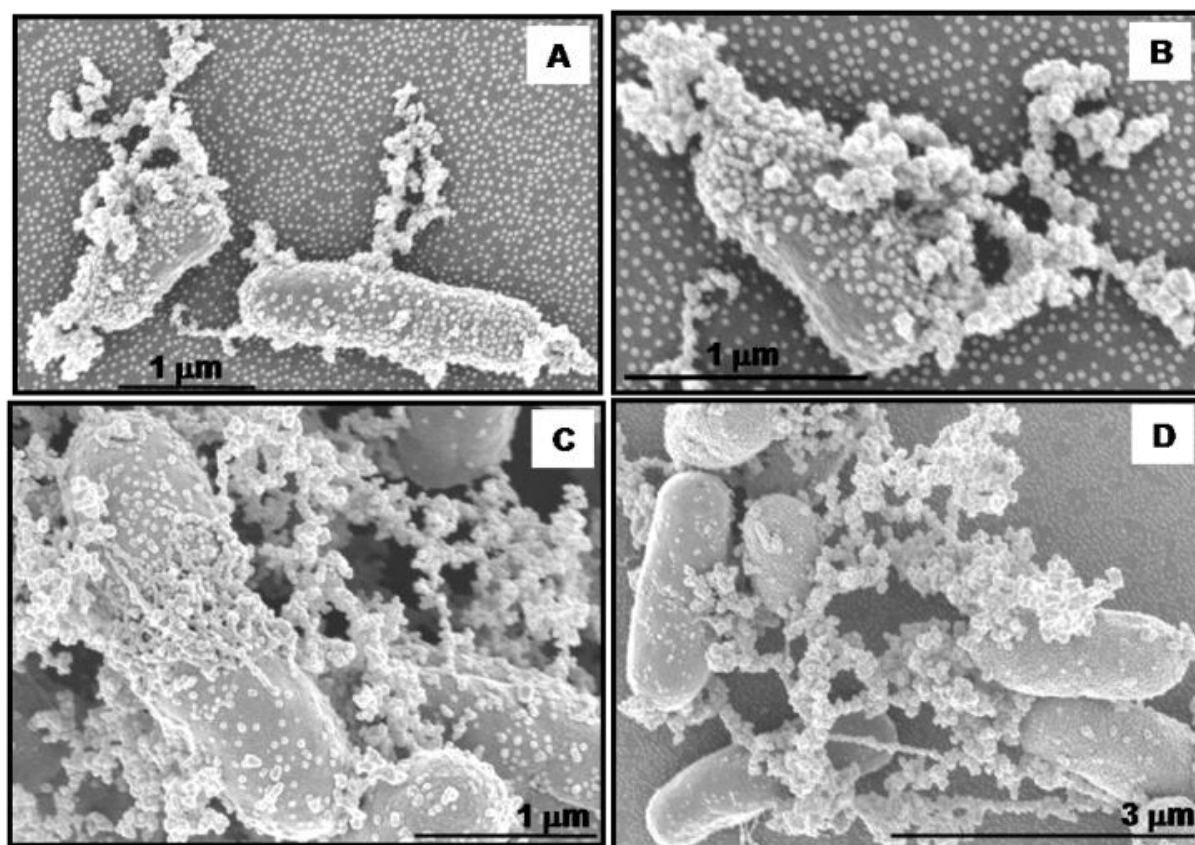


**Figure 3.11.** SEM images for various fixation times of *E. coli* deactivation by TCMTB loaded PS<sub>197</sub>-b-PAA<sub>47</sub> micelles with glutaraldehyde: A, B) immediate fixation; C, D) fixation after two weeks.

#### 3.3.4.2. Dead vs. Live Bacteria

It was also speculated that the micelles might be able to deposit only on dead bacteria. Even though it is known that the bacterial cell surface carries a net negative charge under most physiological conditions,<sup>27</sup> it is possible that the zeta potential of dead vs. live bacteria is different and that the micelles, which are also negatively charged due to the PAA corona, would preferentially deposit on either dead or alive bacteria. The zeta potentials of both, dead and live bacteria, were measured using electrophoretic mobility technique for gram negative *E. coli* bacteria. Two series of experiments were performed on dead and live bacteria in water (control

samples), in the presence of empty PS<sub>197</sub>-b-PAA<sub>47</sub> micelles and TCMTB loaded micelles. The description of the experimental procedure is given in section 1.4.3. in the Appendix to Chapter 3.

The zeta potential values for the dead bacteria samples were the following: – 44 mV for the control sample, – 42 mV for empty micelles and – 42 mV for TCMTB loaded micelles. The zeta potential values for live bacterial samples were the following: – 47 mV for control sample, – 38 mV for empty micelles and – 42 mV for TCMTB loaded micelles. The zeta potential of PS<sub>300</sub>-b-PAA<sub>44</sub> vesicles is approximately -42 mV at pH 7.<sup>31</sup> Micelles are expected to have similar zeta potentials as vesicles. Since the values of zeta potential of bacteria and of micelles are similar, we cannot differentiate between bacteria without vs. bacteria with micelle deposition using the zeta potential technique.

#### 3.3.4.3. Number of Micelles per Monolayer on Bacteria

To better understand micelle deposition on roughly 30 % of the bacteria and also to find out if the micelles are in swollen or collapsed state when deposit on the bacteria, the number of micelles needed per monolayer coverage of bacteria at a given concentration was estimated. The number of micelles per bacterium can be obtained from the SEM image or can be calculated based on knowledge of the average bacteria and micelle sizes. Figure 3.12 shows a SEM image of a typical *E. coli* bacterium covered by deposited TCMTB loaded micelles. The enclosed area on the bacterium corresponds to 100 deposited micelles. The area is magnified on the right side of the picture (Figure 3.12) for better visibility of individual micelles. The calculated bacterium surface, from the SEM image in Figure 3.12, taking the approximate length of 1500 nm, and the width 500 nm, is about  $3.1 \times 10^6 \text{ nm}^2$ ; the size of the area containing 100 micelles is about  $300 \times 350 \text{ nm}^2$  (considering curved surface of bacteria), which equals  $105\,000 \text{ nm}^2$ . Therefore, the

number of micelles deposited on one bacterium is approximately 3000. To calculate the number of micelles per bacterium, considering monolayer coverage, knowing the diameter of micelles from the TEM image, which is 26 nm in the collapsed state (as mentioned in section 3.3.1.), the

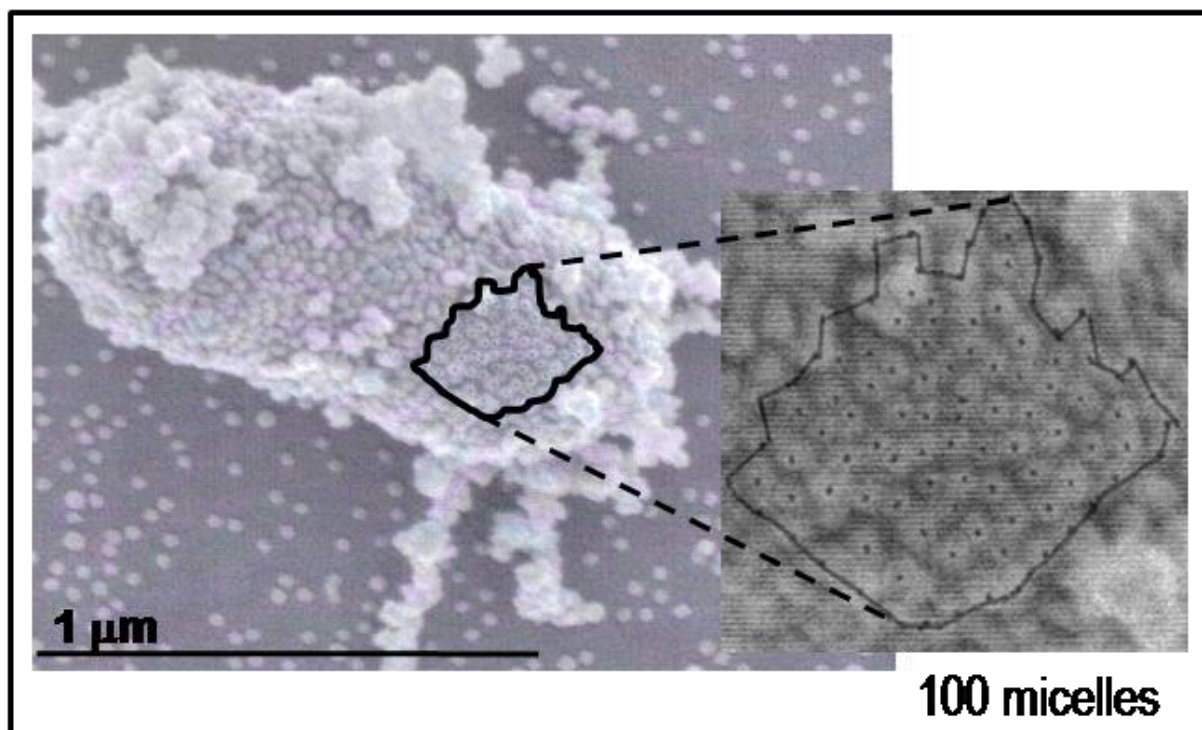


**Figure 3.12.** SEM images of *E. coli*: Number of micelles per monolayer on bacteria.

effective projected surface area of a micelle can be calculated. The effective projected surface area of one micelle ( $\pi r^2/0.55$ ) was found to be approximately 965 nm<sup>2</sup>, from which the number of micelles per bacterium was calculated to be 3 200 micelles/bacterium, which corresponds very well to the number of micelles per bacterium obtained from the SEM image. This agreement shows that the deposited micelles must be in a collapsed state. This suggests that the micelles are not deposited onto the bacteria from solution but that deposition occurred during drying. Based

on these conclusions, we can also conclude that, most likely, no micelles deposit on the bacteria in solution.

#### 3.3.4.4. Drying Effect

Another possibility is that micelle deposit due to a drying artifact. The image in Figure 3.13 was the most useful in this respect. The SEM image shows two *E. coli* bacteria surrounded by micelles in the background. It should be noted that the upper bacterium on the picture is not covered by micelles at all, as opposed to the one on the lower part of the picture which is extensively covered by micelles and which, in addition, released extra-cellular polysaccharides, which are also fully covered by deposited micelles. If the deposition of the micelles on the bacteria were caused by a drying effect, it would be of low probability to have, on the same image, two different bacteria so close to each other, where one is fully covered and, the other not covered at all, even though micelles are seen in the background of both bacteria. As pointed out in the previous section, the micelles on the SEM images (Figure 3.12 and 3.13) are in collapsed state and the deposition of the micelles on the bacteria is caused by the drying effect, because micelles adsorb on the bacteria in collapsed form. In last stage of drying, micelles are collapsed due to the presence of counter ions. Therefore, the deposition occurs late in the drying process, not in the solution. Thus, bacteria must be different in last stage of drying.



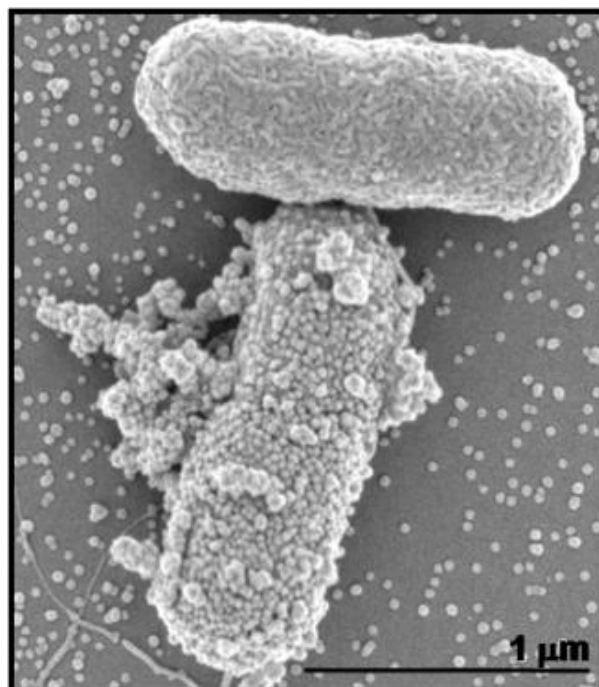


**Figure 3.13.** SEM image of *E. coli* in the presence of TCMTB loaded PS<sub>197</sub>-b-PAA<sub>47</sub> micelles.

### 3.3.5. Proposed Mechanism of Bacteria Deactivation

#### 3.3.5.1. Amount of Biocide in Bacteria

In order to find out how fast and in what quantity the biocide molecules transfer from the biocide loaded micelles to the bacteria, the following experiment was designed: Eight different samples were prepared, with the initial biocide concentration in micelle solution varying slightly from sample to sample (Table 3.3); the *E. coli* bacteria at an absorbance 0.1 were exposed to the TCMTB loaded PS<sub>197</sub>-b-PAA<sub>47</sub> micelles at a polymer concentration of 1 g/L for various times (between 5 and 195 minutes). The samples were then centrifuged for 10 minutes at 3000 RPM and the concentration of TCMTB in the supernatant was compared to the one in the solution before the exposure to the bacteria. TCMTB concentration was measured by UV-vis spectroscopy (described in section 3.2.4.1.). The biocide concentration on/in the bacteria was

estimated by subtraction of concentration after from before bacterial exposure to the biocide loaded micelles. The number of biocide molecules per bacterium can be estimated as follows: From the calibration curve (Figure 2 in Appendix to Chapter 3) one can estimate the number of bacteria in solution at an absorbance of 0.1, which corresponds approximately to  $25 \times 10^9$  bacteria/L. The number of micelles in solution of concentration of 0.01 g of polymer/L is  $\sim 10^{17}$  and the average aggregation number, estimated from the volume of PS per micelle, is  $\sim 250$  chains/micelle.<sup>19</sup> The number of biocide molecules in micelles at saturation is  $2.1 \times 10^3$  biocide molecules.<sup>19</sup> Thus, the number of biocide molecules per bacterium is estimated to be  $\sim 8.4 \times 10^9$ , while the number of micelles per bacterium equals to  $\sim 4 \times 10^6$ .

As seen in the Table 3.3, the concentration of biocide on or in bacteria after 5 minutes exposure is 2.1 w/w %, with exposure times of 10 to 195 minutes exhibit similar concentration values of approximately 3.3 w/w %. Those results prove that the bacteria are “fully loaded” with.

Experiment	#1	#2	#3	#4	#5	#6	#7	#8	
Exposure time $\tau_{\text{exp}}$ (min)	5	10	20	30	60	90	120	195	Av. value
Biocide concentration at $t = 0$ (%)	23.8	23.6	23.6	27.0	27.0	26.7	24.2	23.7	
Supernatant at $t = \tau_{\text{exp}}$ (%)	21.7	19.9	20.6	23.5	24.5	23.2	20.4	20.4	
Biocide ON/IN bacteria at $t = \tau_{\text{exp}}$ (%)	2.1	3.7	3.0	3.5	2.5	3.5	3.8	3.3	3.3 $\pm$ 0.45

**Table 3.3.** Amount of TCMTB biocide in bacteria. Bacteria *E. coli* were starved in the presence of TCMTB loaded for various times (5 to 195 min). The solution was centrifuged and the concentration of TCMTB in the supernatant was compared to the TCMTB concentration in the original samples.

about 10 w/w % of total accessible biocide within about 10 minutes of exposure to the TCMTB biocide from loaded micelles

### 3.3.5.2. Mechanism of Biocide Transfer to Bacteria

The first step in bacteria deactivation consists of the transfer of biocide from the micelle to the bacteria. The transfer cannot occur through the solution since the solubility of the biocide is too low and solutions of these biocides do not deactivate bacteria. The proposed mechanism is based on indirect evidence, i.e. exclusion of mechanisms. The considerations are as follows: i) Micelles are not present inside the bacteria on any images from TEM obtained by microtoming of the *E. coli* bacteria (Figure 3.3), thus, there is no evidence of endocytosis. The absence of endocytosis is not surprising since the micelle is too big to pass through the bacterial membrane; it is known that the outer membrane of bacteria is permeable to solutes of < 600 Daltons.<sup>32</sup> ii) Furthermore, the biocide saturated solution is not strong enough to deactivate the bacteria (section 3.3.2.1. for case of TCMTB and shown in Figure 3.9 for case of TCN). iii) As previously shown,<sup>19</sup> the release of the biocide from the micelles into the solution followed by the uptake of biocide by bacteria is too slow to deactivate the bacteria within a very short time. It is also unlikely that negatively charged micelles spread on negatively charged bacteria. In addition, SEM and TEM images show the absence of micelle adsorption on the most bacteria.

In view of the above considerations, the uptake of biocide by bacteria must involve a different mechanism than the various possibilities excluded in the above discussion. The following mechanism is proposed: The biocide transfers from the micelle into the bacteria by repeated bacteria - micelle contacts. Bacteria come into the contact with the micelle surface, and the biocide molecules are transferred from the micelle surface to the bacteria, while the surface is replenished from the core of the micelle. A schematic illustration of the process is shown in Figure 3.14.

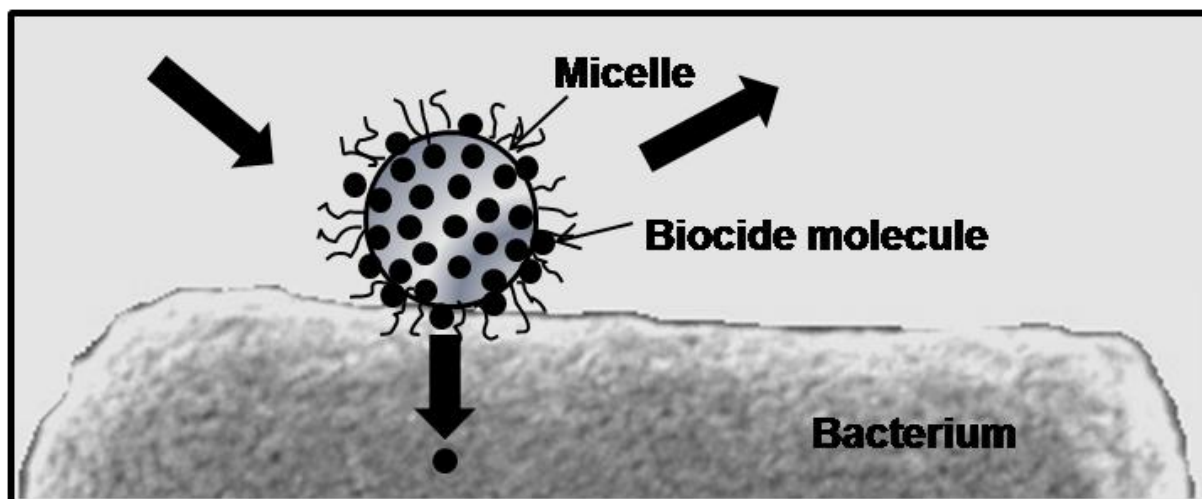


**Figure 3.14.** Schematic representation of mechanism of bacteria deactivation.

Micelle-bacteria contacts occur very frequently. One can estimate the number of micelles colliding per bacterium per second using the Smoluchowski equation:<sup>33</sup>

$$J = \frac{2kTn_2}{3\eta} \frac{(a_1 + a_2)^2}{a_1 a_2}$$

where  $a_1$  is the radius of bacterium ( $\sim 250$  nm),  $a_2$  is the radius of micelle (25 nm by DLS),  $k$  is the Boltzmann constant ( $1.38 \times 10^{-23}$  J/K),  $T$  is the temperature (K),  $\eta$  is the viscosity of water ( $10^{-3}$  Pas) and  $n_2$  is number of micelles per unit volume, which is  $10^{20}$  micelles/m<sup>3</sup>. The number of collisions/bacterium is thus 11500/s.

Since the average concentration of TCMTB biocide in bacteria is approximately 3.3 w/w % (data from Table 3.3), and bacteria are “fully loaded” with about 10 w/w % of the total accessible biocide within about 10 minutes of exposure, one can estimate the number of biocide molecules per collision transferred to the bacterium as follows: Knowing the total amount of biocide transferred from micelles to bacteria in 10 min, which is  $3.3 \times 10^{-2}$  g/L, the amount of biocide transferred to each bacterium is thus  $1.3 \times 10^{-12}$  g of biocide/bacterium at an absorbance

of 0.1 ( $25 \times 10^9$  bacteria/L). The number of molecules of biocide per gram of biocide is  $2.5 \times 10^{21}$ , and thus the number of molecules of biocide taken by one bacterium is  $3.3 \times 10^9$ . Finally, the number of biocide molecules transferred to the bacterium per collision can be estimated based on the above calculations for “full bacteria loading” within 10 min to be roughly 500 TCMTB biocide molecules/collision.

It should be noted that the thickness of the micelle corona and the radius (surface area) of the micelle core could conceivably affect this transfer. For successful transfer of biocide from micelle to the bacteria the permanent deposition of the micelles on the bacteria surface is not necessary.

### 3.4. Conclusions

We have designed and prepared block-copolymer micelles with bactericidal properties from PS-b-PAA (negatively charged corona) or PS-b-P4VP (positively charged corona) loaded with hydrophobic biocides such as Triclosan (TCN) or thiocyanomethylthiobenzothiazol (TCMTB). Block-copolymer micelles were loaded with the hydrophobic bactericidal material up to 20 to 30 % (w/w), depending on their type. Pathogens chosen for this study were *E. coli* (Gram negative bacteria). Block-copolymer micelles of PS-b-PAA loaded with TCMTB exhibit bacteriostatic properties at short exposure times (0-90 min) and only become bactericidal at long exposure times (~ 10 hours) of bacteria to loaded micelles. By contrast, block-copolymer micelles of PS-b-PAA loaded with TCN are bactericidal in exposure times shorter than two minutes. Cationic polyacrylamide, added to the micelle solutions to promote the interaction between micelles and bacteria, was itself found to be a bactericidal agent. PS-b-P4VP block copolymer micelles were also found to exhibit bactericidal properties even when not loaded with biocide.

It was found that the bacteria reach their limiting biocide uptake within about 10 minutes, at which point they have taken up approximately 10 % of the total biocide. The number of biocide molecules per bacterium was estimated to be  $\sim 8.4 \times 10^9$ , while the number of micelles per bacterium equals to  $\sim 4 \times 10^6$ . The proposed mechanism of biocide uptake involves transfer of biocide molecules during transient collisions between loaded micelles and bacteria. As the micelle surface is saturated by biocide, whenever the micelle collides with the bacteria surface, the biocide molecules are transferred from the surface of the core of the micelle to the bacteria. These collisions repeat very frequently. The number of biocide molecules transferred to the bacterium per collision was estimated for “full bacteria loading” within 10 min to be roughly 500 biocide molecules/collision and the number of collisions per one bacterium is approximately 11500/s. The thickness of the micelle corona and the radius (surface area) of the micelle core could conceivably affect this transfer. The deposition of micelles onto the bacterial surface is not necessary for successful transfer of biocide from micelle to the bacteria.

### 3.5. Reference List

(1) Yokoyama, M., *Crit. Rev. Ther. Drug Carrier Syst.*, **1992**, 9, 213 -248.

- (2) Nagasaki, Y., Yasugi, K., Yamamoto, Y., Harada, A., Kataoka, K., *Biomacromolecules*, **2001**, 2,(4), 1067 – 1070.
- (3) Giacomelli, C., Schmidt, V., Borsali, R., *Langmuir*, **2007**, 23, 6947.
- (4) Allen, C., Maysinger, D., Eisenberg, A., *Colloids Surf., B*, **1999**, 16, 3.
- (5) Chiappetta, D., Degrossi, J., Teves, S., D'Aquino, M., Bregni, C., Sosnik, A., *E. J. Pharm. Biopharm*, **2008**, 69, 535 - 545.
- (6) Kabanov, A. V., Bartakova, E. V., *Curr. Pharm. Des.*, **2004**, 10, (12), 1355.
- (7) Torchilin, V. P. *Pharm. Res.*, **2007**, 24 (1), 1.
- (8) Gindy, M. E.; Panagiotopoulos, A. Z., Prud'homme, R. K. *Langmuir*, **2008**, 24, 83.
- (9) Weaver, J. V. M., Armes, S. P., *Macromolecules*, **2003**, 36 (26), 9994–9998.
- (10) Štěpánek, M., Matějček, P., Humpolíčková, J., Havráňková, J., Podhájecká, K., Špírková, M., Tuzar, Z., Tsitsilianis, C., Procházka, K., *Polymer*, **2005**, 46 (23), 10493.
- (11) Gohy, JF., Lohmeijer, B. G. G., Alexeev, A., Wang, X.S., Manners, I., Winnik, M.A., Schubert, U.S., *Chemistry – A European Journal*, **2004**, 10 (17), 4315.
- (12) Nagarajan, R.; Barry, M., Ruckenstein, E., *Langmuir*, **1986**, 2, 210.
- (13) Zhang, L. F.; Eisenberg, A., *Science (Washington, DC, U.S.)*, **1995**, 268, 1728.
- (14) Tao, J.; Stewart, S.; Liu, G. J., *Macromolecules* **1997**, 30, 2738.
- (15) Discher, B. M., Won, Y.-Y.; Ege, D. S.; Lee, J. C.-M.; Bates, F. S.; Discher, D. E.; Hammer, D.A., *Science (Washington, DC, U.S.)*, **1999**, 284, 1143.
- (16) Lodge, T. P.; Pudil, B.; Hanley, K. J., *Macromolecules*, **2002**, 35, 4707.
- (17) Choucair, A., Eisenberg, A., *J. Am. Chem. Soc.*, **2003**, 125 (39), 11993–12000.
- (18) Kataoka, K., Matsumoto, T., Yokoyama, M., Okano, T., Sakurai, Y., Fukushima, S., Okamoto, K., Kwon, G.S., *J. Controlled Release*, **2000**, 64, 143-153.
- (19) Vyhnalkova, R., Eisenberg, A., van de Ven, T.G.M., *J. Phys. Chem. B*, **2008**, 112, 8477.
- (20) Luo, L.; Eisenberg, A.; *Langmuir*, **2001**, 17, 6804.
- (21) Azzam, T.; Eisenberg, A.; *Angew. Chem. Int. Ed.*, **2006**, 45, 7443.
- (22) Zhong, X. F., Varshney, S. K., Eisenberg, A., *Macromolecules*, **1992**, 25, 7160.
- (23) Yu, K., Eisenberg, A., *Macromolecules*, **1998**, 31, 3509.
- (24) H. W. Shen, L. F. Zhang, A. Eisenberg, *J. Am. Chem. Soc.*, **1999**, 121, 2728 - 2740.

- (25) Manninen, A., Auriola, S., Vartiainen, M., Liesivuori, J., Turunen, T., Pasanen, M., *Arch Toxicology*, **1996**, 70, 579.
- (26) Barbolt, T.A., [\*Surg Infect \(Larchmt\)\*](#), **2002**, (3), Suppl 1:S45-53.
- (27) Poortinga, A.T., Bos, R., Norde, W., Busscher, H.J., *Surface Science Reports*, **2002**, 47, 1-32.
- (28) [www.mindfully.org/Pesticide/Triclosan-Lipid-Synthesis](http://www.mindfully.org/Pesticide/Triclosan-Lipid-Synthesis)
- (29) [www.sciencelab.com/xMSDS-Sodium chloride-9927593](http://www.sciencelab.com/xMSDS-Sodium_chloride-9927593)
- (30) Raghavan, S.L., Schuessel, K., Davis, A., Hadgraft, J., *Int. J. Pharmaceutics*, **2003**, 261, 153.
- (31) Luo, L., Eisenberg, A., *Anew. Chem.*, **2002**, 114, 6, 1043.
- (32) Nikaido, H., Vaara, M., *Microbiological Review*, **1985**, 49, 1-32.
- (33) Smoluchowski, M. Z.; *Phys. Chem.*, **1917**, 92, 129.



## **Bridging Section between Chapters 3 and 4**

---

The previous chapter dealt with the bactericidal behaviour of micelles loaded with TCMTB or TCN and also described the mechanism of transfer of biocide from the micelles to the bacteria. Since the micelles are, indeed, bactericidal, with the active agent transferred by collisions in the solution, it is apparent that micellar systems could also be used in bactericidal applications in paper under wet conditions. One possible application was as a bactericidal filter paper, in which the micelles would be attached to the fibres and the water containing the bacteria filtered through such a paper.

The following chapter describes the preparation of such a filter paper using both commercial Whatman filter papers, as well as paper towels as the base. The method of attachment of micelles to the paper is described in Chapter 4, along with the detailed study of bactericidal efficiency over a range of relevant parameters, such as concentration of c-PAM, the polymer used to improve the adhesion of the micelles to the pulp fibres, concentration of the micelles, concentration of bacteria in solution and volume of the bacteria solution passed through the filter. A very brief optimization study was also performed involving these parameters.

## Chapter 4: Bactericidal Filter Paper

---

### Abstract

An antibacterial filter paper was prepared by modifying commercial filter papers or paper towels by first changing the natural negative charge of the pulp fibres to positive by adsorption of cationic polyacrylamide (c-PAM), followed by attachment of negatively charged triclosan loaded micelles to the pulp fibres with roughly monolayer coverage. The micelles are composed of an amphiphilic block copolymer of poly(styrene)<sub>197</sub>-*block*-poly(acrylic acid)<sub>47</sub> (PS-*b*-PAA) loaded with the antibacterial compound triclosan, which is the active component in killing bacteria. As water polluted by bacteria passes through such modified filter paper, the triclosan is transferred by collisions from the micelles to the bacteria which are passing through the filter; the bacteria are killed and the filtrate consists of water which is safe to drink.

### 4.1. Introduction

The killing of bacteria in water is a very important topic because of the obvious public health implications. It is especially relevant in third world countries where a lack of safe drinking water is common. Even in developed countries such as Canada, sometimes, for example while camping in remote areas, drinking water might not be easily accessible. Also, in the case of a major catastrophe, for example a flood, the quality of the drinking water in metropolitan areas can be compromised. Solutions to such problems have already been addressed through many commercially available products such as drinking straws,<sup>1-3</sup> antimicrobial paper<sup>4-7</sup> or disinfecting pills.<sup>8</sup>

\* *The manuscript is to be submitted to Macromolecular Bioscience*

LifeStraw is one example of straws used to drink water directly from a water source.<sup>1</sup> This straw is manufactured by the Vestergaard Frandsen Group in Denmark and is based on a combination of mesh filters, iodine-impregnated beads and active carbon to remove particulate matter and bacteria. Another example of a drinking straw is Survival Straw,<sup>2</sup> produced by Alloy Safe – USA, which is based on alloy media. Yet another example of a drinking straw is Pioneer,<sup>3</sup> manufactured by Pristine - Canada, which does not remove pathogens of size smaller than 3  $\mu\text{m}$ .

An antimicrobial paper was prepared by Intilli;<sup>4</sup> in his method, an antimicrobial additive is incorporated into the binding agent of a heavy-duty, kraft-type paper of substantial density, air impermeability, and improved printability. The antimicrobial additive migrates from within the binding agent onto the paper fibers and eliminates the growth of microorganisms. Other type of antibiotic paper had been patented previously.<sup>5</sup> The author claims that cellulose fibers possess strong antibiotic properties (including antiviral properties) when they have a uniform content of a small amount of a 2-(C<sub>8</sub> -C<sub>18</sub> substantially straight chain alkyl) *pseudourea*. The fibers remain antimicrobial when, in addition, they contain a normal water-soluble thermosetting wet strength resin in the thermoset state. An antibacterial filter paper based on Ag containing glass fibers of size smaller than 1  $\mu\text{m}$  diameter was more recently described in a Japanese patent.<sup>6</sup> Another patent<sup>7</sup> dealing with anti-microbial filters includes a silicon-based filter membrane. This antimicrobial filter device filters out microorganisms in a fluidic system.

Disinfecting pills are another example of bacteria deactivation in water. Commercially available disinfecting pills are manufactured by Camping Survival<sup>8</sup> and usually contain chlorine, chlorine dioxide, iodine or colloidal silver. However, clearly, none of these commercially

available products have the simplicity of passing the water through antibacterial filter paper to achieve potability, while simultaneously removing particulates. To our knowledge, none of the commercially available products are based on block copolymer micelles as carriers for the hydrophobic antibacterial material.

The aim of the present project is to prepare bioactive filter paper for water purification. We propose to achieve this goal by utilizing a hydrophobic biocide, which has very low water solubility and which is incorporated into the hydrophobic cores of amphiphilic block copolymer micelles. These micelles are, in turn, attached to the filter paper. The biocide is transferred to the bacteria as a result of collisions between bacteria and micelles, as shown in a previous paper,<sup>9</sup> and because of the extremely low solubility of an antibacterial agent in water, the water remains safe to drink.

An earlier paper from this project<sup>10</sup> was devoted to the study of the kinetics of loading of biocide into block copolymer micelles of polystyrene<sub>197</sub>-block-poly (acrylic acid)<sub>47</sub> (PS<sub>197</sub>-b-PAA<sub>47</sub>), suspended in water, with biocide, and its subsequent release. Loading was found to be a two- step process. First, the surface of the PS core of the micelles is saturated with biocide, at a rate determined by the transfer of biocide to the micelles during transient micelle – solid biocide collisions. Next, the biocide penetrates as a front into the micelles (Non-Fickian case II diffusion), lowering the glass transition temperature ( $T_g$ ) in the process. The rate of release was found to be governed by the height of the energy barrier which a biocide molecule must overcome to pass from the PS into the water. Because of rapid diffusion of biocide within the micelle above  $T_g$ , a uniform biocide concentration within the micelle is reached and is maintained until the  $T_g$  has increased (as a result of biocide release) to the point that diffusion inside the micelles becomes very slow.

A subsequent paper<sup>9</sup> dealt with deactivation of bacteria in solution using biocide loaded block copolymer micelles of polystyrene-block-poly(acrylic acid) (PS-b-PAA) and polystyrene-block-poly(vinyl pyridine) (PS-b-P4VP). Bacteria were exposed to the hydrophobic biocides of either triclosan or thiocyanomethylthiobenzothiazole, loaded into micelles, and bacterial deactivation was evaluated. Among other results, it was found that the micelles loaded with triclosan are bactericidal; bacteria become non viable in less than two minutes of exposure to a solution of the loaded micelles. It was also shown<sup>9</sup> that the biocide is, most likely, transferred to the bacteria by repeated micelle-bacteria collisions, and not *via* the solution.

The present paper describes in detail the preparation of antibacterial filter paper using commercially available filter papers or paper towels. Such papers are modified to have antibacterial properties by, at first, adsorbing a cationic polymer to change the negative ionic charge of the fibers to a positive one. This step is followed by attaching biocide loaded block copolymer micelles containing a negatively charged corona to the cationic polymer. The purification of water polluted with bacteria is achieved by passing the water through such a modified filter. Bacteria become non-viable in the filter paper as they come into contact with the biocide, which is released from the micelles during collisions as the bacteria pass through the filter paper. In addition, some of the bacteria might be also captured by the filter paper. A schematic drawing of the antibacterial filter paper is shown in Figure 4.1.

In such a modified filter paper, triclosan is the active component in killing the bacteria. It was shown previously<sup>9</sup> that since triclosan is hydrophobic, and therefore has a low water solubility, it is not strong enough to kill the bacteria in a saturated aqueous solution (Figure 3 in Appendix to Chapter 4), even though it is a potent antibacterial material (commercially used in soaps, deodorants, toothpastes, shaving creams, mouth washes, cleaning supplies etc.). Therefore, the

triclosan was loaded into the micelles which serve as a carrier for this biocide which increases the concentration of triclosan in the filter paper.

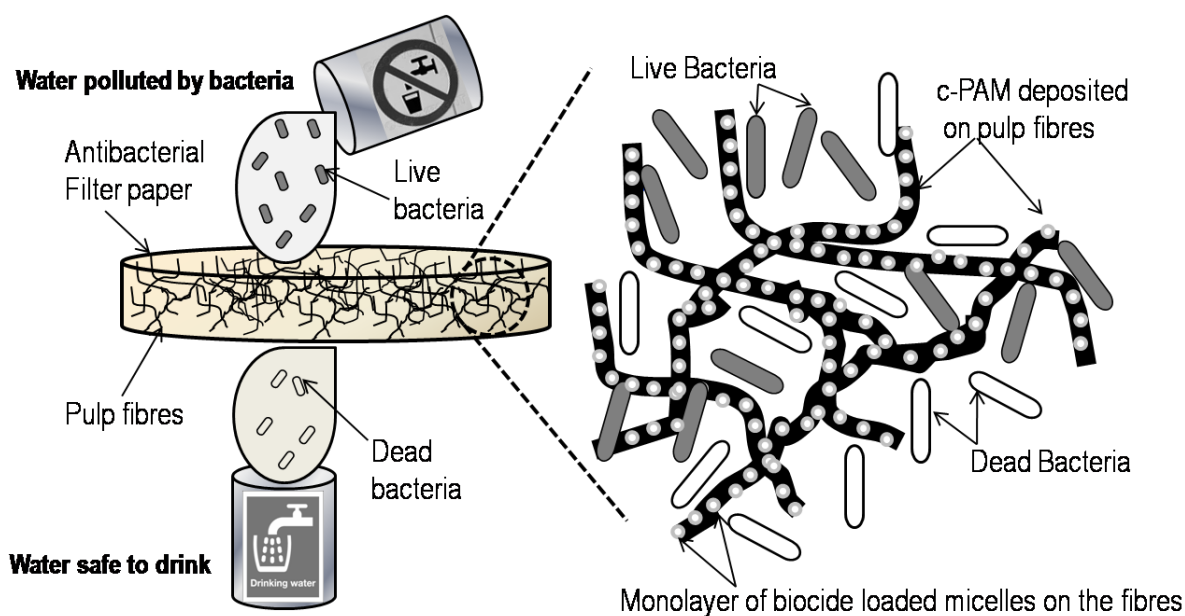


**Figure 4.1.** Schematic representation of antibacterial filter paper. (Not to scale).

In the present study, the results of the efficiency of antibacterial paper are first described for one type of filter paper. This is followed by a discussion of the effect of various relevant parameters, such as paper porosity, initial bacteria concentration, micelle and c-PAM concentration, initial volume of the bacteria solution, re-usability of antibacterial filter paper and bacteria deactivation with a filter sheet left in the bacteria suspension. The effectiveness was tested by passing a solution containing bacteria through the treated paper which had been placed in a funnel. The bacteria became non-viable. It should be noted that the solubility of the triclosan in water is very low; therefore it does not represent a health hazard even when the solution is

saturated<sup>11</sup>. The LD<sub>50</sub> value for triclosan tested on rats is 5 g/kg of animal<sup>12</sup> lower than that for NaCl (3 g/kg).<sup>13</sup> A 50 kg person would have to drink  $0.23 \times 10^5$  Liters of water saturated with triclosan (saturation concentration of triclosan in water is 11.0 mg/L)<sup>9,14</sup> to reach the LD<sub>50</sub> dose for mammals. One cup (300 mL) contains  $10^{-5}$  of the lethal dose. Stated another way, a person would have to drink 2 Liters of saturated triclosan solution for 30 years, without eliminating any of the triclosan, to reach the lethal dose. The mechanism of action of triclosan on the E. coli bacteria is known to be blocking of lipid synthesis in the bacteria.<sup>15</sup> It is also worth noting that the micelles are expected to remain attached to the filter paper and are not expected to be present in significant amounts in the drinking water.

A potential application of such antibacterial filter paper would be in small scale disposable filters for drinking water in remote areas, with additional benefits of filtration such as removal of small particulates. Another potential application could involve filters for sludges in the pulp and paper industry. Many other applications could be anticipated in situations where bacteria free water is important.

## 4.2. Experimental Section

### 4.2.1. Materials

The amphiphilic block copolymer of PS<sub>197</sub>-b-PAA<sub>47</sub> (Table 4.1) was synthesized using atom transfer radical polymerization.<sup>11</sup> The number average molar mass ( $M_n$ ) of the polymer is 23 900 and its polydispersity index is 1.10. The structure and properties of polystyrene-*block*-poly(acrylic acid) co-polymer, along with that of the cationic polyacrylamide, are shown in Table 4.1.

Structural formula		
Composition	PS <sub>197</sub> -b-PAA <sub>47</sub>	degree of substitution: 20 %
M <sub>w</sub> (g/mol)	2.39 x 10 <sup>4</sup>	3 x 10 <sup>6</sup>
PDI	1.10	N/A

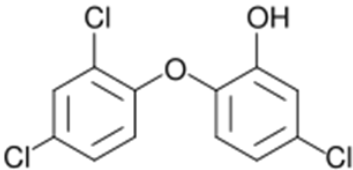
**Table 4.1.** Structure and properties of polystyrene-*block*-poly(acrylic acid) polymer and of cationic polyacrylamide.

Cationic polyacrylamide (c-PAM) of a degree of substitution of 20 % – PERCOL 292 was purchased from Allied Colloids (Canada) Inc. The molecular weight of the c-PAM used in this study is 3 MDa. The hydrophobic antibacterial material, triclosan (TCN) (Irgasan) was purchased from Fluka BioChemika (HPLC grade). The structural formula, together with other properties of triclosan, including water its solubility and oral LD<sub>50</sub>, are shown in Table 4.2.

Dioxane was purchased from Sigma-Aldrich (HPLC grade) and used as received. Milli-Q water was used in all experiments.

Filter papers used in this study were commercial filter papers of various grades made from cellulose fibers and purchased from Whatman. The filter papers differ in pore size and thickness. An overview of various grades of Whatman filter papers used in this study and its corresponding pore size and thickness are given in Table 1 in the Appendix to Chapter 4. The diameters of filter papers used were 90 mm.



Structural formula	
Biocide	Triclosan (TCN)
M <sub>w</sub> (g/mol)	289.5
Water solubility (mg/L)	11.0 <sup>14</sup>
Melting point (°C)	55 - 57
Oral LD <sub>50</sub> (g/kg)	5 (on rats) <sup>12</sup>

**Table 4.2.** Structure and properties of triclosan biocide.

In addition to the Whatman filter papers, white commercial paper towel from Cascades Inc., Canada, was also studied for its antibacterial efficiency as a filter paper. The paper towel was cut into circles shape of 90 mm diameter, similar to that of the Whatman filter paper.

The bacteria used were Gram negative *E. coli* strains ATCC 11229 and were donated by Prof. Mansel Griffiths from the Canadian Research Institute for Food Safety, University of Guelph, Canada. The medium used was Miller-Hinton broth purchased from Fluka (microbiology grade); bacteria were grown in this broth at 37 °C while shaking.

#### 4.2.2. Experimental Techniques

The principal techniques involved in this study were transmission electron microscopy (TEM), dynamic light scattering (DLS), scanning electron microscopy (SEM) and UV-vis spectroscopy. A brief description of the instrumentation and sample preparation methods is given in the Appendix to Chapter 4.

#### 4.2.3. Micelle Preparation

The micelle preparation procedure starting from the amphiphilic block copolymer PS<sub>197</sub>-b-PAA<sub>47</sub> was discussed in detail in a previous paper.<sup>10</sup> Only a very brief description is given here for the convenience of the reader. The block copolymer was dissolved in dioxane at an initial block copolymer concentration of 1% (w/w) and stirred overnight to ensure complete dissolution of the polymer. Milli-Q water was then added drop-wise at a rate of 0.2 % (w/w)/min to induce self-assembly into micelles, until a final water concentration of 50 % (w/w) was reached. No other morphology is observed under these conditions; only micelles are formed. In order to freeze the aggregate morphology, the solution was quenched into a large excess of water, and dialyzed for a period of three days to remove the organic solvent (dioxane). The final micelle concentration in the solution is ca 1 g/L.

#### 4.2.4. Characterization of the Micelles

Characterization of the micelles was discussed in the previous paper.<sup>10</sup> Transmission electron microscopy (TEM) and dynamic light scattering (DLS) were employed to characterize the micelles. The descriptions of the techniques and sample preparation methods are given in the

Appendix to Chapter 4. The micelles consist of a hydrophobic polystyrene core and a hydrophilic poly(acrylic acid) corona. A schematic representation of the micelle structure, both in solution and in the dry state, is shown in Figure 1 in the Appendix to Chapter 4.

#### *4.2.5. Micelle Loading*

After completion of the dialysis of the micelle solution in the preparation step, the micelles were loaded with the triclosan biocide. Prior to loading, the biocide was dissolved in 2 mL of acetone to a concentration of 5 mg/mL and placed in a vial. The acetone was allowed to evaporate overnight from the vial, leaving a thin film of the biocide inside. The micelle solutions (10 mg of polymer in 10 mL) were afterwards transferred to the vials containing the biocide film and vigorously stirred for a period of 1 hour to achieve maximum loading. The excess of biocide was removed by a 0.45  $\mu\text{m}$  filter. The details were described in a previous publication.<sup>10</sup>

#### *4.2.6. Preparation of the Bactericidal Filter Paper*

As mentioned above, commercial Whatman filter papers of various grades (1,2,3) and paper towel samples were used to test the antibacterial properties of the modified papers to be used as antibacterial filters. Preparation of the bactericidal filter paper consists of four steps. The steps are described in detail in the following paragraphs.

Since the charge of the pulp fibers in filter paper is negative, and loaded micelles with a negatively charged corona are to be attached, the ionic charge of the pulp fibers has to be changed; this change is accomplished by depositing a positively charged polymer as a tie-layer. Thus, first step in the preparation of bactericidal filter paper consists of the deposition of cationic polyacrylamide (c-PAM) with a degree of substitution of 20 % onto the filter paper; the relative

amount of the c-PAM is 1 mg of c-PAM/g of paper. Prior to the c-PAM deposition, each filter paper sample is weighed dry and afterwards presoaked in water in a petri dish and weighed again; this is done to determine how much water or solution can be absorbed per gram of dry paper. This information allows one to adjust the c-PAM concentration such that at equilibrium absorption, 1 mg of c-PAM/gram of dry paper has been taken up. The next step consists of drying the filter paper soaked in the c-PAM solution in air overnight.

After drying, the triclosan loaded block copolymer micelles with the negatively charged corona are attached to the positively charged filter paper. Since the volume of solution which can be absorbed by an individual sample of filter paper is known, the paper is now exposed to the micelle solution and a known quantity of micelles is attached to the paper via the interaction of the PAA in the micellar corona and the c-PAM coated fibers of the paper. The final concentration of the loaded micelles on the filter paper is 1mg of micelles/g of paper, which roughly corresponds to half a monolayer of loaded micelles on the pulp fibers. In the final preparatory step, the paper is dried in air overnight.

It should be noted that for each paper sample, controls were also prepared. The first control is the untreated paper without any additives, the second control contains paper coated only with c-PAM but without loaded micelles, and the third control sample contains paper treated with loaded micelles without any c-PAM. Control tests for utilizing empty (unloaded) micelles were not performed since it had previously been found that empty micelles do not affect significantly the growth of bacteria.<sup>9</sup>

#### 4.2.7. Test for Antibacterial Paper Efficiency

To test the efficiency of the antibacterial filter paper, the *E. coli* 11229 bacteria are first incubated over night in growth media at 37 °C while shaking. The concentrations of the bacteria solutions are tested by UV-vis for its absorbance and then diluted to an absorbance of approximately 0.1, which corresponds, according to the calibration curve given in the Supporting Information in Figure 2, to roughly  $25 \times 10^6$  bacteria/mL. The next day the bacteria continue to be incubated in growth media while shaking at 37 °C for about two hours to an absorbance of 0.3 to 0.5, to guarantee the freshness of the bacteria and to be sure that the bacteria concentration is in the linear region of the growth curve. The bacteria solution is then diluted with milli-Q water to reach an absorbance of 0.1.

In the next step, the modified filter paper, containing both c-PAM and triclosan loaded micelles, is placed into a funnel, and attached to a stand below which there is a beaker for the filtrate. A given volume of the solution of bacteria of absorbance of 0.1 is passed through the filter paper and is collected as a filtrate in the beaker below the funnel.

If the filter is effective, the bacteria should be killed after the bacteria solution is passed through the filter paper. Therefore, the efficiency of the filter paper is tested in the following way: After passing through the filter paper, 1 mL of the filtrate bacteria solution is mixed with 9 mL of growth medium to achieve ideal growth conditions for the bacteria. The bacteria solution is then incubated for 3 hours in a shaking incubator at 37 °C while the absorbance is monitored as a function of time. If the absorbance of the filtered bacteria solution in the growth medium continues increasing, the bacteria are growing and the filter paper is considered inefficient. If the absorbance of the filtered bacteria solution in growth medium does not increase, the bacteria are not growing and the filter paper is considered successful. The above mentioned procedure is

repeated also for the control samples, containing only c-PAM, only loaded micelles and also for filter paper without any additives while testing various experimental conditions, one at the time.

We consider the filter paper to be efficient if the relative absorbance after 3 hours of growth did not increase from the original value of 1.0 over the value of 1.03, as typical variations in absorbance for non-growing bacteria are 3%.

### 4.3. Results and Discussion

As an introduction to the presentation of the results of the efficiency of antibacterial paper, bactericidal efficiency of one particular filter paper with one combination of experimental variables will be discussed first. This is followed by a discussion of the effect of various relevant parameters, such as paper porosity, initial bacteria concentration, micelle and c-PAM concentration, initial volume of the bacteria solution, re-usability of antibacterial filter paper and bacteria deactivation with filter left in the bacteria suspension.

#### 4.3.1. Efficiency of Antibacterial Filter Paper

In this experiment, the efficiency of the antibacterial filter paper was studied. A Whatman filter paper was modified first by adsorption of c-PAM, followed by attachment of triclosan loaded micelles. The procedure of the modification of the commercial filter paper was given in detail in section 4.2.6. The modified filter paper was placed into the funnel set up and the *E. coli* ATCC 11229 bacteria solution was passed through the filter paper, as explained in detail in section 4.2.7. Afterwards, the filtrate was tested for bacteria growth (following the protocol described in section 4.2.7). This procedure was repeated also for three control samples; for plain filter paper

without additives, for filter paper modified only by c-PAM and for filter paper modified only by triclosan loaded micelles.

The parameters of the experiment were the following: Whatman filter paper, 90 mm in diameter, grade 3, with a pore size of 6  $\mu\text{m}$  was used. The concentrations of c-PAM and triclosan loaded micelles was 1 mg/g of paper, which roughly corresponds to monolayer coverage of micelles on the fibers. The concentration of the micelles in the solution was 1 g of polymer/L. The biocide loading was approximately 20 wt % of the weight of polymer; i.e. a total loading of 1 gram of micelles/L corresponds to 0.2 g of biocide/L. The absorbance of the bacterial solution was 0.1, which corresponds to roughly  $25 \times 10^6$  bacteria/mL; the total volume of bacterial solution passing through the filter was 100 mL.

The results of these experiments are shown in Figure 4.2. As shown on the graph of relative absorbance as a function of bacteria growth time, it is obvious that the plain filter paper without any additives (control sample) does not influence the growth of the bacteria. The relative absorbance increases from initial value 1 to about 7 in 3 hours.

It is also clear from the figure that bacteria that passed through the filter paper modified with both c-PAM and triclosan loaded micelles do not grow with time at all, since the relative absorbance does not increase above 1. Thus, in this case, the antibacterial filter paper treated with c-PAM and triclosan loaded micelles is efficient in deactivation of *E. coli* bacteria at a concentration of  $25 \times 10^6$  bacteria/mL.

A similar result to that obtained for the filter paper modified by both c-PAM and triclosan loaded micelles is achieved by modifying the paper with only triclosan loaded micelles to the pulp fibers. In this case, the bacteria also do not grow with time, as is evident from the figure. The disadvantage of this paper is that the loaded micelles are not attached to the filter paper and,

thus, are most likely passed through the filter paper along with the bacteria solution. It should be recalled that the charge on the filter paper and on the micelle is negative in both cases, thus preventing electrostatic attraction between them, in contrast to the situation with c-PAM coated fibers. Therefore, the bacteria are killed in the filtrate by triclosan released from the micelles during collisions. For practical applications, it is preferable to keep the micelles attached to the filter paper.

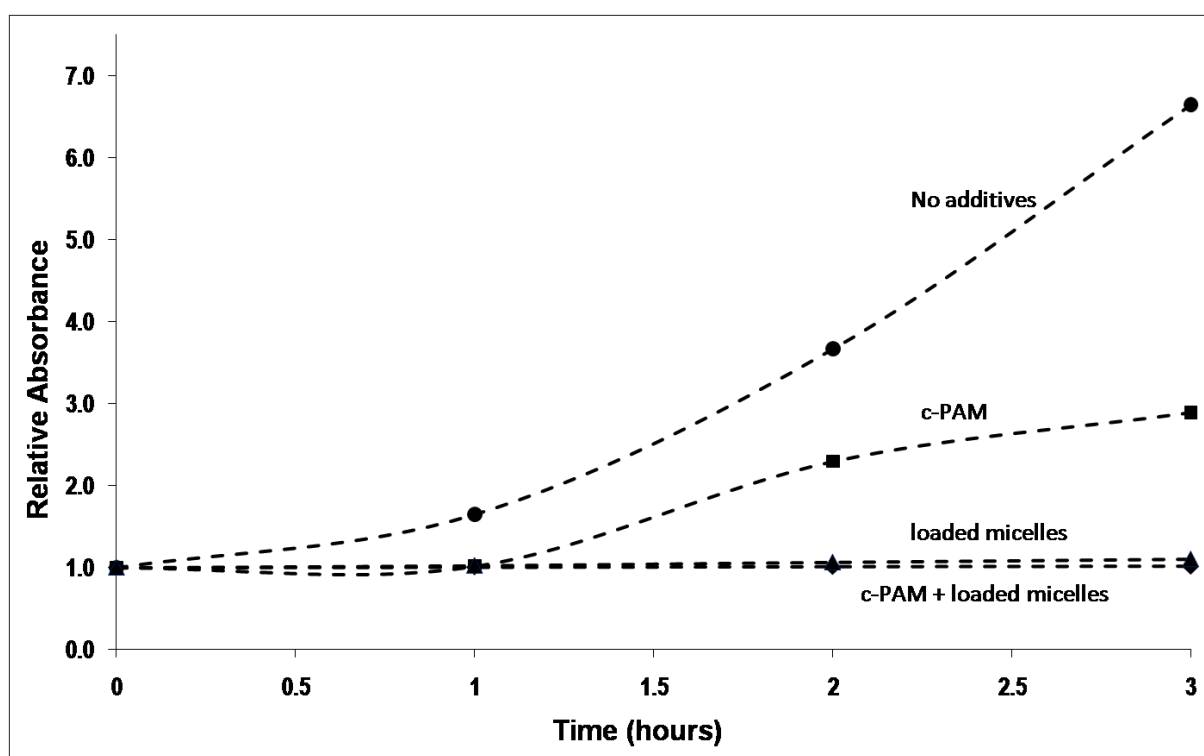


**Figure 4.2.** Efficiency of the variously treated antibacterial filter paper on *E. coli* (ATCC11229 strain) solution passed through a grade 3 Whatman filter paper with a pore size of 6  $\mu\text{m}$ . The experimental conditions were the following: concentration of both c-PAM and triclosan loaded micelles was 1 mg/g of paper each; the volume of 100 mL of bacteria solution of absorbance of 0.1, filtering time was between 30 to 60 minutes, depending on the treatment of the filter paper.

c-PAM by itself adsorbed on the pulp fibers acts as a weak antibacterial agent; this can be deduced from the fact that the relative absorbance of a bacteria solution passed through such



treated paper increases slowly with time; the relative absorbance of a bacteria solution increases in 3 hours from an initial value of 1 to approximately 2.5. By contrast, in a solution of c-PAM without micelles or fibers (previous publication<sup>9</sup>), the c-PAM adsorbs on the bacterial surface and deactivates the bacteria completely; the bacteria do not grow with time at all.<sup>9</sup> The c-PAM adsorbs on the bacteria because in solution the bacteria are negatively charged and c-PAM is positively charged. On the filter paper, the c-PAM is first adsorbed onto the negatively charged pulp fibers, and thus cannot adsorb as easily on the bacteria as they pass by. This is the reason why the c-PAM has a slightly different effect on bacteria in solution than when it is attached to the filter paper. Also, since the bacteria adhere to the pulp fibers, only a small fraction of the bacteria end up in the filtrate.

It should be mentioned that the filtering time in the present experiment was between 30 to 60 minutes, depending on the type of filter paper modification. The fastest filtration of 30 minutes was achieved by plain filter paper without additives.

#### *4.3.2. Effect of Pore Size of Filter Paper on Antibacterial Efficiency*

##### *4.3.2.1. Whatman Filter Papers*

The effect of pore size of Whatman filter paper on the antibacterial efficiency was studied. Since the size of the *E. coli* bacteria is approximately 1.5 x 0.5  $\mu\text{m}$  (as determined by SEM and reported in a previous publication<sup>9</sup>), the filter paper used to filter the bacteria solution had to be chosen to optimize empirically the bactericidal action. For that purpose, Whatman filter papers of three pore sizes were chosen; i.e. filter papers of grades 3, 2 and 1 with pore sizes of 6, 8 and 11  $\mu\text{m}$ , respectively.

The present experiment was performed in the same way as the experiment described in section 4.3.1., except that papers with various pore sizes were tested. The results of the experiments are shown in Figure 4.3, where the relative absorbance of bacteria solution filtered through papers of various porosities and modifications is plotted as a function of incubation time. As shown in the graph, plain filter papers, filter papers modified with c-PAM only, with triclosan loaded micelles only and those containing triclosan loaded micelles along with c-PAM were tested in three various pore sizes.

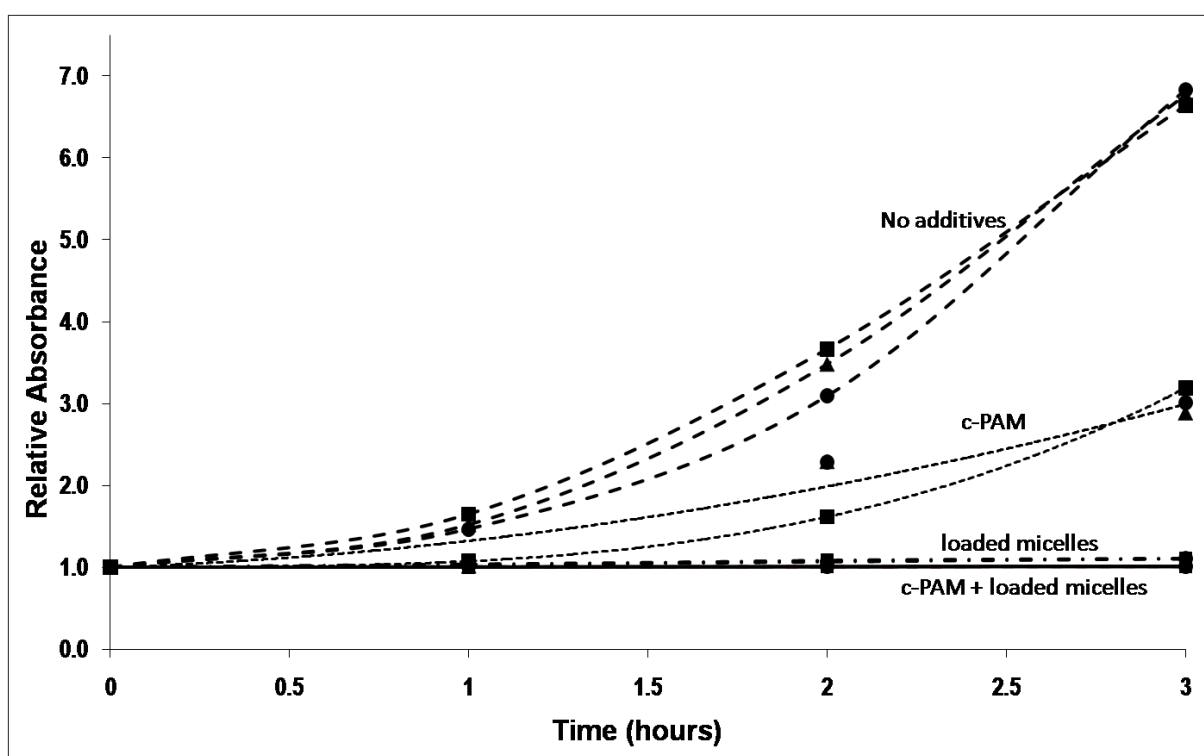


**Figure 4.3.** Efficiency of the variously treated filter papers on solution of *E. coli* (ATCC11229 strain) passing through Whatman filter papers of 90 mm diameter of various pore sizes. Symbols: square - grade 3 (pores size 6  $\mu\text{m}$ ), triangle –grade 2 (pore size 8  $\mu\text{m}$ ), circle – grade 1 (pore size 11  $\mu\text{m}$ ). The experimental conditions were the following: weight ratios of c-PAM and triclosan loaded micelles were 1 mg/g of paper each, the volume was 100 mL of bacteria solution of absorbance of 0.1, and the filtering time was between 30 to 60 minutes, depending on the treatment of the filter paper.

As shown in the figure, there is no appreciable difference in the growth of bacteria passed through the filter paper of various pores without additives (plain paper); bacteria growth is the

same after an incubation period of three hours, which means that the pore size of 6  $\mu\text{m}$  is big enough to pass the bacteria without deactivating them.

The results for the filter papers treated with only biocide loaded micelles and those treated with c-PAM along with biocide loaded micelles are very similar; the curves for the different treatments and for various pore sizes overlap. As shown on the graph, in both cases, the relative absorbance of bacteria after three hours of incubation remains unchanged. Thus, the bacteria passed through the various filters treated with biocide loaded micelles only and those treated with c-PAM along with biocide loaded micelles, are killed in all cases. As explained in connection with the previous experiment in section 3.1., even though the same results are achieved for both modifications of the filter paper, the filter paper treated only with triclosan loaded micelles is not useful since the loaded micelles are not attached to the filter and may pass through to the filtrate along with the bacteria solution, where the bacteria are killed subsequently by the triclosan released from the micelles, probably transferred during collisions.

As in the previous series of experiments, the filtering times in the present experiment were between 30 to 60 minutes, depending on the type of filter paper modification. The fastest filtration of 30 minutes was achieved by plain filter paper without additives. The filtering time of the bacteria solution through papers of various pore sizes was not dependent on the pore size, but on the modification of the filter paper. Thus, one can conclude that in this range the pore size is not an important parameter in the antibacterial filter paper efficiency for the given experimental conditions.

#### 4.3.2.2. Commercial Paper Towel

In addition to the modified Whatman filter paper, a modified commercial textured paper towel was also tested for its antibacterial efficiency. The pore size of that paper towel is much larger than that of the Whatman filter paper.

The commercial paper towel was cut to a circular shape of 90 mm diameter, similar to that of Whatman filter paper. The thickness of the paper towel is roughly 450  $\mu\text{m}$ , which, under compression, decreases to 100  $\mu\text{m}$ ; it is much thicker than the filter paper. The paper towel was treated the same way as the filter paper, i.e. either with triclosan loaded micelles along with c-PAM, or with only c-PAM, or with only triclosan loaded micelles, and was also tested for its efficiency without any additives. The experimental techniques of modification of the paper towel along with the technique of testing the antibacterial efficiency was the same as that employed in case of the filter paper, and described in section 4.3.1. The experimental conditions were the following: weight ratio of c-PAM and of triclosan loaded micelles was 1 mg/g of paper each. The concentration of the micelle solution was 1 g of polymer/L, and the biocide loading was approximately 20 wt % (0.2 g of biocide/L). 100 mL of bacteria solution of absorbance of 0.1 was utilized in each test.

The results for the antibacterial efficiency of the differently modified paper towels are shown in Figure 4.4, where the relative absorbance of bacterial solutions which passed through the paper towels is plotted as a function of re-growth time. As seen from the figure, the antibacterial paper towel is not as efficient as the modified filter paper; the bacteria start to re-grow slowly after 1 hour of incubation time. After passing through the paper towel modified with c-PAM, the bacteria grow almost as fast as do in the control sample of unmodified paper towel; in three hours of re-growth, the relative absorbance reaches the same value for the c-PAM modified filter

paper as for the plain one. Also, in the case of the paper towel modified with c-PAM along with triclosan loaded micelles, the efficiency of the paper is not very high; the bacteria are not killed and continue to grow after one hour of incubation, although they continue to grow more slowly. The most efficient modification of the paper towel in regard to bacteria deactivation is the modification by only triclosan loaded micelles, in which case the mechanism involves deactivation by micelles in the filtrate, not in the paper towel while filtering, since the triclosan loaded micelles are not attached to the paper towel.

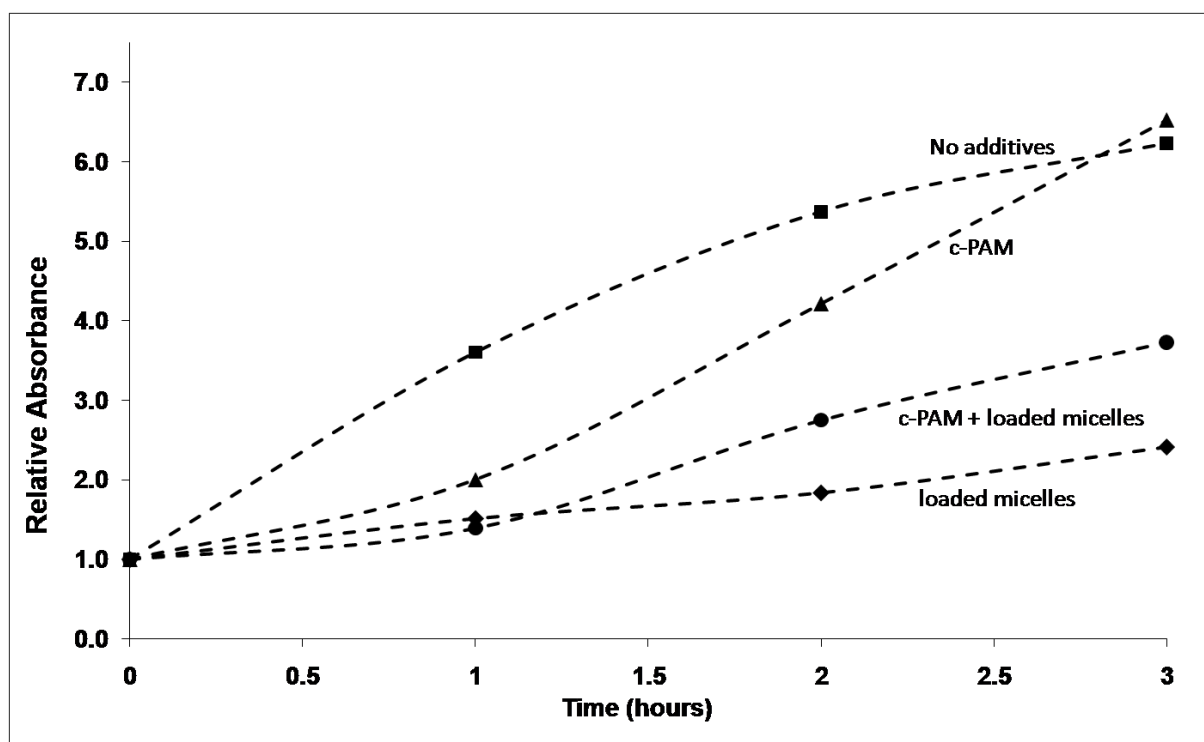


**Figure 4.4.** Efficiency of the modified paper towel on *E. coli* ATCC11229 strain. The experimental conditions were the following: weight ratios of c-PAM and triclosan loaded micelles was 1 mg/g of paper each, the volume was 100 mL of bacteria solution of absorbance of 0.1, and the filtering time was slower than one minute.

The low efficiency of the paper towel treated with c-PAM and triclosan loaded micelles can be explained by the very short filtering time of the bacteria solution through it. The filtering time was shorter than one minute, as opposed to the case of the modified filter paper, where the filtering time was 30 to 60 minutes, thus, the contact time of bacteria with micelles was much shorter. Therefore, it is not surprising that the modified paper towel was not as efficient as the filter paper, since the bacteria, according to the previous paper,<sup>9</sup> need a few minutes of contact time with triclosan loaded micelles to be killed. In this experiment, the short contact time of bacteria with the triclosan loaded micelles, which is related to the thickness and porosity of the paper, explains the low efficiency of the antibacterial properties of the paper towel. The most successful modification of the paper towel involved triclosan loaded micelles only, since the micelles are not attached to the paper towel but are filtered, along with the bacteria solution, into the filtrate, where their bactericidal action continues. However, since the filtering time was short (less than 1 minute), it is likely that not enough of the triclosan loaded micelles passed through the filter paper along with bacteria solution to kill the bacteria completely. Therefore, the bacteria continued to grow slowly on incubation.

As seen from the figure, the modified paper towel is still reasonably efficient in bacteria deactivation in spite of its high porosity and very short contact time. Probably multiple layers of the modified paper towel, or a decrease in its pore size, might be efficient in killing the bacteria.

#### *4.3.3. Optimization of Bactericidal Efficiency of Filter Paper*

In order to optimize the efficiency of the antibacterial filter paper, the effect of four additional variables was tested. The parameters which were tested, in addition to the pore size, were the

weight ratio of the deposited biocide loaded micelles to the filter paper, the weight ratio of the deposited c-PAM to the filter paper, the concentration of bacteria solution passed through the paper and the volume of bacteria solution passed. Those parameters were tested on three grades of Whatman filter paper (1 – 3) with three controls for each grade: filter paper without additives, filter paper modified only with c-PAM and filter paper modified only with biocide loaded micelles. In the principal experiment, the filter papers modified with c-PAM along with the triclosan loaded micelles were investigated.

For the convenience of the reader, the experimental conditions, along with the results for the parameters tested, are summarized in Table 4.3. For brevity, only results for filter paper of grade 3 (smallest pore size) treated with c-PAM together with triclosan loaded micelles under various conditions are shown in Table 4.3. The results for the control samples showed very similar trends to the previous experiments and will be discussed at the end of this section.

All experiments were conducted using an approach similar to that explained in section 4.3.1., i.e the filter paper was modified with biocide loaded micelles along with the c-PAM (as explained previously in detail in section 4.2.6.). Then, the modified filter paper was placed into a funnel and a solution containing *E. coli* ATCC 11229 bacteria was passed through the filter paper (as explained in section 4.2.7). Afterwards, the filtrate was tested for bacteria growth (following the protocol described in section 4.2.7). This procedure was repeated also for the three control samples.

The results for the experiments involving the filtrate of the bacteria solution incubated for 3 hours in growth media, while monitoring the absorbance, are shown in Table 4.3 in the far right column in the form of relative absorbance. As mentioned in section 4.2.7., the filter paper is considered to be efficient in killing the bacteria if the relative absorbance of the filtrate after 3

hours of incubation did not increase above the value of 1.03 from the original value of 1.00. The results of experiments involving conditions which were inefficient in killing the bacteria are highlighted in gray in Table 4.3. As seen from the Table, the inefficient conditions are a concentration of bacteria in a solution of an absorbance of 0.2 (corresponding to a bacteria concentration of  $50 \times 10^6$  bacteria/mL) and 200 mL of bacteria solution passed through the modified filter paper.

Variable	Micelles weight ratio* (mg/g of paper)	c-PAM weight ratio* (mg/g of paper)	conc. of bacteria solution** (absorbance)	Volume of bacteria solution (mL)	Relative absorbance after 3 hours of filtrate incubation
Micelle weight ratio on the filter paper	0.5	1	0.1	100	1.02
	1				1.02
	2				1.01
c-PAM weight ratio on the filter paper	1	0.5	0.1	100	1.02
		1			1.02
		5			1.01
Concentration of bacteria solution before filtering	1	1	0.05	100	1.01
			0.1		1.02
			0.2		1.11
Volume of bacteria solution before filtering	1	1	0.1	100	1.02
				200	1.13

\* Triclosan loaded micelles. The biocide loading is approximately 20 wt % (0.2 g of biocide/L).

\*\* Concentration of bacteria solution is expressed in terms of absorbance deduced from the bacteria calibration curve given in Figure 2 in the Appendix to Chapter 4: absorbances 0.05, 0.1 and 0.2 correspond to bacteria concentrations of  $12.5 \times 10^6$ ,  $25 \times 10^6$  and  $50 \times 10^6$  bacteria/mL, respectively.

**Table 4.3.** The antibacterial efficiency of the filter paper as influenced by changes in various parameters: weight ratio of biocide loaded micelles deposited onto the filter paper, weight ratio of c-PAM deposited onto the filter paper, concentration of bacteria solution passed through the filter paper and volume of bacteria solution passed through the filter paper. Boxes highlighted in grey refer to conditions inefficient in bacteria deactivation since the value of relative absorbance is higher than 1.03.



Based on the results from Table 4.3, one can conclude that the optimal parameters to prepare an antibacterial filter paper based on 20 wt % triclosan loaded PS<sub>197</sub>-b-PAA<sub>47</sub> block copolymer micelles are the following: for 100 mL of bacteria solution, a concentration corresponding to an absorbance of 0.1 ( $25 \times 10^6$  bacteria/mL), triclosan loaded micelles and c-PAM at a weight ratio of 0.5 mg/g of paper for each. Depending on the treatment of the filter paper, the filtering time of the bacteria solution varied, in all the experiments shown in Table 4.3, between 30 and 60 minutes.

It should be noted that in Table 4.3 only results are given for the filter paper treated with both c-PAM and with triclosan loaded micelles for various optimization parameters. The paper treated with only c-PAM shows weak antibacterial properties (not shown in the Table 4.3), as mentioned previously in section 4.3.1. Filter paper treated only with triclosan loaded micelles (also omitted from Table 4.3), is efficient in bacteria deactivation under all tested experimental conditions, since the bacteria do not grow with time, as was also explained previously. The disadvantage of this paper, as discussed in section 4.3.1., is that the loaded micelles are not attached to the filter paper and, most likely, pass through the paper along with the bacteria solution to the filtrate where they continue the deactivation process.

#### 4.3.4. Re-usability of Antibacterial Filter Paper

It was of interest to find out if the antibacterial filter paper is reusable after drying, i.e. still efficient in killing bacteria. In this experiment, the filter papers were prepared and tested in the same way as in the experiment described in section 4.3.1. After passing the *E. coli* bacteria solution through the modified filter paper, the filtrate was tested for the bacteria re-growth (as described in section 4.2.7), the filter was then dried at room temperature on air overnight and a

fresh *E. coli* bacteria solution was passed through the once used filter paper to test its antibacterial efficiency. The filtrate from the second pass of bacteria was then tested for the bacteria re-growth. This procedure was repeated, as in the previous experiments, for control samples such as plain filter paper, filter paper modified with only c-PAM, with only biocide loaded micelles and with c-PAM along with biocide loaded micelles. All three grades (1, 2 and 3) of Whatman filter paper were tested. The results of paper of grade 1 and 2 were the same as for that of grade 3. For the convenience of the reader, only results obtained from filter papers of grade 3 will be discussed here.

In the second pass of the bacteria solution through the unmodified filter paper, it was found for plain Whatman filter paper (without any additives, i.e. control samples) that the relative absorbances increase with time at similar speeds for both passes. Furthermore, it was found that the c-PAM affects the growth of the bacteria, but that in both passes through such a modified filter, it does not deactivate the bacteria, but only slow their growth.

In the case of bacteria passed for the first time through either the filter paper modified with only loaded micelles or with biocide loaded micelles along with c-PAM, it was found that both modified filters are efficient in bacteria deactivation in the c-PAM concentration ranges applied in the present experiment (see section 4.3.1.). The filters are efficient since the relative absorbance of the bacteria solution incubated for three hours does not increase with time (it stays within the limit of absorbance of 1.03).

In the second pass (in the reusability test) of bacteria through the filter paper modified either with only loaded micelles or with biocide loaded micelles along with c-PAM, the modifications cannot be considered efficient in bacteria deactivation. The filters are inefficient as can be seen from the fact that the relative absorbance of the bacteria solution incubated for three hours

increased slightly with time above the limit of absorbance of 1.03. For the second pass for the filter paper modified with only micelles, the relative absorbance increases in three hours to the value of 1.31. In case of filter paper modified with loaded micelles along with c-PAM, the relative absorbance grows in 3 hours to the value of 1.12, which is above the absorbance limit of 1.03.

#### *4.3.5. Bacteria Deactivation with the Paper Left in the Bacteria Suspension*

The following experiment was designed to ascertain whether the antibacterial filter paper can kill the bacteria if it is not used as a filter paper for filtration, but is instead immersed in the bacteria suspension, and how long it takes to kill the bacteria. The filter papers were prepared as described in section 4.3.1.; Whatman filter papers of grade 3 were tested either as plain filter paper, or modified with only c-PAM, or with only biocide loaded micelles, or with c-PAM along with biocide loaded micelles. All these filter papers were immersed into 100 mL of *E. coli* bacteria suspension of absorbance 0.1 for various periods of time: 0, 20, 40 and 60 min. At each time period, 1 mL sample of the suspension was removed, mixed with 9 mL of growth media and incubated for three hours while monitoring the absorbance as a function of time. The procedure is described in detail in the second part of section 4.2.7.

From the relative absorbance vs. time for each sample, it was found that most of the bacteria in suspensions which were exposed for various times to the variously modified filter papers do grow with time, which means that the modified antibacterial filter paper is not efficient in killing the bacteria within the limits of the test. Only three combinations of filter paper modification and exposure times did not result in any bacteria growth within three hours (relative absorbance did not increase above the value of 1.03), which means that only those modified filter papers are

efficient in killing the bacteria within those exposure times. The successful combinations are the following: Filter paper modified with triclosan loaded micelles along with c-PAM immersed in the bacteria suspension for 40 and 60 minutes and filter paper modified only with triclosan loaded micelles immersed in the suspension for 60 min.

#### 4.4. Conclusions

The present project describes the preparation of antibacterial filter papers designed mainly for small scale water purification. The preparation of the antibacterial filter papers involved a hydrophobic biocide, triclosan, which has very low water solubility and which is incorporated into the hydrophobic core of amphiphilic block copolymer micelles. Biocide incorporation into micelles is needed because the saturated solution of triclosan is not efficient in killing bacteria. Thus, a reservoir is required to increase the concentration of the hydrophobic biocide and the micelles provide such a reservoir. In addition, a collisional transfer mechanism is available to transport the biocide molecules to the bacteria without introducing micelles into the body since they are attached to filter paper. These biocide loaded micelles were attached to commercially available Whatman filter papers. Since the ionic charge of both the pulp fibres of the filter paper and also of the amphiphilic block copolymer corona of the micelles is negative, the charge on the pulp fibres had to be changed to positive by deposition of cationic poly(acryl) amide (c-PAM) prior to the attachment of the biocide loaded micelles to the filter paper. The biocide is transferred to the bacteria primarily during collisions between triclosan loaded micelles and bacteria (due to its extremely low solubility in water).

After this modification of the commercially available filter paper, the paper was tested for its efficiency in deactivation or killing of the bacteria. The test consisted of passing the *E. coli*

bacteria suspension through the modified filter paper. The sample of the filtrate was taken, mixed with growth media and incubated for three hours to monitor bacterial growth with time by measuring the absorbance of the sample. A constant values of the relative absorbance of the sample as a function of time proves that the bacteria do not grow, presumably because they have been killed. For comparison, a set of control samples was prepared for each filter paper modified with c-PAM and biocide loaded micelles to prove that it is these modifications which prevent the bacteria from growing. The control samples consisted of plain filter paper without any modification and filter papers modified either with only c-PAM or with only biocide loaded micelles.

In the present study, we first showed that we had, indeed, prepared antibacterial filter paper by proving that this paper has antibacterial properties when a bacteria solution is passed through it, and that it is efficient in killing the bacteria when modified with c-PAM along with biocide loaded micelles. Whatman filter paper treated with only triclosan loaded micelles kills the bacteria, but since the micelles are not attached to the paper, they are filtered into the filtrate along with the bacteria and killed in solution. Such water, containing the amphipilic block copolymer micelles, may not be safe to drink. Filter paper treated with c-PAM and triclosan loaded micelles kills the bacteria, but, more importantly, the micelles do not come into the filtrate, since they are attached to the filter paper. It was also found, that c-PAM itself, when attached to the filter paper, slows the growth of the bacteria, but does not kill them; thus, it acts as a weak biocide. Also, commercially available paper towel modified with c-PAM along with biocide loaded micelles, was tested for its antibacterial efficiency; it was found that even a short contact time with the modified paper towel of high porosity already shows an appreciable deactivation of bacteria.

Secondly, in this study, we also wanted to find optimal experimental conditions to prepare an antibacterial filter paper; therefore, we explored the effect of varying several relevant experimental parameters, such as paper porosity, initial concentration of bacteria solution passed through the filter, initial volume of the bacteria solution, weight ratios of biocide loaded micelles and c-PAM to weight of paper, re-usability of the antibacterial filter paper and, finally, bacteria deactivation with the active filter left in the bacteria suspension. It was found that the optimal parameters for the successful killing of the bacteria are the following: Whatman filter paper of 90 mm diameter of grade 1 to 3 with pore sizes of 11 to 6  $\mu\text{m}$ , respectively. Furthermore, the weight ratio of c-PAM and triclosan loaded PS-b-PAA micelles was in both cases 0.5 mg/g of paper, the micelle loading by triclosan was approximately 20 % (w/w), and the *E. coli* bacteria concentration in 100 mL of solution passed through the filter was approximately  $25 \times 10^6$  bacteria/mL, which corresponds to an absorbance of 0.1; time of filtration was between 30 and 60 min.

The test for re-usability of the filter paper was performed on bacteria suspensions. The tests showed that in the case of a second pass of bacteria through the filter paper modified either with only loaded micelles or with biocide loaded micelles along with c-PAM, the modifications cannot be considered efficient in bacteria deactivation. Re-used filters were found inefficient since the relative absorbance of the bacteria solution incubated for three hours increased slightly with time above the limit of absorbance of 1.03. In case of filter paper modified with loaded micelles along with c-PAM, the relative absorbance increased in 3 hours to the value of 1.12, which is clearly above the absorbance limit of 1.03. The antibacterial filter paper, after reuse, has only marginal antibacterial properties; therefore, re-use does not appear advisable at this time.

In the present study, bacteria deactivation was also tested for filters left in the bacteria suspension for various times. It was found that the antibacterial filter paper of c-PAM and biocide loaded micelles of concentrations of 1 mg/g of paper is efficient in killing *E. coli* bacteria from 100 mL suspension of concentration of  $25 \times 10^6$  bacteria/mL, when left in the bacteria.

#### 4.5. Reference List

- (1) <http://www.vestergaard-frandsen.com/lifestraw.htm>
- (2) [http://www.alloysafe.com/search.php?search=survival straw](http://www.alloysafe.com/search.php?search=survival%20straw)
- (3) <http://www.airport.ca/news/Water-Purifier-for-Your-Travels-PRISTINE-Pioneer-mergency-Water-Filter-System-022497.php>
- (4) Intilli, H.S., U.S. patent 4533435, 1985
- (5) United States Patent 3728213
- (6) U.S. patent 7201846, 2007
- (7) Japanese Patent JP06285314
- (8) <http://www.campingsurvival.com/watpur.html>
- (9) Vyhnalkova, R., Eisenberg, A., van de Ven, T.G.M., to be submitted
- (10) Vyhnalkova, R., Eisenberg, A., van de Ven, T.G.M., *J. Phys. Chem. B*, **2008**, 112, 8477.
- (11) Azzam, T.; Eisenberg, A.; *Angew. Chem. Int. Ed.*, **2006**, 45, 7443.
- (12) Barbolt, T.A., *Surg Infect (Larchmt)*, **2002**, (3), Suppl 1:S45-53.
- (13) [www.sciencelab.com/xMSDS-Sodium\\_chloride-9927593](http://www.sciencelab.com/xMSDS-Sodium_chloride-9927593)
- (14) Raghavan, S.L., Schuessel, K., Davis, A., Hadgraft, J., *Int. J. Pharmaceutics*, **2003**, 261, 153.
- (15) [www.mindfully.org/Pesticide/Triclosan-Lipid-Synthesis](http://www.mindfully.org/Pesticide/Triclosan-Lipid-Synthesis)
- (16) <http://www.whatman.com/QualitativeFilterPapersStandardGrades.aspx>

## **Bridging Section between Chapters 4 and 5**

---

The preceding three chapters dealt with block copolymer micelles as carriers of biocides, both, in solution and on paper. While micellar systems are convenient delivery systems for hydrophobic materials such as the biocides used here, the total amount of biocide that can be incorporated into the micelles is at most 30 %. Furthermore, block copolymers are relatively expensive materials and the preparation of the systems, i.e. polymer synthesis, self assembly and loading, represent multiple relatively complex steps. Emulsions, on the other hand, are composed almost entirely of the active ingredient (except for a relatively minor stabilizing component), and involve a much more simple preparation sequence. Naturally, the total cost of the delivery materials is expected to be much lower than that of the block copolymer micelles. Because of the features discussed above, it was decided to explore emulsions as delivery systems for bactericidal systems under conditions similar to those described in Chapter 3. The specific topics to be discussed thus include preparation of bactericidal emulsions using two different stabilizing agents, effectiveness of these emulsions, as well as the mechanism of bacteria deactivation.



## Chapter 5:

# Effect of Stabilizers on the Deactivation Efficiency of Bactericidal Emulsions

---

### Abstract

Biocide emulsions stabilized with various stabilizing agents were prepared and characterized, and their efficiency in bacteria deactivation was evaluated. A number of stabilizing agents was tested for their stabilizing effect on emulsions of thiocyanomethylthiobenzothiazole (TCMTB) biocide. Two agents, successful in stabilizing the biocide, were chosen for further studies: high molecular weight polyethyleneimine (PEI) and an amphiphilic block copolymer of poly(caprolactone)-b-poly(acrylic acid) (PCL<sub>33</sub>-b-PAA<sub>33</sub>). The most stable emulsions were prepared from 50/50 wt. % and 66/33 wt % ratios of stabilizing agent/biocide. The emulsion droplet sizes, measured by DLS, varied between 325 and 500 nm. Deactivation of bacteria was studied by exposing *E. coli* ATCC 11229 bacteria dispersions to the emulsions stabilized by positively charged PEI or negatively charged PCL-b-PAA micelles and by measuring their absorbance (which is related to bacteria concentration) by UV-vis. The time dependence of the absorbance of bacteria deactivated by emulsions was compared to the absorbance of bacteria in water and to those exposed to solutions containing only the stabilizing agent. It was found that *E. coli* do not grow with time in the presence of biocide emulsions. PEI molecules alone act as biocide and deactivate the bacteria. PCL-b-PAA micelles as stabilizing agent do not affect the growth of the *E. coli*; bacteria are deactivated by TCMTB released from the emulsion droplets. The kinetics of emulsion dissolution were studied for both stabilizing agents by measurements of the emulsion droplet size, which decreases with time while the emulsions were subjected to dialysis. Kinetic curves revealed that the biocide is released from the emulsions within ~ 250 min; the droplet shells consist mostly of PEI or PCL-b-PAA insoluble complexes with the biocide in solution; which do not dissolve during dialysis. SEM images confirm the presence of residual crumbled shells with holes after 24 hours of dialysis.

\* The manuscript is to be submitted to *Journal of Colloids and Surfaces B, Biointerfaces*

## **5.1. Introduction**

Emulsions are of great interest both academically and industrially. Milk is perhaps the best known naturally occurring emulsion, while mayonnaise is an excellent example of a manmade food product. Water based paints are an example of a large scale commercial application. Many other examples could be cited from a wide range of fields, and many books and review articles are available on the topic.

Since emulsions frequently involve small drops of, for example, a hydrophobic material in water, and are thus subject to a high interfacial energy, stable emulsions require the use of a stabilizer, which coats the hydrophobic droplets and prevents their aggregation and the formation of a macroscopic phase. Many types of stabilizers are available; among these, polar homopolymers or amphiphilic block-copolymers are very often used. In the homopolymer case, adsorption of the polymer chain onto the interface of the colloidal droplet can lead to steric or electrostatic stabilization, while in the case of the block copolymers, the hydrophobic segment can be associated with a hydrophobic drop while the hydrophilic segment provides, again, steric or electrostatic repulsive interactions between the hydrophobic drops. Emulsions prepared in this way can remain stable for extended time periods.

Over the last decades, polymeric surfactants, mainly block copolymers, came into frequent use for a variety of applications such as emulsifiers, dispersion stabilizers, wetting agents, and others due to their well defined structure, molecular weight, and composition; their usefulness is mainly due to their unique solution and associative properties.<sup>1</sup> Polymeric surfactants have, in general, much lower diffusion coefficients and critical micelle concentrations than “classic” surfactants, but in spite of that, amphiphilic block copolymers, composed of hydrophilic and hydrophobic blocks, behave in many ways similarly to low-molecular-weight surfactants.<sup>1</sup> Due to the very low

critical micelle concentration (CMC) and low diffusion coefficients, and also the possibility of strong attachment to the colloidal particles while providing excellent steric or electrosteric stabilization against flocculation and coalescence, block copolymers may, under some conditions, have advantages over conventional low-molecular-weight surfactants.<sup>1</sup> Parameters like surface or interfacial tension or CMC influence the block copolymer stabilization efficiency, which results from an extensive interaction between the block copolymer sequences and the immiscible phases. Since the block copolymers are suitable for the preparation of polymeric water-in-water emulsions, they present a wider range of possibilities than the low-molecular-weight surfactants.<sup>1</sup> Compared with conventional surfactants, block copolymers in latex technology may serve not only as a stabilizer in the polymerization process, but also as an active component in the finished product formulation, for example, as plasticizers, compatibilizers, antistatic agents and oil and/or water repellents.

The use of block copolymers, and of polymeric surfactants in general, as stabilizing agents has one minor limitation, which is that their efficiency as stabilizers decreases with increasing molecular weight by surfactant entrapment in the latex particles, followed by decrease of the diffusion coefficient of these agents. Therefore, the ideal molecular weight for industrial applications is in the range of about 1 000 to 20 000.<sup>1</sup>

It should be stressed that the use of block copolymers as emulsion stabilizers is very extensive and only a small sampling of the relevant literature can be given here. Armes *et al.*<sup>2</sup> recently demonstrated that nanostructured colloidal particles have a potential use also in advanced technologies such as information storage, controlled drug delivery and photonic devices, which might be accessible with ABC triblock copolymers and stimuli responsive latexes.

The work of Molau,<sup>3</sup> in the mid 1960s, pioneered the research on block copolymers and their colloidal behaviour when used as polymeric surfactants. The colloidal aspects of block copolymers in solution have then continued to be studied experimentally and theoretically by Price,<sup>4</sup> Piirma,<sup>5</sup> Tuzar and Kratochvil,<sup>6</sup> Riess,<sup>7</sup> Alexandridis and Hatton,<sup>8</sup> and by Alexandridis and Lindman.<sup>9</sup>

Burguieree *et al.*<sup>10</sup> studied block copolymers of PS-*b*-PAA of various molar masses, topologies and compositions as emulsion stabilizers. They found that the diblock copolymers with 10 styrene units and a maximum of 50 acrylic acid units are the most efficient stabilizers. The authors also pointed out that an increase in the size of the hydrophilic segment does not lead to any improvement in stability. The diblocks were found to be very efficient stabilizers, and the triblock or starblock copolymers did not behave differently from the diblocks. In addition, it was found that the efficiency of triblocks with an internal hydrophilic segment strongly depends on the lengths of both blocks.<sup>10</sup>

Application of block copolymers with one charged block as emulsion stabilizers was investigated by Antoinetti *et al.*<sup>11</sup> The stabilizing properties of these polyelectrolyte block copolymers were found to be strongly dependent on the ionic strength and the architecture of the charged block; the lower the ionic strength, the better are the stabilizing properties of the biocide copolymers for latex particles.<sup>11</sup>

PEO-PPO-PEO triblock copolymers at the emulsion droplet-water interface were studied by Prestidge *et al.*<sup>12</sup> It was found that the thickness of the absorbed layer depends on the copolymer structure, the level of cross-linking within the droplets and on the surface chemistry of the absorbent.<sup>12</sup>

Curvature and phase inversion effects on the thermodynamics of particle-stabilized emulsions were investigated by Lips *et al.*<sup>13</sup> They found that if the particles are not densely packed, the interfacial bending moment and the spontaneous curvature (due to the particles) are equal to zero; if the particles are closely packed, then the particle adsorption monolayer possesses a significant bending moment, and the interfacial energies of bending and dilatation become comparable. In such a case, the bending energy can either stabilize or destabilize the emulsion, depending on whether the particle contact angle is smaller or greater than 90°. <sup>13</sup>

Double emulsions containing water-in-oil-in-water were recently prepared by Deming *et al.*<sup>14</sup>. Both water-soluble and oil-soluble compounds can be delivered in the same droplet in these oil-coated water droplets of a diameter of 100 nm. The authors showed that these emulsions can be prepared in a simple process and stabilized for many months using single-component, synthetic amphiphilic diblock copolypeptide surfactants (poly(L-lysine HBr)<sub>x</sub>-b-poly(racemic-leucine)<sub>y</sub>). These surfactants even stabilize droplets subjected to extreme flow, leading to the direct production of robust double nanoemulsions that are amenable to nanostructured encapsulation applications in foods, cosmetics and drug delivery.<sup>14</sup>

The literature describing bactericidal emulsions is very limited, only one patent on the topic was found. An invention, presented by Lipecki *et al.*,<sup>15</sup> deals with a process of preparing stable emulsions of biologically active compounds that are water insoluble or have low water solubility directly before introducing them to an environment of use. Emulsions of water insoluble biocides (isothiazolones) which do not require significant quantities of added surfactants and solvents to form stable micro-emulsions were prepared in a micro-mixing device directly before use. These emulsions were found to be stable toward the phase separation for periods measured in years.<sup>15</sup>

Because of the wide occurrence of pathogens, a range of biocides has been developed commercially. Some of these are hydrophilic, but many others, especially some of those which combine high effectiveness and low toxicity, are hydrophobic. Therefore, to make these materials useful for particular applications, they need to be incorporated into a medium, which allows them to interact with the pathogens, such as bacteria, while at the same time permitting their localization in the environment of interest. Emulsions or block-copolymer micelles are thus convenient vehicles for biocide incorporation. A separate publication<sup>16</sup> dealt with the use of block-copolymer micelles in biocide applications, in which the hydrophobic biocide was incorporated into the hydrophobic micelle core, the corona of which consisted of the hydrophilic polymer chain segments.

The present publication describes the use of biocide emulsions stabilized with polymeric stabilizers. These stabilizers consist either of polar polymer chains, i.e. polyethyleneimine (PEI), or of amphiphilic block-copolymer micelles of poly(caprolactone)-b-poly(acrylic acid) (PCL-b-PAA). The work described here is part of a comprehensive study aimed at producing a bactericidal paper. The use of emulsion droplets or micelles is, therefore, very tempting because of the range of strategies available which can be used to attach them to the paper while maintaining their bactericidal action. Emulsion droplets are of particular interest because of the high loading capacity, i.e. because the ratio of weight of active ingredient to total weight of a carrier plus ingredient can be very high.

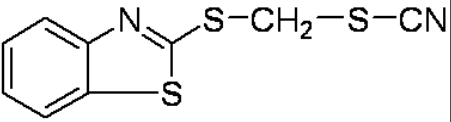
Thiocyanomethylthiobenzothiazol (TCMTB) was chosen for the present study as the bactericidal agent because it had already been proven effective in a micellar environment.<sup>16</sup> The material combines a low toxicity to humans, low melting point, low water solubility and high

effectiveness in bacterial deactivation. Emulsions of TCMTB are used commercially as biocides in the pulp and paper industry.

## 5.2. Experimental Section

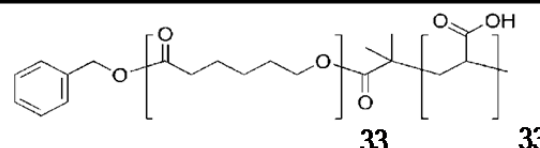
### 5.2.1. Materials

Thiocyanomethylthiobenzothiazole (TCMTB), the hydrophobic bactericidal material (biocide), was provided by Buckman laboratories. The structure and properties of the TCMTB, are shown in Table 5.1.

<b>Molecular structure</b>	
<b>Biocide</b>	Thiocyanomethylthiobenzothiazole (TCMTB)
<b>M<sub>w</sub> (g/mol)</b>	238
<b>Water solubility (mg/L)</b>	12.7 <sup>16</sup>
<b>Melting point (°C)</b>	34
<b>Density (g/cm<sup>3</sup>)</b>	0.95
<b>Oral LD<sub>50</sub> (g/kg)</b>	0.75 (on rats) <sup>17</sup>

**Table 5.1.** Structure and properties of thiocyanomethylthiobenzothiazole biocide.<sup>16,17</sup>

Branched Polyethyleneimine (PEI) of  $M_w$  of 750 000 g/mol as a 50 wt % solution in water was purchased from Aldrich. Amphiphilic block copolymer of poly(caprolactone)<sub>33</sub>-*b*-poly(acrylic)<sub>33</sub> acid (PCL-*b*-PAA) was prepared from the selective hydrolysis of a poly( $\epsilon$ -caprolactone)-*b*-poly(*tert*-butyl acrylate) (PCL-*b*-PtBA) precursor, which was synthesized by ring opening polymerization (ROP) of  $\epsilon$ -caprolactone ( $\epsilon$ -CL), followed by atom transfer radical polymerization (ATRP) of *tert*-butyl acrylate (*t*BA).<sup>18</sup> The number average molar mass ( $M_n$ ) of PCL-*b*-PAA polymer was 6 400 and its polydispersity index was 1.10. Structures of PEI and PCL-*b*-PAA are shown in Table 5.2.

<b>Molecular structure</b>	$\text{H}_2\text{N}-(\text{CH}_2\text{CH}_2\text{N})_x-(\text{CH}_2\text{CH}_2\text{NH})_y-\text{H}_2\text{CH}_2\text{NH}_2$	
<b>Polymer</b>	<b>PEI</b>	<b>PCL<sub>33</sub>-<i>b</i>-PAA<sub>33</sub></b>
<b><math>M_w</math> (g/mol)</b>	<b>750 000</b>	<b>6 400</b>
<b>PDI</b>	<b>N/A</b>	<b>1.10</b>

**Table 5.2.** Structure and properties (molecular weight and polydispersity indices) of stabilizing agents of polyethyleneimine and poly(caprolactone)<sub>33</sub>-*b*-poly(acrylic)<sub>33</sub> acid polymer.

1-4-dioxane, dextran of  $M_w$  of 188 000 g/mol, sodium dodecyl sulphate 98.5 %, poly(acrylic acid) of  $M_w$  of 2 000 g/mol and poly(ethylene oxide) of  $M_w$  of 100 000 g/mol were obtained from Sigma-Aldrich and used as received. A cationic (quaternary amine-substituted) starch, CATO-237, was received from National Starch in powder form. Prior to use, starch was dispersed in milli-Q water, obtaining a solution of 1 %, which was heated for 40 minutes in a 93 °C water bath and then cooled down.<sup>19</sup> Poly(vinyl) alcohol 99% hydrolyzed was purchased from MCIB - Supply Assured. Pluronic F88 Prill (ethylene oxide-propylene oxide copolymer) was



received from BASF and Triton X-100 (4-octylphenol polyethoxylate) was purchased from SPI Suppliers Division, Structure Probe, Inc.

The bacteria consisted of gram negative *E. coli* (strain ATCC 11229), and were donated by Prof. Mansel Griffiths from the Canadian Research Institute for Food Safety, University of Guelph, Canada. The medium was Miller-Hinton broth purchased from Fluka (microbiology grade); bacteria were grown in this broth at 37 °C while shaking. The bacteria fixative, glutaraldehyde, was donated by Dr. Hojatollah Vali, Facility for Electron Microscopy Research, McGill University. The pH of the milli-Q water used in all experiments was approximately 6. A 1 % phosphotungstic acid solution was obtained from Sigma-Aldrich and used as stain for TEM images.

### *5.2.2. Experimental Techniques*

The principal techniques involved in this study were transmission electron microscopy (TEM), dynamic light scattering (DLS), scanning electron microscopy (SEM), UV-vis spectroscopy and inductively coupled plasma (ICP). A brief description of the instrumentation and sample preparation methods is given in the Appendix to Chapter 5.

### *5.2.3. Micelle Preparation*

The PCL<sub>33</sub>-b-PAA<sub>33</sub> block copolymer was dissolved in dioxane at an initial block copolymer concentration of 10 % (w/w) and stirred for 2 hours to ensure complete dissolution of the polymer. Milli-Q water was then added drop-wise at a rate of 50 mL/hour to induce self-assembly into micelles, until a final concentration of polymer of 2 % (w/w) was reached. Under

these conditions, a mixture of micelles and small number of small vesicles is observed in the solution. The solution was then dialyzed for a period of three days to remove the organic solvent (dioxane). The final solid content in the solution is ca 20 mg/L.

#### *5.2.4. Characterization of the Micelles*

Transmission electron microscopy (TEM) and dynamic light scattering (DLS) were employed to characterize the micelles. The descriptions of the techniques and sample preparation methods are given in the Supporting Information. Since the vast majority of the aggregates consist of micelles, we refer to this family of aggregates as to micelles. As will become clear later, the presence of a small number of vesicles is of absolutely no consequence to the conclusions. The micelles consist of a hydrophobic poly(caprolactone) core and a hydrophilic poly(acrylic acid) corona. A schematic representation of the micelle structure, both in solution and in the dry state together with TEM micelle image, is shown in Figure 1 in the Appendix to Chapter 5.

#### *5.2.5. Emulsion Preparation*

Before preparing the emulsion, the stabilizing agent was dissolved in milli-Q water. The concentration of the stabilizing agent varied for each agent, as will be described in results section for those stable agents which yielded stable emulsions. A given amount solution of the stabilizing agent was placed into a vial. A given amount of solid TCMTB was weighed in a separate vial. Afterwards, both vials, the one containing the solution of the stabilizing agent and the other one with solid TCMTB, were heated to 60°C (a temperature well above the 34 °C, melting point of TCMTB and  $T_m$  of PCL) on which the TCMTB became liquid. The contents of

both vials were then mixed and sonicated using a Ultrasonic Processor sonicator for 5 min at the amplitude of 80, while cooling the sonicating solution in an ice bath. After 5 min of sonication, the emulsion was quenched drop wise in an excess of cold water while stirring. The stability of the emulsion was then tested visually without stirring the sample. The emulsion is considered to be unstable if it precipitates at any time. It should be noted that the weight ratios of biocide and stabilizing agent in emulsions were 50/50 %, except when mentioned otherwise.

#### *5.2.6. Bacteria Deactivation Using Emulsion*

Bacteria deactivation by an emulsion was tested using UV-vis spectroscopy. Each emulsion sample of a given concentration was mixed with growth media and *E. coli* bacteria. All samples (containing either the biocide emulsion or only the stabilizing agent as a control) were incubated at 37 °C for 6 hours while shaking. The absorbance at 600 nm of each sample was monitored with time. To express the efficiency of the emulsion on bacteria deactivation, the absorbance was plotted as relative absorbance vs. time. No absolute values of the efficiency were measured. We use the term loosely to compare the performance of several biocide emulsions. An increase in relative absorbance of the sample with time indicates growth of the number of bacteria, and demonstrates that the bacteria are not deactivated; if the absorbance value decreases or does not change with time, the bacteria are considered to be deactivated. The details of the technique employed to measure bacteria deactivation using emulsions are given along with the calibration curve for the bacteria in the Appendix to Chapter 5 in sections 1.5 and 1.6.

#### *5.2.7. Kinetics of Emulsion Dissolution*

Each biocide emulsion (20 mL) was placed after its preparation into a dialysis bag (of  $M_w$  cut-off of 14 000 g/mol), which was placed into a 15 L beaker with external milli-Q water which acts as a sink for the biocide molecules. The sample was dialyzed for 1500 min (25 hours) to release the biocide completely from the emulsion, while 15  $\mu$ L of the sample was taken periodically. Each 15  $\mu$ L sample was then diluted with Milli-Q water and the average diameter of the emulsion droplets was measured by DLS. To express the kinetics of emulsion dissolution, the average diameter of the emulsion droplets for each stable emulsion was plotted as a function of time for each ratio of biocide to stabilizing agent.

### **5.3. Results and Discussion**

#### *5.3.1. Emulsions Properties*

##### 5.3.1.1. Stability of TCMTB Emulsions

Several stabilizing agents were tested in the preparation of stable emulsions of TCMTB (prepared by the experimental procedure described in section 5.2.5): Cationic starch, sodium dodecyl sulphate (98.5 %), branched poly(ethylene imine) 50 % ( $M_w = 750\,000$  g/mol) (PEI), dextran ( $M_w = 188\,000$  g/mol), poly(vinyl alcohol) (99 % hydrolyzed), PCL<sub>33</sub>-b-PAA<sub>33</sub> block copolymer micelles, poly(acrylic acid) ( $M_w = 2\,000$  g/mol), poly(ethylene oxide) ( $M_w = 100\,000$  g/mol), Pluronic F88 and Triton X-100. Except for the starch and the PCL<sub>33</sub>-b-PAA<sub>33</sub> block copolymer micelles, all materials were used as received; preparation of the emulsions with TCMTB followed the protocol described in section 5.2.5.

The stability of the emulsion was evaluated visually, without stirring the sample; samples were considered unstable if they precipitated. Visual evaluation showed that TCMTB emulsions

stabilized by starch, sodium dodecyl sulphate, dextran, poly(vinyl alcohol), poly(ethylene oxide), were stable only for few hours; TCMTB emulsions prepared using stabilizing agents of poly(acrylic) acid, Pluronic F88 and Triton X-100 were stable for approximately one day. The most stable TCMTB emulsions were those stabilized by PEI (stable for over several days) and PCL<sub>33</sub>-b-PAA<sub>33</sub> micelles (stable for over ten months); these were chosen as stabilizing agents for further studies, described in the following sections.

#### 5.3.1.2. Emulsions Stabilized by PEI

Since it had been found that (the positively charged) PEI is a good stabilizing agent for TCMTB at a 50/50 ratio, additional PEI/TCMTB ratios were also explored; i.e. 29/71 and 66/33, respectively. The stability of the emulsions were studied for each PEI/TCMTB ratio both visually, and also by measuring their average diameters using DLS (briefly described in the Appendix to Chapter 5 in section 1.1.). It was found that at a ratio of 29/71 PEI/TCMTB emulsions are stable only for a few hours before they precipitate; the average diameter was 1508 nm. Both the 66/33 and 50/50 ratios of PEI/TCMTB were found to be stable for more than two days. The average diameter measured by DLS for the PEI/TCMTB emulsion of 50/50 ratio (PEI/TCMTB) was found to be 373 nm, while that of the 66/33 ratio was 508 nm.

It should be noted that to prepare stable 50/50 and 66/33 PEI/TCMTB emulsions, a large excess of PEI in solution (compared to monolayer coverage) was added. Perhaps the low molecular weight fraction of PEI has to adsorb between high molecular weight fraction to make sufficiently stable droplets.<sup>20</sup>

Figure 5.1 shows TEM images (A, B) and SEM images (C – E) of the 50/50 ratio (PEI/TCMTB) emulsions. The descriptions of the sample preparation technique for TEM and

SEM imaging are given in the Appendix to Chapter 5 in sections 1.2. and 1.3. The dark regions in the TEM images are due to the phosphotungstic acid stain.

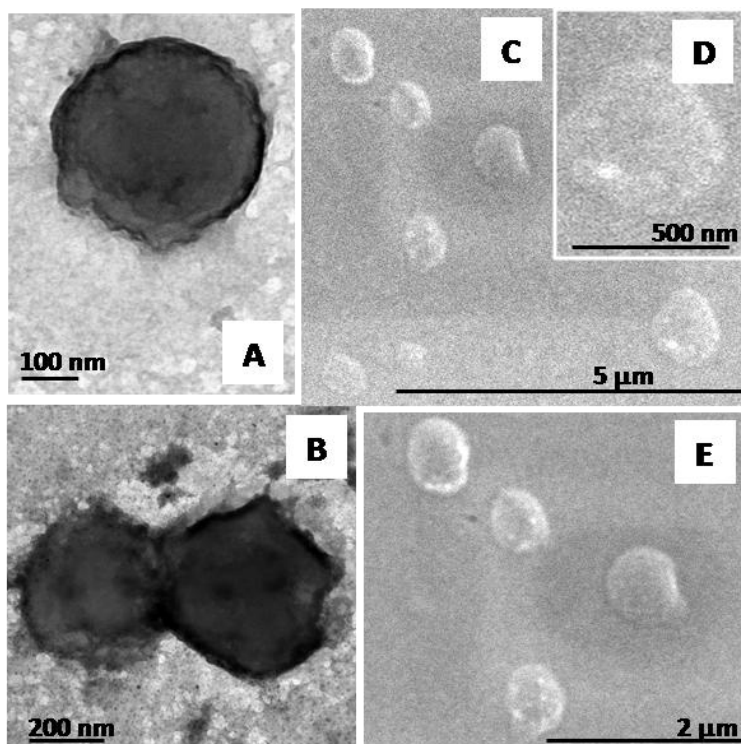


**Figure 5.1.** TEM (A, B) and SEM (C - E) images of 50/50 ratios of PEI/TCMTB emulsion.

#### 5.3.1.3. Emulsions Stabilized by PCL-b-PAA Micelles

In order to prepare emulsions of TCMTB stabilized with PCL-b-PAA, first the micelles of PCL<sub>33</sub>-b-PAA<sub>33</sub> block copolymer were prepared as described in section 5.2.3. DLS and TEM techniques were employed to measure the size of PCL-b-PAA micelles. By DLS, it was found that this solution has a bimodal size distribution, in that it contains two species with average sizes 17 and 168 nm, respectively. The average diameter was found to be 63 nm. The TEM images of the PCL-b-PAA solution revealed the presence of micelles along with a small number of vesicles, as shown in Figure 1 in the Appendix to Chapter 5. The average diameter of the

aggregates was measured using Sigma Scan program to be  $48 \pm 16$  nm, lower than that measured by DLS, since in the TEM image the corona is collapsed, and also because DLS measures a z-average rather than a number average as calculated from TEM images. Because the micelles are used as a protective coat on the emulsion, the presence of an occasional vesicle is unlikely to change the protective mechanism of this stabilizing agent since the vesicles are only slightly larger than the micelles and their exterior is identical to that of the micelles.

Since it was found that PCL<sub>33</sub>-b-PAA<sub>33</sub> micelles (with a negatively charged corona) act as a good stabilizing agent for the TCMTB (it stabilizes the TCMTB/PCL-b-PAA of a 50/50 ratio for over ten months), additional PCL-b-PAA/TCMTB ratios were also explored; i.e. 66/33, 33/66, 9/91 and 4/96. All five ratios of PCL-b-PAA/TCMTB emulsions were studied for their stability both visually, and by DLS. It was found that the ratios of 33/66, 9/91 and 4/96 (PCL-b-PAA/TCMTB) were stable only for a few hours before they precipitated. The average diameters of 9/91 and 4/96 ratios of PCL-b-PAA/TCMTB were found to be 1520 and 1230, respectively, by DLS. The average diameter for the PCL-b-PAA/TCMTB ratio of 33/66 was not measured because of its instability. The average diameter measured for the PCL-b-PAA/TCMTB emulsion of 50/50 ratio was found to be 325 nm while that of 66/33 ratio was 378 nm.

Figure 5.2 shows TEM images (A, B) and SEM images (C) of 50/50 ratio of PCL-b-PAA/TCMTB emulsion. As seen from the TEM images (A and B), the large dark regions appear to be stabilized emulsion droplets with the darkness due to the phosphotungstic acid stain. The much smaller features surrounding the emulsion droplets are probably PCL-b-PAA micelles or vesicles, with the pattern formed during the drying process. The structures on the SEM image (C) are also emulsion droplets, some of which might be irregular drops.

It is interesting to note that both PEI (which is positively charged) and PCL-b-PAA micelles (which have negatively charged corona), stabilize the emulsions at the same stabilizing agents/biocide ratios, namely 50/50 and 66/33.

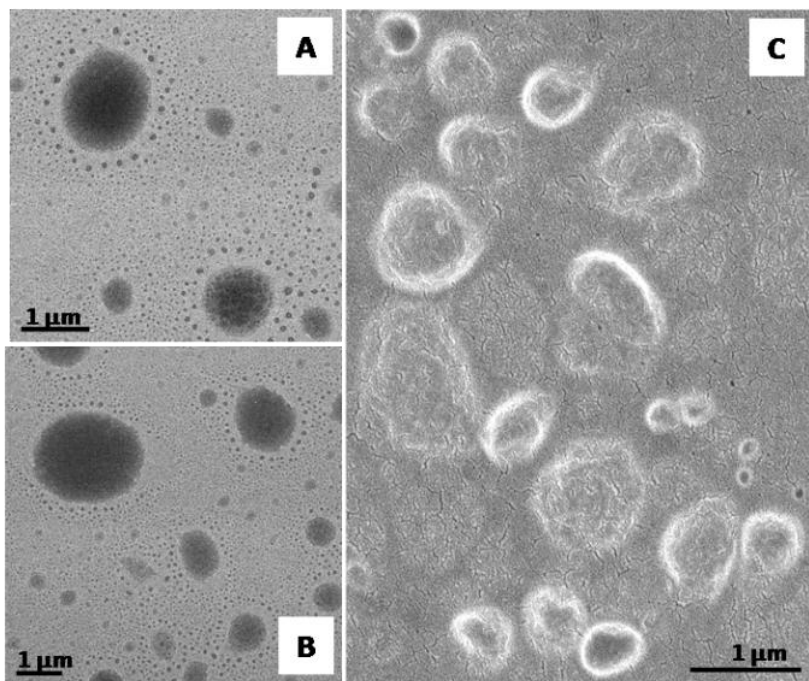


**Figure 5.2.** TEM (A,B) and SEM (C) images of 50/50 ratios of PCL-b-PAA/TCMTB emulsion.

### 5.3.2. Bacteria Deactivation by Emulsions

Stable emulsions of TCMTB with stabilizing agents of either PEI or PCL-b-PAA were prepared to study *E. coli* bacteria deactivation. The results for each stabilizing agent are given in the following sections.



#### 5.3.2.1. Bacteria Deactivation by PEI/TCMTB Emulsions

TCMTB emulsions stabilized with PEI were stable at ratios of 50/50 and 66/33. Only the emulsion of 50/50 PEI/TCMTB was chosen to study the efficiency on bacteria deactivation since the mechanism of deactivation is likely to be identical for both ratios. The concentration of both, TCMTB and PEI, in the emulsion (at a 50/50 ratio) was varied between 0.045 g/L and 0.45 g/L. The description of the experimental procedure was given in the section 2.6., and in much greater detail in the Appendix to Chapter 5 in sections 1.5. and 1.6.

The results of the bacteria deactivation experiments are given in Figure 5.3., where the relative absorbance of the bacteria dispersion exposed to the various concentrations of PEI/TCMTB emulsions is plotted as a function of incubation time. As seen from the figure, the efficient PEI/TCMTB concentrations in killing the bacteria were above 0.136 g/L for both, PEI and TCMTB (the bacteria concentration corresponded to  $25 \times 10^9$  bacteria/L). For the concentration of 0.045 g/L, not all the bacteria were killed, as seen from the increase of the relative absorbance with bacteria incubation time above the relative absorbance of 1. All tested concentrations of PEI/TCMTB emulsions were compared to the control sample (containing no biocide emulsion); as shown in Figure 5.3 the relative absorbance of this sample increased in 6 hours to approximately 10. Of all the other samples only that which a concentration of 0.045 g/L showed a slight bacteria growth.

It should be noted that in the case of PEI/TCMTB concentrations of 0.45 g/L for each component, the sample precipitated, most likely due to the positively charged PEI adsorption onto the negatively charged bacteria.

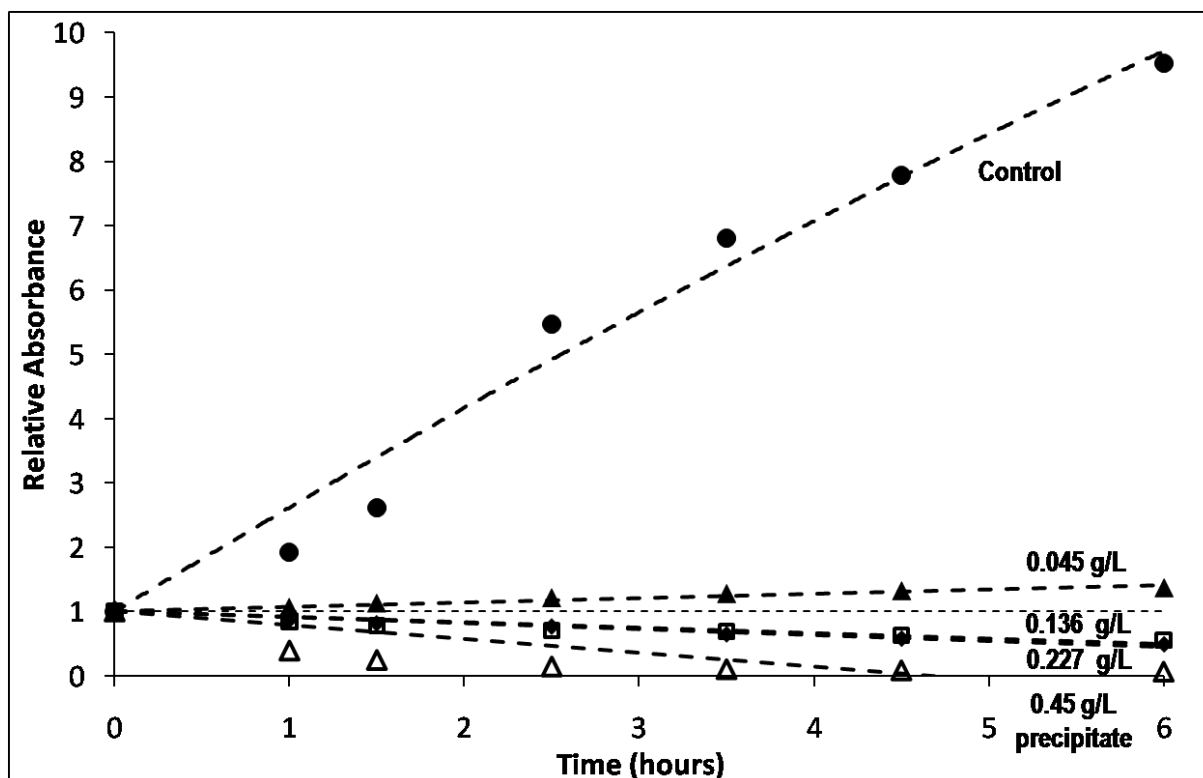


**Figure 5.3.** Bacteria deactivation by PEI/TCMTB emulsions.

Since PEI is a cationic amine, and some amines are known to have biocidal properties,<sup>21</sup> it was necessary to ascertain whether the bacteria are deactivated by the biocide in the emulsion, rather than by the stabilizing agent (PEI) alone. For that purpose, the bacteria were exposed to the control samples containing only PEI, as described below, and the experiments were conducted in the same manner as described above for bacteria deactivation by the emulsion. The control samples were prepared as follows: A PEI/TCMTB emulsion was prepared according to the protocol given in section 5.2.5. The emulsion was then centrifuged for 10 minutes at 3 000 RPM; the supernatant was filtered through a 0.22  $\mu\text{m}$  filter to remove all the emulsion droplets from the sample in order to make sure only PEI molecules are left in the supernatant; this solution served

as a control for the experiment. Afterwards, various volumes of the supernatant were mixed with the bacteria and the growth medium to keep the same concentrations as in the experiments of bacteria deactivation by emulsions (except for the absence of the emulsion droplets themselves) and bacteria were incubated for 6 hours while monitoring the absorbance of each sample.

The results of these experiments are shown in Figure 5.4, where the relative absorbance of the *E. coli* bacteria exposed to the various concentrations of the PEI emulsion supernatants are plotted as a function of incubation time. As seen from the figure, the supernatant of PEI/TCMTB emulsion of concentration of 0.045 g/L does not kill the bacteria; it only slows the growth of the bacteria. The relative absorbance of the sample after 6 hours of incubation is only slightly lower than that of the control sample without supernatant. By contrast, the supernatant of the emulsion of concentration of 0.136 g/L kills the bacteria since the relative absorbance stays lower than 1 and, in addition, it acts the same way as the 0.136 g/L emulsion itself (control sample), since the curves overlap. The identity of the results for the emulsion and for its supernatant means that the bacteria are not killed by the TCMTB in the emulsion, since the saturation concentration of TCMTB does not kill the bacteria as shown in a previous publication<sup>22</sup>; rather, and unexpectedly they are killed by the free PEI molecules in the emulsion solution. In this case, free positively charged PEI molecules act as the stronger biocide than the TCMTB. It should be also mentioned that the supernatant from the 0.136 g/L emulsion precipitated the bacteria. The bacteria precipitated most likely because of the presence of the positively charged PEI adsorbing on the negatively charged bacteria. The mechanism of bacteria deactivation by PEI will be discussed in section 5.3.3. Thus, it appears that the emulsion is not needed to kill the bacteria, since the PEI itself is sufficient and since the saturated solution of TCMTB does not kill the bacteria. But since the supernatant containing only PEI at 0.045 g/L is not as potent as the emulsion (compare

results for the concentration of 0.045 g/L for emulsion in Figure 5.3 and for supernatant without emulsion in Figure 5.4), one can conclude from these results that TCMTB droplets do contribute to bacteria deactivation.

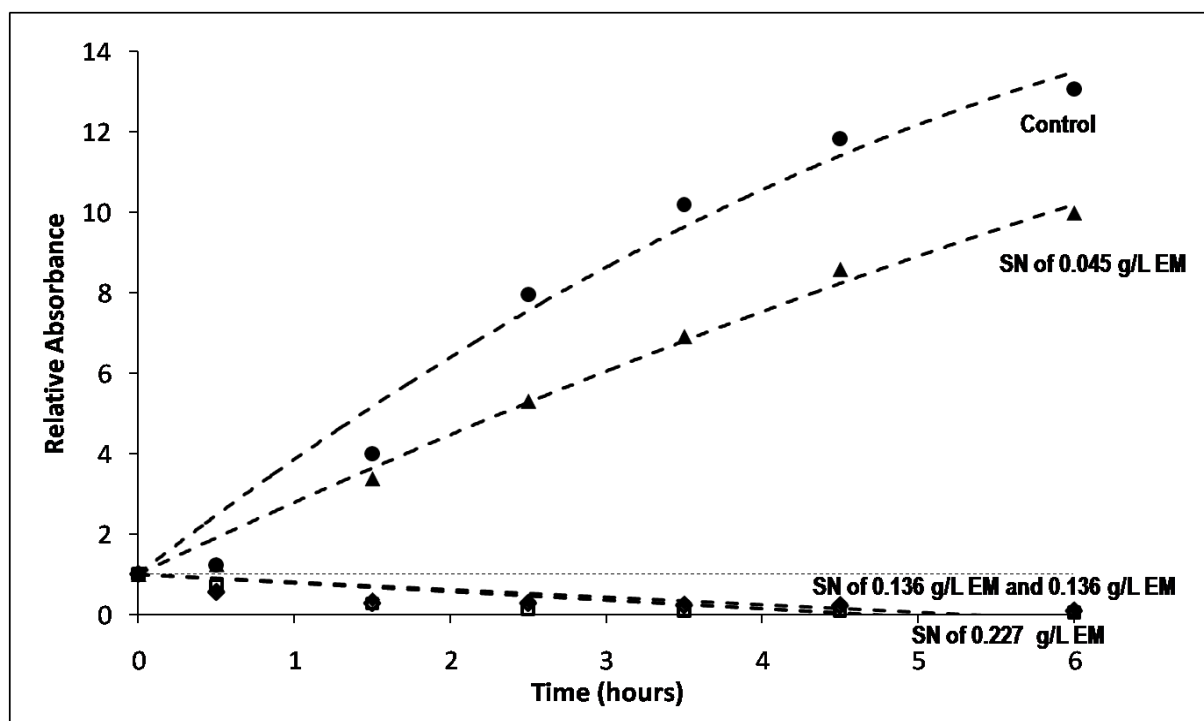


**Figure 5.4.** Effect of supernatant of PEI/TCMTB emulsions on bacteria deactivation (control experiment). (SN) - emulsion supernatant, (EM) – emulsion

#### 5.3.2.2. Bacteria Deactivation by PCL-b-PAA/TCMTB Emulsions

PCL-b-PAA micelles were found to be a good stabilizer for TCMTB emulsions in ratios of 50/50 and 66/33. Similar to the case of PEI/TCMTB emulsions, for the PCL-b-PAA/TCMTB emulsions the ratio of 50/50 was also chosen for bacteria deactivation study. The concentration of both, PCL-b-PAA and TCMTB, in the emulsion (50/50 ratio) varied between 0.045 g/L and 0.45 g/L. The details of the experimental procedure of the bacteria deactivation experiment were given in section 5.2.6., and also in sections 1.5. and 1.6 of the Appendix to Chapter 5.

The results of the bacteria deactivation experiment are given in Figure 5.5, where the relative absorbance of *E. coli* bacteria dispersions exposed to the various concentrations of PCL-b-PAA/TCMTB emulsions are presented as a function of incubation time. As seen from the figure, the PCL-b-PAA/TCMTB concentrations efficient in killing the bacteria were concentrations above 0.136 g/L for both, PCL-b-PAA and TCMTB (the bacteria concentration corresponded to  $25 \times 10^9$  bacteria/L). A concentration of 0.045 g/L is not high enough to kill the bacteria since the bacteria continued to grow during the 6 hours of incubation as seen from the relative absorbance, which was higher than 1; the bacteria growth was slowed down when compared the relative absorbance of the control sample (which does not contain any emulsion).

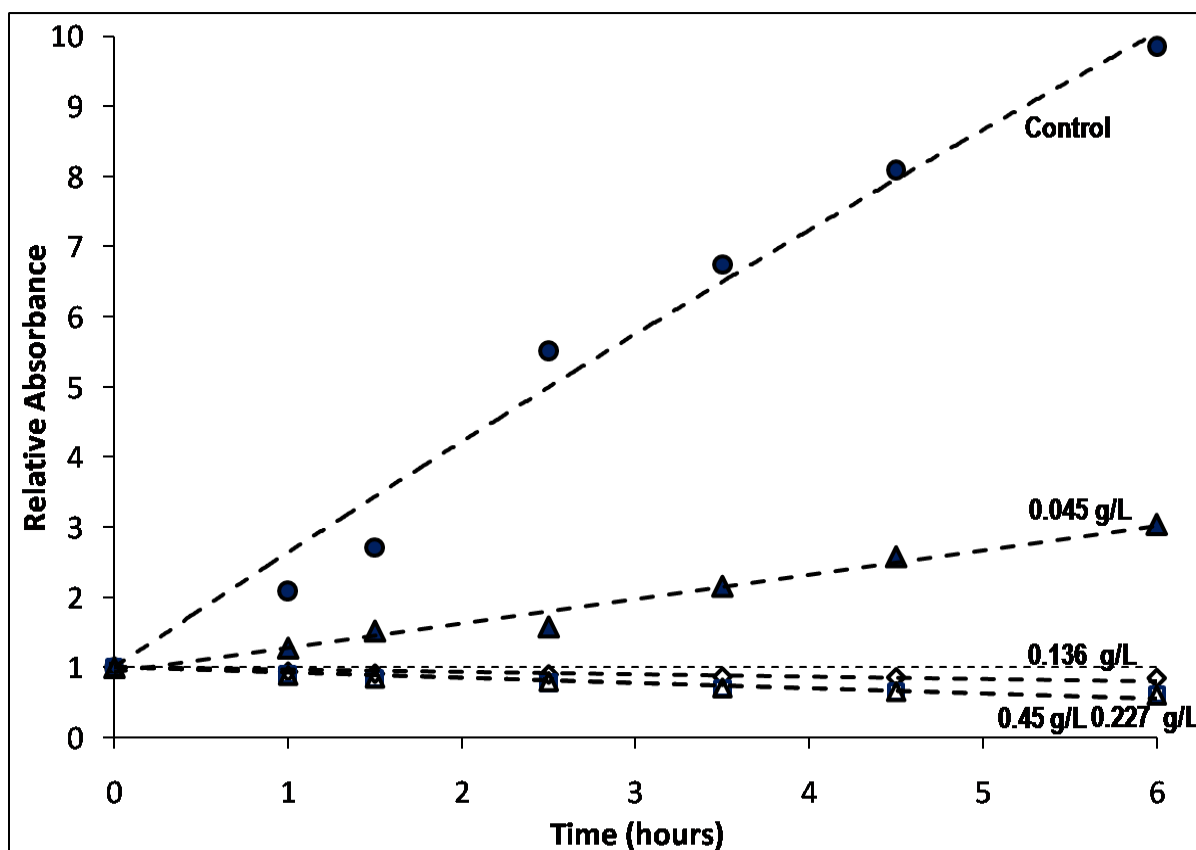


Figure 5.5. Bacteria deactivation by PCL-b-PAA /TCMTB emulsions.

In parallel to the study of emulsions of PEI/TCMTB, as control samples for the PCL-b-PAA/TCMTB emulsions various PCL-b-PAA micelle concentrations were also tested for bacteria deactivation. The experiment was conducted in the same manner as the one involving PCL-b-PAA/TCMTB emulsions; PCL-b-PAA micelle concentrations varied from 0.045 to 0.45 g/L. PCL-b-PAA micelles were mixed with *E. coli* bacteria and the growth medium, and were incubated for 6 hours at 37 °C, while the absorbance of the solution was monitored with time. The plot of the relative absorbance vs. time of each sample was compared to the one for the control sample (which does not contain PCL-b-PAA micelles). The plot of relative absorbance vs. time of incubation is not given in the main text of the thesis, it is shown only in Figure 2 in the Appendix to Chapter 5, because it was found that the PCL-b-PAA micelles of any concentration do not disturb the growth of the bacteria at all; the relative absorbances of the bacteria exposed to the PCL-b-PAA micelles were the same as those of the control sample (reaching a value of approximately of value of 10 after incubation for 6 hours).

From the results described above, it can be concluded that PCL-b-PAA/TCMTB emulsions kill the bacteria at concentrations above 0.136 g/L, and that the negatively charged PAA micelle corona does not disturb the growth of the bacteria; the bacteria deactivating agent in this case is the TCMTB biocide as opposed to the system containing PEI as the stabilizing agent. The mechanism of bacteria deactivation by PCL-b-PAA micelles will be discussed in section 5.3.3.

#### 5.3.2.3. Comparison of PEI and PCL-b-PAA/TCMTB Emulsions in Bacteria Deactivation

As seen from the results discussed above, TCMTB emulsions stabilized either by PEI or by PCL-b-PAA micelles, are efficient in killing bacteria. In the case of PEI stabilized TCMTB emulsion, the free PEI molecules are the primary agents in killing the bacteria. This behavior

contrasts with that of the TCMTB emulsions stabilized by PCL-b-PAA micelles, where the micelles alone do not affect the growth of bacteria; therefore, the TCMTB is in this system the biocide. This difference can, most likely, be attributed to the charge of the stabilizing agent; positively charged PEI deposits on the negative bacteria, while the micelles with a negatively charged corona do not influence the bacteria; thus, TCMTB molecules become the primary bactericidal agent in the solution. The mechanisms of bacteria deactivation by TCMTB emulsions stabilized by PEI and PCL-b-PAA micelles will be discussed in the following sections.

### *5.3.3. Mechanisms of Bacteria Deactivation*

#### *5.3.3.1. Kinetics of Emulsion Dissolution*

To determine over what period of time and to what extent the biocide emulsion dissolves, the kinetics of emulsion dissolution were studied. The TCMTB emulsions stabilized by PEI or PCL-b-PAA micelles were prepared by following the protocol described in section 5.2.5. The kinetic study was performed as described in section 5.2.7. The average diameters of the emulsion droplets were evaluated using DLS, the description of which is given in section 1.1. in the Appendix to Chapter 5. The results are given in the following sections.

##### *5.3.3.1.1. PEI/TCMTB Emulsion*

The average diameters of the emulsion droplets for the 50/50 and 66/33 ratios of PEI/TCMTB emulsions were plotted as a function of time, as shown in Figure 5.6, which illustrates the decrease in the emulsion diameter as the biocide is released from the emulsion droplets. As can be seen from the figure, the biocide is released from 66/33 ratio of PEI/TCMTB in emulsion

within a time of approximately 250 minutes, while for 50/50 ratio the biocide is released within 150 minutes. After the biocide is released from the emulsions, the diameters of the remaining structure become more or less constant, since data of the average diameters show plateaus in both cases and do not change with time.

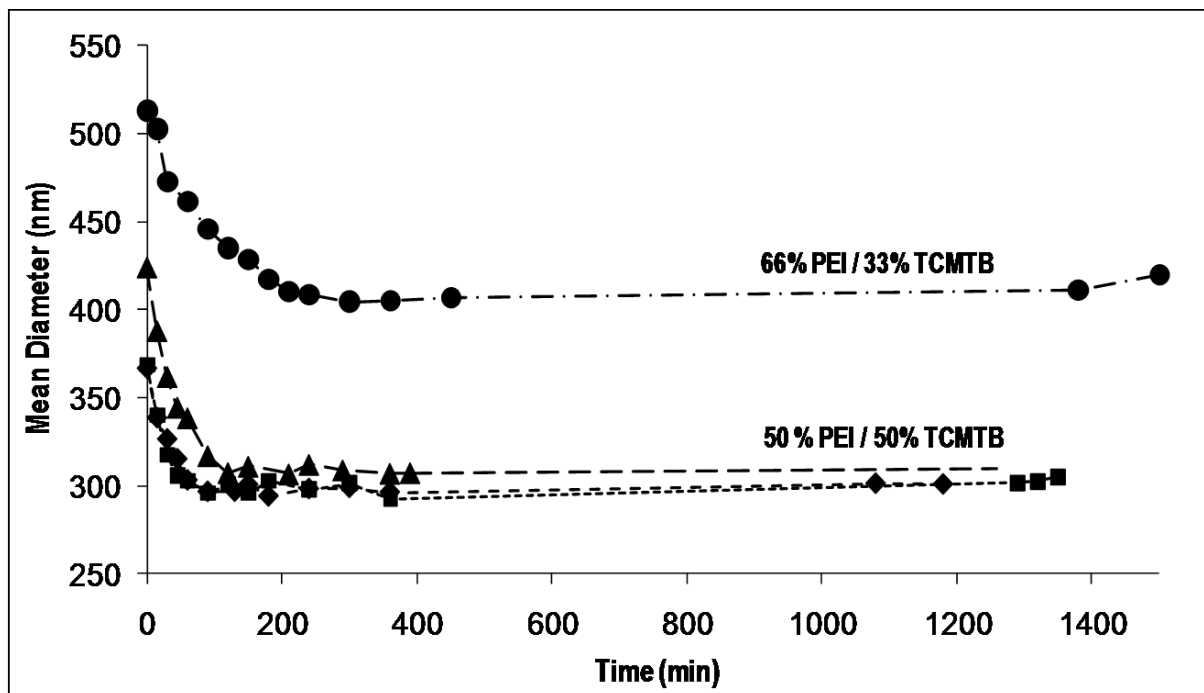


**Figure 5.6.** Kinetics of PEI/TCMTB emulsion dissolution for 66/33 and 50/50 % ratios of PEI and TCMTB in emulsion.

For the 66/33 PEI/TCMTB emulsion, the average diameter of the emulsion droplets decreases from an initial value of 508 nm to 419 nm (at 1500 min), which corresponds to a total decrease of 89 nm or 18 %, while for the 50/50 emulsion it decreases from the initial value of 373 nm to 305 nm, corresponding to a decrease of 68 nm or again 18 %.



As shown in the figure, for the 50/50 PEI/TCMTB emulsion, the reproducibility of the data was verified three times (three independent data curves); the diameters of emulsion droplets did not show any significant differences within the experimental error.

For the 66/33 PEI/TCMTB emulsion the average slope of droplet size plot was found to correspond to approximately  $7 \times 10^{-3}$  nm/s (the biocide is released in  $\sim 250$  min), while that for the 50/50 emulsion the rate of decrease was also estimated to be  $7 \times 10^{-3}$  nm/s (in this case the biocide is released in  $\sim 150$  min). The difference in the time of the biocide release for the two ratios can be attributed to the initial diameter of the droplets; it takes longer for the biocide to be released from the larger emulsion droplets.

The desorption constant can be estimated from the initial slopes of biocide release  $k$  divided by the density of the biocide  $(0.95)^{23}$ . This yields a value of  $(0.8 \pm 0.1) \times 10^{-8}$  kg m<sup>2</sup> s<sup>-1</sup> for the desorption rate constant for the 50/50 emulsion and a value of  $(0.7 \pm 0.1) \times 10^{-8}$  kg m<sup>2</sup> s<sup>-1</sup> for the desorption rate constant for the 66/33 emulsion; the values are the same within experimental error.

#### 5.3.3.1.2. PCL-b-PAA/TCMTB Emulsion

To express the decrease in the emulsion diameter as the biocide is released from the emulsion droplets with time (kinetics of emulsion dissolution), the average diameters of the emulsion droplets for the 50/50 and 66/33 ratios of PCL-b-PAA/TCMTB emulsions were plotted vs. time, as shown in Figure 5.7. The biocide is released from droplets prepared from both ratios of PCL-b-PAA/TCMTB in the emulsions within 270 minutes, at which point the diameters of the emulsions droplets become approximately constant, as can be seen from the figure.

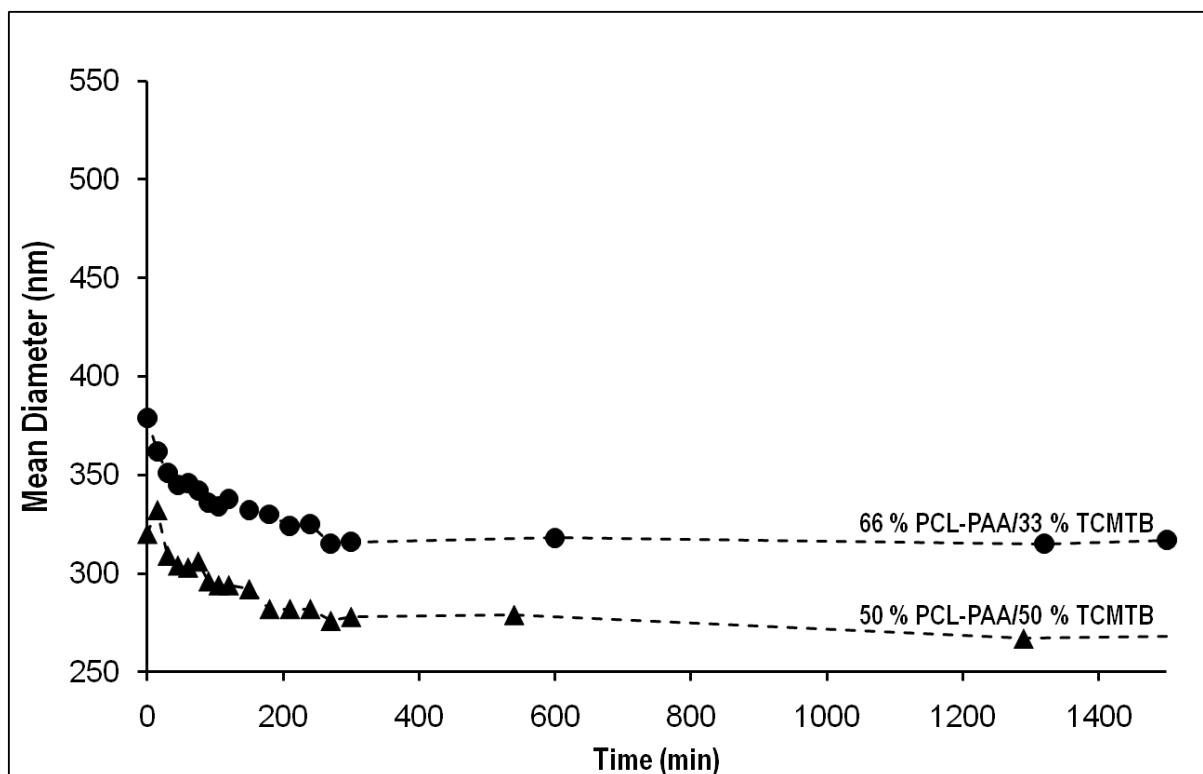


**Figure 5.7.** Kinetics of PCL-*b*-PAA/TCMTB emulsion dissolution for 66/33 and 50/50 % ratios of PCL-*b*-PAA and TCMTB in emulsion.

For 66/33 PCL-*b*-PAA/TCMTB emulsion the average diameter of the droplets decreases in 1500 minutes from the initial average diameter of 378 nm to 317 nm, which corresponds to the total average diameter decrease of 61 nm or 16 %, while for 50/50 emulsion ratio it decreases from initial average diameter of 325 nm to 267 nm, which corresponds to the total average diameter decrease of 58 nm or 18 %. Again, the percentage decrease in diameter is quite similar for the two systems.

The average slopes of biocide release were found for both ratios of PCL-*b*-PAA/TCMTB in the emulsions to have a similar value, for the initial 270 minutes estimated as  $3.5 \times 10^{-3}$  nm/s in.

Similar to the case of PEI/TCMTB emulsions, the desorption rate constant was also estimated for PCL-b-PAA/TCMTB emulsions. Since the average slopes for both ratios were the same, the desorption constant was found to be the same for both ratios  $(0.4 \pm 0.1) \times 10^{-8} \text{ kg m}^2 \text{ s}^{-1}$ .

It should be noted that, as the biocide is released from the emulsion droplets, the droplets do not dissolve completely with time; this behavior is similar to the case of PEI/TCMTB emulsions. This phenomenon will be discussed in detail below.

#### 5.3.3.1.3. Comparison of Kinetic Results for PEI and PCL-b-PAA/TCMTB Emulsions

As seen from the dissolution experiments, the biocide is released from the PCL-b-PAA/TCMTB over a comparable time period (in 270 min) as from PEI/TCMTB emulsion, in which case it is released completely within 250 min for the 66/33 ratio and in 150 minutes for the 50/50 ratio. Due to this similarity, the average slopes and desorption rate constants for biocide release are also similar for emulsion containing both stabilizing agents. A possible explanation for smaller desorption constant in the case of PCL-b-PAA/TCMTB emulsions (0.4 vs. 0.7) is that PCL-b-PAA forms hemi-micelles on the droplets with an approximate coverage of 50 %.

It is known that sizes of emulsion droplets are a function of a range of parameters, among them preparative conditions. Therefore, no easy explanation can be given for difference in sizes of the droplets for the two ratios. In this particular case, under identical preparative conditions, the 66/33 ratio yields larger droplets than the 50/50 for the emulsions containing either of the two stabilizing agents, which could be most likely attributed to a kinetic effect during emulsion preparation (emulsion droplets get stabilized before they break up into smaller drops during emulsification).

Another noteworthy feature of the release study involves the similarity in scattering intensity observed before and after the release of the biocide from the emulsion droplets. Since a plateau was reached and since the uptake capacity (solubility limit) in the water in the dialysis step is not exceeded (see calculations in the Appendix to Chapter 5 in section 1.7.), it can be concluded that all of the biocide has probably been released. The scattering of light by the remaining solution after release is most likely due to residual shells, consisting mostly of the stabilizing agent. The fact that the emulsion droplets do not dissolve with time completely, as the biocide is released, was unexpected. A priori, one should expect both the biocide and the stabilizer (PEI or PCL-b-PAA micelles) to be water soluble and to dissolve with time at similar rates. It appears that the stabilizing material does not dissolve or dissolves only incompletely and thus leaves a shell behind.

#### 5.3.3.2. Deactivation Mechanisms

As was highlighted in section 5.3.2.3, the mechanisms of bacteria deactivation are different for the two emulsions. Here, first, the mechanism of bacteria deactivation by each emulsion will be discussed, which will be followed by a comparison of the two mechanisms.

##### 5.3.3.2.1. Mechanism of Bacteria Deactivation by PEI/TCMTB Emulsions

Bacteria deactivation by the PEI/TCMTB emulsion was discussed in section 5.3.2.1. It was found that a PEI/TCMTB emulsion of 50/50 ratio at a concentration of 0.136 g/L, and also its supernatant only, are efficient in killing bacteria, since the exposed bacteria did not grow during 6 hours of incubation. After 6 hours of incubation, the sample containing the killed bacteria and the emulsion droplets was taken for imaging by SEM in order to visualize bacteria after

deactivation by the emulsion. Prior to SEM imaging, samples were prepared for SEM analysis by following the protocol described in section 1.3. of the Appendix to Chapter 5.

SEM images (A – D) in Figure 5.8 show bacteria in the presence an emulsion of PEI/TCMTB of a 50/50 ratio. For comparison, the images of the control sample of *E. coli* bacteria with no emulsion are given in images E and F. In contrast to the smooth and intact surface of the bacteria (without any holes) for the control sample, one can see, in images A and B for bacteria after exposure to the emulsion, that the surface is rough, and it contains holes; the bacteria are clearly dead. In images A (upper right part of image), C and D, the spherical particles are the emulsion droplets, which also appear to have a rough surface, containing holes, seen most clearly in image D. As was found and described in section 5.3.2.1., the bacteria, in case of PEI/TCMTB emulsion, are killed primarily by the free PEI molecules, but TCMTB also partially contributes to the bacteria deactivation; PEI molecules in solution could have TCMTB molecules associated with them and could help in the deactivation of bacteria (see more details in section 5.3.3.3.1.).

It is interesting to note that the random coil size of the PEI molecule of  $M_w$  of 750 000 is  $\sim 40$  nm, (see calculations in the Appendix to Chapter 5 in section 1.8.), the size of the surface holes in the bacteria is  $23.6 \pm 6.6$  nm, as measured from SEM images A, B and D using Sigma Scan size analysis. Knowing that the free PEI molecules are the primary biocide, and that their size is  $\sim 40$  nm, it is tempting to suggest that the holes on the bacteria surface are caused by the free PEI molecules, which penetrate through the bacteria membrane, leaving the holes and killing the bacteria. The opposite charge of the PEI molecules (positive) and that of the bacteria surface (negative) leads to the deposition of the PEI on the bacteria because of the electrostatic interactions.

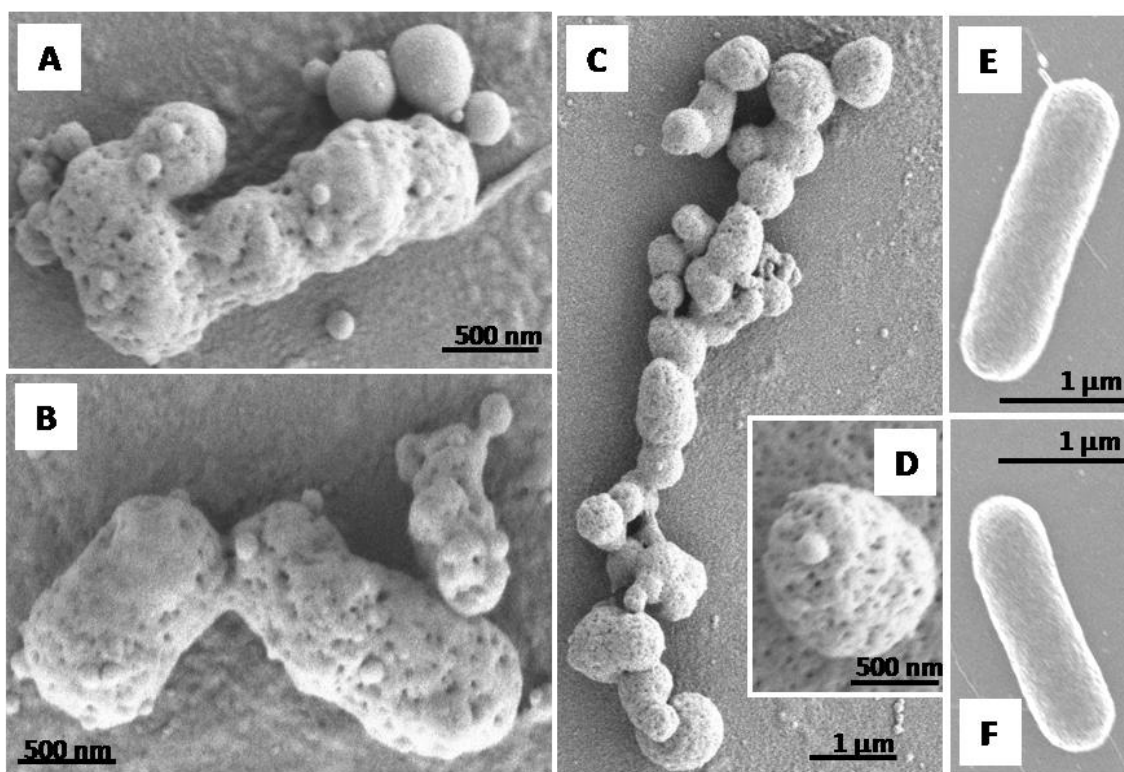


**Figure 5.8.** SEM images (A-D) of *E. coli* bacteria deactivated by PEI/TCMTB emulsion (0.136 g/L of PEI and TCMTB), (E, F) – *E. coli* control.

#### 5.3.3.2.2. Mechanism of Bacteria Deactivation by PCL-b-PAA/TCMTB Emulsions

As was discussed in section 5.3.2.2., the PCL-b-PAA/TCMTB emulsion of 50/50 ratio and a concentration of 0.136 g/L is efficient in bacteria deactivation, since the exposed bacteria did not grow during 6 hours of incubation. A sample of killed bacteria and emulsion droplets was taken after 6 hours of incubation for imaging by SEM to visualize bacteria deactivation by the emulsion as was done in the case of PEI/TCMTB emulsions. (The preparative protocol for the SEM analysis is described in section 1.3. of the Appendix to Chapter 5.)

*E. coli* bacteria after exposure to a 50/50 ratio emulsion of PCL-b-PAA/TCMTB are shown on SEM images (A – E) in Figure 5.9. The bacteria exhibit visual differences from those of the control sample (Figure 5.8, E, F); their surfaces are also smooth but not intact, since a few holes

can be seen in all the images (A – E). The spherical particles seen in these images correspond to the emulsion droplets, which appear to have a rough surface, with PCL-b-PAA micelles on it.

The bacteria, in the case of the PCL-b-PAA/TCMTB emulsion, are killed by the TCMTB for emulsions of a concentration of 0.136 g/L; the PCL-b-PAA micelles do not disturb the growth of the bacteria at all, as described in section 5.3.2.2. and shown in Figure 2 in the Appendix to Chapter 5. Since the corona of the PCL-b-PAA micelles is negatively charged, as is also the bacteria surface, the PCL-b-PAA micelles stabilizing the PCL-b-PAA/emulsion do not deposit on the bacteria surface. The TCMTB biocide must, therefore, be transferred to the bacteria by repeated emulsion-bacteria contacts (similar to the case of the transfer of the hydrophobic biocide triclosan from PS-b-PAA micelles to the bacteria<sup>22</sup>), or *via* the solution.

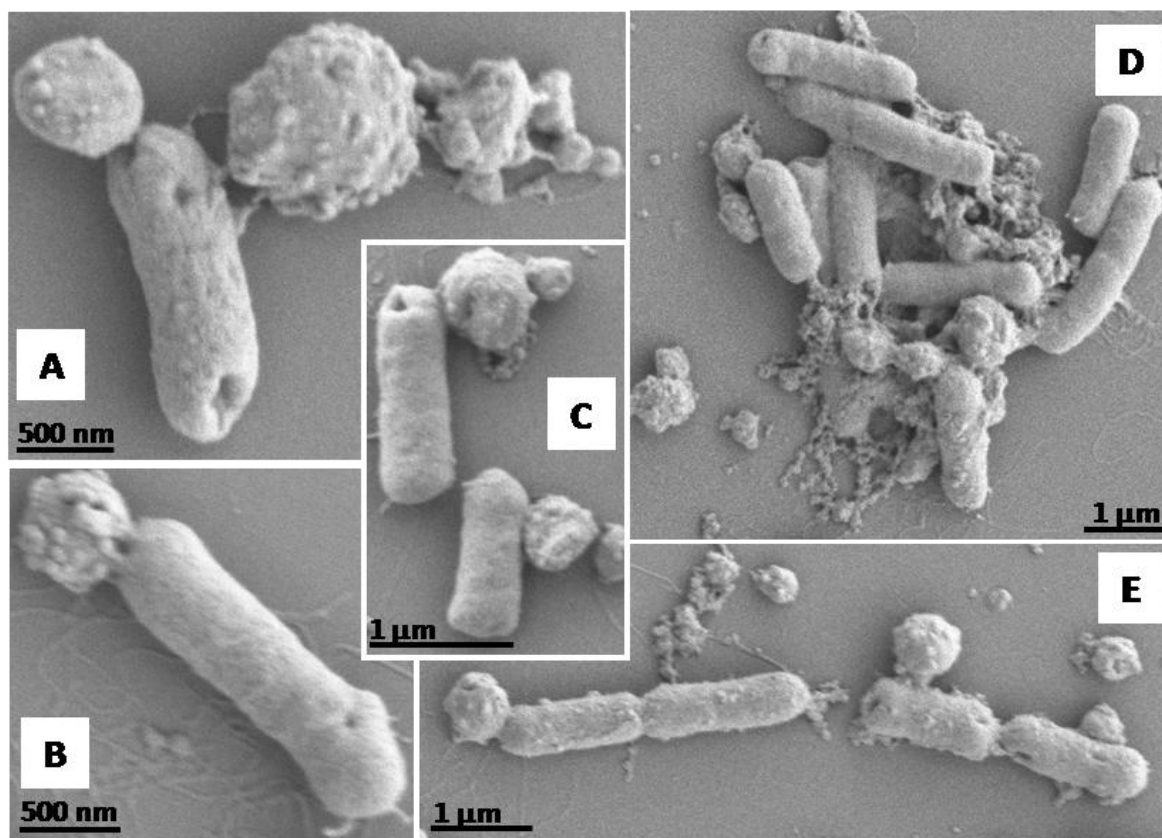


Figure 5.9. SEM images of bacteria deactivated by PCL-b-PAA/TCMTB.

Simple calculations were performed to explore how many emulsion droplets (in relation to the number required for monolayer coverage on the bacteria) are needed to kill the bacteria. The calculation is given in the Appendix to Chapter 5 in section 1.9. It can be concluded from these calculations that the emulsion solution effective in killing bacteria contains roughly enough droplets for a monolayer coverage number of emulsion droplets per bacterium. The theoretical monolayer coverage of 22 droplets/bacterium is in agreement with the concentration efficient in killing the bacteria found from the bacteria deactivation experiment.

#### 5.3.3.2.3. Comparison of Mechanisms of Bacteria Deactivation by PEI/TCMTB and PCL-b-PAA /TCMTB emulsions.

The mechanisms of bacteria deactivation by PEI/TCMTB and PCL-b-PAA/TCMTB emulsions are different, as was discussed for each emulsion individually in the sections above. Figure 5.10 shows a schematic representation of mechanisms of bacteria deactivation by emulsions stabilized by the two stabilizing agents. The key difference in the mechanisms can be attributed to the charge of the stabilizing agent; PEI molecules are positively charged, while the PCL-b-PAA micelles corona has a negative charge. Therefore, the PEI molecules are attracted to the negatively charged sites on the bacterial cell wall; these electrostatic interactions will cause the bacteria to die of perturbations in the cell wall (Figure 5.10 A1). After adsorption, the PEI molecules penetrate through the bacteria membrane and kill the bacteria, leaving small holes on the surface of it. A number of other positively charged polymers, for example cationic polyacrylamide, are also known to be bactericidal.<sup>21</sup> In addition to the PEI adsorption followed



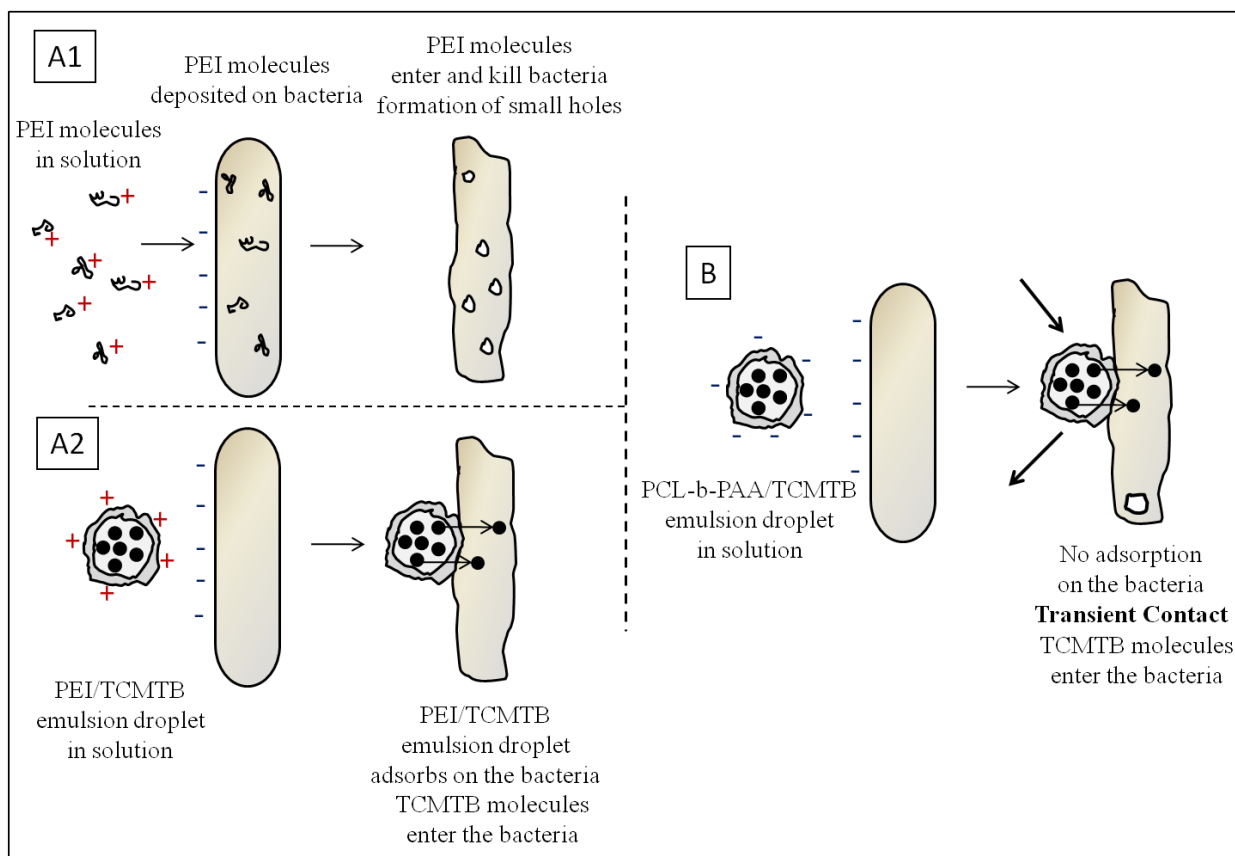


**Figure 5.10.** Schematic representation of mechanisms of bacteria deactivation by PEI/TCMTB (A1 and A2) and PCL-b-PAA /TCMTB (B) emulsions.

by its penetration into the bacteria, also the PEI/TCMTB emulsion droplets deposit on bacteria and transfer TCMTB molecules, which will penetrate through the bacteria cell wall (Figure 5.10 A2). Thus, in case of PEI/TCMTB emulsions, the killing mechanism is a combination of killing the bacteria by PEI molecules along with TCMTB molecules, transferred from the emulsion droplets adsorbed on the bacteria.

In contrast to the PEI, the PCL-b-PAA micelles are not attracted to the bacteria and thus another mechanism of transfer which does not involve electrostatic interactions has to be considered. TCMTB molecules are transferred upon a transient contact of the emulsion droplets with bacteria (Figure 5.10 B). The bacteria are killed by TCMTB molecules after they enter the

bacteria. The mechanism involving the release of the biocide from the emulsion into the solution followed by the penetration of biocide from solution through the bacteria wall is too slow process, and therefore, such mechanism is not applicable.

#### 5.3.3.3. Properties of Emulsion Droplets after Deactivation

As can be seen in Figures 5.11 and 5.12, after all the biocide has been released from the emulsions, residual shells remain in the solutions of both stabilizing agents. Since the stabilizing agents, in both cases, consist of water soluble species (PEI homopolymer or PCL-b-PAA micelles), it is of interest to inquire why such water soluble materials survive in the form of a shell without dissolving in aqueous solution.

The reason for the presence of an insoluble shell from the emulsion after dialysis is not right away obvious since both the stabilizing agents (PEI and PCL-b-PAA micelles) are water soluble. One possibility that might explain the insolubility is the formation of a hydrogen bonded complex between TCMTB biocide and the stabilizing agent. It is known that complexes of a polyelectrolyte with an organic material of opposite charge can yield water insoluble polyelectrolyte complexes.<sup>24-29</sup> Hydrogen bonding between the components can also lead to the formation of such complexes. If such a complex is formed, then the residual shell should contain both, the TCMTB biocide and polymeric stabilizer. The formation of such a complex is plausible because the TCMTB has a nitrogen containing a lone electron pair, while both stabilizing polymers contain protons capable of H bonding, either as hydroxyl groups on the PAA or NH groups on the PEI.

To ascertain whether such complexes are actually formed, elemental analysis was performed on the residual shells remaining in the emulsion solution after extensive (24 hours) dialysis

against the large excess of water. It should be recalled that the TCMTB should be present only if the complex is formed, and that it contains three sulphur atoms per molecule. Sulphur is easy to detect by the inductively coupled plasma (ICP) technique with an optical emission spectrophotometer, which method is used in the present case. (Details of ICP technique are given in section 1.10. in the Appendix to Chapter 5).

The results for the emulsions protected by the two stabilizing agents do, indeed, show the presence of TCMTB. Specifically, the results suggest that for the 50/50 PEI/TCMTB emulsion, there are 17 PEI repeat units per TCMTB molecule, while for the 50/50 PCL-b-PAA/TCMTB emulsion; there are approximately 11 PAA units per TCMTB molecule. These ratios are probably too low for the formation of a stable hydrophobic complex. It should be noted, however, that these results are subject to considerable experimental error. ICP measurements are performed on the solution of the analyte. In this particular case, the material was very difficult to digest, so it is entirely possible that undigested particles remained. The component that went into solution is, most likely, composed of the material containing the least amount of TCMTB. Thus, there are likely higher concentrations of TCMTB than indicated by the analysis, and the formation of hydrophobic complexes cannot be excluded, and may well be responsible for the formation of the insoluble shell detected by electron microscopy and DLS.

The proposed mechanisms for the two stabilizing agents are somewhat different. They are described below, starting with the PEI system.

#### 5.3.3.3.1. Residual Shells of PEI after Bacteria Deactivation

As can be seen in Table 5.1, the TCMTB contains nitrogen in a heterocycle. This nitrogen is expected to be the negative end of a dipole, and thus receptive to hydrogen bonding by a species containing a proton which is susceptible to H bonding. The PEI has such a hydrogen atom; one can therefore expect an H bond to be formed between the amine proton of the PEI and the nitrogen of the TCMTB heterocycle. If the binding constant of such hydrogen bonded structure is sufficiently strong, a substantial number of the PEI repeat units would be expected to undergo such complexation. Since the hydrophobic component of the complexed chain would now be considerable, the polymer is expected to become water insoluble, and thus cause the survival of the shell in solution. Such shells, shown in Figure 5.11, are seen both by TEM (A - C), where they were stained with phosphotungstic acid, and by SEM (D - F).

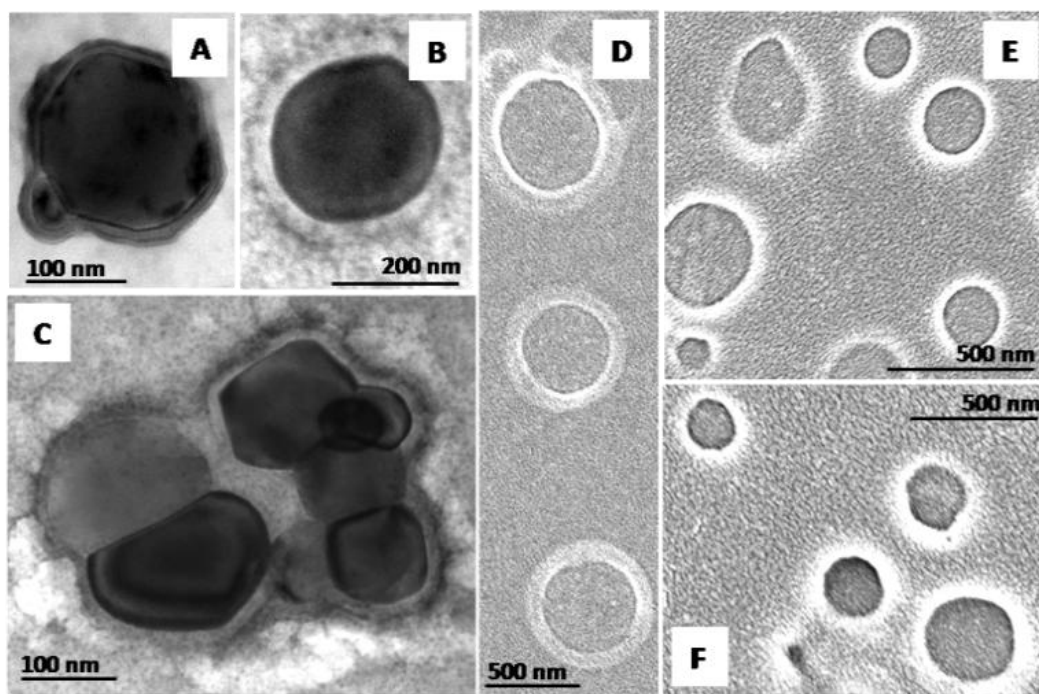


**Figure 5.11.** TEM (A – C) and SEM (D – F) images of PEI/TCMTB shells remaining after emulsion dissolution for 50/50 % ratios of PEI and TCMTB after 1400 minutes of dialysis (at the end of the kinetics of emulsion dissolution experiment).

In view of the above discussion of the water insolubility of the complex, the question arises as to why one finds in the solution some free PEI homopolymer, which acts as the primary biocide in the system. To understand this aspect, it is useful to recall that the emulsion is prepared from a 50/50 ratio of the two ingredients, PEI and TCMTB. The formula weight of a PEI repeat unit is 43, while that of the TCMTB is 238. There is, thus, a ca. four fold excess of the PEI. One can envisage equilibrium between the complex with TCMTB and free PEI molecules in the aqueous solution, possibly even involving two phases.

#### 5.3.3.3.2. Residual Shells of PCL-b-PAA after Bacteria Deactivation

The mechanism of shell formation in PCL-b-PAA/TCMTB emulsions shows considerable similarity to that of the PEI stabilized emulsions. It should be recalled that the stabilized emulsions are prepared at 60 °C, above the melting point of the poly(caprolactone) micelle cores, as well as that of the TCMTB. It is, therefore, reasonable to suggest that the micelles are placed on the surface of the liquid TCMTB drop in the form of hemi-micelle, which would maximize the hydrophobic interactions between the hydrophobic PCL core and the hydrophobic TCMTB.

In addition, in parallel to the situation with the PEI stabilizer, a strong hydrogen bond is expected to form between the proton of the PAA and the heterocyclic nitrogen on the TCMTB. Such complexation, as before, would decrease the hydrophilicity of the PAA corona, and lower its solubility in water. However, since equilibrium is expected to be operative between the TCMTB and the PAA, it is tempting to suggest that a certain number of uncomplexed PAA units will remain on the surface of emulsion drop. Under the pH prevailing in neutral water, many of these PAA units are expected to be ionized, which would give the emulsion drop a negative charge and maintain its stability in water. After the release of the TCMTB from the emulsion, the

decreased solubility of the PAA resulting from the complexation keeps the shell intact, as can be seen in Figure 5.12 from TEM (A, B) and SEM (C – E) images. Clearly, the shell does not maintain its spherical structure, but collapses (Figure 5.12 D and E).

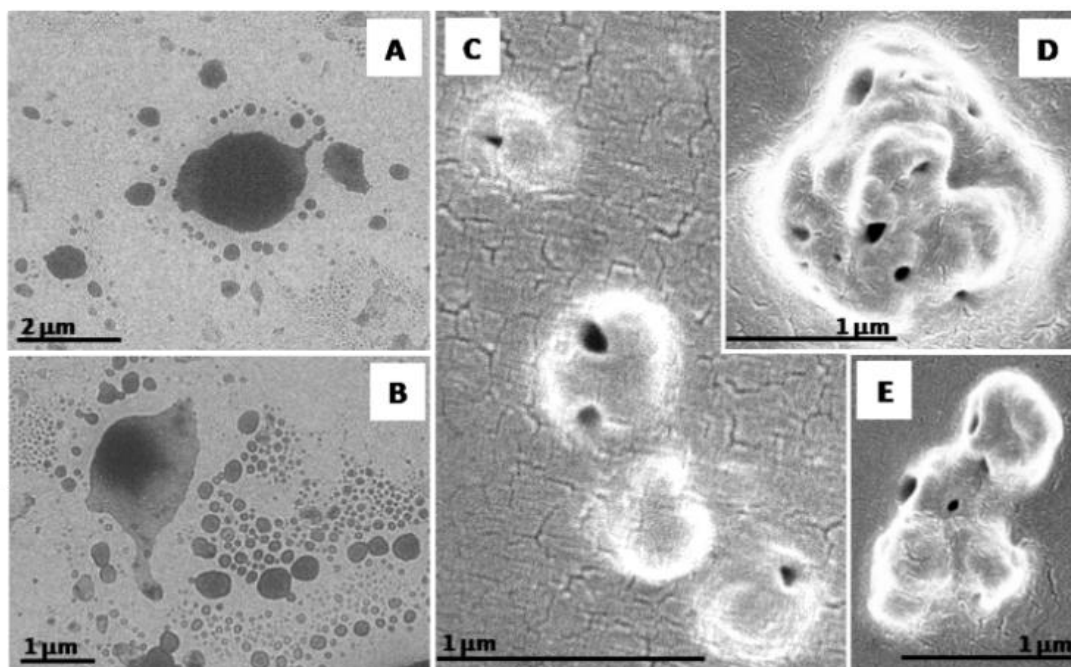


**Figure 5.12.** TEM (A, B) and SEM (C – E) images of PCL-*b*-PAA /TCMTB shells remaining after emulsion dissolution for 50/50 % ratios of PCL-*b*-PAA and TCMTB after 1400 minutes of dialysis (at the end of the kinetics of emulsion dissolution experiment).

#### 5.4. Conclusions

The effect of stabilizers on the deactivation efficiency of bactericidal emulsions was studied. Stable thiocyanomethylbenzothiazol biocide emulsions, stabilized by poly(ethyleneimine) (stable for few days) and by micelles of poly(caprolactone)<sub>33</sub>-*b*-poly(acrylic acid)<sub>33</sub> block copolymer (stable over ten months) were prepared; emulsions using the two stabilizing agents were found to be stable in 50/50 and 66/33 ratios of stabilizing agent/TCMTB. The average diameters measured by DLS for the 50/50 PEI/TCMTB emulsion was found to be 373 nm, while that of the

66/33 ratio was 508 nm; the 50/50 PCL-b-PAA/TCMTB emulsion contains droplets of 325 nm, while in that of 66/33 ratio the size is 378 nm.

Bacteria deactivation using TCMTB emulsions stabilized by PEI homopolymer and by PCL-b-PAA micelles was studied. It was found that the primary biocidal material using PEI/TCMTB emulsion are the positively charged free PEI molecules combined with an effect of TCMTB from emulsions. In contrast to the case of PEI as a stabilizing agent, for PCL-b-PAA/TCMTB the negatively charged PAA micelle corona does not disturb the growth of the bacteria; the bactericidal agent is the TCMTB biocide. This difference in the bactericidal action can be attributed to the charge of the stabilizing agent; the positively charged PEI molecules adsorb on the negative bacteria, while the micelles with a negatively charged corona, do not deposit on the bacteria. Concentrations above 0.136 g/L are efficient in killing the bacteria for both types of emulsions at a bacteria concentration of  $25 \times 10^9$  bacteria/L, which corresponds to an absorbance of 0.1.

The kinetics of emulsion dissolution was studied for both emulsion types. It was found that the biocide is released from the PCL-b-PAA/TCMTB (both 50/50 and 66/33) over a comparable time period (270 min) as from the PEI/TCMTB emulsion, in which case it is released to a steady state within 300 min for the 66/33 ratio and in 150 minutes for the 50/50 ratio. Interestingly and unexpectedly, neither of the biocide emulsions dissolves completely when dialyzed against a large excess of water; plateaus in the curves of average diameters vs. time were seen by DLS in all the tested emulsions after the biocide was released in spite of the fact that both stabilizing agents are water soluble. From the emulsion dissolution curves it appears that residual shells are left in solution after the release is complete.

The mechanisms of bacteria deactivation were found to differ for emulsions of the two stabilizing agents. The key difference in the mechanisms is due to the charge of the stabilizing agent; PEI molecules are positively charged, while the PCL-b-PAA micelle corona has a negative charge. Therefore, PEI molecules are attracted to the negatively charged sites on the bacterial cell wall; these electrostatic bonds cause the bacteria to die, likely of stresses in the cell wall. In addition, after adsorption, the PEI molecules penetrate through the bacteria membrane and kill the bacteria, leaving small holes on their surface. By contrast, the PCL-b-PAA micelles are not attracted to the bacteria, and thus a mechanism of transfer other than electrostatic interactions has to be considered. TCMTB molecules are either released from the emulsion and then enter the bacteria from solution or are transferred upon contact of the emulsion drop with the bacteria. The bacteria are killed by the TCMTB molecules after they enter the bacteria.

The existence of the residual shells in the emulsion solution, in case of PEI, can be ascribed to H bond formation between the amine proton of the PEI and the nitrogen of the TCMTB heterocycle; the PEI repeat units undergo complexation and the polymer becomes water insoluble, thus preventing the dissolution of the shell. In the PCL-b-PAA/TCMTB emulsions, the mechanism of shell formation shows considerable similarity to that of the PEI stabilized emulsions. Due to emulsion preparation at temperature above melting points for both materials, TCMTB and the PCL in the PCL-b-PAA micelles, the micelles are, most probably, placed on the surface of the liquid TCMTB drop in the form of hemi-micelles, which maximizes the hydrophobic interactions between the hydrophobic PCL core and the hydrophobic TCMTB. In addition, a strong H bond is expected to form between the proton of the PAA and the heterocyclic nitrogen on the TCMTB, which decreases the hydrophilicity of the PAA corona, and lowers its solubility in water. Since equilibrium is expected to be operative between the



TCMTB and the PAA, most likely a certain number of uncomplexed PAA units remains on the surface of the emulsion drop. Under the pH prevailing in neutral water, many of these PAA units are ionized, which gives the emulsion drop a negative charge and maintains its stability in water. After the release of the TCMTB from the emulsion, the decreased solubility of the PAA resulting from the complexation keeps the shell intact.

### 5.5. Reference List

- (1) Riess, G., Labbe, C., *Macromol. Rapid Commun.*, 2004, 25, 401.
- (2) Amalvy, J.I., Armes, S.P., Brinks, B.P., Rodrigues, J. A., G. F. Unali, G. F., *Chem. Commun.*, **2003**, 15, 1826.
- (3) Molau, G. E., *Colloidal and Morphological Behavior of Block and Graft Copolymers*, in: *Block Copolymers*, S.L. Aggarwal, Ed., Plenum Press, New York, **1970**, 79.
- (4) Price, C., *Colloidal Properties of Block Copolymers*, in: *Developments in Block Copolymers I*, S. L. Aggarwal, Ed., Applied Science, London, **1982**, 39.
- (5) Piirma, I., *Polymeric Surfactants*, in: *Surfactant Science Series 42*, Marcel Dekker, New York, **1992**, 1.
- (6) Tuzar, Z., Kratochvil, P., *Micelles of Block and Graft Copolymers in Solution*, in: *Surface and Colloid Science*, E. Matijevic, Ed., Plenum Press, New York, **1993**, Vol. 15, 1, 1.
- (7) Riess, G., Dumas, P., Hurtrez, G., *Block Copolymer Micelles and Assemblies*, in: *MML Series 5*, Citus Books, London, **2002**, 69.
- (8) Alexandridis, P., Hatton, T.A., *Block Copolymers*, in: *Polymer Materials Encyclopedia 1*, CRC Press, Boca Raton, **1996**, 743.
- (9) Alexandridis, P., Lindman, B., *Amphiphilic Block Copolymers: Self Assembly and Applications*, Elsevier, Amsterdam, **2000**, 1.
- (10) Burguiere, C., Pascual, S., Bui, Ch., Vairon, J.-P., Charleux, B., Davis, K.A., Matyjaszewski, K., Betremieux, I., *Macromolecules*, **2001**, 34, 4439.
- (11) Muller, H., Leube, W., Tauer, K., Forster, S., Antoinety, M., *Macromolecules*, **1997**, 30, 2288.

- (12) Barnes, T.J., Prestidge, C.A., *Langmuir*, **2000**, 16, 4116.
- (13) Kralchevsky, P.A., Ivanov, I.B., Ananthapadmanabhan, K.P., Lips, A., *Langmuir*, **2005**, 21, 50.
- (14) Hanson, J.A., Chang, C.B., Graves, S.M., Li, Z., Mason, T.G., Deming, T.J., *Nature*, **2008**, 455, 85.
- (15) European Patent 1508276, Lipiecki, F.J., Maroldo, S.G., Pendell, B.J., Simon, E.S., Rohm and Hass, **2005**.
- (16) Vyhnalkova, R., Eisenberg, A., van de Ven, T.G.M., *J. Phys. Chem. B*, **2008**, 112, 8477.
- (17) Manninen, A., Auriola, S., Vartiainen, M., Liesivuori, J., Turunen, T., Pasanen, M., *Arch Toxicology*, **1996**, 70, 579.
- (18) Edward, Q.Z., Remsen, E., Wooley, K.L., *J. Am. Chem. Soc.* **2000**, 122, 3641.
- (19) Poraj-Kozminski, A., Hill, R., van de Ven, T.G.M., *J. Coll. Inter. Sci.*, **2007**, 309, 1, 99.
- (20) Alince, B., Vanerek, A., van de Ven, T.G.M., *Ber. Bunsenges. Phys. Chem.*, **1996**, 100, 954.
- (21) [www.lenntech.com/biocides.htm](http://www.lenntech.com/biocides.htm)
- (22) Vyhnalkova, R., Eisenberg, A., van de Ven, T.G.M., to be submitted
- (23) Kamiti, M., van de Ven, T.G.M., *Macromolecules*, **1996**, 29 (4), 1191.
- (24) Smitha, B., Sridhar, S., Khan, A. A., *Macromolecules*, **2004**, 37 (6), 2233.
- (25) Wallin, T., Linse, P., *Langmuir*, **1998**, 14, 2940.
- (25) Kuhn, P.S., Levin, Y., Barbosa, M.C., *Chemical Physics Letters*, **1998**, 298, 51.
- (26) Chodanowski, P., Stoll, S., *Journal of Chemical Physics*, **2001**, 115, (10), 4951
- (27) Schatz, Ch., Lucas, J-M., Viton, Ch., Domard, A., Pichot, Ch., Delair, T., *Langmuir*, **2004**, 20, 7766.
- (28) Tsuchida, E., *Journal of Macromolecular Science, Part A*, **1994**, 31, (1), 1.
- (29) Chavasit, V., Kienzle-Sterzer, C., Torres, J.A., *Polymer Bulletin*, **1988**, 19, (3), 223.

## **Chapter 6:**

# **Conclusions, Contributions to Original Knowledge and Suggestions for Future Work**

---

### **6.1. Conclusions and Contributions to Original Knowledge**

The main objective of the present dissertation was to prepare antibacterial filter paper while using hydrophobic materials with antibacterial properties of very low water solubility. This goal was achieved by choosing two different strategies, i.e. by employing amphiphilic block copolymer micelles which were loaded with biocides, followed by their attachment to the pulp fibres, or by using biocide emulsions stabilized with polymeric materials.

The summary of the main findings of the work employing the two above mentioned strategies, together with the original aspects of the studies, are given in this chapter of the thesis. The discussion is divided into four subsections, corresponding to the four main chapters of the dissertation. Sections 6.1.1.- 6.1.3. summarize the study of biocide loaded micelles, while section 6.1.4. deals with biocide emulsions.

### 6.1.1. Loading and Release Mechanisms of a Biocide in PS-*b*-PAA Block-copolymer Micelles

As discussed in Chapter 2, crew cut micelles of PS<sub>197</sub>-*b*-PAA<sub>47</sub> were self assembled following well known procedures and loaded with the hydrophobic antibacterial material, thiocyanomethylthiobenzothiazole (TCMTB). The TCMTB loading capacity of the PS-*b*-PAA micelles was measured using UV-vis spectroscopy; it was found that maximum loading was achieved in one hour and reached values around 32 % (w/w).

The loading process was found to be a two step process; in the first, the micelle surface is saturated with TCMTB molecules, which takes about 10 minutes and reaches approximately 10 % (w/w) of loaded biocide. The biocide molecules are transferred from the biocide film (which coats the glass container) by transient contacts between micelles and the film. In the next step, after the micelle surface is saturated with TCMTB molecules, the biocide starts to penetrate as a front into the hydrophobic polystyrene core, while lowering the glass transition temperature of the PS in the process. The front was found to move towards the inside of the PS core with the velocity of 0.2 nm/min following Non-Fickian case II diffusion, which was demonstrated because the data fit the equation for case II diffusion. The velocity of the moving front depends on how fast the biocide molecules plasticize the PS core. This process continues until the micelles are loaded with biocide molecules to the thermodynamic limit. The second part of the process, i.e. the internalization step of the biocide molecules from the micelle surface into the PS core of the micelles, is much slower than the adsorption of the biocide molecules on the micelle surface, and thus is the rate-determining step of biocide loading.

Based on the partition coefficient experiments and calculations, it was found that the biocide has a similar preference for the PS core as for ethylbenzene over water, indicating that maximum loading is governed by thermodynamics.

Two techniques of biocide loading into micelles were tested; loading of the biocide from the biocide film and the loading from biocide grains. It was found that the loading from the biocide film is more effective than that from the biocide grains. The loading from the biocide grains is not as effective because the micelles adsorb onto the biocide grains and are filtered off along with the excess of biocide after the loading is completed; therefore, it appears that not as many biocide molecules can be loaded into the micelles.

From the kinetics of the biocide release experiments it was found that the release of the biocide from the micelles is a slower process than loading, which is completed within one hour. The rate determining step of the release was found to be the release of the biocide molecules from the surface of the micelles; for this step to take place, the biocide molecules have to pass over an energy barrier to go into the aqueous solution. After the release of biocide molecules from the micelle surface, the surface is replenished by diffusion of biocide molecules from the micelle interior in the early stage of release. As the biocide molecules are released from the micelle, the glass transition temperature of the core increases, and the diffusion coefficient of the molecules decreases progressively. Due to the glass transition temperature increase with decreasing biocide content, not all the biocide molecules can be released from micelle interior within a short time.

### 6.1.2. Bactericidal Block-copolymer Micelles

Chapter 3 of this thesis dealt with bacteria deactivation by biocide loaded micelles in solution. The block copolymer micelles used were composed of amphiphilic block copolymers of PS-*b*-PAA with a negatively charged corona and of PS-*b*-P4VP with a positively charged corona under some pH conditions. Two different hydrophobic biocides, TCMTB and triclosan, of very low water solubility, were loaded from the film into the micelles; the loading reached a plateau in one hour in both cases at a maximum loading of about 20 to 30 % (w/w), depending on the type of biocide. The loading of the TCMTB biocide reached higher loading levels (30 % (w/w)) than triclosan (20 % (w/w)). *E. coli* bacteria (Gram negative) are very commonly used as a model pathogen since they can be grown easily and their genetics are simple and easily-manipulated or duplicated; thus, they were chosen as a model pathogen in this study.

It was found that TCMTB biocide released from block copolymer micelles of PS-*b*-PAA is only bacteriostatic (rather than bactericidal) on *E. coli* for exposure times ranging from 0 to 90 minutes. TCMTB becomes bactericidal only after long exposure times to the bacteria, such as ~ 10 hours. By contrast, triclosan released from PS-*b*-PAA block copolymer micelles exhibits bactericidal properties on *E. coli* upon exposure times shorter than 2 minutes under the same experimental conditions. These results show that triclosan, even though its loading capacity is approximately 10 % (w/w) lower than that of the TCMTB, is a much more efficient and more potent biocide than TCMTB.

The effect of cationic polyacrylamide (c-PAM) on the bacteria deactivation was also studied, since c-PAM promotes the interaction between negatively charged PS-*b*-PAA micelles and bacteria. It was found that when c-PAM is added to the micelle/bacteria solution, it acts as a

bactericidal agent by itself in that it kills the bacteria. In the absence of micelles, c-PAM adsorbs on the bacterial surface and deactivates the bacteria. However, in the presence of micelles, the surface area of the micelles is 100 times larger than that of the bacteria, and the bacteria are unaffected because the c-PAM adsorbs mainly on the micelles. It was also found that combining TCMTB loaded micelles and c-PAM causes flocculation of *E. coli*.

PS-b-P4VP block copolymer micelles loaded with TCMTB biocide were also tested for their bactericidal properties. TCMTB loaded PS<sub>297</sub>-b-PVP<sub>30</sub> micelles exhibit bactericidal properties, but furthermore, by contrast with the PS-b-PAA micelles, which affect the bacterial growth only minimally, empty PS<sub>297</sub>-b-PVP<sub>30</sub> micelles (without TCMTB loading) act as a bactericidal agent also. The difference lies in the bactericidal nature of the P4VP itself and also because P4VP is positively charged and the charge of the bacteria is overall negative; positively charged PS-b-P4VP micelles are attracted to the negatively charged sites on the bacterial cell wall and deposit on the bacteria. These electrostatic bonds cause the bacteria to die, likely because of stresses in the cell wall.

Based on experiments of various exposure times of *E. coli* bacteria to the TCMTB loaded PS<sub>197</sub>-b-PAA<sub>47</sub> micelles, it was found that the bacteria reach their limiting biocide uptake within about 10 minutes, at which point they have taken up approximately 10 % of the total biocide. The number of biocide molecules per bacterium was estimated to be  $\sim 8.4 \times 10^9$ , while the number of micelles per bacterium equals to  $\sim 4 \times 10^6$ .

The proposed mechanism of biocide uptake by the bacteria involves transfer of biocide molecules during transient collisions between loaded micelles and bacteria. As the micelle surface is saturated by biocide, whenever the micelle collides with the bacteria surface, some biocide molecules are transferred from the surface of the core of the micelle to the bacteria; these

collisions repeat very frequently. The number of biocide molecules transferred to the bacterium per collision was estimated for “complete loading of bacteria” within 10 min to be roughly 500 biocide molecules/collision and the number of collisions per one bacterium was calculated to be 11500/s. The thickness of the micelle corona and the radius (surface area) of the micelle core could conceivably affect this transfer. The deposition of micelles onto the bacterial surface was not found to be necessary for successful transfer of biocide from the micelles to the bacteria.

### *6.1.3. Bactericidal Filter Paper*

Chapter 4 was focused on a practical application of biocide loaded micelles, namely, on the preparation of antibacterial filter paper intended mainly for water purification. For that purpose, existing and commercially available filter papers were used. The preparation of the antibacterial filter papers involved a hydrophobic biocide, triclosan, which has very low water solubility and which was incorporated into the hydrophobic core of negatively charged (in the corona) amphiphilic block copolymer micelles. Since the micelles are negatively charged as are the pulp fibres of the paper as well, an intermediate compound, cationic polyacrylamide (c-PAM), was attached to the pulp fibres to change the ionic charge of the filter paper carrier prior to the attachment of triclosan loaded micelles. Due to the extremely low solubility of the biocide in water, the biocide is transferred to the bacteria primarily during the transient collisions between the triclosan loaded micelles and bacteria, as was discussed in more detail in Chapter 3.

The antibacterial filter paper was, after its preparation, tested on bacteria for its efficiency in deactivation. A bacterial suspension was passed through variously modified filter papers. The filtrate was then taken, mixed with growth media, and incubated for three hours to examine the bacterial growth with time by measuring its absorbance. Bactericidal filter paper was considered



efficient in killing the bacteria if the bacteria did not reproduce themselves, i.e., when the relative absorbance of the incubated sample passed through the filter paper did not increase with time. To verify if the bacteria in the samples were killed by triclosan released from the filter paper, a set of control samples was prepared for each filter paper at the same time and the results were compared; these control samples consisted of plain filter paper without any modification and filter papers modified either with only c-PAM or with only biocide loaded micelles.

In Chapter 4 it was shown that we had indeed prepared antibacterial filter paper from commercial papers modified with c-PAM along with biocide loaded micelles. The bactericidal effectiveness was confirmed by proving that this paper has antibacterial properties when a bacteria solution is passed through it, and that it is efficient in killing the bacteria. Filter paper treated with only triclosan loaded micelles also deactivates the bacteria, but since it is not attached to the filter paper through the modification (with c-PAM) of the ionic charge of the pulp fibers, these triclosan loaded micelles are filtered into the filtrate along with the bacteria. Therefore, some bacteria are also killed in the solution due to the presence of these triclosan loaded micelles. The presence of the triclosan loaded micelles in the filtrate may not be favorable since it contains the amphiphilic block copolymer micelles and, therefore, may not be safe to drink. Filter paper treated with both c-PAM and triclosan loaded micelles kills the bacteria, but, more importantly, the micelles do not come into the filtrate, since they are attached to the filter paper.

The attachment of c-PAM alone to the filter paper fibers was found to slow down the growth of the bacteria in the filtrate after passing the bacterial suspension through the paper, but not to kill them. As was proven already in Chapter 3, c-PAM itself acts as a weak biocide.

A commercially available paper towel material was also modified with c-PAM and triclosan loaded micelles to test the bactericidal efficiency of that system. Appreciable bacterial deactivation was achieved even though the contact time of bacteria with loaded micelles was very short due to the high porosity of the paper towel.

In addition, optimal parameters and conditions for bactericidal efficiency of the filter paper were studied in the work described in Chapter 4. The effect on the bacterial deactivation of varying several relevant experimental parameters was studied, specifically, the initial concentration of bacteria in solution which passed through the filter, the initial volume of the bacteria solution, the weight ratios of biocide loaded micelles and c-PAM to weight of paper, paper porosity, re-usability of the antibacterial filter paper and, finally, bacteria deactivation with the active filter placed in the bacteria suspension. Optimal parameters to prepare an efficient bactericidal filter paper were found to be as follows: Whatman filter paper of 90 mm diameter of grade 1 to 3 with pore sizes of 11 to 6  $\mu\text{m}$ , respectively. The weight ratio of c-PAM and triclosan loaded PS-b-PAA micelles was in both cases 0.5 mg/g of paper, the micelle loading by triclosan was approximately 20 % (w/w), and the *E. coli* bacteria concentration in 100 mL of solution passed through the filter was approximately  $25 \times 10^6$  bacteria/mL, which corresponds to an absorbance of 0.1; time of filtration was between 30 and 60 min.

The tests for re-usability of the filter paper on bacteria suspensions showed that in the case of a second pass of bacteria through the filter paper modified either with only loaded micelles or with biocide loaded micelles along with c-PAM, the modifications were not found efficient in bacteria deactivation. Re-used filters were found inefficient since the bacteria grew slightly above the absorbance limit with incubation. Re-use of the antibacterial filter paper does not appear advisable at this time since the paper has only marginal antibacterial properties after reuse.

Antibacterial filter papers (90 mm diameter) left in the bacteria suspension of c-PAM and biocide loaded micelles of concentrations of 1 mg/g of paper were found efficient in killing *E. coli* bacteria from 100 mL suspension of concentration of  $25 \times 10^6$  bacteria/mL, when left in the bacteria suspension for times longer than 20 minutes.

#### 6.1.4. Effect of Stabilizers on the Deactivation Efficiency of Bactericidal Emulsions

The topic of Chapter 5 was to study the effect of polymeric stabilizers on the bacterial deactivation by emulsions containing a hydrophobic biocide. Stable emulsions containing thiocyanomethylbenzothiazol were prepared using either polymeric stabilizers, such as poly(ethyleneimine) (stable for few days) or micelles of poly(caprolactone)<sub>33</sub>-b-poly(acrylic acid)<sub>33</sub> block copolymer (stable over ten months). Both emulsions were found to be stable in 50/50 and 66/33 ratios of stabilizing agent/TCMTB. DLS was employed to measure the average diameter of the emulsion droplets. The 50/50 PEI/TCMTB emulsion droplets had a diameter of 373 nm, while in those of the 66/33 ratio it was 508 nm; the 50/50 PCL-b-PAA/TCMTB emulsion contained droplets of 325 nm, while in that of the 66/33 ratio the size was found to be 378 nm.

Both emulsions containing TCMTB biocide in solution were examined for *E. coli* bacteria deactivation and found to be efficient. In case of TCMTB emulsion stabilized with PEI, the primary biocidal material was found to be the positively charged free PEI molecules while the TCMTB had a weaker effect. In contrast to the case of PEI as a stabilizing agent, for the PCL-b-PAA/TCMTB emulsion the negatively charged PAA micelle corona does not disturb the growth of the bacteria; the bactericidal agent is the TCMTB biocide alone. The difference in the bactericidal mechanism is based on the stabilizing agent; the positively charged PEI molecules adsorb on the negatively charged sites of bacteria, while the micelles with a negatively charged

corona, do not deposit on the bacteria. The concentrations efficient in killing bacteria for both types of emulsions were those above 0.136 g/L at a bacteria concentration of  $25 \times 10^9$  bacteria/L.

As studied in Chapter 5, it was found from the measurements of kinetics of emulsion dissolution that the biocide is released from the PCL-b-PAA/TCMTB (both 50/50 and 66/33) over a time period of ca 270 min; this value is similar to that for the PEI/TCMTB emulsion, in which case it is released completely within 300 min for the 66/33 ratio and in 150 minutes for the 50/50 ratio. In addition, the experiments of kinetics of dissolution revealed, interestingly and unexpectedly, that for neither of the biocide emulsions did the droplets dissolve completely when dialysed against a large excess of water for 24 hours. It was found that in both cases the curves of average diameter *vs.* time measured by DLS exhibited a plateau in all the tested emulsion samples after the release of biocide, in spite of the fact that the two stabilizing agents by themselves are water soluble. Based on these data and on SEM images it appeared that residual shells are left in solution after the release of the biocide comes to a stop.

The mechanisms of bacteria deactivation differ for the emulsions stabilized by the two stabilizing agents. The key difference in the mechanisms lies in the ionic charge of the stabilizing agents; the charge of PEI molecules is positive, while that of the PCL-b-PAA micelle corona is negative. Since the bacterial cell wall is overall negatively charged, PEI molecules are attracted to the negatively charged sites on the bacteria cell wall and, therefore, PEI molecules deposit on the bacteria; these electrostatic interactions cause the bacteria to die, likely of stresses in the cell wall. After adsorption, the PEI molecules penetrate through the bacteria cell wall and kill the bacteria, leaving small holes on their surface. By contrast, since the ionic charge of PCL-b-PAA micelles core is negative and the micelles are not attracted to the bacteria, the mechanism of the biocide transfer to the bacteria is not of an electrostatic nature. Most likely, the TCMTB

molecules are either transferred upon contact of the emulsion droplet with bacteria and then enter the bacteria cell wall, which causes the deactivation of bacteria.

H bond formation between the amine proton of PEI and the nitrogen of the TCMTB heterocycle possibly causes the formation of an insoluble complex of PEI repeat units with TCMTB molecules and might thus explain the existence of the water insoluble residual shells in the emulsion PEI/TCMTB solution. The mechanism of shell formation in the PCL-b-PAA/TCMTB emulsions shows considerable similarity to that of the PEI stabilized emulsions. Since these emulsions are prepared at temperatures above the melting points of both materials, i.e. TCMTB and the PCL in the PCL-b-PAA micelles, the micelles, most probably, form hemi-micelles on the surface of the liquid TCMTB drop, which maximizes the hydrophobic interactions between the hydrophobic PCL core and the hydrophobic TCMTB. A strong H bond is expected to form between the proton of the PAA and the heterocyclic nitrogen on the TCMTB, which decreases the hydrophilicity of the PAA corona, and lowers its solubility in water. Since there is an equilibrium between the TCMTB and the PAA, a certain number of uncomplexed PAA units remains on the surface of the emulsion drop. Under the pH prevailing in neutral water, many of these PAA units are ionized, which gives the emulsion drop a negative charge and keeps these emulsion droplets stable in water over long period of time. The decreased solubility of the PAA resulting from the complexation keeps the shell intact after the release of the TCMTB from the emulsion.

## **6.2. Suggestions for Future Work**

The following paragraphs provide some suggestions for follow up studies, useful for modification of bactericidal filter paper. The discussion is divided in the following four sections.

### 6.2.1. Loading and Release Mechanisms of a Biocide in PS-*b*-PAA Block-copolymer Micelles

As discussed in Chapter 2, thiocyanomethylthiobenzothiazol biocide was chosen as a model antibacterial material to study mechanisms of loading into and release from PS-*b*-PAA amphiphilic block copolymers micelles. As a follow up, it would be interesting to elucidate loading capacities, partition coefficients, and the effects of the antibacterial materials as plasticizing agents on the glass transition temperature for the hydrophobic core, as well as loading and release mechanisms for other types of hydrophobic antibacterial agents. These studies could be used to find an ideal bactericidal material to be incorporated into and subsequently released from the PS-*b*-PAA micelles with negatively charged corona. It could be also of interest to provide the above mentioned studies on micelles prepared from other types of amphiphilic block copolymers, for example from block copolymers which, when micellized, contain a positively charged corona, such as poly(styrene)-*b*-poly(4-vinyl pyridine). Similar studies could also be performed on block copolymers, which are biocompatible and thus safe for human use, such as those currently used in drug delivery, for example poly(caprolactone)-*b*-poly(ethylene oxide) amphiphilic block copolymers.

### 6.2.2. Bactericidal Block-copolymer Micelles

*E. coli* bacteria deactivation by biocide loaded micelles in solution was described in Chapter 3. The block copolymer micelles used in that part of the study were composed of amphiphilic block copolymers of PS-*b*-PAA with a negatively charged corona and of PS-*b*-P4VP with a positively charged corona. Two different hydrophobic biocides, TCMTB and triclosan, of very low water solubility, were loaded from the film into the micelles and the deactivation of *E. coli* bacteria

was tested. *E. coli* bacteria were chosen in this study as a model system. Since there are many pathogens which are dangerous to humans, it would be of interest to perform similar studies of bacteria deactivation as those described in Chapter 3, also on other types of gram negative bacteria, such as, for example, *Salmonella*, *Pseudomonas*, *Shigella* and others, or on gram positive bacteria, such as, for example, *Micrococcus Luteus*, *Staphylococcus*, *Streptococcus* and others.

It was shown that block copolymer micelles of PS-b-PAA with negatively charged corona deposit only on some bacteria of which the wall is also of overall negative charge, while the surfaces of other bacteria remains unaffected. In an attempt to elucidate the difference, only a few studies were performed since this aspect was not principal thrust of this thesis. Therefore, it would be of interest to continue with the study of the micelle deposition on bacteria surfaces. A detailed understanding of the reasons for the difference and of the mechanism of deposition of negatively charged corona of the micelles on some negatively charged bacteria remains unknown.

### 6.2.3. Bactericidal Filter Paper

The study described in Chapter 4 dealt with bactericidal paper. It was shown that *E.coli* were deactivated when passing through a filter loaded with block copolymer micelles containing triclosan. The deactivation process was followed by optical absorption measurements. It would be of interest to provide a number of additional experiments and validations as well as to broaden the range of block copolymer micelles and bactericidal agents to obtain optimum bactericidal properties of the filter paper.

To avoid the intermediate step of using c-PAM to change the charge of the pulp fibers, biocide loaded micelles with a positively charged corona could be attached directly to the filter paper; such a filter paper could be tested following the same procedures as described in Chapter 3.

In addition, the bacteria deactivation could be probed by supplementary techniques which are more sensitive than optical density, such as, for example, growing colonies of bacteria on agar plates which evaluate the survival of bacteria. Optical density measurements were chosen to study the deactivation because that technique is very fast; however, it has typically an accuracy of only around 1%. Thus it is sometimes impossible to conclude from such data whether all the bacteria are killed or if 1 or 2 percent survive, which might not be acceptable for some applications. Therefore, more precise techniques to test the efficiency of bacteria deactivation should be used in further studies.

The possibility exists that some micelles leak out from the filter during filtration. Although the micelles are bound to the filter by electrostatic attraction and the shear forces exerted on them during filtration are small, this possibility cannot be excluded completely. Therefore, additional experiments to explore micellar leakage from the filter paper would be needed. Fluorescently labelled micelles might be useful for such studies.

An additional series of experiments should be performed which explore the effect of bacteria concentration in the water on bactericidal efficiency of filter papers.

Since antifungal papers have a number of interesting applications, it would be also useful to investigate the possibility of producing antifungal papers, by testing the deactivation of yeast and other fungi with the micelle-loaded filters.



#### 6.2.4. Effect of Stabilizers on the Deactivation Efficiency of Bactericidal Emulsions

The efficiency in *E. coli* bacteria deactivation by TCMTB biocide emulsions stabilized either by PEI polymer or by PCL-b-PAA micelles in bacteria suspension was investigated and was discussed in Chapter 5. As it was shown, both types of stabilizing agents are good stabilizers for the TCMTB biocide. In addition, both types of TCMTB biocide emulsions are efficient in bacteria deactivation, even though the mechanisms of the bacteria deactivation are different for the two types of emulsions. The difference was found to be due to the opposite ionic charges; PEI is positive, while PCL-b-PAA micelles have negative a charge.

As the next step of expanding the study in the future, it would be advisable to prepare an antibacterial filter paper while using those emulsions. If a similar strategy as that described in Chapter 4 is used, i.e. the attachment of the emulsion droplets to the pulp fibres of existing filter paper, the use of the PEI stabilized biocide emulsion would involve a smaller number of steps, since the PEI is positively charged while bacteria cell wall surface is negative. By contrast, similar to the strategy of preparation of the filter paper described in Chapter 4, an intermediate step would have to be used to prepare antibacterial filter paper when using the biocide emulsion stabilized by PCL-b-PAA micelles, since the corona of the micelles and the surface of the bacteria cell wall are both negative. This would involve, first, a change of the ionic charge of the pulp fibres by attaching positively charged polymer, for example c-PAM, followed by the attachment of the biocide emulsion stabilized by the PCL-b-PAA micelles in the next step. This approach would have an advantage over that involving PEI stabilized emulsions, which has improved stability of the PCL-b-PAA stabilized emulsions (longer than ten months).

After the filter paper based on both types of the biocide emulsions is prepared, it should be tested for its antibacterial efficiency employing experiments similar to those described in Chapter 4. The system could also be optimized to provide the best efficiency in bacteria deactivation by using various biocides or changing relevant parameters of the bactericidal paper.

# Appendix to Chapter 1:

---

## A) Commercial Consumer Products for Filtering Water

Type of approach	Name of product	Company	Based on
Straw	LifeStraw	Vestergaard Fransten Group - Denmark	Combination of mesh filters, iodine-impregnated beads and active carbon to remove particulate matter and bacteria
	Survival Straw	AlloySafe - USA	Alloy media (Mechanism not disclosed on web site)
	Pioneer	Pristine	Does not remove bacteria or viruses of size < than 3 $\mu\text{m}$
Antimicrobial paper	Anti-microbial filter	patent	Anti-microbial filter device filters out microorganisms in a fluidic system, could be coated (Ag) to kill the microorganisms
	Antibacterial filter paper	patent	Ag containing glass fibbers < 1 $\mu\text{m}$ diameter
Disinfecting pills		Camping Survival	Contain usually chlorine, chlorine dioxide, iodine or colloidal silver
Chlorination	Potable Aqua, Military Water etc.		Chlorine is added to drinking water at treatment plants

**Table Appendix 1:** Products on market to filter

## B) Parameters Affecting Morphology of Block Copolymer Aggregates

The self-assembled morphology of block copolymers is influenced primarily by three components of the free energy of aggregation: i) *core-chain stretching*, ii) *interfacial energy* and iii) *inter-coronal chain interactions*.<sup>1,2</sup> The morphogenic components are dependent on the structural parameters of the micelles, such as the core dimensions, the density of the corona on the surface of the core, and the aggregation number.<sup>1,2</sup> The stress of any of these free energy parameters, for example further water addition or reduction of the hydrophilic block length, may

lead to morphological transition to another structure. The most common sequence of the structures is formation of micelles (after cwc is exceeded), followed by rods, vesicles and finally large compound micelles (LCMs).

To understand better the parameters of the free energy of aggregation, the following example is given: only the hydrophilic block length is varied. Using a block copolymer with a constant polystyrene block length and starting with a relatively long poly(acrylic acid), PAA, block, spherical micelles are observed initially. As the PAA length is decreased, the repulsive interactions between coronal block chains decrease, thus more PS chains can aggregate in the core, leading to larger spheres. Some of the PS blocks, however, must reach from the center of the core to the core-corona interface; thus, in general, the larger the PS core, the greater the average degree of core-chain stretching. When the aggregates become very large, the entropic penalty of core-block stretching renders simple spheres thermodynamically less stable, and rods with a decreased core diameter are formed. Reducing the PAA block to an even greater degree leads to an increase in the rod diameter as the aggregation number increases again due to reduce coronal block repulsion. Ultimately, in the same manner as for the simple sphere-rod transitions, the core-block stretching term will dictate a further morphological transition to bilayer structures, manifested, for example, as lamellae or vesicles.<sup>1,2</sup>

On the other hand, starting with a diblock copolymer of a particular composition in pure common solvent, as the water water is added to the system, the block copolymers self-assemble at the critical water concentration. As the water content is increased forward, the interfacial energy increases and minimizes the total interface surface area. In the limit, a single styrene sphere would minimize the interfacial energy, but the finite block length precludes this option. As soon as the chain stretching and coronal terms exceed the interfacial energy term, a new rod-

like morphology of a smaller radius becomes favorable and is formed. If the PAA block length is too long, however, then the spherical micelles formed are thermodynamically locked and do not undergo the transition. In such case the net surface area decrease does not compensate for the electrostatic repulsion implied by the long acrylic acid block. If the PAA block is short enough, the rod to bilayer morphology change can be induced by more water addition.<sup>1,2</sup>

### **C) Main Techniques Used in the Thesis**

#### Dynamic Light Scattering

Dynamic light scattering was used to determine the diameter of the micelles and emulsion droplets. The light scattering experiments were performed on a Brookhaven light scattering instrument with a BI9000 AT digital correlator. The data were collected by monitoring the scattered light intensity at a 90° scattering angle at 25 °C.

#### Scanning Electron Microscopy

Scanning Electron Microscopy (SEM) was employed to explore visually the effect of the biocide on the bacteria. SEM was performed on a Hitachi instrument model S- 4700. The bacteria were exposed to the micelles for a certain period of time (details given for each experiment in the Results section), the sample was then centrifuged for 10 min at 3000 RPM and supernatant replaced by 2.5 % glutar-aldehyde, which served as a fixative. One drop of the well dispersed bacterial sample was placed for one hour on a glass slide, pre-coated with (poly) L-lysine, which polymerizes the sample. The sample drop was then washed out with milli-Q water and the samples were then dehydrated in alcohol. The alcohol dehydration was done by soaking the glass slide for 10 min periods in increasing concentrations of ethanol: 30, 50, 70, 80, 90, 95

and 100 %. The samples were then dried in air and stained by Au-Pd sputter coating before the SEM images were taken. The images of the emulsion samples were prepared by deposition of a drop of emulsion solution on the glass slide. Sample was then dried on air and sputter coated with Au/Pd.

### Transmission Electron Microscopy

TEM was performed on a JEOL microscope model JEM 2000.FX. The principles of operation of an electron microscope are shown schematically in Figure Appendix 1. This technique relies on the transmission of electrons through the sample. Therefore, typically only very thin samples ( $< 10 \mu\text{m}$ ) can be visualized in detail.<sup>3</sup>

Electrons, produced from a heated tungsten hairpin filament or a pointed lanthanum hexaboride rod, provide the illumination of the microscope; the electrons are then accelerated in the illumination system into a narrow beam by an electron gun under high vacuum. The resolution of the TEM depends on the wavelength, which is a function of the accelerating voltage; the higher the voltage, the higher the resolution.<sup>3</sup> The electron beam passes through a series of condenser lenses, which serve to gather the electrons, control the intensity of the beam onto the specimen and determine the illuminated specimen area. The beam will then strike the specimen, where some of the electrons are absorbed or scattered, and then pass through the system of lenses.<sup>3,4</sup>

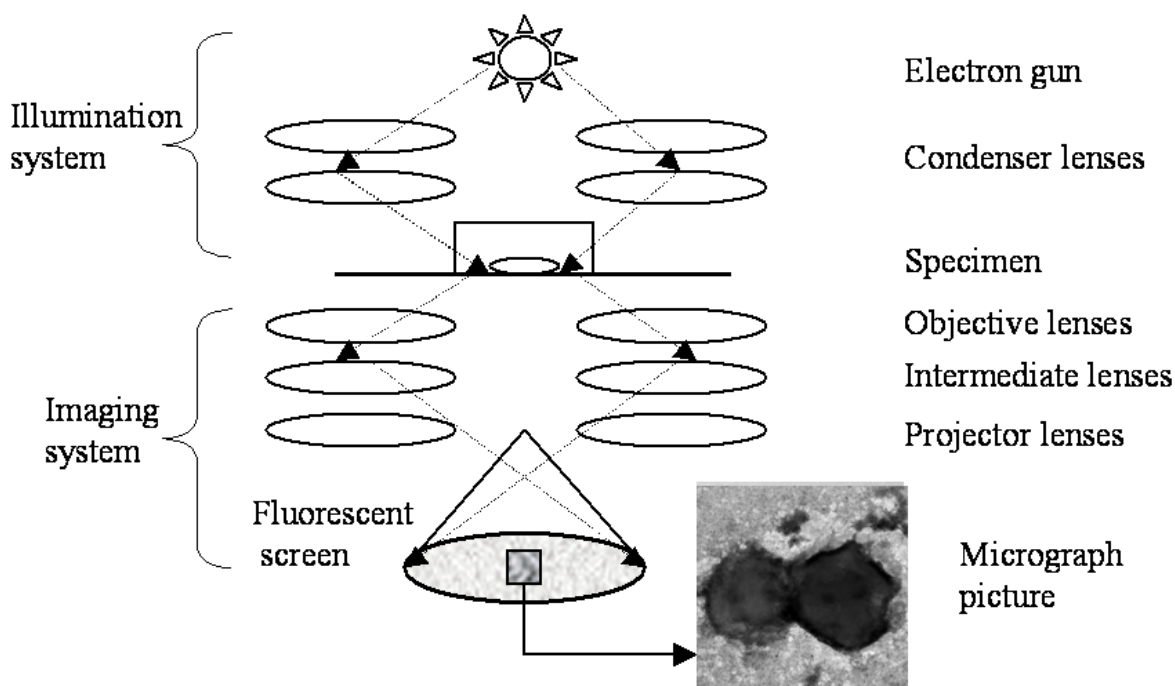


**Figure Appendix 1.** Schematic representation of transmission electron microscope technique.

The imaging system consists of the objective, intermediate and projector lenses and fluorescent screen.<sup>(73)</sup> The image of the specimen is created and magnified with objective lenses, and further magnified with intermediate and projector lenses. The final image is viewed on a fluorescent screen in green color, for which the human eye has the maximum sensitivity.<sup>(73)</sup>

The image is recorded using a charge-coupled device camera and the morphology, size and size distribution of the aggregates is determined. The sizes of aggregates were measured using SigmaScan Pro 5 software.

### UV-vis Spectroscopy

The concentration of the biocide in the loaded micelles was evaluated using UV-vis spectroscopy. All UV measurements were performed on a Varian UV-vis spectrophotometer

(model Cary 300 Bio). First, a calibration curve of the absorbance vs. concentration for various known biocide concentrations in dioxane/water 95/5 % (w/w) was constructed at three various wavelengths which show peaks in the spectrum at 300.2, 290.0 and 280.4 nm; absorbance increases linearly with the concentration. Samples of unknown biocide concentrations were also dissolved in dioxane/water ratio at 95/5 % (w/w), (in such mixture the micelles are completely dissolved) and then compared to the calibration curves. An example of a calibration curve for TCMTB biocide is given in Figure Appendix 2.

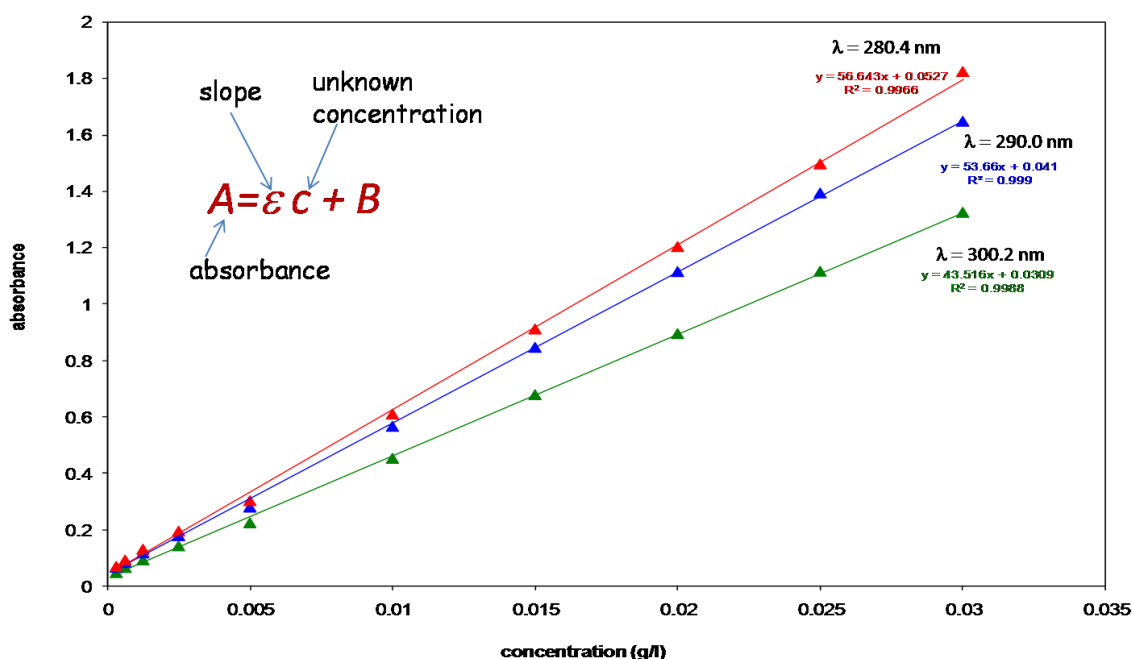


**Figure Appendix 2.** Calibration curves for TCMTB biocide in dioxane/water at 95/5 % (w/w).

The efficiency of loaded micelles on bacteria deactivation was tested by UV-vis measurements, which were performed on a Varian UV-vis spectrophotometer, model Cary 300 Bio. The turbidity at a wavelength of 600 nm was measured for each sample right after addition of the growth medium and at various times to see if the absorbance value of the sample increases with time. To express the efficiency of the biocide in micelles on bacteria deactivation, the



absorbance was plotted as relative absorbance vs. time. Relative absorbance is the absorbance taken at a given time divided by the absorbance at time 0 of the experiment (when the growth medium is added). An increase of the absorbance with time indicates growth of the number of bacteria and demonstrates that the bacteria are not deactivated; if the absorbance does not change with time or decrease, the bacteria are considered to be deactivated.

References for Appendix:

- (1) Zhang, L., Eisenberg, A.; *Polym. Adv. Technol.*, **1998**, 9, 677.
- (2) Israelachvili, J. N., *Intermolecular and Surface Forces*, 2<sup>nd</sup> ed., Academic Press, London, **1992**.
- (3) Evans, R.J., *Encyclopedia of Physical Science and Technology*, 1<sup>st</sup> ed., Meyers, R.A., Ed.; Academic Press Inc., **1987**, vol. 8
- (4) Reimer, L., *Transmission Electron Microscopy: Physics of Image Formation and Microanalysis*, 4<sup>th</sup> ed., Springer – Verlag, Berlin, **1997**

## Appendix to Chapter 3:

---

### 1.1. Micelle Preparation

The PS<sub>197</sub>-b-PAA<sub>47</sub> block copolymer was dissolved in dioxane, a good solvent for both blocks. The initial block copolymer concentration was 1% (w/w). The sample was then stirred overnight to ensure complete dissolution of the polymer. To induce self-assembly of the chains into micelles, milli-Q water was added drop-wise at a rate of 0.2 % (w/w)/min. Water addition was continued until a final water concentration of 50 % (w/w) was reached. The water concentration determines the resulting morphology.<sup>1</sup> Only micelles are formed under these conditions, no other morphology is observed. The solution was quenched into a large excess of water in order to freeze the aggregate morphology, and dialyzed for a period of three days to remove the organic solvent (dioxane). The final concentration of the micelle in solution was 1 g/L.

### 1.2. Characterization of the Micelles

To characterize the micelles transmission electron microscopy (TEM) and dynamic light scattering (DLS) were employed. The micelles are composed of a hydrophobic polystyrene core and a hydrophilic poly(acrylic acid) corona.

#### *1.2.1. Transmission Electron Microscopy (TEM)*

TEM was one of the techniques used to characterize the micelles. Samples for the TEM studies were prepared from the micellar solutions by applying one drop of the solution to a copper grid,

which had been pre-coated with 0.5 % formvar solution and a layer of carbon. The drop was allowed to evaporate over night. TEM (without staining) was performed on a JEOL microscope model JEM 2000FX. The average size of the micelles was evaluated from TEM images using the Sigma Scan image analysis. The representative image of PS<sub>197</sub>-b-PAA<sub>47</sub> micelles with schematic representation of micellar structure is shown in Figure 1.

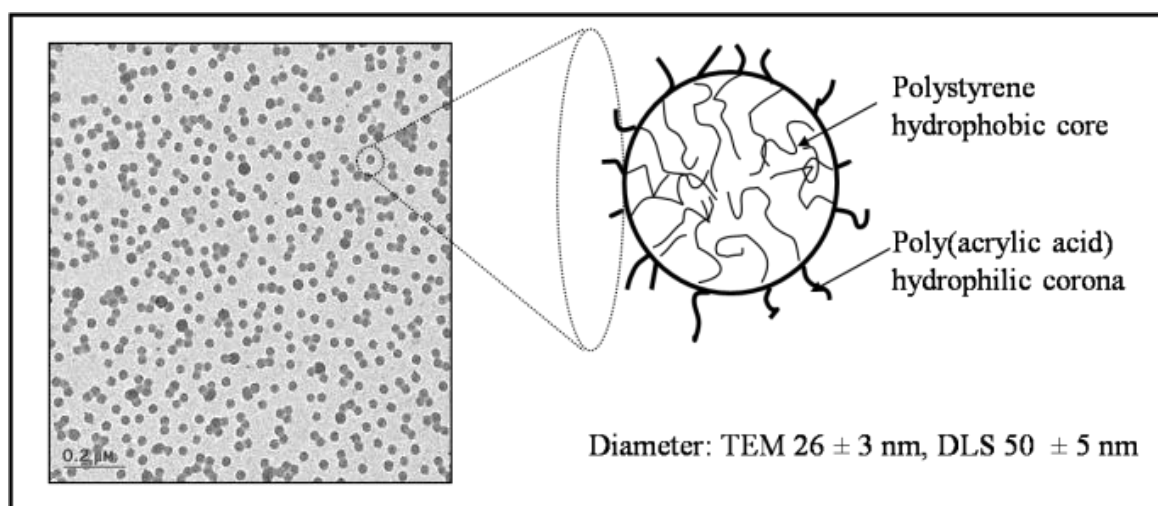


**Figure 1.** TEM image of PS<sub>197</sub>-b-PAA<sub>47</sub> micelles with schematic representation of micellar structure.<sup>2</sup>

#### 1.2.1.1. Microtomy of the Bacteria Samples - TEM

TEM was also used in the present study to find out what effect the micelles have on the bacteria. Samples for the TEM studies were prepared from the micellar solutions by exposing the bacteria to the loaded micelles. The bacteria solution was then centrifuged and the supernatant was replaced by glutaraldehyde. After re-dispersion of the bacteria in the fixative and letting the sample stay in the fridge for few days, the sample was centrifuged again and bacteria were washed 3 times with washing buffer for a total time of 30 min. Next, the samples

were post-fixed with 1% aqueous OsO<sub>4</sub> and 1.5 % aqueous potassium ferrocyanide for 2 hrs. The bacteria samples were then washed 3 times again with washing buffer for a total time of 15 min. Afterwards, the samples were dehydrated with acetone in increasing concentrations: 30, 50, 70, 80, 90, 3 times 100% each at 15 min. The samples were infiltrated with epon/acetone 1:1 overnight, 2:1 all day, 3:1 overnight and with pure epon next day for 4 hrs. The bacteria samples were then polymerized at 58 °C for 48 hrs, trimmed and cut into 90-100 nm thick sections and placed on a 200 mesh copper grid. Then the sections were stained first with uranyl acetate for 6 min and then with Reynold's lead for 5 min.

#### *1.2.2. Dynamic Light Scattering (DLS)*

In addition to electron microscopy, dynamic light scattering was used to determine the diameter of the micelles. The light scattering experiments were performed on a Brookhaven light scattering instrument with a BI9000 AT digital correlator. The data were collected by monitoring the scattered light intensity at a 90° scattering angle at 25 °C. The micelle solutions were prepared as described in section 1.1. above.

#### *1.3. Micelle Loading*

After completion of the dialysis of the micelle solution, the micelles were loaded with TCMTB or TCN biocide. Prior to loading, the biocide, in a vial, was dissolved in 2 mL acetone to a concentration of 5 mg/mL. Acetone was allowed to evaporate over night from the vial, leaving a thin film of the biocide inside. The micelle solutions (10 mg of polymer in 10 mL) was afterwards transferred to the vials containing the biocide film and vigorously stirred for a period

of 1 hour to achieve maximum loading. The excess of biocide was removed by a 0.45  $\mu\text{m}$  filter. The detailed description of the micelle loading can be found in a previous publication.<sup>2</sup>

It should be noted that the loading technique discussed above was used for both types of block copolymer micelles (PS-*b*-PAA and PS-*b*-P4VP) and both types of biocide (TCMTB and TCN).

#### *1.3.1. Concentration of the Biocide in Loaded Micelles*

The concentration of the TCMTB or TCN biocide in the loaded PS-*b*-PAA or PS-*b*-P4VP micelles was evaluated using UV-vis spectroscopy. UV-vis measurements were performed on a Varian UV-vis spectrophotometer, model Cary 300 Bio. First, calibration curves of the absorbance vs. concentration for various known biocide concentrations in dioxane/water 95/5 % (w/w) were constructed: in case of the TCMTB biocide, three calibration curves were constructed at three various wavelengths at which the biocide shows peaks in the spectrum - 300.2, 290.0 and 280.4 nm; in case of the TCN biocide, one calibration curve was constructed at one wavelength at which the biocide shows the maximum in the spectrum - at 281.4 nm. For both biocides, the absorbance was found to increase linearly with the concentration in agreement with the Lambert-Beer law. Samples of unknown biocide concentrations in micelles of PS-*b*-PAA and PS-*b*-P4VP were also dissolved in dioxane/water ratio at 95/5 % (w/w), (in such mixture the micelles are completely dissolved) and then compared to the calibration curves of the given biocide. In the case of TCMTB, unknown sample concentrations were obtained by comparing its absorbance value with three calibration curve of various wavelengths, and the average value was then calculated from the three resulting values of the biocide concentration.

It should be noted that UV-vis spectra of block copolymer micelles without biocide show a low PS peak at a wavelengths shorter than those used for the preparation of the calibration curves; this peak does not interfere with the biocide spectra.

#### 1.4. Bacteria Deactivation

In most of the bacteria experiments of this study, the bacteria were exposed to the micelle solution for various periods of time; subsequently, the samples were centrifuged and supernatant was replaced by growth medium (Miller-Hinton broth). The bacteria were then re-dispersed and incubated at 37 °C while shaking in the incubator for various periods of time; finally the samples were evaluated for the bacteria deactivation. Details of each experiment are given in the Results section.

To evaluate the deactivation of bacteria by loaded micelles, UV-vis spectroscopy, scanning electron microscopy, transmission electron microscopy (microtomy) and zeta potential measurements were employed.

##### *1.4.1. UV-vis Spectroscopy – Absorbance*

Several techniques to measure concentration of bacteria in solution, such a plating or measurement of optical density (absorbance), can be used to determine efficiency of loaded micelles on bacteria deactivation. The technique chosen for this study is optical density since it is fast.

The efficiency of loaded micelles on bacteria deactivation was tested by UV-vis measurements, which were performed on a Varian UV-vis spectrophotometer, model Cary 300 Bio. The turbidity at a wavelength of 600 nm was measured for each sample right after addition

of the growth medium and at various times (details of each experiment are given in Results section) to see if the absorbance value of the sample increases with time. To express the efficiency of the biocide in micelles on bacteria deactivation, the absorbance was plotted as relative absorbance vs. time. Relative absorbance is the absorbance taken at a given time divided by the absorbance at time 0 of the experiment (when the growth medium is added). An increase of the absorbance with time indicates growth of the number of bacteria and demonstrates that the bacteria are not deactivated; if the absorbance does not change with time or decrease, the bacteria are considered to be deactivated.

#### *1.4.2. Scanning Electron Microscopy*

Scanning Electron Microscopy (SEM) was employed to explore visually the effect of the biocide on the bacteria. SEM was performed on a Hitachi instrument model S- 4700. The bacteria were exposed to the micelles for a certain period of time (details given for each experiment in the Results section), the sample was then centrifuged for 10 min at 3000 RPM and supernatant replaced by 2.5 % glutar-aldehyde, which served as a fixative. One drop of the well dispersed bacterial sample was placed for one hour on a glass slide, pre-coated with (poly) L-lysine, which polymerizes the sample. The sample drop was then washed out with milli-Q water and the samples were then dehydrated in alcohol. The alcohol dehydration was done by soaking the glass slide for 10 min periods in increasing concentrations of ethanol: 30, 50, 70, 80, 90, 95 and 100 %. The samples were then dried in air and stained by Au-Pd sputter coating before the SEM images were taken.

#### 1.4.3. Electrophoretic Mobility Measurements - Zeta Potential

The Rank Brothers Micro-Electrophoresis Apparatus MKII<sup>4</sup> was used to measure the electric charge and an electrophoretic mobility (EM) of the live and dead bacteria in the presence and the absence of biocide. The rectangular cell and platinum black electrodes were used. The effective length ( $l$ ) of the cell was calculated from the measurements of cross-section area of the cell and the conductivity in the 7.5 mM NaCl solution. The effect of suspended particles on the cell constant has been ignored. From velocity ( $v$ ) of bacteria measured on a calibrated monitor screen in an applied electric field, one can calculate the electrophoretic mobility ( $EM$ ). EM is defined as the velocity of the moving particle (bacteria) divided by the strength of the electric field (ca. 50 V).

For each experiment the velocity of 30 bacteria was measured at stationary plane and averaged for EM calculations. From the size of the bacteria (TEM) and an estimation of the ionic strength of the buffer used as the medium, the Smoluchowski equation was used to convert EM into the zeta potential ( $\zeta$ ) of the bacteria samples.<sup>5</sup> The Smoluchowski equation is defined as ratio of viscosity of the medium multiplied by the EM and the permittivity of medium.

The procedure to prepare samples of dead bacteria to measure the zeta potential was the following: The bacteria were incubated in the growth medium to an absorbance of 1 at 600 nm. The bacterial samples were then centrifuged at 3000 RPM for 10 minutes, the supernatant was exchanged for 2% glutaraldehyde (the fixative) to kill the bacteria, and shaken for 1 hour. Afterwards, the bacteria samples were centrifuged again and the supernatant was exchanged for milli-Q water to remove the glutaraldehyde. This process was repeated two times to make sure the samples are free of glutaraldehyde and growth medium. Then 0.1 mL of sample (TCMTB loaded micelles, empty polymer micelles or water for the control) was added to the bacteria,



along with 9.9 mL of 7.5 mM NaCl in milli-Q water. After one hour, the zeta potential of each sample was measured. The final concentration in the sample was 0.5 g/L of polymer and 0.167 g/L of TCMTB. The pH of all three samples was 7.

#### 1.4.3.1. Dead vs. Live Bacteria

The procedure to prepare samples to measure zeta potential of live bacteria (section 3.4.2.) was the following: The bacteria were grown in the growth medium to an absorbance of 1 at 600 nm. The bacteria samples were then centrifuged at 3000 RPM and the supernatant was exchanged for milli-Q water to remove the growth medium. This process was repeated two times to make sure the samples were free of growth medium. Then 0.1 mL of sample (TCMTB loaded micelles, empty polymer micelles or water for the control) was added to the bacteria along with 9.9 mL of 7.5 mM NaCl in milli-Q water. After one hour, the zeta potential of each sample was measured. The final concentration in the sample was 0.5 g/L of polymer and 0.167 g/L of TCMTB. The pH of all three samples was 7.

#### 1.5. Bacteria Calibration Curve

To know how many bacteria/mL are present in the bacterial solution of a certain absorbance, a calibration curve for the number of *E. coli* bacteria as a function of absorbance was made. Figure 2 shows such a calibration curve, which was constructed by counting the bacteria of bacterial solutions of given absorbance using a hemocytometer. The hemocytometer is shown schematically in the inset. Details of a hemocytometer can be found elsewhere.<sup>6,7</sup> *E. coli* bacteria were grown in an incubator at 37°C in the growth medium until each of the three bacterial samples reached a given absorbance (0.333; 0.633; and 0.935). Each sample was then diluted

two times by the fixative (glutaraldehyde) to prevent bacteria from continuing to grow. Each sample had to be diluted with water an additional two times to decrease the number of bacteria to a level at which they were easy to count. 15  $\mu\text{L}$  of each sample was individually placed into the hemocytometer and bacteria were counted at a magnification of 40x. Next, the final number of bacteria/mL at each absorbance was calculated, taking in account all the dilutions.

### 1.5.1. Calibration Curve of Absorbance vs. Bacteria Concentration in Solution

The concentration of the bacteria in solution is expressed by absorbance at the wavelength of 600 nm. To know how many bacteria/mL are present in the bacterial solution of a certain absorbance, the calibration curve for *E. coli* was constructed according to the procedure described in section 2.7. The number of bacteria in solution as a function of absorbance at 600 nm is shown in Figure 2. As seen in that Figure, the absorbance increases linearly with an increase in the number of bacteria/mL as the bacteria multiply.

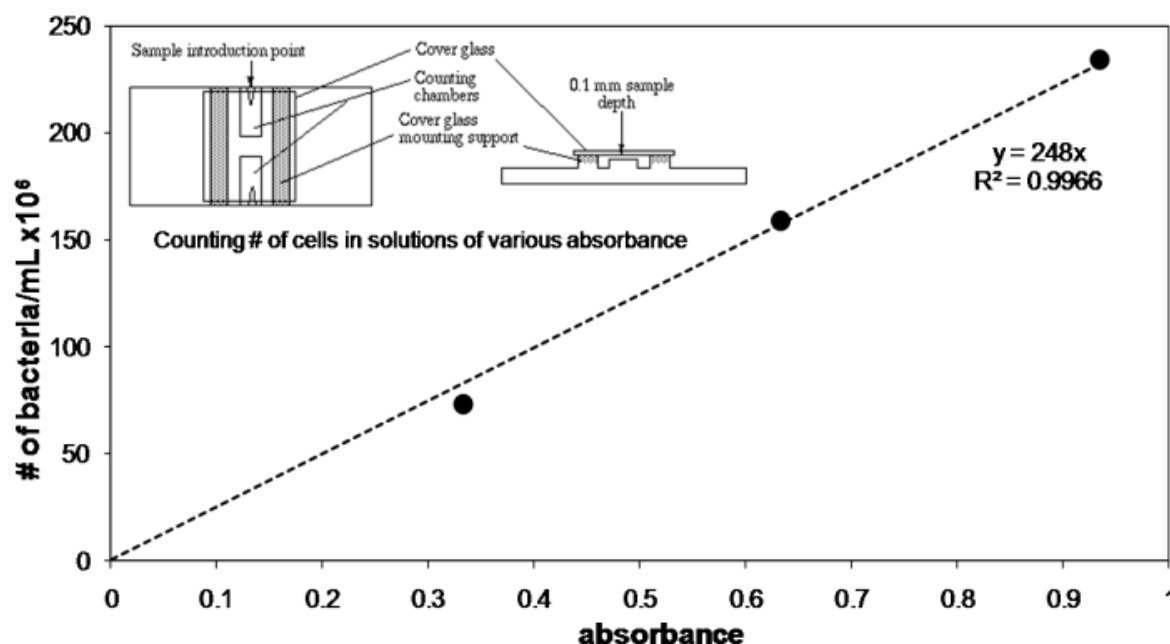


**Figure 2:** Number of *E. coli* in solution as a function of absorbance at 600 nm.

Reference list

- (1) Nagarajan, R.; Barry, M., Ruckenstein, E., *Langmuir*, **1986**, 2, 210.
- (2) Vyhnalkova, R., Eisenberg, A., van de Ven, T.G.M., *J. Phys. Chem. B*, **2008**, 112, 8477.
- (3) Eloff, J.N., *Planta-Med*, **1998**, 64 (8), 711-713.
- (4) [www. rankbrothers.co.uk](http://www.rankbrothers.co.uk)
- (5) Hunter, R.J., *Introduction to Modern Colloid Science*, Oxford University Press, New York, **1993**.
- (6) [www.cascadebio.com/uploads/File/pdf/hemat.pdf](http://www.cascadebio.com/uploads/File/pdf/hemat.pdf)
- (7) [www.animal.ufl.edu/hansen/Protocols/hemacytometer.htm](http://www.animal.ufl.edu/hansen/Protocols/hemacytometer.htm)

## Appendix to Chapter 4:

---

Grade	Pore size ( $\mu\text{m}$ )	Thickness
1	11	Fine
2	8	Medium
3	6	Thick

**Table 1.** An overview of various grades of Whatman filter papers and its corresponding pore size.<sup>16</sup>

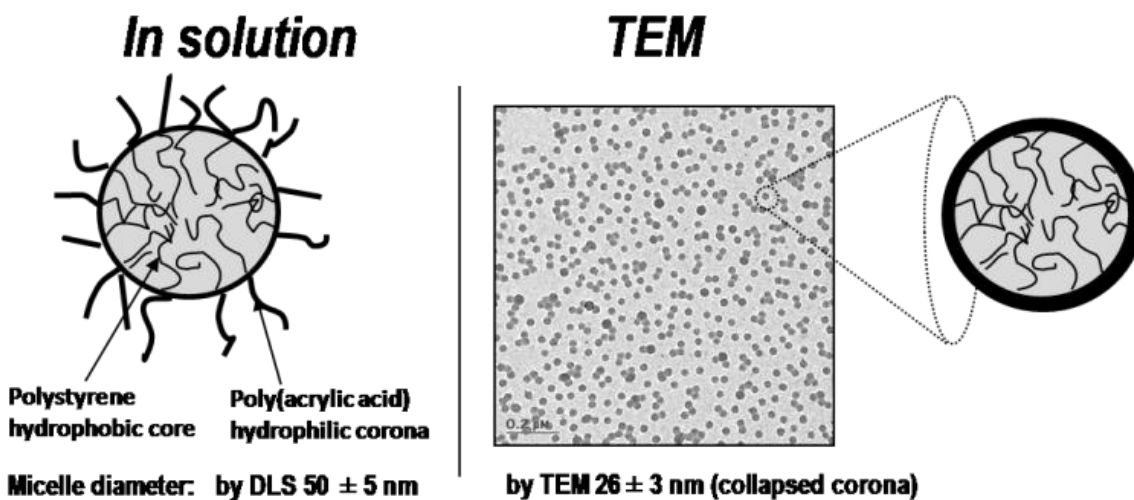


**Figure 1.** Schematic representation of micelles in solution and on TEM grid and TEM image.

### 1. Experimental Techniques

#### 1.1. Transmission Electron Microscopy

Samples for the TEM studies were prepared from the micellar solutions by applying one drop of the solution to a copper grid, which had been pre-coated with 0.5 % formvar solution and a

layer of carbon. The drop was allowed to evaporate over night. TEM (without using any staining) was performed on a JEOL microscope model JEM 2000FX. The average size of the micelles was evaluated from TEM images using the Sigma Scan image analysis.

### *1.2. Scanning Electron Microscopy*

Scanning Electron Microscopy (SEM) was employed to explore visually the effect of the biocide on the bacteria. SEM was performed on a Hitachi instrument model S- 4700. The bacteria were exposed to the micelles for a certain period of time, the sample was then centrifuged for 10 min at 3000 RPM and supernatant replaced by 2.5 % glutar-aldehyde, which served as a fixative. One drop of the well dispersed bacterial sample was placed for one hour on a glass slide, pre-coated with (poly) L-lysine, which polymerizes the sample. The sample drop was then washed out with milli-Q water and the samples were then dehydrated in alcohol. The alcohol dehydration was done by soaking the glass slide for 10 min periods in increasing concentrations of ethanol: 30, 50, 70, 80, 90, 95 and 100 %. The samples were then dried in air and stained by Au-Pd sputter coating before the SEM images were taken.

### *1.3. Dynamic Light Scattering*

Dynamic light scattering was used in addition to electron microscopy to determine the diameter of the micelles. The light scattering experiments were performed on a Brookhaven light scattering instrument with a BI9000 AT digital correlator. The data were collected by monitoring the scattered light intensity at a 90° scattering angle at 25 °C.

#### 1.4. UV-vis Spectroscopy

As described in the previous paper,<sup>9</sup> the concentration of triclosan biocide in the loaded micelles was evaluated using UV-vis spectroscopy. All UV measurements were performed on a Varian UV-vis spectrophotometer (model Cary 300 Bio). First, a calibration curve of the absorbance vs. concentration for various known biocide concentrations in dioxane/water 95/5 % (w/w) was constructed at wavelengths which shows peak in the spectrum at 281.4 nm; absorbance increases linearly with the concentration. Samples of unknown biocide concentrations were also dissolved in dioxane/water ratio at 95/5 % (w/w), (in such mixture the micelles are completely dissolved) and then compared to the calibration curve. Then, the concentration of triclosan in the unknown sample was calculated based on the height of the peak at 281.4 nm wavelength from the calibration curve.<sup>9</sup> The loading of triclosan into PS<sub>197</sub>-b-PAA<sub>47</sub> typically reaches values around 20 % (w/w).<sup>9</sup>

It should be noted that UV-vis spectra of PS<sub>197</sub>-b-PAA<sub>47</sub> micelles without biocide show a low PS peak at wavelengths lower than those used for the preparation of the calibration curves; this peak does not interfere with triclosan biocide spectra.

#### 2. Calibration Curve of Absorbance vs. Bacteria Concentration in Solution

The concentration of the bacteria in solution is expressed by absorbance at the wavelength of 600 nm. To know how many bacteria/mL are present in the bacterial solution of a certain absorbance, the calibration curve for *E. coli* was constructed using hemocytometer by counting the bacteria of bacterial solutions of given absorbance. *E. coli* bacteria were grown in an incubator at 37°C in the growth medium until each of the three bacterial samples reached a given absorbance (0.333; 0.633; and 0.935). Each sample was then diluted two times by the fixative

(glutaraldehyde) to prevent bacteria from continuing to grow. Each sample had to be diluted with water an additional two times to decrease the number of bacteria to a level at which they were easy to count. 15  $\mu\text{L}$  of each sample was individually placed into the hemocytometer and bacteria were counted at a magnification of 40x. Next, the final number of bacteria/mL at each absorbance was calculated, taking in account all the dilutions.

The number of bacteria in solution as a function of absorbance at 600 nm is shown in Figure 2. As seen in that Figure, the absorbance increases linearly with an increase in the number of bacteria/mL as the bacteria multiply. The hemocytometer is shown schematically in the inset.

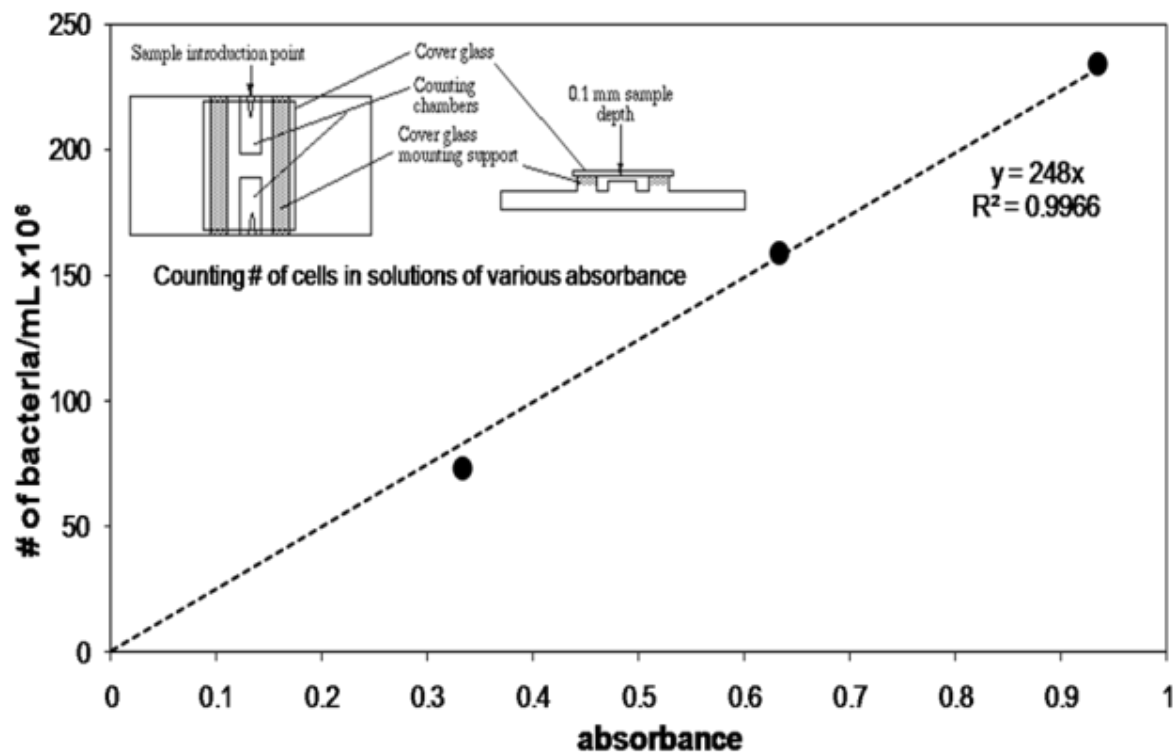


**Figure 2:** Number of *E. coli* in solution as a function of absorbance at 600 nm.

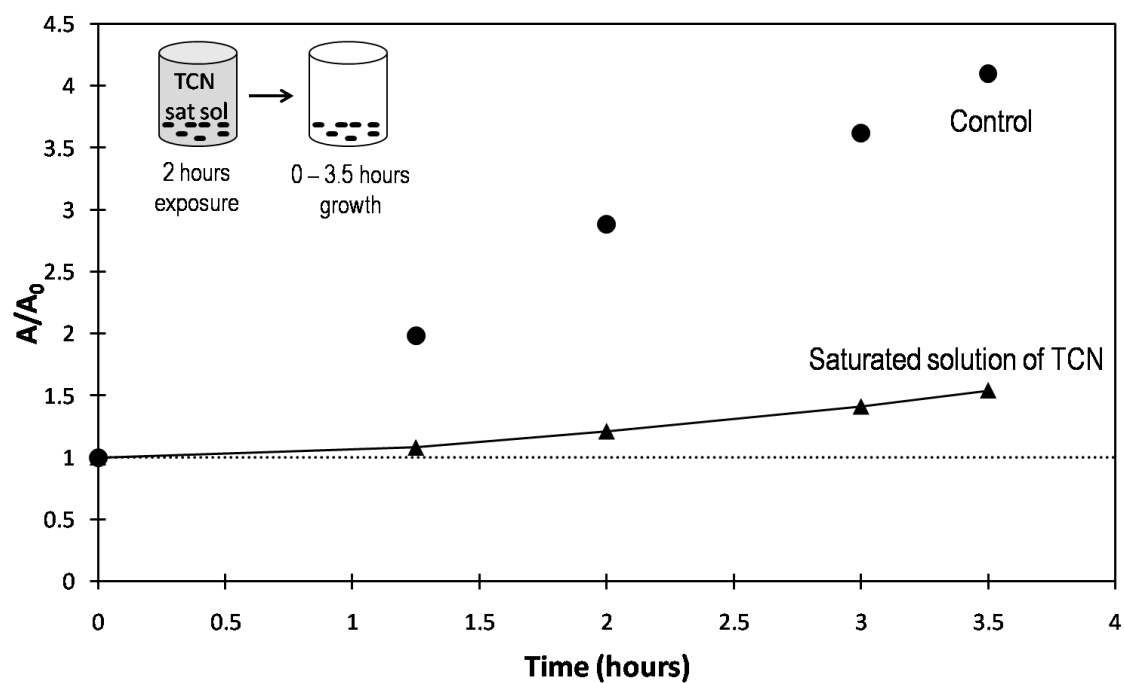


**Figure 3.** Deactivation of *E. coli* ATCC11229 by exposure of the bacteria to a saturated solution of Triclosan for 2 hours, followed by incubation of the bacteria for various time periods.

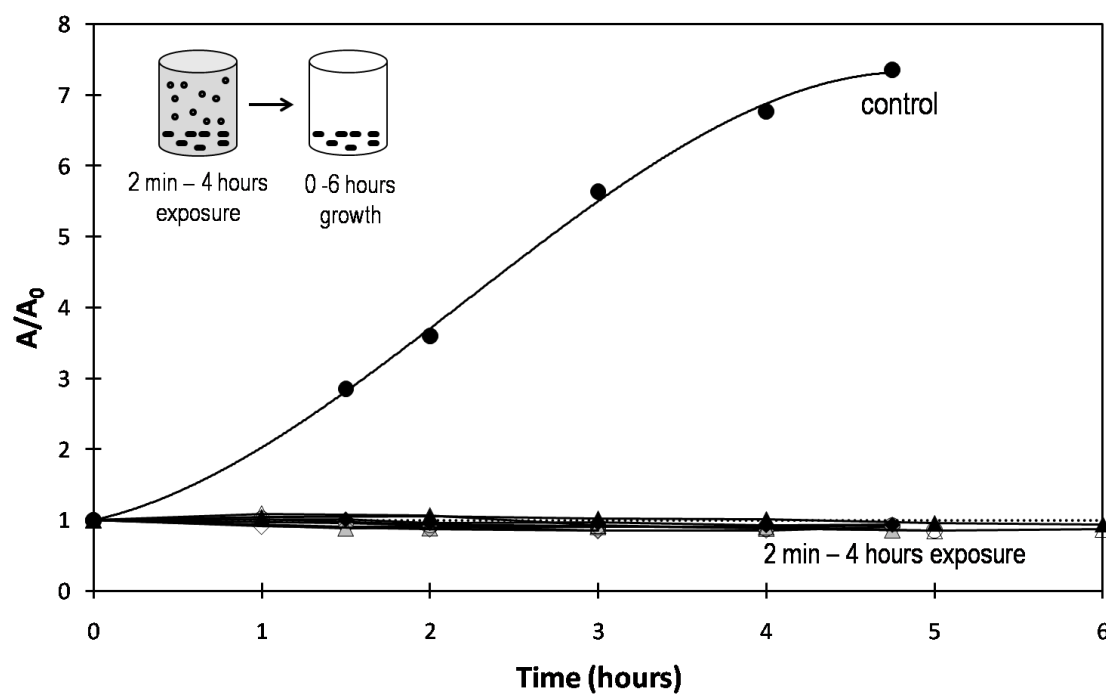


**Figure 4.** Killing time of *E. coli* ATCC11229 by Triclosan loaded micelles of PS<sub>197</sub>-b-PAA<sub>47</sub> as an effect of various exposure times of bacteria to loaded micelles prior to re-growth.



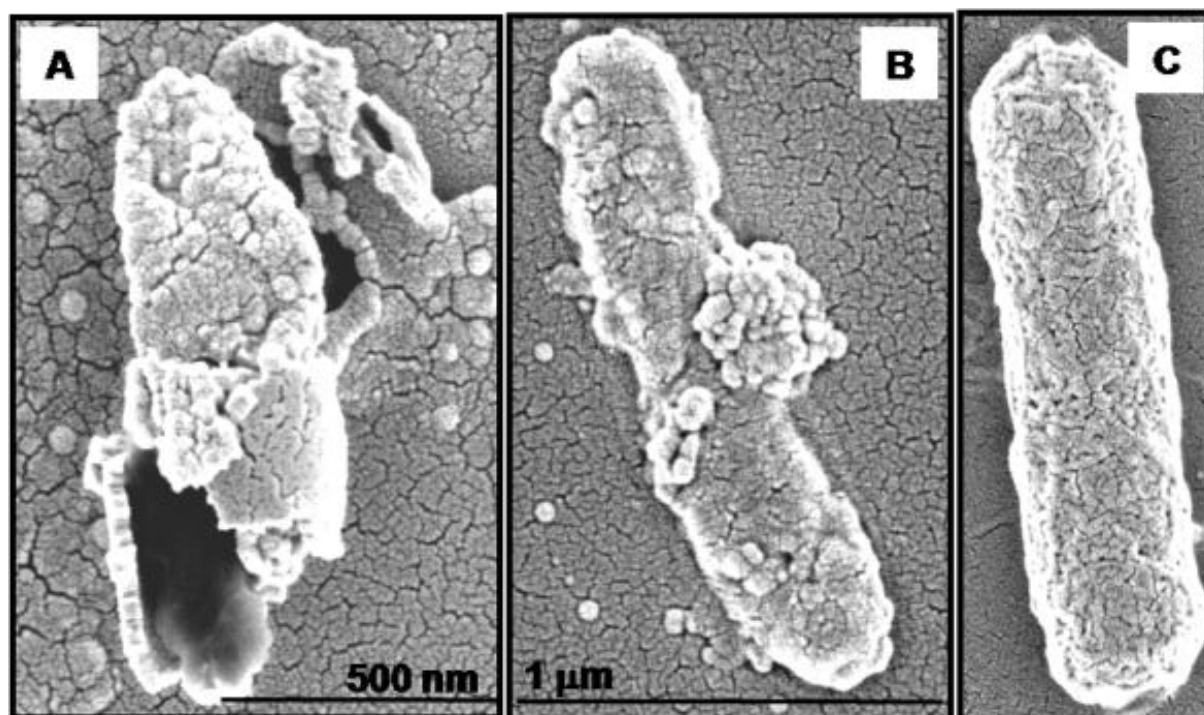


**Figure 5.** SEM images of *E. coli* bacteria killed by micelles of PS<sub>197</sub>-b-PAA<sub>47</sub> loaded with Triclosan (images A and B); image C is bacteria in absence of Triclosan loaded micelles (control sample). (The image scale for image C is the same as in case of image B)

Material	Supplier	Laboratory Cost (\$)	Large scale cost (\$)	Cost / g or unit (\$)	Amount needed/sheet	Laboratory scale cost (\$)	Est. large scale cost (\$)
Filter paper – grade 3	Whatman	14.76 / 100 sheets	1 / kg	0.1476	1 sheet	0.1476	0.0015
PS <sub>275</sub> -PAA <sub>47</sub> Polymer	Polymer Source	250 / g	20 / kg	0.02	0.022 g	5.5	0.0004
Triclosan	Sigma	90 / 25 g	15 / kg	3.6	4.4 x 10 <sup>-3</sup> g	0.0158	0.000066
c-PAM	Sigma	129 / 500 g	7 / kg	0.258	1.1406 x 10 <sup>-3</sup> g	0.000294	0.000008
<b>Total cost</b>						<b>5.66</b>	<b>0.002 = 0.2 ¢</b>

**Table 2.** Estimate of Material Cost per One Filer Paper

## Appendix to Chapter 5:

---

### *1.1. Dynamic Light Scattering*

Dynamic light scattering was used in addition to electron microscopy to determine the average diameter of the emulsion droplets. The light scattering experiments were performed on a Brookhaven light scattering instrument with a BI9000 AT digital correlator. The data were collected by monitoring the scattered light intensity at a 90° scattering angle at 25 °C.

### *1.2. Transmission Electron Microscopy*

Samples for the TEM studies were prepared from the micellar (in case of PCL-b-PAA micelles used as stabilizing agent to verify the initial size of micelles) and emulsion (in case of PEI and PCL-b-PAA micelles used as stabilizing agent) solutions by applying one drop of the solution to a copper grid. The copper grid had been pre-coated with 0.5 % formvar solution and a layer of carbon. The drop of the sample was allowed to evaporate for few minutes from the grid, the excess of the sample was removed by drying the rest of the drop by filter paper by capillary forces. Sample was afterwards stained with 1% phosphotungstic acid in case of PCL-b-PAA containing sample. Sample containing PEI was not stained. TEM was then performed on a JEOL microscope model JEM 2000FX. The average size of the micelles was evaluated from TEM images using the Sigma Scan image analysis.

### *1.3. Scanning Electron Microscopy*

Scanning Electron Microscopy (SEM) was employed to explore visually the shape and the size of emulsion droplets and the effect of the biocide incorporated in emulsion on the bacteria in case of TCMTB emulsions stabilized by PEI and PCL-b-PAA micelles. In addition, the emulsion droplets were studied after biocide release. SEM was performed on a Hitachi instrument model S-4700. In case of bacteria deactivation experiments by emulsions, the bacteria were exposed to the emulsions for a certain period of time, the sample was then centrifuged for 10 min at 3000 RPM and supernatant replaced by 2.5 % glutar-aldehyde, which served as a fixative. One drop of the well dispersed bacterial sample was placed for one hour on a glass slide, pre-coated with (poly) L-lysine, which polymerizes the sample. The sample drop was then washed out with milli-Q water and the samples were then dehydrated in alcohol. The alcohol dehydration was done by soaking the glass slide for 10 min periods in increasing concentrations of ethanol: 30, 50, 70, 80, 90, 95 and 100 %. The samples were then dried in air and stained by Au-Pd sputter coating before the SEM images were taken. In case of evaluation of the size and the shape of the emulsion droplets when prepared and after release of biocide, the drop of the sample was placed on the glass slide, let evaporate on air over night followed by Au-Pd sputter coating before the SEM images were taken.

### *1.4. Characterization of the micelles*

Transmission electron microscopy (TEM) and dynamic light scattering (DLS) were employed to characterize the micelles. The micelles consist of a hydrophobic poly(caprolactone) core and a hydrophilic poly(acrylic acid) corona, as shown schematically in Figure 1.

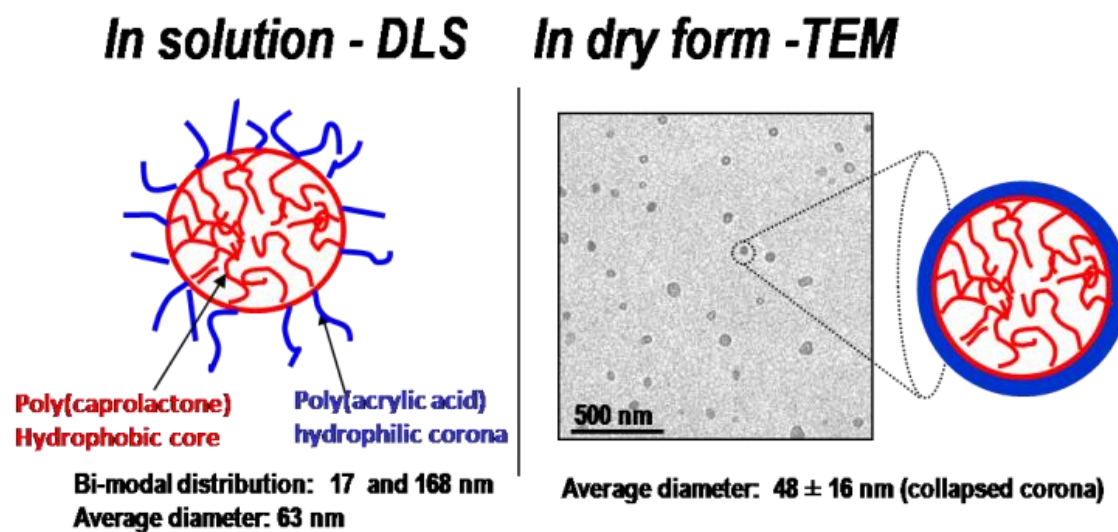


**Figure 1.** Schematic representation of PCL<sub>33</sub>-b-PAA<sub>33</sub> micelles in solution and in a dry form on TEM grid and its supporting TEM image.

### 1.5. Bacteria Deactivation - UV-vis Spectroscopy

Several techniques, such as plating or measurement of optical density (absorbance), can be used to evaluate bacteria deactivation in solution. The technique chosen for this study is an optical density, primarily because of its speed.

To evaluate deactivation the bacteria were exposed to emulsions of various concentrations, or to the control samples solutions which not contain any biocide (for comparison). Biocide emulsions containing as stabilizing agents PEI or PCL-b-PAA micelles of various concentrations, or stabilizing agent solutions without biocide, were mixed with constant volumes of growth media and *E. coli* bacteria. The total volume was kept the same for all the samples. The samples were then incubated at 37 °C for 6 hours while shaking; the absorbance of each sample was monitored with time using UV-vis spectroscopy at 600 nm. To assure the freshness of the *E. coli* sample, the bacteria were incubated over night, and the next day diluted with growth medium to a concentration corresponding to an absorbance of 0.1, incubated again to the

concentration of absorbance of 1, and finally diluted to an initial absorbance of 0.1. The concentration of bacteria at an absorbance of 0.1 corresponds to a bacteria concentration of  $25 \times 10^6$  bacteria/mL (as determined from the bacteria calibration curve). The efficiency of the emulsions in bacteria deactivation was tested by UV-vis measurements using a Varian UV-vis spectrophotometer, model Cary 300 Bio. The turbidity at a wavelength of 600 nm was followed for each sample as a function of time to see if the absorbance value of the sample increases. To express the efficiency of the emulsion, the absorbance was plotted as relative absorbance vs. time. The relative absorbance is the absorbance taken at a given time divided by the absorbance at time 0 of the experiment (at the point of addition of the growth medium and the *E. coli* to the emulsion or to the control sample containing only the stabilizing agent). An increase in the relative absorbance of the sample with time indicates growth of the number of bacteria and demonstrates that the bacteria are not deactivated in that run; if the absorbance value decreases or does not change with time, the bacteria are considered to be deactivated.

In addition to UV-vis spectroscopy, scanning electron microscopy and transmission electron microscopy were also employed to evaluate visually the deactivation of bacteria by the emulsions.

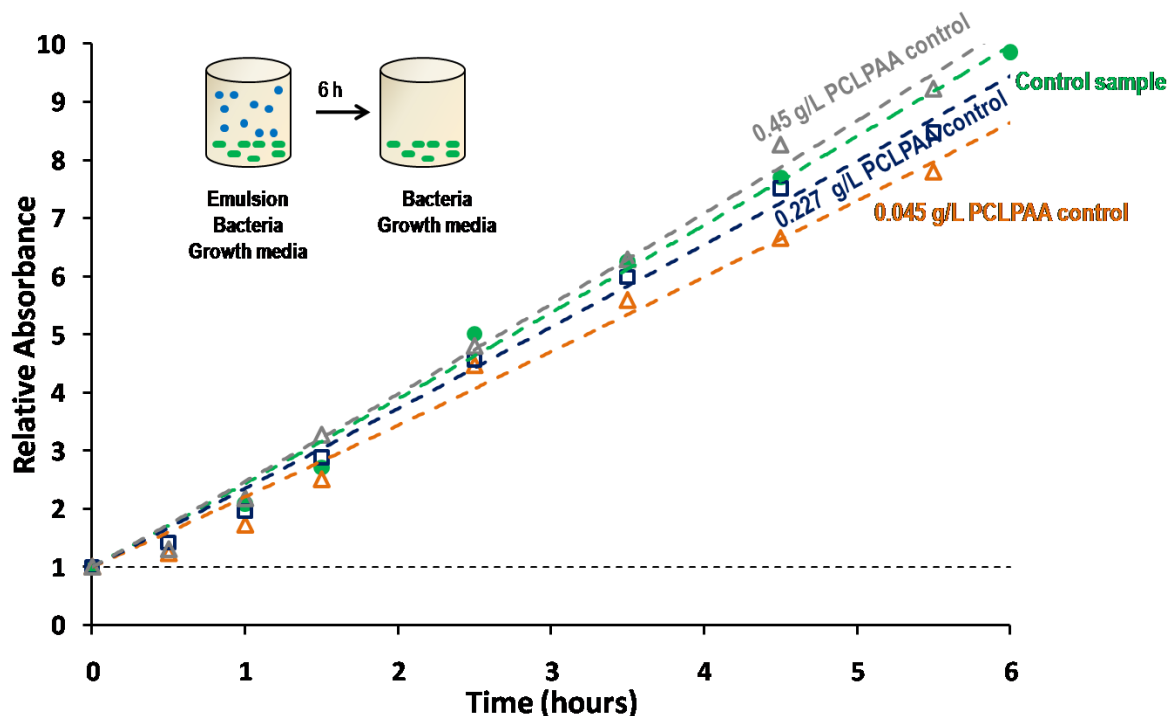


**Figure 2.** Effect of PCL-b-PAA micelles control sample on bacteria deactivation

### 1.6. Bacteria Calibration Curve

To know how many bacteria/mL are present in the bacterial solution of a certain absorbance, a calibration curve for the number of *E. coli* ATCC11229 (bacteria as a function of absorbance) was made. Figure 3 shows such a calibration curve, which was constructed by counting the bacteria of bacterial solutions of given absorbance using a hemocytometer. The hemocytometer is shown schematically in the inset. Details of a hemocytometer can be found elsewhere.<sup>6,7</sup> *E. coli* bacteria were grown in an incubator at 37°C in the growth medium until each of the three bacterial samples reached a given absorbance (0.333; 0.633; and 0.935). Each sample was then diluted two times by the fixative (glutaraldehyde) to prevent bacteria from continuing to grow. Each sample had to be diluted with water an additional two times to decrease the number of bacteria to a level at which they were easy to count. 15  $\mu$ L of each sample was individually

placed into the hemocytometer and bacteria were counted at a magnification of 40x. Next, the final number of bacteria/mL at each absorbance was calculated, taking in account all the dilutions. As seen in that Figure, the absorbance increases linearly with an increase in the number of bacteria/mL as the bacteria multiply.

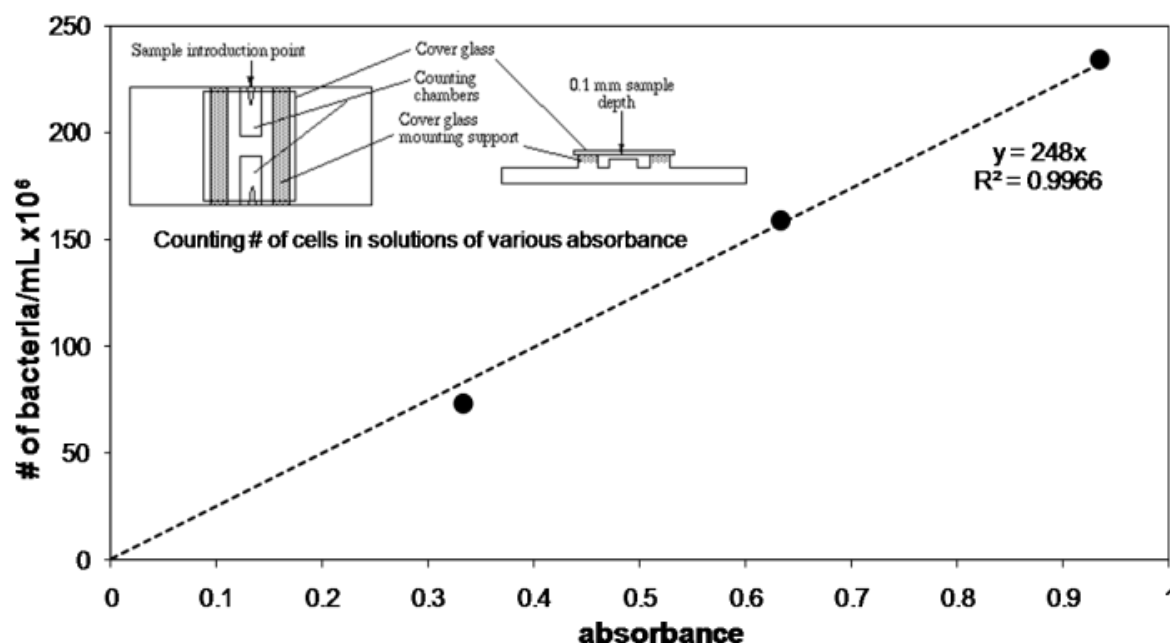


**Figure 3:** Number of *E. coli* in solution as a function of absorbance at 600 nm.

### 1.7. Calculations of Uptake Capacity of Water in the Dialysis Step

Since the solution is dialyzed in large excess of water (15 L), all biocide should diffuse from emulsion droplets into the surrounding water. The saturation concentration of biocide in the water is 12.7 mg/L,<sup>20</sup> which corresponds to 0.195 g in 15 L dialysis bath. To prepare the 50/50 ratio emulsion, 0.02 g of biocide was used. Therefore, the weight of the biocide in each emulsion solution (20 mL) is approximately 10 times lower than the weight which corresponds to the capacity at the saturation concentration in 15 L of dialysis bath (for 50/50 emulsion). In case of

66/33 ratio the biocide weight capacity is exceeded 20 times in 15 L. Thus the biocide is most likely depleted from emulsion droplets and they are empty.

### *1.8. Calculations of the unperturbed end to end distance for PEI molecule*

Since the  $M_w$  of PEI molecule is 750 000 g/mol and  $M_w$  of one repeat unit corresponds to 43 g/mol, one can calculate that one molecule contains  $\sim 17\,400$  repeat units. Knowing the number of repeat units, the number of backbone atoms is  $\sim 52\,000$  or 26 000 atom pairs. Taking 2.5 Å/pair, the unperturbed end to end distance can be estimated to be  $\sim 40$  nm.

### *1.9. Calculation of Monolayer Coverage at Emulsion Concentration Efficient in Bacteria Deactivation*

In order to calculate how many emulsion droplets are needed to kill the bacteria, first, the number of emulsion droplets needed to cover 1 bacterium was calculated, using the diameter of PCL-b-PAA/TCMTB droplet of  $\sim 325$  nm and the size of the bacteria of  $\sim 1\,500 \times 500$  nm. Considering the projected surface of bacterium to be  $2.3 \times 10^6 \text{ nm}^2$  and the surface of emulsion droplet to be  $1.05 \times 10^5 \text{ nm}^2$  (assuming square packing of emulsion droplets on the bacterial surface), there is a space for roughly 22 emulsion droplets on 1 bacterium.

Knowing the concentration of PCL-b-PAA/TCMTB emulsion (0.136 g/L) required to kill the bacteria at a concentration of  $25 \times 10^9$  bacteria/L (from the calibration curve in the Supporting Information), which corresponds to an absorbance of 0.1, one can estimate number of emulsion droplets/bacterium in such a solution. Since the efficient emulsion solution contained 3 mL of the PEI/TCMTB emulsion, while the total volume of the solution was 22 mL, one can calculate that there is  $1.23 \times 10^{10}$  emulsion droplets of diameter of 325 nm in 22 mL solution. (The number of emulsion droplets per liter of solution was calculated to be  $4.1 \times 10^{12}$  droplets/L from the



knowledge of the average weight of 1 droplet, which is  $3.3 \times 10^{-7}$  g). Finally, the number of emulsion droplets/bacterium in the emulsion solution effective in killing the bacteria was estimated to be 22 emulsion droplets/bacterium, since the number of bacteria in the total volume of that solution was  $0.55 \times 10^9$  bacteria/22 mL.

#### *1.10. Inductively Coupled Plasma - Emission Optical Spectrophotometry (ICPEOS)*

Atomic analysis by inductively coupled plasma involves several well defined steps. In the first, the nebulization step, the liquid is converted to an aerosol. In the second step, desolvation/volatilization takes place. The water is driven off, and the remaining solid and liquid portions of the sample are converted to gasses. Atomization takes place in the third step, bonds are broken and only atoms or ions are present. An inert chemical environment is important at this point, because the temperature is very high (up to ca 10 000 K), and oxidation has to be avoided. In the fourth (simultaneous) step, the atoms gain energy by collisions, during which electrons are promoted to excited states. The pattern of frequencies of light emitted when electrons fall back to their lower energy or ground states is different for each element. Therefore, from a spectroscopic analysis of the emitted light, the elements present in the sample can be identified.

Because sulfur is present in the TCMTB biocide, which was suspected to be complexed with the polymeric stabilizing agents in the residual emulsion shells, the wavelengths characteristic of the sulfur emission (182 nm) were monitored in the ICP spectrum. The specific steps of the procedure involved mixing of the emulsion with nitric acid, followed by sample digestion *via* boiling for an hour. This step was needed to break down the polymeric components and to oxidize all the material. The product of the digestion was diluted with water, and injected into the

argon plasma at a temperature of ca 10 000 K. The instrument used was an ICPEOS Trace Scan Model from Thermo Jarrell Ash.